National Library
of Canada

Acquisitions and
Bibliographic Services Branch

395 Wellington Street
Ottawa, Ontario
K1A 0N4

Bibliothèque nationale
du Canada

Direction des acquisitions et
des services bibliographiques

395, rue Wellington
Ottawa (Ontario)
K1A 0N4

Your file Votre référence

Our file Notre référence

NOTICE

The quality of this microform is heavily dependent upon the quality of the original thesis submitted for microfilming. Every effort has been made to ensure the highest quality of reproduction possible.

If pages are missing, contact the university which granted the degree.

Some pages may have indistinct print especially if the original pages were typed with a poor typewriter ribbon or if the university sent us an inferior photocopy.

Reproduction in full or in part of this microform is governed by the Canadian Copyright Act, R.S.C. 1970, c. C-30, and subsequent amendments.

AVIS

La qualité de cette microforme dépend grandement de la qualité de la thèse soumise au microfilmage. Nous avons tout fait pour assurer une qualité supérieure de reproduction.

S'il manque des pages, veuillez communiquer avec l'université qui a conféré le grade.

La qualité d'impression de certaines pages peut laisser à désirer, surtout si les pages originales ont été dactylographiées à l'aide d'un ruban usé ou si l'université nous a fait parvenir une photocopie de qualité inférieure.

La reproduction, même partielle, de cette microforme est soumise à la Loi canadienne sur le droit d'auteur, SRC 1970, c. C-30, et ses amendements subséquents.

Canada

UNIVERSITY OF ALBERTA

THE GEOCHRONOLOGY, GEOCHEMISTRY AND ISOTOPE GEOLOGY OF THE TYPE-NUK GNEISSES OF THE AKIA TERRANE, SOUTHERN WEST GREENLAND.

©

BY

MICHAEL JOHN MACLACHLAN DUKE

A thesis submitted to the Faculty of Graduate Studies and Research in partial fulfilment of the requirements for the degree of Doctor of Philosophy.

DEPARTMENT OF GEOLOGY

Edmonton, Alberta
Fall 1993

National Library
of Canada

Acquisitions and
Bibliographic Services Branch

395 Wellington Street
Ottawa, Ontario
K1A 0N4

Bibliothèque nationale
du Canada

Direction des acquisitions et
des services bibliographiques

395, rue Wellington
Ottawa (Ontario)
K1A 0N4

Your file Votre référence

Our file Notre référence

The author has granted an irrevocable non-exclusive licence allowing the National Library of Canada to reproduce, loan, distribute or sell copies of his/her thesis by any means and in any form or format, making this thesis available to interested persons.

L'auteur a accordé une licence irrévocable et non exclusive permettant à la Bibliothèque nationale du Canada de reproduire, prêter, distribuer ou vendre des copies de sa thèse de quelque manière et sous quelque forme que ce soit pour mettre des exemplaires de cette thèse à la disposition des personnes intéressées.

The author retains ownership of the copyright in his/her thesis. Neither the thesis nor substantial extracts from it may be printed or otherwise reproduced without his/her permission.

L'auteur conserve la propriété du droit d'auteur qui protège sa thèse. Ni la thèse ni des extraits substantiels de celle-ci ne doivent être imprimés ou autrement reproduits sans son autorisation.

ISBN 0-315-88312-X

Canada

UNIVERSITY OF ALBERTA
RELEASE FORM

NAME OF AUTHOR: Michael John Maclachlan Duke

TITLE OF THESIS: 'The geochronology, geochemistry, and isotope geology of the type-Nûk gneisses of the Akia terrane, southern West Greenland'.

DEGREE: Doctor of Philosophy

YEAR THIS DEGREE GRANTED: 1993

Permission is hereby granted to the University of Alberta Library to reproduce single copies of this thesis and to lend or sell such copies for private, scholarly or scientific research purposes only.

The author reserves all other publication and other rights in association with the copyright in the thesis, and except as hereinbefore provided neither the thesis nor any substantial portion thereof may be printed or otherwise reproduced in any material form whatever without the author's prior written permission.

John Duke

3635 - 51st Street,
Edmonton, Alberta,
CANADA. T6C 1C7.

Date: 16th June 1993

UNIVERSITY OF ALBERTA

FACULTY OF GRADUATE STUDIES AND RESEARCH

The undersigned certify that they have read, and recommend to the Faculty of Graduate Studies and Research for acceptance, a thesis entitled 'The geochronology, geochemistry, and isotope geology of the type-Nûk gneisses of the Akia terrane, southern West Greenland' submitted by Michael John Maclachlan Duke in partial fulfilment of the requirements for the degree of Doctor of Philosophy.

H. Baadsgaard

Dr. H. Baadsgaard (Supervisor)

R A Burwash

Dr. R.A. Burwash

Dr. T. Chacko

Dr. R. Luth

D.I. Gough

Dr. D.I. Gough

Z.E. Peterman

Dr. Z.E. Peterman (external)

Date: 18 MAY 1993

Dedication

I dedicate this thesis to Professor Lloyd George Stephens-Newsham for the role model, mentor and friend he has been to me over the years.

I owe many things to Lloyd, not least of which was the opportunity to emigrate to Canada because of the position he secured for me at the University of Alberta SLOWPOKE reactor Facility after months of exchange with the 'authorities' while I was completing my M.Sc in geology at the University.

He both encouraged me to return to graduate studies to obtain this Ph.D. and throughout its duration.

In Lloyd I see many qualities that I aspire to and I am better for knowing him.

Abstract

The Godthåbsfjord region of southern West Greenland is now considered to consist of a minimum of three terranes including: the Akia terrane, the Akulleq terrane, and the Tasiusarsuaq terrane. The geochronology and geochemistry of the mid-Archaean Akia terrane, which is dominated by the type-Nûk gneisses, is the focus of this study.

Chemical and isotopic analyses lead to the conclusion that the type-Nûk gneiss igneous precursors were produced by partial melting of basic crust with variable amounts of garnet in the residue. Large volumes of tonalitic magmas produced in this manner underwent subsequent fractionation of hornblende (and to a lesser degree plagioclase) producing melts of trondhjemitic and granodioritic composition.

Precise U-Pb zircon analyses, determined by both ion microprobe and small sample techniques, of a number of type-Nûk gneisses show a range of ages from 2920 to 3040 Ma. The data are insufficient in number to confidently conclude whether magmatic activity was of a prolonged or episodic nature, though there appears to be a clustering of ages at about 3000 Ma.

Regions within the Akia terrane previously identified as being composed of Amîtsoq gneisses show no isotopic evidence of being Amîtsoq in nature. Ion microprobe data do suggest that some of these areas may be remnants of felsic crust some 3250 - 3400 (?) Ma old.

Uranium-Pb SHRIMP zircon analyses gave an age of 3193 ± 7 Ma (2σ) for the dioritic protoliths of the Nordlandet granulites of the region, with peak granulite-facies metamorphism occurring at 3014 ± 7 Ma (2σ). Consequently, the Nordlandet protoliths are $\geq$ 150 Ma older than the igneous precursors of the type-Nûk gneisses and proves the two are not contemporaneous.

The granulites show *extreme* depletion in many of the LILE, especially Rb, Th, U, K, and Cs making them the most depleted granulites on record (K/Rb up to 11000). Geochemical evidence does not indicate LILE depletion *via* partial melt extraction though locally this may have been a factor. LILE depletion *via* a fluid phase is the favoured mechanism of depletion.

Finally, the 'refined' single-bead zircon technique, developed as part of this study, provides a simple and elegant means of Pb separation for single-zircon work, with a very small Pb blank.

Acknowledgements

First, and most of all, I thank Margaret my wife for her support throughout the duration of this degree. She has sacrificed much and her patience, encouragement, and perspective have been a blessing to me.

Special thanks to my supervisor Dr. Bud Baadsgaard for his tutelage in the art of geochronology, for providing the facilities to carry out this work, for financing the research and, particularly in the latter stages of this thesis, for his patience.

Dr. Allen Nutman is especially acknowledged for organizing the fieldwork in Greenland and for his assistance in selecting and collecting samples for study. Without his aid this thesis would not have been possible. I greatly benefited from his knowledge of the Archaean geology of Greenland and his expertise in the field. Thanks also to Drs. Clark Friend and Vic McGregor for their aid in the field.

In the isotope geology groups of the departments of Geology, and Physics Pat Cavell, Wayne Day, Alex Stelmach, and Dragan Krstic have all taught me a lot during the past many years. However, it is their friendship and kindness that I will remember the most.

Friendship is a difficult thing to quantify or define. Socrates is reported to have asked an old man what he valued most when he reflected on his life. He replied "the friends I have had". In addition to many of the people I have already mentioned I would especially like to thank Brian Turner of the Department of Animal Sciences at the University for his friendship over the years and the many ways he has assisted me in my work and in general. Similarly to Chuck and Vel Box who have always been there both the happy times and not so happy ones, and for their support to Margaret and me during this thesis. I thank Steve Prevec and Steve (Hello) Johnston for their company and good humour over the years of studying together.

I am doubly grateful to the personnel of the SLOWPOKE Nuclear Reactor Facility at the University of Alberta. Firstly, for permitting me the use of NAA facilities to carry out a significant portion of my work, and secondly to Dr. Ron

Kratochvil (Chairman) and Dr. Len Wiebe (Acting Director) of the Facility for allowing me time from my work to finish writing-up this thesis.

Finally, I have been very fortunate and am extremely grateful for the financial support I received during my Ph.D. studies and research. The majority of the work was carried out during the tenure of an Izaak Walton Killam predoctoral Memorial Scholarship (University of Alberta), a Ralph Steinhauer Award (Alberta Heritage Scholarship Fund), a Province of Alberta Graduate Fellowship, and an Andrew Stewart Graduate Prize.

Table of Contents.

Chapter Page

1. Introduction 1
  1.1 Rationale for this Study 3
  1.2 Research Procedures 6
2. Geological Setting 8
  2.1 Synopsis of the Archaean geology of the Godthåbsfjord Region 8
    2.1.1 The Terrane Model of southern West Greenland 8
      2.1.1.1 The Akulleq terrane 9
      2.1.1.2 The Akia terrane 10
      2.1.1.3 The Tasiusarsuaq terrane 10
    2.1.2 Overview of the geology of the Amîtsoq, Nûk, and Ikkattoq gneisses 10
      2.1.2.1 The Amîtsoq Gneisses 11
      2.1.2.2 The Ikkattoq Gneisses 14
      2.1.2.3 The Nûk Gneisses 15
3. The type-Nûk gneisses 18
  3.1 Introduction 18
  3.2 Geochemical and isotopic results 21
    3.2.1 Classification 21
    3.2.2 Geochemistry 27
      3.2.2.1 Major element chemistry 27
      3.2.2.2 Trace element chemistry 42
    3.2.3 Geochronology and isotope geology 59
      3.2.3.1 Zircon geochronology 59
      3.2.3.2 Whole-rock isotopic data 83
      3.2.3.3 Comparison of the type-Nûk and Amîtsoq gneisses 96
    3.2.4 Summary 101
4. Nordlandet granulites 102
  4.1 Introduction 102

4.1.1 Previous work 103
4.1.2 Description of granulites 104
4.2 Geochemistry 106
4.2.1 Major element chemistry 109
4.2.2 Trace element chemistry 109
4.3 Geochronology and isotope systematics 127
4.3.1 Zircon geochronology 127
4.3.1.1 Ion microprobe 130
4.3.1.2 Small sample uranium-lead analyses 130
4.3.2 Whole-rock isotope systematics 136
4.3.2.1 Lead-Lead 136
4.3.2.2 Rubidium-Strontium 141
4.3.2.3 Samarium-Neodymium 142
4.4 Discussion 147
4.4.1 Origin of granulites 147
4.4.2 Depletion of LILE 149
4.5 Conclusions 151
5. Late granite sheets 154
5.1 Introduction 154
5.2 Classification 154
5.3 Geochemistry 159
5.3.1 Major element chemistry 159
5.3.2 Trace element chemistry 161
5.4 Geochronology and isotopic systematics 162
5.4.1 Uranium-Lead zircon analyses 162
5.4.1.1 Ion microprobe results 164
5.4.1.2 Conventional Uranium-Lead results 164
5.4.2 Whole-rock isotopic analyses 167
5.4.2.1 Lead-Lead 167
5.4.2.2 Rubidium-Strontium 170
5.4.2.3 Samarium-Neodymium 171

5.5 Conclusions 173
6. Origin of the type-Nûk gneisses 174
6.1 Review of the origin of Archaean granitoids 174
6.2 Possible modes of formation of the type-Nûk gneisses 175
6.3 Summary 176
7. Summary and conclusions 177
Bibliography 185
Appendix 1: Sample location 208
Appendix 2: Analytical methods 212
Appendix 3: Single bead U-Pb zircon analyses 239
Appendix 4: Elemental and isotopic results 246
Appendix 5: CIPW norms 266
Appendix 6: Whole-rock normalized plots 279

List of Tables.

Table Page

3.1 Key of symbols used to identify the various type-Nûk gneisses in geochemical plots 28

3.2 Average major and minor oxide composition of the type-Nûk gneisses by rock-type 41

3.3 Comparison of the mean and median values of the major heat-producing elements of the type-Nûk gneisses with average crustal values 54

3.4 Ion microprobe data for zircons separated from gneisses G87-17 and G87-85 60

3.5 Results of conventional U-Pb zircon analyses 74

3.6 Whole-rock Pb isotopic composition of Amîtsoq gneisses 91

3.7 Type-Nûk gneiss whole-rock Sm-Nd data 94

3.8 Isotopic data for analyzed Amîtsoq gneisses 100

4.1 Ion microprobe data for G87-67 and G87-70 131

4.2 Conventional U-Pb zircon results for G87-67 and G87-70 133

4.3 Pb-Pb data for the Nordlandet granulites 137

4.4 Comparison of granulite- and amphibolite-facies grade dioritic and quartz-dioritic gneisses of the Akia terrane 152

5.1 Elemental data for the granitic sheets 157

5.2 Isotopic data for the granite sheets 168

7.1 The Archaean geochronology of the Akia terrane 184

A2.1 Results of multiple XRF analyses of G87-35 216

A2.2 X-ray fluorescence results for Ailsa Craig microgranite, AC-E . . . 219

A2.3 X-ray fluorescence results for trace elements in AC-E 220

A2.4 X-ray fluorescence results for USGS W1 221

A2.5 X-ray fluorescence results for USFS SDC-1 222

A2.6 X-ray fluorescence results for USGS SCo-1 223

A2.7 X-ray fluorescence results for CCRMP soil SO-2 224

A2.8 Nuclear data on elements determined by INAA 230

List of Figures.

Figure Page

1.1 Location of study area in southern West Greenland 2

1.2 Folded and fragmented amphibolitized basic dyke from the Akia terrane 'Amîtsoq gneisses' southern Sadelø 5

3.1 Amphibolite xenoliths engulfed by Nûk gneiss 20

3.2 Normative feldspar granitoid classification of the Nûk gneisses . . . 24

3.3 Classification of the type-Nûk gneisses 26

3.4 Harker diagrams for Al_2O_3, FeO^*, and MgO 29

3.5 Harker diagrams for CaO, Na_2O, and K_2O 30

3.6 Harker diagrams for TiO_2, MnO, and P_2O_5 31

3.7 AFM diagram of the type-Nûk gneisses 34

3.8 MgO *vs* TiO_2 for the type-Nûk gneisses 36

3.9 Na-K-Ca ternary diagram for the type-Nûk gneisses 37

3.10 Shand's Index for the type-Nûk gneisses 38

3.11 Mean major and minor element Harker diagrams by rock-type 40

3.12 Harker diagrams of Ni, Co and V 43

3.13 Harker diagrams of Sc, Zn and Cu 44

3.14 Harker diagrams of Ta, Nb and Y 45

3.15 Harker diagrams of Ba, Sr and Yb 46

3.16 Type-Nûk gneiss Th, U, Rb and Cs Harker diagrams 47

3.17 U *vs* Th for the type-Nûk gneisses 50

3.18 Th/U *vs* La/Th for the type-Nûk gneisses 51

3.19 Rb *vs* K for the type-Nûk gneisses 53

3.20 Yb_N *vs* La_N/Yb_N for the type-Nûk gneisses 56

3.21 Y *vs* CaO, TiO_2 and MnO 58

3.22 SHRIMP U-Pb results for zircons from G87-85 61

3.23 SHRIMP U-Pb results for zircons from G87-17 62

3.24 SHRIMP U-Pb results for zircons from G87-89a and G87-80 63

3.25 SHRIMP U-Pb results for zircons from G87-92 64

3.26 Type-Nûk gneiss picked and abraded zircons a) G87-18 b) G87-24 67

3.27 Type-Nûk gneiss picked and abraded zircons a) G87-34 b) G87-94 68

3.28 Type-Nûk gneiss picked and abraded zircons
a) G87-103 b) G87-111 69

3.29 Zircons from G87-5 70

3.30 Type-Nûk gneiss picked and abraded zircons
a) G87-16 b) G87-90 71

3.31 Two zircon populations from type-Nûk gneiss G87-149 72

3.32 U-Pb concordia diagram of zircon analyses 75

3.33 U-Pb concordia diagram for samples G87-5, G87-16,
G87-111, G87-112 and G87-113 76

3.34 Histograms of ^{207}Pb-^{206}Pb zircon ages of analyzed
type-Nûk gneisses 82

3.35 Type-Nûk gneiss Rb-Sr scatterchron for whole-rock data
determined solely by TIMS 84

3.36 Type-Nûk gneiss scatterchron for whole-rock data
determined by TIMS and XRF 86

3.37 Strontium evolution diagram 89

3.38 Effect of variable ^{87}Rb/^{86}Sr ratios on Sr model ages 89

3.39 Pb-Pb isochron for type-Nûk gneisses 90

3.40 Type-Nûk gneiss whole-rock Sm-Nd errorchron 92

3.41 Nd evolution diagram showing the type-Nûk gneisses
and the trajectory of the Amîtsoq gneisses 95

3.42 ϵ_{Nd} *vs* ϵ_{Sr} diagram for the type-Nûk gneisses at 3.0 Ga 97

3.43 U-Pb concordia diagram for Amîtsoq gneiss sample G87-140 99

4.1 Igneous protolith classification of the Nordlandet granulites 107

4.2 Shand's Index for the Nordlandet granulites 108

4.3 Harker diagrams for Al_2O_3, FeO*, and MgO 110

4.4 Harker diagrams for CaO, Na_2O, and K_2O 111

4.5 Harker diagrams for TiO_2, MnO, and P_2O_5 112

4.6 AFM plot of the Nordlandet granulites 113

4.7 Na-K-Ca ternary diagram for Nordlandet granulites 113

4.8 Harker diagram of Ni, Cr, and V 114
4.9 Harker diagrams of Zn, Co, and Sc 115
4.10 Rb vs K for the Nordlandet granulites 117
4.11 K vs K/Rb for the Nordlandet granulites 118
4.12 Sr vs Rb variation diagram for the Nordlandet granulites 120
4.13 K vs K/U for the Nordlandet granulites 122
4.14 K vs K/Th for the Nordlandet granulites 123
4.15 Th/U *vs* La/Th for the Nordlandet granulites 124
4.16 Chondrite normalized REE plot of the Nordlandet granulites together with the average Scourian granulite 125
4.17 Sr vs Ba for the Nordlandet granulites and dioritic type-Nûk gneisses (+) 126
4.18 Zircons from the Nordlandet granulite G87-70 128
4.19 Zircons from the Nordlandet granulites a) G87-70 and G87-67 . . 129
4.20 SHRIMP U-Pb results of zircons from G87-67 and G87-70 132
4.21 Concordia plot of conventional U-Pb zircon analyses from G87-67 and G87-70 134
4.22 ^{207}Pb/^{204}Pb vs ^{206}Pb/^{204}Pb plot of the Nordlandet dioritic granulites 139
4.23 ^{207}Pb/^{204}Pb vs ^{206}Pb/^{204}Pb plot of the Nordlandet dioritic granulites (without sample LR-341938) 140
4.24 Sm-Nd whole-rock isochron plot of fresh granulites 143
4.25 Mixed whole-rock Sm-Nd isochron plot 144
4.26 Effect of partial melt extraction on Nd model ages 146
5.1 Normative feldspar granitoid classification of the granite sheets . . 156
5.2 Granite sheet classification after DeBon and Le Fort (1982) 158
5.3 Normative Q-A-P plot of the granite sheets 158
5.4 Na-K-Ca diagram of the granite sheets 160
5.5 Granite sheets plotted on the pseudo-ternary Q-Ab-Or system . . . 160
5.6 K *vs* K/U ratio of the granite sheets 163
5.7 K *vs* K/Th ratio of the granite sheets 163
5.8 U-Pb Concordia plot of SHRIMP analyses of G87-19 165

5.9 U-Pb concordia diagram for samples G87-114 and G87-27 166
5.10 Nd evolution diagram related to the origin of the granite sheets . . 172

List of Abbreviations.

BABI - Basaltic Achondrite Best Initial
CA - Calc-Alkaline
CHUR - CHondritic Uniform Reservoir
DM - Depleted Mantle
DNC - Delayed Neutron Counting
HREE - Heavy Rare Earth Elements
HFSE - High Field Strength Elements
INAA - Instrumental Neutron Activation Analysis
LILE - Large Ion Lithophile Elements
LREE - Light Rare Earth Elements
MSID - Mass Spectrometry Isotope Dilution
MSWD - Mean Squared Weighted Deviation
REE - Rare Earth Elements
TIMS - Thermal Ionization Mass Spectrometry
TTG - Tonalite-Trondhjemite-Granodiorite
WR - Whole-rock
XRF - X-Ray Fluorescence

CHAPTER 1

Introduction

The focus of this thesis is the geochronology, isotope geology, and geochemistry of the mid-Archaean[1], type-Nûk gneisses of southern West Greenland and the Archaean history of the Akia terrane, which is largely made up of the type-Nûk gneisses. The field area, centred about Nuuk (formerly Godthåb), the capital of Greenland, forms part of the Archaean gneiss complex of southern West Greenland. This complex is part of a much larger block that makes up a significant portion of the North Atlantic Craton as defined by Bridgwater *et al.* (1973) (Figure 1.1). In the context of North American geology the area, together with the Archaean of Labrador, is considered part of the Nain province (Hoffman, 1988).

The Archaean of southern West Greenland has been important in the development of our understanding of the origin and evolution of the Earth's continental crust (*e.g.*, Moorbath and Taylor, 1981). By the mid-1980's some ten to fifteen years of field- and isotopic-studies had resulted in a fairly comprehensive understanding of the origin and history of the high-grade Archaean rocks of the Godthåbsfjord region. McGregor (1973) divided the grey gneisses of the area into one of two major litho-stratigraphic complexes on the basis of the presence or absence of the now amphibolitized, basic Ameralik dykes. In this manner he was able to differentiate the older, early Archaean, polygenetic, Amîtsoq gneisses (that contain relicts and fragments of the Ameralik dykes) from the younger, mid- to late-Archaean Malene supracrustals and Nûk gneisses (from which Ameralik dykes are absent). McGregor (1973) defined the Nûk gneisses as all those quartzo-feldspathic gneisses in the Nuuk area that did not contain Ameralik dykes and which

---

[1] Within this thesis the Archaean is divided into early- (4000 - 3400 Ma), mid- (3400 - 2900 Ma) and late- (2900 - 2500 Ma) after Harland *et al.*, 1982.

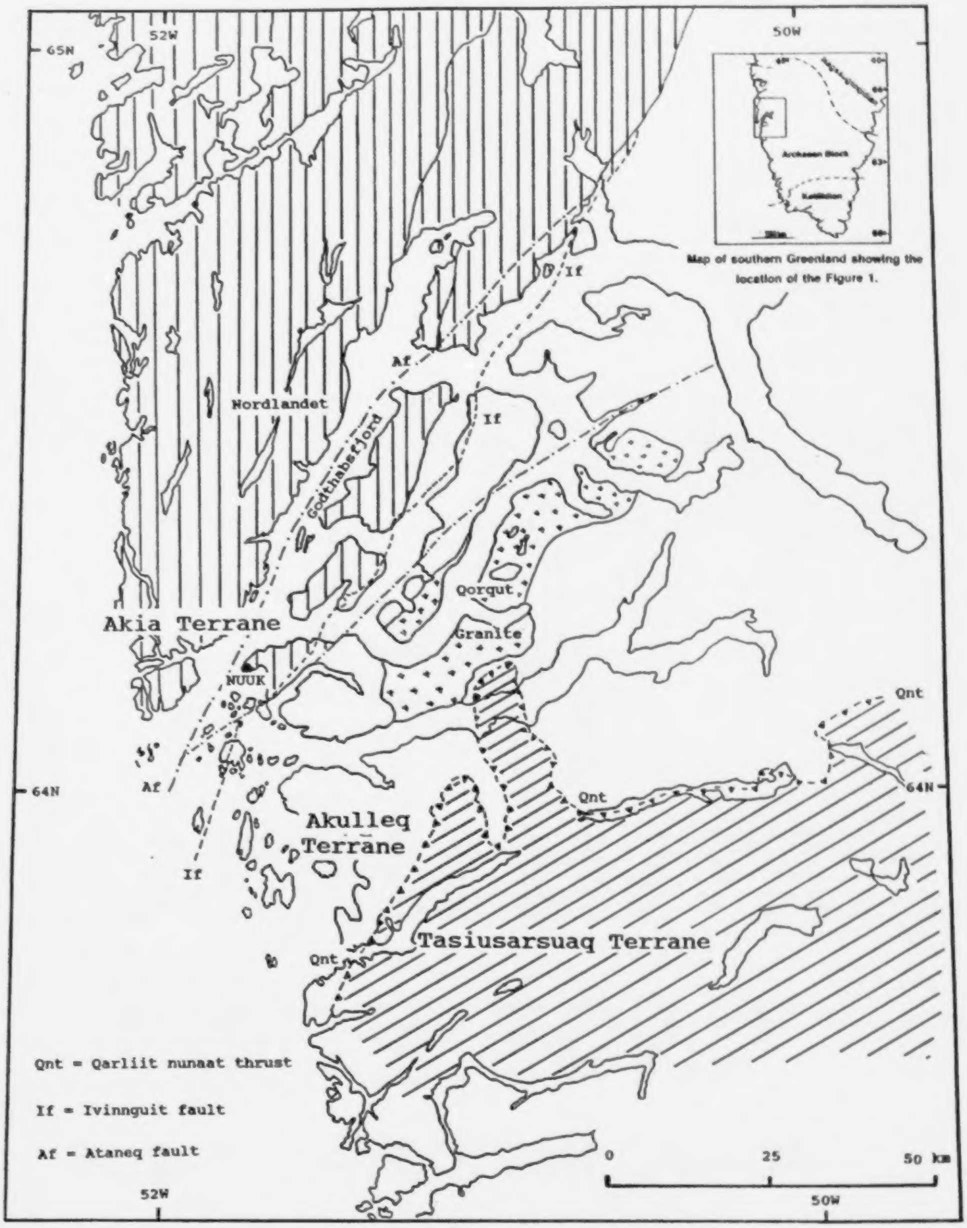
65N
52W
50W
Map of southern Greenland showing the location of the Figure 1.
Archaean Block
If
Af
Nordlandet
Godthabsfjord
If
Qorqut
Granite
Akia Terrane
NUUK
Qnt
64N
Af
Qnt
64N
Akulleq Terrane
If
Tasiusarsuaq Terrane
Qnt
Qnt = Qarliit nunaat thrust
If = Ivinnguit fault
Af = Ataneq fault
0
25
50 km
52W
50W

Figure 1.1 Location of study area in southern west Greenland

intruded the Amîtsoq gneisses, Malene supracrustals, and leucogabbro-anorthositic rocks of the region. When mapping outside the Godthåbsfjord region other workers employed this definition, which led to a division of the "Nûk gneisses" into Nûk gneisses *sensuo stricto* (the type-Nûk gneisses from the Nuuk townsite and environs), and Nûk gneisses *sensuo lato*, which also included those from outside the immediate Godthåbsfjord region. However, mapping the Buksefjorden region south of Nuuk, Chadwick and Coe (1973) and Chadwick *et al.*, (1974) were always opposed to the application of McGregor's terminology, particularly in regard to the Nûk gneisses (*s.l.*) which they showed had been produced by remobilization of older gneisses. At that time conventional dating methods demonstrated that the Amîtsoq gneisses were *ca*. 3650 Ma old, whereas the Nûk gneisses (*s.l.*) ranged in age from 3070 - 2650 Ma.

1.1 Rationale for this Study

In comparison to the older Amîtsoq gneisses the Nûk gneisses have received significantly less study. Prior to this study, no thorough integrated isotopic and geochemical study of the type-Nûk gneisses, with or without strict age control, had been carried out **on the same samples**. Consequently, a detailed isotopic and geochemical investigation of these rocks was considered worthwhile for a number of reasons.

Firstly, conventional U-Pb zircon analyses of sized fractions from fourteen type-Nûk gneisses yielded Concordia upper intercept apparent crystallization ages that spanned 175 Ma (ranging from 3065 to 2890 Ma) (Baadsgaard and McGregor, 1981). Similarly, previous dating of the Nûk gneisses (*s.l.*) of southern West Greenland using whole-rock Rb-Sr and U-Pb bulk zircon techniques gave dates that spanned some 400 Ma (*i.e.*, 3065 - 2650 Ma). Either interval seemed an inordinate length of time for a supposed single 'super event' of continental crust generation (Moorbath *et al.* 1986). Thus at the beginning of this study it was believed that a detailed

U-Pb zircon study of the various phases of the type-Nûk gneisses, employing current methodologies (*e.g.*, single zircon and ion microprobe dating techniques) might explain this enigma and reveal evidence of an episodic history of magmatism as opposed to a single, protracted period of activity. In this sense the study parallels that of Baadsgaard *et al.*, (1986) who showed the Amîtsoq gneisses at Isukasia to be comprised of three lithologies of significantly different ages.

Secondly, soon after this study was initiated the geology of the Godthåbsfjord region was reinterpreted in the context of a 'terrane model' (Friend *et al.*, 1987, 1988; Nutman *et al.*, 1989; McGregor *et al.*, 1991). Under this model the study area comprises a significant portion of the Akia terrane, a small section of the adjacent Akulleq terrane, and part of the tectonic boundary between these two terranes (the Ivinnguit fault). As defined in the terrane model the Akia terrane does not contain any early Archaean Amîtsoq gneisses - in the model they are confined to the Akulleq terrane. However, the region now defined as the Akia terrane has numerous areas that were originally mapped by McGregor as being Amîtsoq gneiss, largely on the basis of the presence of amphibolitized basic dykes (Figure 1.2) presumed to be Ameralik dykes. Prior to this study there were no geochemical, isotopic or geochronologic data on the gneisses from these areas (hereafter referred to as Akia terrane 'Amîtsoq gneisses') and it was solely on the basis of the terrane model was their original designation was questioned. The existence of Amîtsoq gneisses in the Akia terrane would call into question the validity of the Akia terrane as a distinct, separate entity from the Akulleq terrane. Consequently, samples of the Akia terrane 'Amîtsoq gneisses' were collected for geochemical and isotopic study with the expectation that the results would permit an objective decision to be made as to their age and hence the integrity of the Akia terrane.

Thirdly, the early Archaean Amîtsoq gneisses and mid- to late-Archaean Nûk gneisses (*s.l.*) are considered to be the products of two major

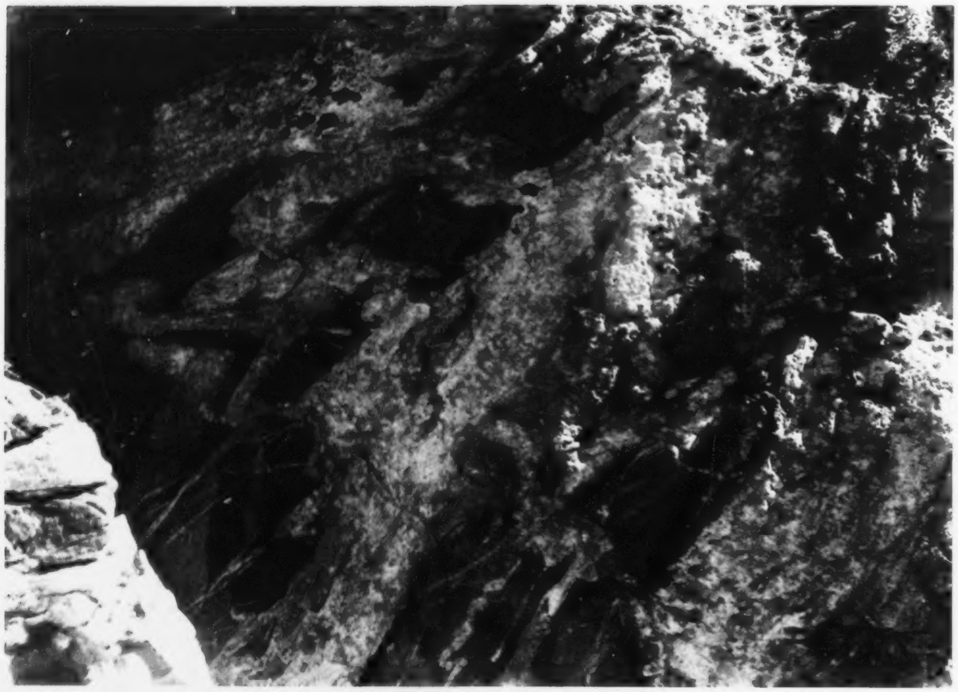

Figure 1.2 Folded and fragmented amphibolitized basic dyke from the Akia terrane 'Amîtsoq gneisses' southern Sadelø (penknife = 9 cm).

episodes of continental crust accretion (Moorbath, 1977). Although the salient features of the two phases are similar, it was hoped that a detailed geochemical study of the type-Nûk gneisses (when compared with data on the Amîtsoq gneisses) might reveal differences related to changes in the Earth in the intervening 600 Ma or so (particularly the effect of its dwindling thermal budget).

It was also considered that the results of this study might enable stricter constraints to be placed on geological processes that operated in the Archaean, particularly processes that are poorly understood; *e.g.*, the generation of tonalitic and trondhjemitc magmas (with the associated implications on the origin of the early continental crust), the formation and depletion of granulites in heat-producing and related large-ion lithophile elements.

In regards to the generation of tonalitic and trondhjemitic magmas in the Archaean there have, in recent years, been numerous experimental studies performed to elucidate the origin of Archaean, sodium-rich 'grey gneisses'. It was considered that it would be useful to compare the results these studies with the geochemically and isotopically well-characterized type-Nûk gneisses of this study.

1.2 Research Procedures.

Samples were collected largely by the author and Dr. Allen Nutman during a five week period spanning part of June and July, 1987. Drs. Clark Friend and Vic McGregor also participated in sampling towards the latter part of this five week period. Details of sample locations, sampling procedures and sample preparation are given in Appendix 1.

With the above research questions in mind, samples were selected for zircon geochronology and/or whole-rock isotopic studies, and elemental analysis. One hundred and twenty-three samples were collected, all of which were analyzed by X-ray fluorescence (XRF) and instrumental neutron activation analysis (INAA) as described in Appendix 1. Whole-rock Sm-Nd and Pb-Pb analyses were performed on all but a few samples, and Rb-Sr analyses on the majority of samples. Zircons were separated from some twenty-five samples and analyzed by single - small sample chemical techniques and/or high resolution ion microprobe mass spectrometry. Details of the chemical procedures and mass spectrometric determinations are described in Appendices 2 and 3, respectively.

CHAPTER 2

Geological Setting

Before reporting the results of the investigations of this study, a synopsis of the Archaean geology of southern West Greenland is presented to provide a geological framework in which to interpret the findings.

2.1 Synopsis of the Archaean geology of the Godthåbsfjord Region

Prior to 1987 the geology of the Godthåbsfjord region (as outlined above) was considered to be applicable through-out the region (McGregor *et al.*, 1986).

The recognition of a number of major tectonic breaks within the Godthåbsfjord region in the late mid- to late-1980's by Friend *et al.*, (1987, 1988) coupled with detailed U-Pb zircon studies, led to a reinterpretation of the geology of the area in terms of discrete tectono-stratigraphic terranes or blocks analogous to those identified in Phanerozoic and Proterozoic orogenic belts and formed by plate tectonic processes (Windley, 1984). Amalgamation of the terranes is inferred to have taken place in the late-Archaean, prior to the intrusion of the Qorqut granite at 2530 ± 30 Ma (Baadsgaard, 1976; Moorbath *et al.*, 1981).

This reinterpretation provides a model to test both new and old hypotheses, has significant implications regarding the operation of plate tectonic-like processes in the Archaean, and in a broader sense tests the universality of the principle of uniformitarianism.

2.1.1 The Terrane Model of southern West Greenland.

Between Færinghaven and Tre Brødre, some 50 km south of Nuuk, three terranes were initially identified in the late mid-1980's (Friend *et al.*, 1987). They included the Færinghaven terrane, the Tre Brødre terrane, and the Tasiusarsuaq terrane. Further mapping and geochronological studies led to the definition of a fourth terrane, the Akia terrane (which encompasses the type-Nûk gneisses); and the realisation that differences in the Færinghaven and Tre Brødre terranes were in fact local and not regional. With no major distinction made between these two, the 'Akulleq terrane' was introduced for those rocks previously defined as belonging to the Færinghaven and Tre Brødre terranes (the latter two 'terranes' being demoted to sub-terrane status).

The boundaries of the various terranes are tectonic in nature. The Qarliit nunaat thrust separates the Akulleq and Tasiusarsuaq terranes, while the Ivinnguit fault separates the Akulleq and Akia terranes (Figure 1.1).

Apparently, the individual terranes amalgamated just prior to about 2700 Ma (probably at *c.* 2720 Ma) as indicated by the age of numerous granitic (*s.l.*) sheets that occur throughout the Godthåbsfjord region.

In addition to the Færinghaven, and Tre Brødre sub-terranes in the south, the Akulleq terrane was also divided into the Isukasia sub-terrane in the northeast.

The salient features of the three terranes comprising the Nuuk region as synthesized from Friend *et al.*, 1987, 1988; Nutman, *et al.*, 1989, and McGregor *et al.* (1991) are as follows:-

2.1.1.1 The Akulleq terrane

Also referred to as the Central block, this terrane forms a NE-SW trending linear belt some 150 kms in length that stretches from south of the mouth of Bukesfjorden (south of Nuuk) to the Isukasia area in the northeast. As previously mentioned it is divided into three sub-terranes namely, the Færinghaven, Tre Brødre, and Isukasia sub-terranes. Amîtsoq gneisses dominate the Færinghaven and Isukasia sub-terranes, while late Archaean Ikkattoq quartzo-feldspathic gneisses (Nûk gneisses, *s.l.*) are the major gneissic component of the Tre Brødre sub-terrane, and locally intrude Amîtsoq gneisses.

There are at least three supracrustal sequences within this terrane. Two of the sequences are older than the Amîtsoq gneisses (the Akilia association, and the Isua supracrustal sequence) and one younger (formerly known as the Malene supracrustals).

2.1.1.2 The Akia terrane

The extent of the Akia terrane is shown in Figure 1.1. Prior to this study the terrane was believed to be dominated by 3070 - 2900 Ma tonalitic to dioritic amphibolite-facies, type-Nûk gneisses, which underwent granulite-facies metamorphism in its northwestern parts at *c*. 3000 Ma.

The type-locality for the Malene supracrustals is situated within the Akia terrane. They are comprised of amphibolites and pelitic to semi-pelitic metasedimentary gneisses. Amphibolites, on the southeast of the island of Bjørneøen, contain recognizable pillow lava structures. A full description of the various lithologies comprising this sequence may be found in McGregor (1973) and McGregor *et al.*, (1986).

The Akia terrane is also referred to as the northern block.

2.1.1.3 The Tasiusarsuaq terrane

Also referred to as the southern block, this terrane is dominated by *ca*. 2900 Ma tonalitic to dioritic gneisses which underwent granulite-facies metamorphism at *ca*. 2800 Ma. There has been extensive retrogression of the granulites to amphibolite-facies grade (McGregor and Friend, 1992). The well-studied Fiskenæsset Complex (Myers 1981, 1985; Ashwal *et al.*, 1989) belongs to this terrane.

2.1.2 Overview of the geology of the Amîtsoq, Nûk, and Ikkattoq gneisses.

In addition to a major section of the Akia terrane, the study area comprises parts of the Akulleq terrane that border the Akia terrane. Consequently, a summary of previous work on the Amîtsoq, Ikkattoq, and type-Nûk gneisses is presented to familiarize the reader with the rocks most relevant to this study.

2.1.2.1 The Amîtsoq Gneisses.

As defined by McGregor (1973), the Amîtsoq gneisses are a polyphase suite of early Archaean quartzo-feldspathic, banded, grey orthogneisses that include remnants of basic dykes. Tonalitic to granodioritic compositions predominate. However, almost a third of the Amîtsoq gneisses that crop out on the southside of Ameralik fjord are comprised of a distinctive, atypical suite of Fe-rich augen gneisses and minor ferrodiorites (Lambert and Holland, 1976; Nutman *et al.*, 1984a).

In outer Godthåbsfjord most of the Amîtsoq gneisses have been intensely deformed, and practically all intrusive relationships have been obliterated. Fortuitously, at Isukasia an augen of low deformation some 10 kms in diameter preserves both the Isua supracrustal sequence, and the cross-cutting relationships of various components of the Amîtsoq gneisses (*e.g.*, Allaart, 1976; Nutman *et al.*, 1984b; Nutman and Bridgwater, 1986; Baadsgaard *et al.*, 1986).

Within the Amîtsoq gneiss complex, and particularly at the mouth of Ameralik fjord and the islands northwest of Bukesfjorden, enclaves of supracrustal rocks termed the Akilia association occur (McGregor and Mason, 1977). These metabasaltic and metasedimentary rocks were interpreted as representing possible fragments of a greenstone belt-like sequence. Similarly, at Isukasia the Isua supracrustal belt is surrounded and locally intruded by Amîtsoq gneisses. At *ca*. 3800 Ma old, this is the world's best preserved early Archaean supracrustal sequence (see Nutman, 1986 for a superbly detailed study of the sequence). As such it has been extensively studied in an effort to place limits on early Archaean crustal processes and mantle evolution (*e.g.*, Hamilton *et al.*, (1978, 1983); Moorbath *et al.*, (1986); Jacobsen and Dymek, (1988)). McGregor and Mason (1977) tentatively correlated the Akilia and Isua supracrustal sequences because both are intruded by Amîtsoq gneisses. However, as shown below this is not now considered to be the case.

Although the mineralogy of the Amîtsoq gneisses is indicative of upper amphibolite-facies metamorphism, relict high pressure granulite-facies mineral assemblages occur in the cores of many of the basic and ultrabasic rocks of the Akilia association (McGregor and Mason, 1977). From their study Griffin *et al.*, (1980) concluded that the Amîtsoq gneisses were depleted in Rb and U during a granulite-facies metamorphic event that reached its maximum at *ca.* 3600 Ma. The depletion in U, which must have occurred soon after emplacement of the igneous precursors of the Amîtsoq gneisses, has resulted in a characteristic unradiogenic Pb-isotopic signature for the gneisses (Black *et al.*, 1971). However, care must be exercised when utilizing older published data on some "Amîtsoq gneisses" because of possible misidentification in the field (see Chapter 3 for details).

Geothermometry and geobarometry of the granulite mineral assemblages permits limits to be placed on the thickness and geothermal gradient of the early Archaean Amîtsoq crust. Analyses indicate that the crust was likely at least 20 km thick, with a geothermal gradient $\leq 30°\mathrm{C}\ \mathrm{km}^{-1}$ at *ca.* 3600 Ma. This implies that the greater radiogenic heat production of early Archaean times (some 3 times that of today, Lambert, 1976) was not dissipated through the continental crust, and suggests that the rheological properties of the continental crust were likely not significantly different than those of the continental crust today. A corollary to this is that the excess radiogenic heat must therefore have been lost through the oceanic crust, possibly by longer ridge lengths (hence smaller plates, *e.g.* Hargraves, 1986) and/or by greater spreading rates (Bickle, 1978).

Because of their great age (Black *et al.*, 1971; then the oldest known terrestrial rocks) the Amîtsoq gneisses have been intensely studied (*e.g.*, Moorbath *et al.*, 1972; McGregor, 1973; Baadsgaard, 1973; Baadsgaard *et* *al.* 1976; Griffin *et al.*, 1980). Initial geochronological investigations centred on whole-rock Rb-Sr and Pb-Pb studies and yielded ages in the range 3.65 - 3.55 Ga. Rubidium-Sr isochrons mostly gave initial Sr ratios in the range 0.700 to 0.701 suggestive of a mantle (or Rb-depleted lower continental crust) derivation. The first U-Th-Pb studies of zircons separated from Amîtsoq gneisses [from the Færinghaven sub-terrane] (Baadsgaard, 1973) yielded an upper Concordia intercept age of 3650 ± 50 Ma (recalculated to 3595 ± 50 Ma in Baadsgaard (1976)). In a combined U-Pb bulk zircon, and whole-rock Sm-Nd, Rb-Sr, and Pb-Pb study of the Amîtsoq gneisses from Isukasia, Baadsgaard *et al.*, (1986) were able to demonstrate the polygenetic nature of the gneisses. They concluded that the most probable ages for the grey, white, and pegmatitic gneisses of the area were 3690 ± 50 Ma, 3590 ± 40 Ma, and 3370 ± 60 Ma, respectively; and that the white and pegmatitic gneisses were likely derived by partial melting of grey gneiss-like crust. Moorbath and Taylor (1986) reported a seven point whole-rock Sm-Nd isochron date of 3740 ± 84 Ma ($^{143}Nd/^{144}Nd_{in}$ = 0.50792 ± 7, ϵ_{Nd} = +2.3 ± 1.2) for granulite and amphibolite facies samples from the Godthåbsfjord region (from the Færinghaven sub-terrane).

Pb-Pb whole-rock and mineral analyses of the Isua banded iron formation gave an age of 3710 ± 70 Ma (Moorbath *et al.*, 1973). Bulk analyses of zircons separated from both the Akilia and Isua supracrustal sequences gave upper Concordia intersection ages of 3587 ± 38 Ma and 3813 +21-14 Ma, respectively (Baadsgaard *et al.*, 1984). The former date was considered to record the granulite facies metamorphic event that affected the area (the Færinghaven sub-terrane) at *ca.* 3600 Ma, and to have no bearing on the true age of the Akilia association (except to provide a lower age limit).

The advent of the Sensitive High Resolution Ion MicroProbe or SHRIMP (Compston, *et al.*, 1984), coupled with the fact that Archaean zircons generally contain significant quantities of radiogenic Pb because of their great age, has resulted in previously unattainable detailed U-Pb dating of Archaean samples. Using the SHRIMP, notable geological discoveries have been made (*e.g.*, Froude *et al.*, 1983, Compston *et al.*, 1985, Bowring *et al.*, 1989a,) and advances in our understanding of Archaean geology resulted (this is particularly the case in southern West Greenland).

Using the ion-microprobe Kinny (1986) demonstrated that components of a zircon population separated from an Amîtsoq gneiss from outer Ameralik were at least 3820 Ma old, and that previous bulk zircon analyses had been biased by younger, U-rich zircon zones that mantle the old cores. Three analyses of some very low U and Th rims gave a date of 3632 ± 24 Ma (2σ) which was considered to represent a minimum estimate of the age of granulite facies metamorphic event.

SHRIMP U-Pb zircon analyses of detrital zircons from the Isua supracrustal sequence have yielded ages of 3811 ± 18 Ma (Compston *et al.*, 1986) and 3808 ± 4 Ma (2σ) for a layered felsic rock of the Isua supracrustals (Nutman, 1990).

Nutman (1990) obtained a weighted $^{207}Pb/^{206}Pb$ age of 3877 ± 10 Ma for an Amîtsoq gneiss sample from the Færinghaven sub-terrane that intrudes the type-Akilia association. This is the oldest measured age for a rock from Greenland, and means that the Akilia association, at least at this locality, must be $\geq$ 3880 Ma, making it the world's oldest known supracrustal sequence, and at least 30 Ma older than the Isua supracrustals.

2.1.2.2 The Ikkattoq Gneisses.

A significant portion of the Tre Brødre sub-terrane is made up of the *ca*. 2820 Ma quartzo-feldspathic, amphibolite facies, Ikkattoq gneisses. The group is predominantly granodioritic in composition; dioritic gneisses are of minor importance, and tonalites are rare. As a consequence of being mainly granodioritic in composition the Ikkattoq gneisses are characterized by a high Rb/Sr ratio *vs.* the type-Nûk gneisses, for example.

Whole-rock Rb-Sr, Pb-Pb, and Sm-Nd isotopic studies indicate that many of these gneisses were derived in part from pre-existing Amîtsoq-like crustal material (Baadsgaard, *pers. comm.*, 1993).

2.1.2.3 The Nûk Gneisses

The type-Nûk gneisses comprise the metamorphosed equivalents of apparently earlier, more basic phases (including diorites and hornblende gabbros) which are intruded by younger tonalites, granodiorites, and trondhjemites. Over the last decade a variety of workers have obtained whole-rock isochron and U-Pb zircon ages for the Nûk gneisses (*s.l.*) in the range 3080-2750 Ma, together with initial $^{87}Sr/^{86}Sr$ ratios in the range 0.7015 - 0.7025 (*e.g.*, Pankhurst and Moorbath (1976), Taylor *et al.*, (1980, 1984), Baadsgaard and McGregor, 1981). The low Sr initial ratios led Pankhurst and Moorbath (1976) to conclude that the magmatic precursors of the Nûk gneisses were not partial melts of the *c.* 3.7 Ga Amîtsoq gneisses. The values indicate that the parental materials of the gneisses were derived from a source region with mantle-type Rb/Sr ratios not more than 200-300 Ma before the measured isochron ages. Thus, the mantle, and a Rb-depleted, low Rb/Sr lower crust, have been postulated as possible source regions for the igneous precursors of the Nûk gneisses. Whole-rock Pb-Pb analyses by Taylor *et al.* (1980) led them to conclude that the Nûk gneisses in the Godthåbsfjord region are contaminated with Pb of an unradiogenic isotopic signature indicative of the older Amîtsoq gneisses. Migration of Pb from lower in the crust (induced by granulite facies metamorphism at depth) in fluids and/or direct assimilation of older Amîtsoq gneiss, for example, were postulated as possible mechanisms of contamination. When one plots the Pb isotopic data it can be seen that there is a geographical control on the contamination which decreases towards the northwest. Taylor *et al.* (1980) also suggested that identification of the Pb contaminant might be useful for the detection and delineation of old continental crust. Samarium-Nd isotopic studies of the Nûk gneisses should readily identify the presence of an older crustal component if direct assimilation has taken place. In addition, such data may provided a means to differentiate the possible modes of contamination.

Chemically the Nûk gneisses of the study area show similarities with more recent calc-alkaline (CA) suites. Differences include a somewhat greater Na/K ratio, lower U content, and larger (and more variable) Th/U and K/U ratios for the Nûk gneisses in comparison with younger CA suites. The chemical similarities between the Nûk and Amîtsoq gneisses of the region (McGregor, 1979) may indicate a similar mechanism involved in the origin of both complexes. The similarity rules out derivation of the Nûk gneisses by partial melting of the Amîtsoq gneiss as this would require almost total melting of the latter, and as such is most improbable.

Compton (1978) determined the REE concentration of Nûk gneisses (*s.l.*) from Bukesfjorden, to the southeast of Godthåbsfjord. The variation in the chondrite normalized REE patterns led him to conclude that the igneous precursors of the Nûk gneisses were not cogenetic, but were derived from widely differing sources. To date, however, only four whole-rock REE analyses have been published for the type-Nûk gneisses (previously unpublished data of J.G. Arth, in McGregor *et al.*, (1986)).

Prior to this study it was not known whether the type-Nûk gneisses belonged to a single, cogenetic suite, or whether they were intruded during periods of unrelated activity, possibly separated by major intervals of time. Baadsgaard and McGregor (1981) concluded from their U-Th-Pb zircon study of fifteen samples of type-Nûk gneisses and Qârusuk dykes (McGregor *et al.*, 1983) from southern Bjørneøen and the Nuuk townsite that the range of apparent crystallization ages (3065-2890 Ma) likely resulted from varying degrees of Pb loss rather than multiple intrusion. This is contrary to the conclusion drawn by Compton (1978) for Nûk gneisses in Bukesfjorden. The scatter of Rb-Sr data (Baadsgaard and McGregor, 1981) from samples taken about Nuuk townsite may, however, be indicative of multiple intrusion.

Prior to the development of the terrane model for the region, mid-Archaean supracrustal rocks throughout the Godthåbsfjord area were collectively called the 'Malene supracrustals'. Subsequent work led a number of workers to suggest that the term should be abolished except for the supracrustal sequence of the Akia terrane (*e.g.*, McGregor, *et al.*, 1991). However, as shown later, there are at least two supracrustal sequences within the Akia terrane with distinct ages. Therefore, if use of the term 'Malene supracrustals' is to be continued, it will have to be more rigorously defined.

CHAPTER 3

The type-Nûk gneisses

3.1 Introduction

The purpose of this chapter is to report the results of a detailed study of the geochemistry, geochronology and isotopic geology of the type-Nûk gneisses from the Akia terrane. To this end sixty-nine type-Nûk gneiss samples were collected for geochemical and isotopic study. A number of the samples were collected from areas mapped previously by McGregor (1973) as being Amîtsoq gneiss material (*i.e.*, Akia terrane 'Amîtsoq gneisses' as mentioned in Chapter 1). On the basis of the terrane model the hypothesis was that these supposed 'Amîtsoq gneisses' were in fact Nûk gneisses. It was expected that chemical and isotopic analyses might resolve this issue. Sample locations for the various samples are given in Appendix 1.

The type-Nûk grey gneisses and associated amphibolites (formerly known as part of the Malene supracrustal sequence) of the Akia terrane exemplify the bimodal character typical of many high-grade Archaean terranes (Barker and Peterman, 1974). The gneisses are made up of rock-types that range in composition from gabbros/diorites, through quartz-diorites, tonalites and trondhjemites, to granodiorites and granites (*s.s.*), with tonalites and trondhjemites making up the vast majority of the terrane and samples studied.

On an outcrop scale, cross-cutting relations (where discernable) show that the dioritic and quartz-dioritic gneisses are the oldest phases and the granites the youngest. As explained under the isotopic section of this chapter, the granites (*s.s.*) are considered to be the products of the partial melting of pre-existing grey gneisses (*i.e.*, $\geq$ 2.9 Ga) and as such are considered separately (Chapter 5) from the tonalitic, trondhjemitic, quartz-dioritic, and dioritic gneisses.

The tonalitic and trondhjemitic gneisses are composed chiefly of quartz, plagioclase feldspar (oligoclase), hornblende and biotite, with the trondhjemitic gneisses (by definition) containing less than 10 % mafic minerals. The dioritic and quartz-dioritic gneisses contain significantly more amphibole than the tonalitic gneisses.

Jahn *et al.*, (1981) coined the term 'tonalite-trondhjemite-granodiorite suite (TTG)' to describe the dominant rock-types making up typical high-grade Archaean grey gneiss terranes. The type-Nûk gneisses are a fairly typical TTG-suite.

The high-grade gneisses are associated with amphibolites which occur both as massive sheets/sills, and as abundant lenses and 'exploded' xenoliths engulfed by the grey gneisses (Figure 3.1a). Presumably the precursors of the amphibolites were quite 'wet' when the igneous precursors of the grey gneisses were intruded. The rapid expansion of water fragmented the xenoliths, permitting the magma to be injected further along fractures accentuating the effect. The various stages of the break-up and 'assimilation' of these amphibolite xenoliths by intense ductile deformation can be traced in the field (Figure 3.1b). An awareness and understanding of the possible isotopic and geochemical effects of this process is important when studying the grey gneisses. In very rare areas of low strain primary volcanic structures, such as pillow lavas, are preserved (*i.e.*, S.E. Bjørneøen).

As recorded by McGregor (1973, 1979) most of the type-Nûk gneisses are heterogeneous in outcrop. He described three types including: polyphase gneisses, pegmatite-layered gneisses, and streaky gneisses. Exceptions to the generally heterogeneous nature of the type-Nûk gneisses are the occasional, apparently late, large granodioritic gneissose bodies (*e.g.*, east coast of Bjørneøen).

Field relationships suggest that many of the type-Nûk gneiss precursors were deformed during emplacement. Generally, however, the original structures have since been intensely deformed by severe ductile deformation; intrusive relations being rotated and largely obliterated. There are, however, some instances where cross-cutting relations are clear.

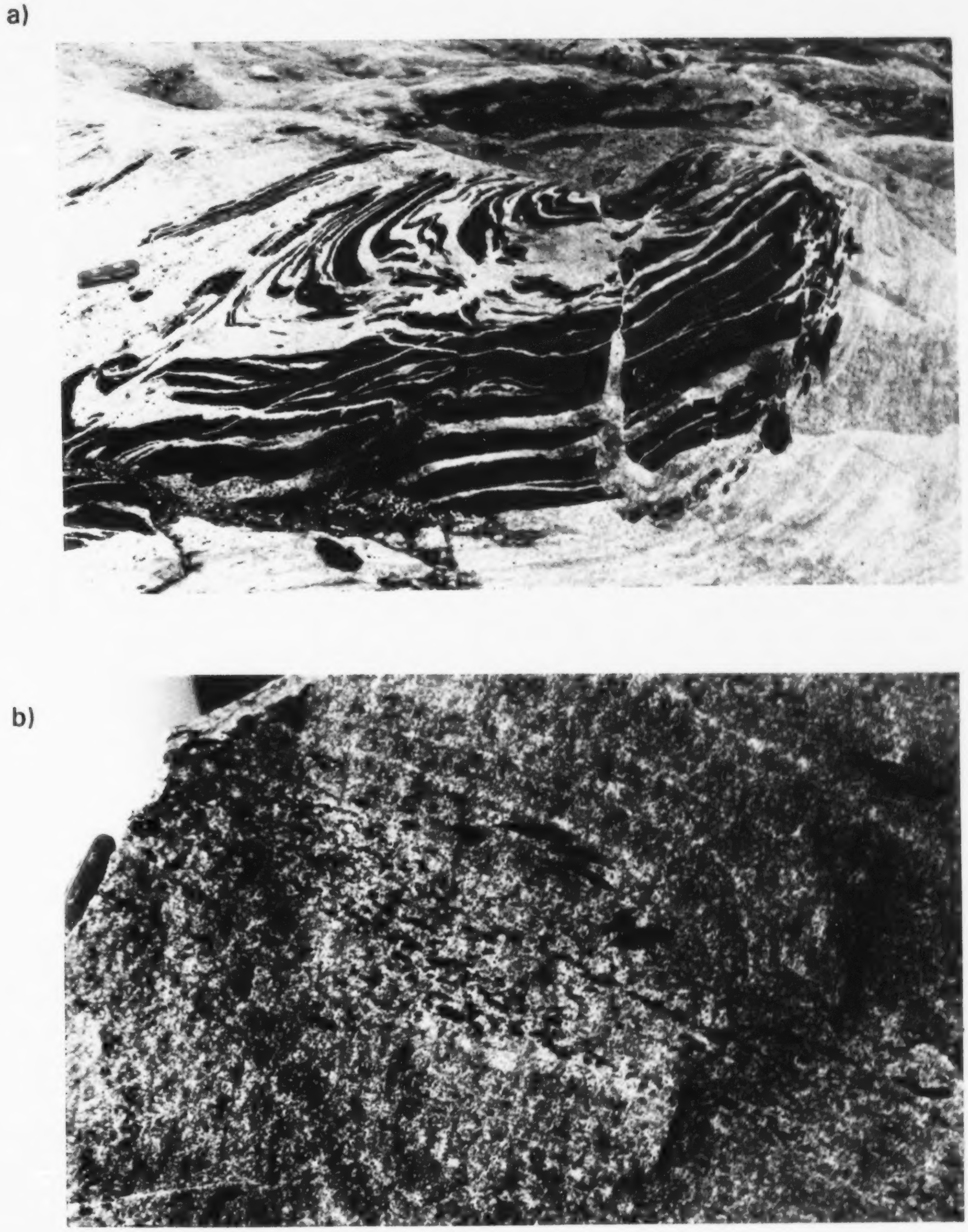

Figure 3.1 a). Amphibolite 'exploded' by effects of the intrusion of the protolith of the type-Nûk gneiss. b). 'Assimilation' of amphibolite fragments by intense ductile deformation (pen knife = 9 cm).

3.2 Geochemical and Isotopic Results

The following sections report the basis of rock-type classification employed for the various type-Nûk gneisses, the results of major and trace element analyses of the gneisses, zircon U-Pb analyses for the gneisses, and the results of whole-rock Rb-Sr, Pb-Pb and Sm-Nd isotopic analyses.

3.2.1 Classification

Grey gneisses of high-grade metamorphic terranes are now commonly described using their inferred pre-metamorphic igneous character as deduced from their major element chemistry, *e.g.*, trondhjemitic gneiss, tonalitic gneiss, *etc*. This approach became popular as evidence accumulated suggesting that the great majority of these rocks were orthogneisses. Prior to this, such gneisses were typically described by a characteristic mineral *e.g.*, hornblende gneiss, pyroxene gneiss, microcline gneiss, *etc*. In describing the grey gneisses of this study, the practice of using their igneous character as a descriptor is employed. In an attempt to determine this igneous character a variety of igneous rock-type classification schemes were examined. Only those schemes utilized by previous workers to study grey gneisses were considered.

Mineral point counting and classification on the basis of the modal quartz-alkali feldspar-plagioclase feldspar content was not employed because of the difficulty of determining reliable mineral estimates due to mineral heterogeneity. This heterogeneity is the result of the extreme deformation and recrystallization suffered by the gneisses.

The majority of samples were named using a combination of classification schemes including: a) the normative feldspar granitoid classification scheme of O'Connor (1965) [with modifications by Barker (1979)], b) major element data together with Barker's chemical definition of trondhjemite (Barker, 1979) [to aid in differentiating tonalites from trondhjemites], and c) the QAP classification (Streckeisen, 1973) using an estimation of the modal mineral content based on major-oxide chemical data (Kalsbeek and Petersen, 1974).

Strictly speaking O'Connor's (1965) classification scheme is applicable only to rocks containing $\geq$ 10% quartz (either normative or modal). O'Connor (1965) stated unequivocally that:

> "If the chemical analysis does not contain sufficient silica to produce the feldspars and 10 percent quartz, the rock will not fit into the classification proposed here." (O'Connor, 1965, p.B83).

Consequently, the scheme has not been applied to the quartz-poor rocks of this study. For example, the dioritic gneisses contain $\leq$ 10% normative quartz as determined by CIPW norm calculation (see Appendix 5).

As noted in Appendix 1 only total iron (reported as FeO^*) was determined for the majority of samples studied. However, the FeO/Fe_2O_3 ratio does not affect the normative feldspar percentages (and hence the applicability of the classification scheme). The feldspars are determined prior to the ferromagnesian minerals (where the ferrous:ferric ratio plays an essential role). The normative quartz content of a CIPW norm is calculated from the residual SiO_2 content after the percentages of all other minerals have been determined. Consequently, the normative quartz content will vary with the ferrous:ferric ratio. For rocks of tonalitic-trondhjemitic-granodioritic composition this is of little concern in the case of the normative feldspar classification scheme because a cursory visual examination of a hand specimen shows that these rock-types contain $\geq$10 % modal quartz. For borderline cases this is not always readily apparent, and the need for reasonably accurate ferrous:ferric ratios becomes important. Consequently, an empirical relationship between Fe_2O_3 and FeO for type-Nûk gneisses was determined from the literature (McGregor *et al.*, 1986) and applied to the type-Nûk gneisses of this study. In addition, FeO was determined in a number samples by titration. The agreement between the empirical ferric:ferrous ratios (Fe_2O_3 = 0.25 * FeO) and those calculated from the titration measurements was fairly good and considered satisfactory for the purposes intended. Using this approach, CIPW norms were calculated for each sample (reported in Appendix 5). The normative quartz content calculated in this manner was used to divide the samples into quartz-rich ($\geq$ 10 % quartz) and quartz-poor ($<$ 10% quartz) categories giving greater confidence in the choice of samples which may be classified using O'Connor's scheme.

Using the normative feldspar classification scheme the majority of the Nûk gneisses plot in either the tonalite or trondhjemite field (Figure 3.2). Of note is the total **absence** of samples falling in the granodiorite field! Numerous workers studying other Archaean grey gneiss terranes have also reported a rarity of gneisses of granodioritic composition (*e.g.*, Glikson, 1979; Tarney *et al.*, 1979; Jahn *et al.*, 1981; Nutman and Bridgwater, 1986). This is in keeping with the generally more sodic nature of granitoids in the early- to mid-Archaean *vs* the late Archaean (and thereafter). However, McGregor (1979) reported that granodioritic gneisses form some of the largest continuous bodies of Nûk gneiss. Consequently, the possibility that the absence of granodioritic gneisses (as implied by the O'Connor classification scheme) was an artifact, or bias, of sampling was considered. Because samples were not collected on the basis of apparent rock-type (which is often ambiguous because of the severe deformation that has taken place) this was considered unlikely. Given that a number of the samples have K_2O contents in the 2 to 3 wt% range it was decided that a number of samples identified as 'trondhjemites' using the normative feldspar classification scheme were in fact granodioritic in composition. Caution should therefore be exercised when utilizing this scheme, particularly when classifying gneisses of granodioritic composition. Potential misidentification can minimized by interpreting the normative feldspar triangular diagram in conjunction with major element rock data (particularly the K_2O content).

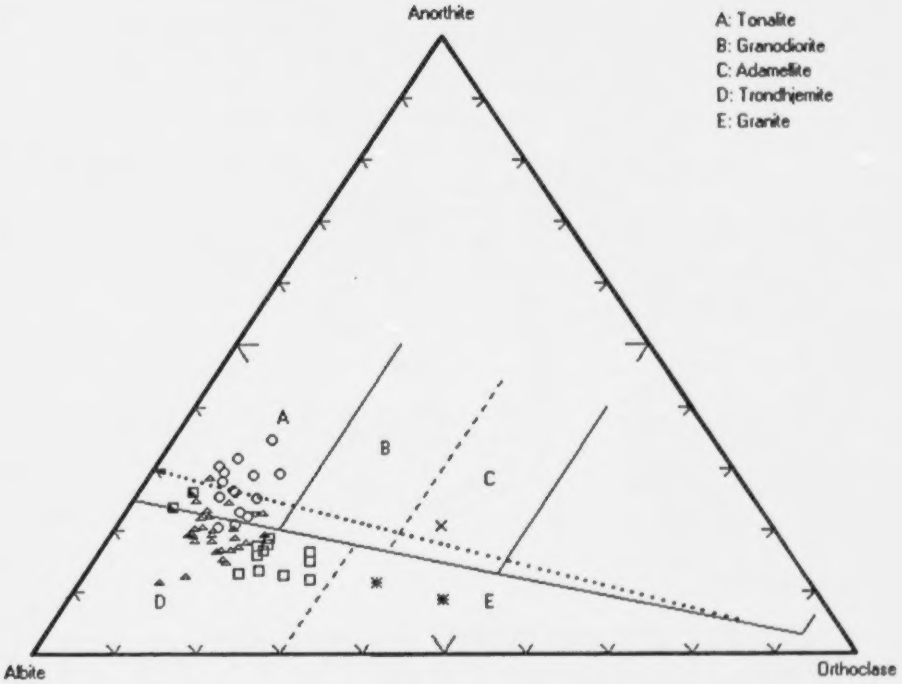

Figure 3.2 Normative feldspar granitoid classification of the Nûk Gneisses (containing ≥ 10 % normative quartz, after O'Connor, 1965). The dotted line represents a modification Barker (1979). (for symbols see Table 3.1)

In addition to the normative feldspar classification scheme the QAP classification scheme (Streckeisen, 1973), employing an *estimation* of the mode calculated predominantly from major element chemical data, was also investigated. The approach was specifically developed to be applied to grey gneisses of Greenland (Kalsbeek and Petersen, 1974). In addition to the major elemental data (usually determined by XRF) some basic petrological information is required for each sample, *i.e.*, the An content of the plagioclase feldspar, the presence or absence of K-feldspar, hornblende, and biotite, for example. Petersen (1977) described and listed a programme written in FORTRAN to perform the mode calculation. This author transcribed the code to run in a PC environment (using Microsoft® QuickBasic) and added a number of routines, one of which takes the calculated quartz-alkali feldspar-plagioclase feldspar content and classifies the rock according to Streckeisen (1973). As the majority of igneous rock-type classification schemes are incapable of distinguishing tonalites from trondhjemites (including the QAP scheme), this author wrote another subroutine to differentiate these sodic granitoids using the calculated modal ferromagnesium mineral content.

On the basis of the above mentioned classification schemes, almost all the gneisses studied were identified as being either dioritic, quartz-dioritic, tonalitic, trondhjemitic, granodioritic, or granitic in nature. Individual rock-type names are reported in Appendix 1, together with the sample location map coordinates. As expected, some samples fall close to the borderline or boundary of two rock-types. In these cases the author attempted to make an objective decision as to which term to use (bearing in mind that such divisions, although not arbitrary, have their limitations).

Finally, to assess the reliability of the descriptive terms given on the basis of the above mentioned schemes the names were compared with the igneous rock classification scheme of Debon and Le Fort (1982). Sample data, plotted by assigned rock-type, are displayed in Figure 3.3. The

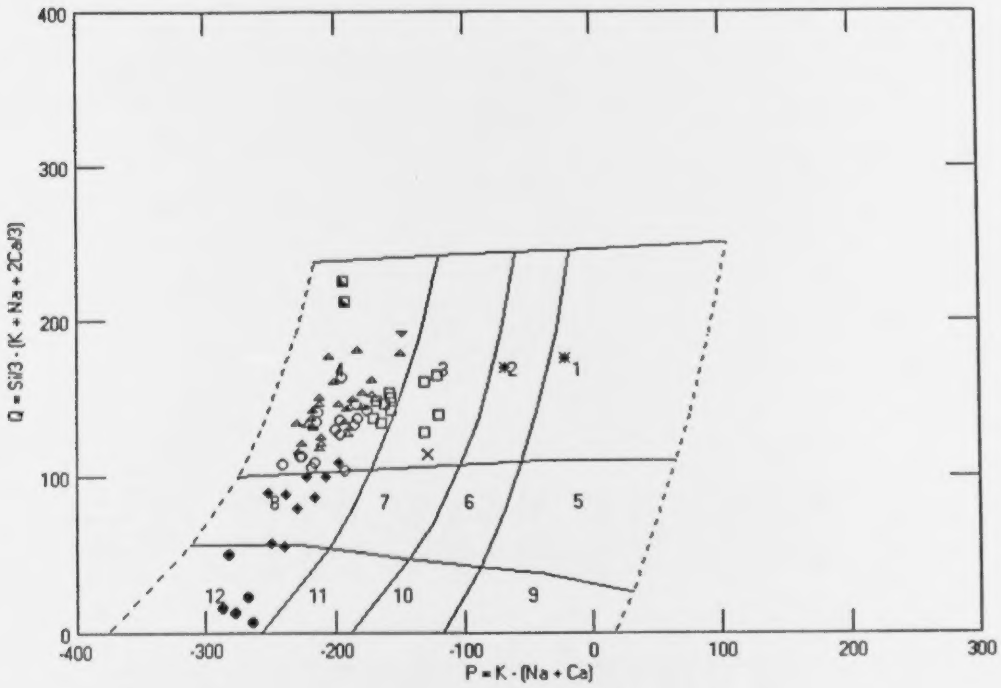

1 = granite
2 = adamellite
3 = granodiorite
4 = tonalite
8 = quartz diorite
12 = gabbro / diorite

Figure 3.3. Classification of the type-Nûk gneisses according to DeBon and LeFort, (1982) (symbols as in Table 3.1).

agreement between the two approaches is in general very good. All of the tonalitic and trondhjemitic gneisses plot within the tonalite field. With one exception all the gneisses designated as quartz-dioritic plot in that field. Some of the gneisses identified as granodioritic in composition plot within the tonalite field, but lie close to the boundary separating the tonalite-granodiorite fields, and form a group discrete from the tonalites and trondhjemites. The dioritic gneisses are confined to the gabbro field, and the two samples identified as granitic gneisses plot in the granite and adamellite fields.

Given the general agreement between the two approaches the descriptive names given on the basis of the previously described schemes was considered reliable and is utilized here on.

3.2.2 Geochemistry

3.2.2.1 Major Element Chemistry.

Major element data for the samples studied, as determined by XRF, are listed in Appendix 4. Silica variation diagrams (*i.e.*, Harker diagrams) of all the samples, identified by rock-type, are displayed in Figures 3.4 to 3.6. A key for the rock-type symbols utilized are given in Table 3.1 and are as follows: dioritic gneisses - filled circles; quartz-dioritic gneisses - filled diamonds; tonalitic gneisses - open circles; trondhjemitic gneisses - open triangles, granodioritic gneisses - open boxes. Two 'granitic' samples are identified by asterisks. Unusual samples have their own symbols and are identified when discussed.

The silica content of the amphibolite-facies grey gneisses from the Akia terrane ranges from 51 to 78 wt % (*i.e.*, dioritic to granitic in composition); excluding the granitic and other late sheets reduces the upper SiO_2 limit of the range to a little below 75%. This span is essentially identical to that reported by McGregor (1979) *i.e.*, 49 to 76 wt % SiO_2 [$n \approx 37$]. He noted that intermediate Nûk gneisses, with silica contents

Table 3.1. Key of symbols used to identify the various type-Nûk gneisses in geochemical plots.

Gneiss-Type	**Symbol**
dioritic gneiss	●
quartz-dioritic gneiss	♦
tonalitic gneiss	○
trondhjemitic gneiss	△
granodioritic gneiss	□

between 56 and 63 wt %, were apparently absent. The additional type-Nûk gneiss analyses of this study confirm the presence of such a gap (Figures 3.4 to 3.6) albeit slightly narrower (55 to 60 % SiO_2) than originally described. This compositional break corresponds to the Daly Gap, and its presence argues against an origin for the tonalites and trondhjemites by fractional crystallization of dioritic magmas.

The TiO_2 content of the gneisses decreases in a fairly monotonous fashion from about 1.1 wt% in the dioritic gneisses to about 0.1 wt% in those of granodioritic and granitic composition. Tarney (1976) used TiO_2 *vs* SiO_2 to discriminate ortho- and paragneisses of the Lewisian of N.W.Scotland. The boundary between the two types is marked on Figure 3.6a and it can be seen that all of the type-Nûk gneisses plot in the igneous field.

Alumina varies from 14 to 20 wt % with almost all the samples having greater than 15 wt % Al_2O_3 (Figure 3.4a). The tonalitic gneisses have fairly constant Al_2O_3 values, while the trondhjemitic and granodioritic gneisses show a steady decrease with increasing SiO_2. This may be indicative of plagioclase or hornblende fractional crystallization. The trondhjemites are of the high-Al_2O_3 type (following Barker's division of trondhjemites into high- and low-Al_2O_3 types, Barker, 1979).

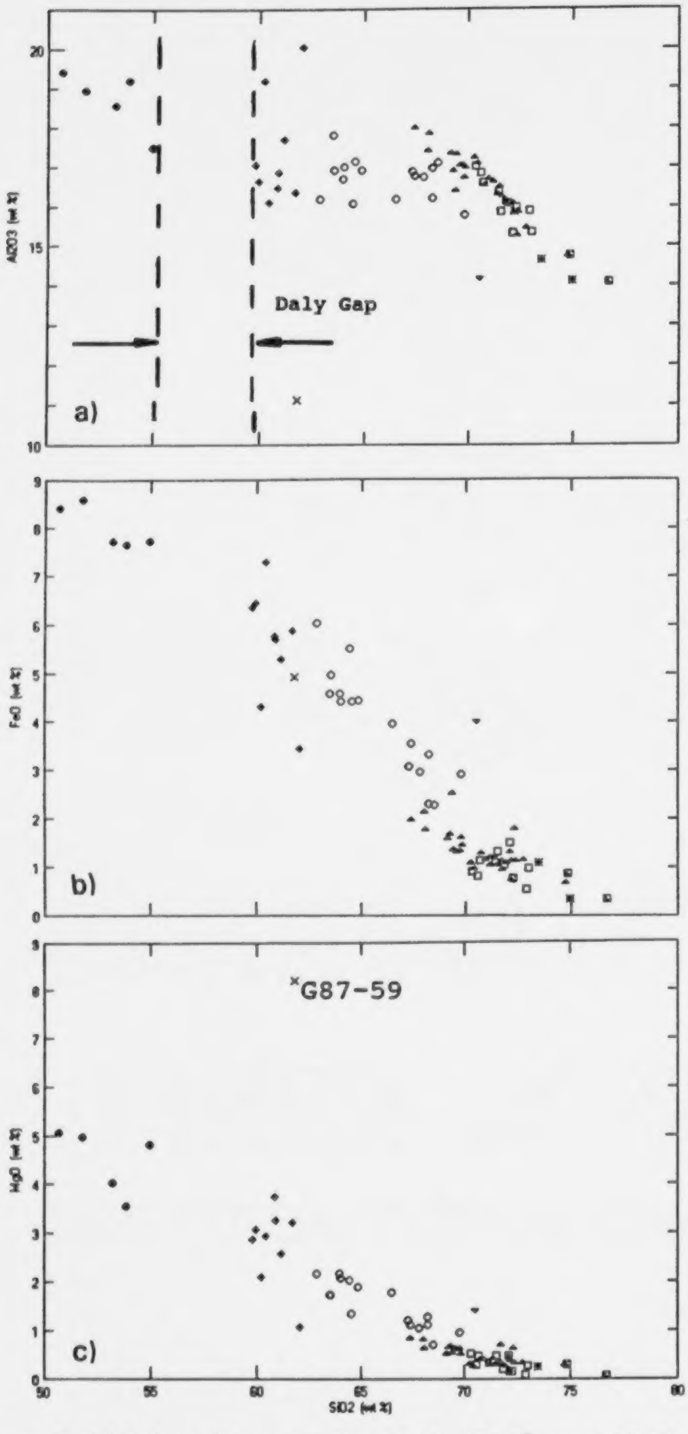

Figure 3.4 Harker diagrams for Al_2O_3, FeO^*, and MgO

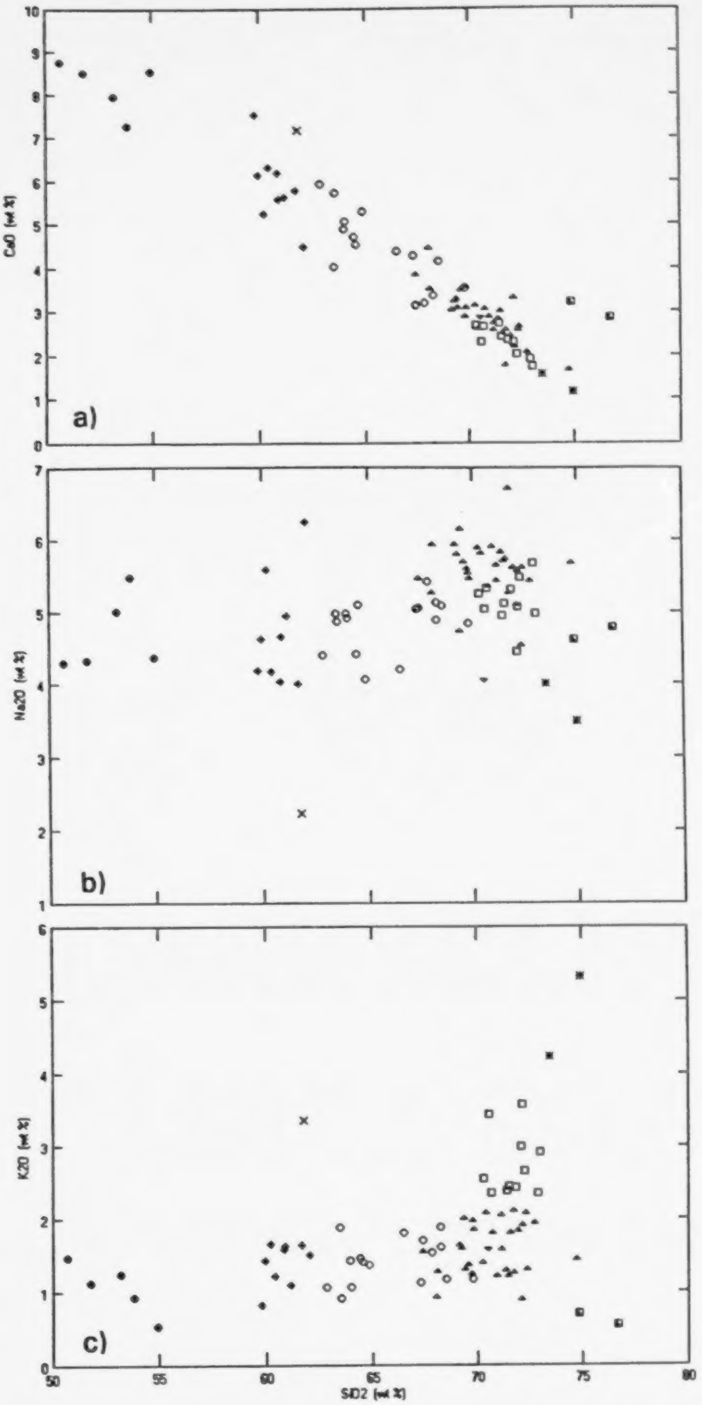

Figure 3.5 Harker diagrams for CaO, Na_2O, and K_2O

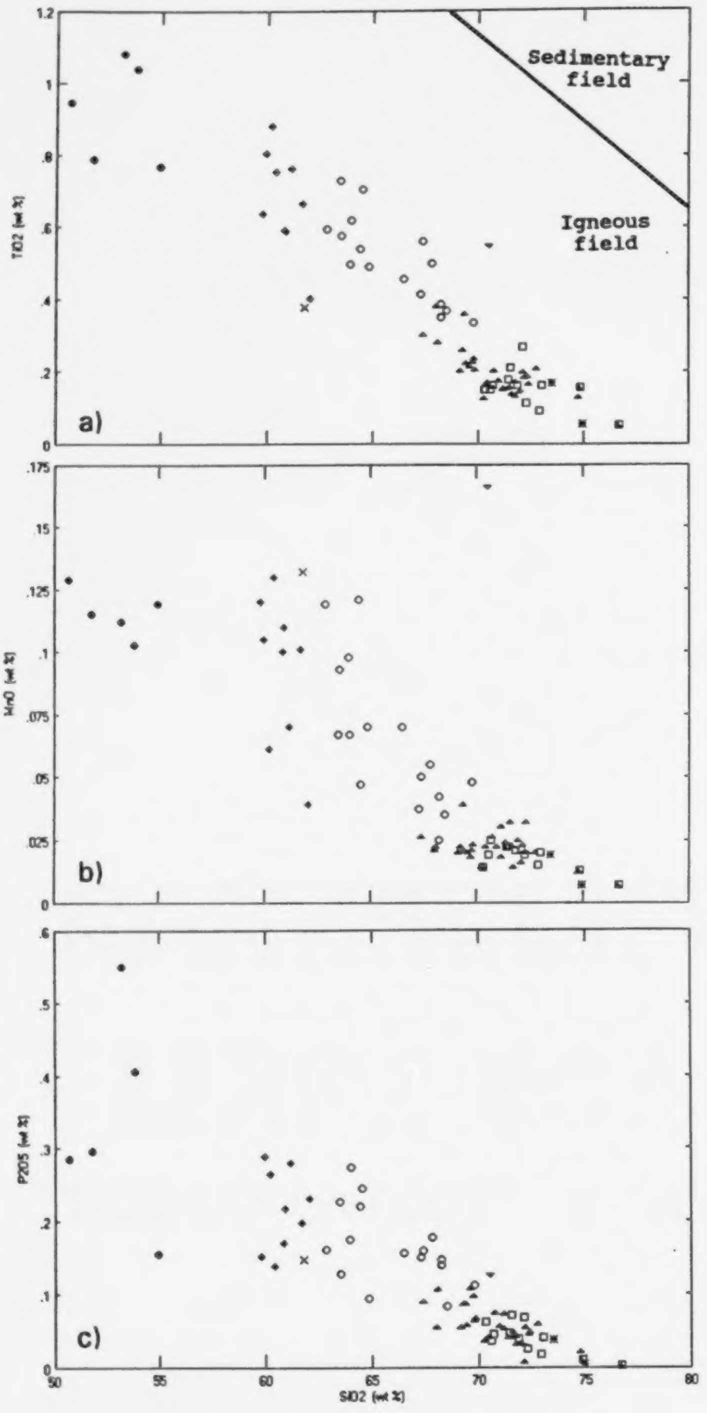

Figure 3.6 Harker diagrams for TiO_2, MnO, P_2O_5

Total iron (as FeO*) displays a steady decline with increasing SiO_2 (Figure 3.4b). The quartz diorites show a wide range (*c.* 3.5 - *c.*7.5%) in total iron for a narrow silica range (*c.* 2.5 wt%). These samples also show a wide scatter in MgO content.

With the exception of sample G87-59, the MgO content of the type-Nûk gneisses mimics that of total iron, decreasing from slightly over 5 wt% to almost 0 wt% for the 51 to 75 wt % silica change (Figure 3.4c).

Again, except for G87-114 and G87-115, the CaO content of the gneisses decreases systematically with increasing SiO_2 content (Figure 3.5a). The two granite sheets plot well above the trend for their particular SiO_2 content.

The Nûk gneiss TTG suite shows the early- to mid-Archaean characteristic enrichment in Na_2O (Glikson, 1979). Without exception analyzed dioritic, tonalitic, and trondhjemitic gneisses contain > 4 wt% Na_2O (Figure 3.5b). As McGregor (1979) also noted, the Na_2O data show a great deal of scatter.

The K_2O *vs* SiO_2 diagram (Figure 3.5c) displays two trends; one is a slight, but steady increase in K_2O with increasing silica content (from dioritic to trondhjemitic compositions) and the second a significant increase in K_2O with SiO_2 content for the granodioritic and granitic gneisses. Sample G87-59 plots by itself not following either of the two trends described. For its SiO_2 content it is strongly elevated in potash. Similarly, the two late 'trondhjemitic' sheets, G87-114 and G87-115, do not follow either of the above trends, and display very low K_2O values for their high silica contents.

Engel *et al.*, (1974) reported that the majority of rocks from Archaean terranes had K_2O/Na_2O ratios < 1, and often < 0.7. Samples from this study show even smaller values. The dioritic, quartz-dioritic, tonalitic, and trondhjemitic gneisses all have K_2O/Na_2O ratios < 0.5, with values as low as 0.17! Even the granodioritic gneisses have values < 0.7 (see Table 3.2).

Except for the extreme elevation of MnO in G87-143 (a mylonite), the trends for the minor oxides MnO and P_2O_5 are not unusual, displaying a negative correlation with increasing SiO_2 (Figures 3.6b and c).

Examination of Figures 3.4 - 3.6 shows that there are a few samples that invariably lie off the main oxide variation trends. In particular, sample G87-59 (represented by a cross), G87-143 (represented by an inverted, open triangle), and samples G87-114 and -115 (represented by half-filled boxes) appear anomalous compared to the other samples and as such need some explanation.

Sample G87-59 has an unusual composition. Compared to other samples of similar SiO_2 content, G87-59 contains approximately two-thirds the Al_2O_3, less than half the Na_2O, double the K_2O, and triple the MgO content. The sample also appears to be elevated in CaO and MnO. The excessive MgO causes the sample to plot far off the calc-alkaline trend on an AFM diagram (Figure 3.7).

Sample G87-143, a mylonite from the Ivinnguit fault which is interpreted as part of the boundary of the Akia and Akulleq terranes, also plots off many of the main oxide trends. This is especially apparent in the plots of SiO_2 *vs.* FeO^*, MgO, Al_2O_3, and MnO (Figures 3.4 and 3.6b).

From stable isotope studies mylonite zones are known to act as conduits for fluids, and consequently can be enriched and/or depleted in a variety of elements. In an attempt to ascertain the original nature of the mylonite, a TiO_2 *vs.* MgO plot of all the type-Nûk gneisses was generated (with the exception of G87-59) and is shown in Figure 3.8. These two elements were chosen because of their generally immobile character, at least to amphibolite facies conditions (Garde *et al.*, 1986; Nutman and Bridgwater, 1986). From Figure 3.8 a fairly linear trend of increasing TiO_2 with increasing MgO is apparent. This trend flattens somewhat above *c.* 2.5 wt % MgO.

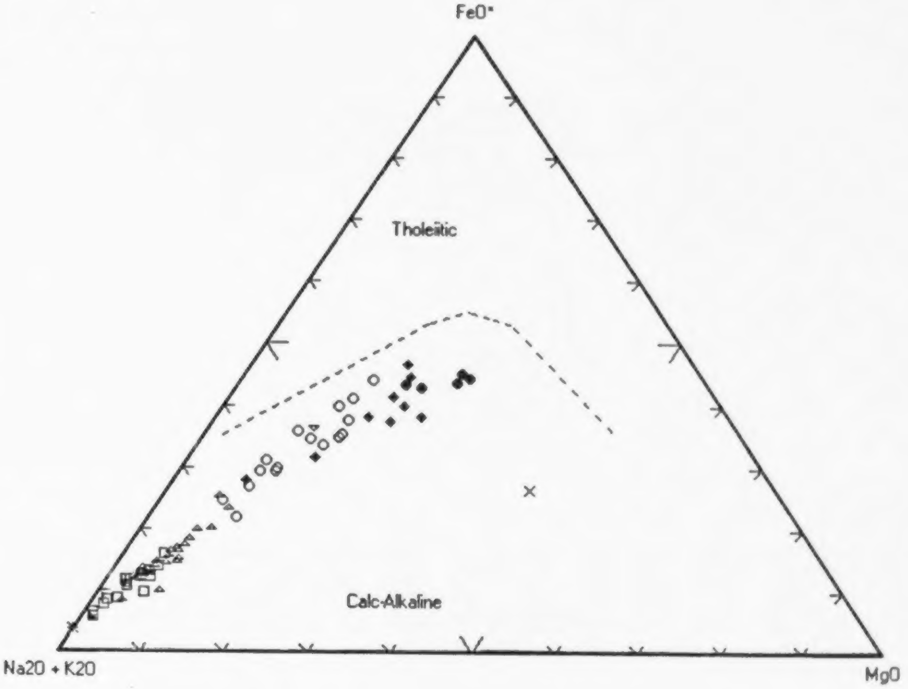

Figure 3.7 AFM diagram of the type-Nûk gneisses (after Irvine and Baragar, 1971).

Of particular note are the well defined fields for the dioritic, quartz dioritic, and tonalitic gneisses. It can be seen that sample G87-143 falls well within the tonalitic gneiss field. This suggests that prior to mylonitization the mylonite precursors at this location were possibly tonalitic in composition. If this was the case, then on the basis of the TiO_2, MgO, and FeO^* Harker diagrams the mylonite has gained *c.* 4 to 5 % SiO_2. Furthermore, on the basis of other Harker diagrams it can be concluded that G87-143 has experienced a loss of *c.* 2 wt % Al_2O_3, *c.* 1.5 wt% CaO, and *c.* 0.5 wt % Na_2O, apparently little or no net gain or loss in K_2O or P_2O_5, and a doubling of the MnO content. Except for the MnO variation, the major element changes would be consistent with the formation of a more sodic plagioclase at the expense of more calcic plagioclase feldspar. On the basis of field relations it is possible that sample G87-143 represents mylonitized Amîtsoq gneiss material and is not derived from type-Nûk gneiss material. This is further discussed under the 'Trace Element Chemistry' section.

The trondhjemitic sheets, G87-114 and -115, are unlike other analyzed trondhjemitic gneisses from the Akia terrane in that they are significantly depleted in K_2O, have reduced Na_2O contents, and are enriched in CaO. Again a mineralogical control is indicated. The CaO composition of the trondhjemitic sheets is explained by the presence of a more calcic plagioclase feldspar than occurs in the other trondhjemites.

Finally, sample G87-152, ostensibly a dioritic gneiss, has a low K content in comparison to the other dioritic gneisses. The whole-rock composition of this sample is very similar to the average of 39 granulite-grade, pyroxene gneisses from the Lewisian of the Drumbeg area of Assynt, N.W. Scotland (Sheraton *et al.*, 1973). Under the 'Trace element chemistry' section of this chapter further evidence is presented that suggests that sample G87-152 may have experienced granulite grade metamorphism. The sample was collected from the northwestern tip of Sadelø fairly close to the granulites of Nordlandet.

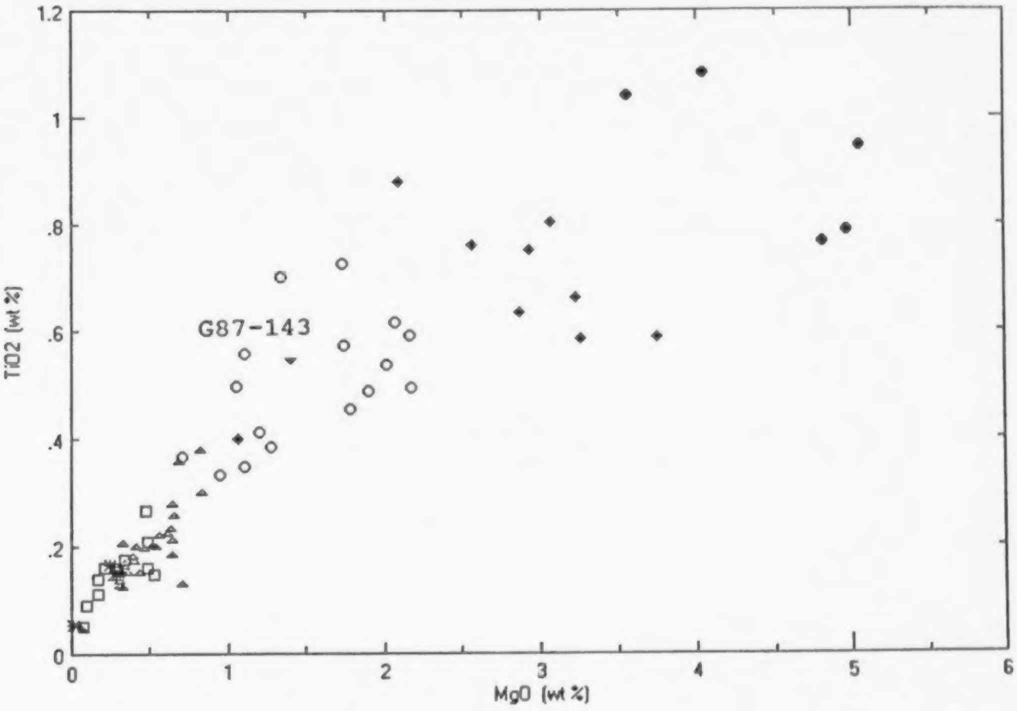

Figure 3.8 MgO *vs* TiO_2 for the type-Nûk gneisses

On an AFM diagram (Irvine and Baragar, 1971) the type-Nûk gneisses fall in the calc-alkaline field (Figure 3.7) and display a trondhjemitic trend (Arth *et al.*, 1978). Compared to modern calc-alkaline trends, the type-Nûk gneisses show extreme enrichment in Na_2O. Compositional variation of the type-Nûk gneisses, together with trends for recognized calc-alkaline (*e.g.*, Southern California Batholith) and trondhjemitic suites (Arth, *et al.*, 1978) are plotted on a Na-K-Ca ternary diagram in Figure 3.9. With their late enrichment in K_2O, the type-Nûk gneisses more closely resemble a calc-alkaline trend *vs.* the gabbro-trondhjemite trend from SW Finland (Arth *et al.*, 1978).

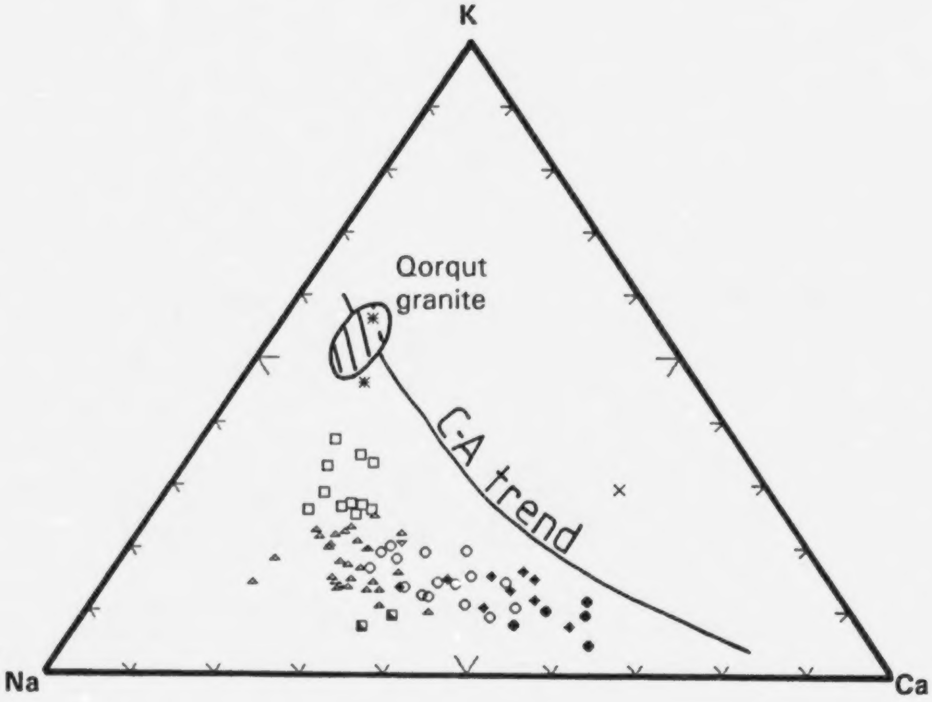

Figure 3.9 Na-K-Ca ternary diagram for the type-Nûk gneisses.

The major difference between the modern calc-alkaline trend and that displayed by the type-Nûk gneisses is the shift of the gneiss data towards the Na apex of the ternary diagram brought about by the higher Na/K ratios of most Archaean granitoids. The pattern displayed by the type-Nûk gneisses is very similar to that shown by the early Archaean Uivak gneisses of Labrador (Collerson and Bridgwater, 1979) and the Amîtsoq banded grey gneisses (Nutman *et al.*, 1984).

The meta-igneous nature of the type-Nûk gneisses is indicated using Shand's Index (Figure 3.10).

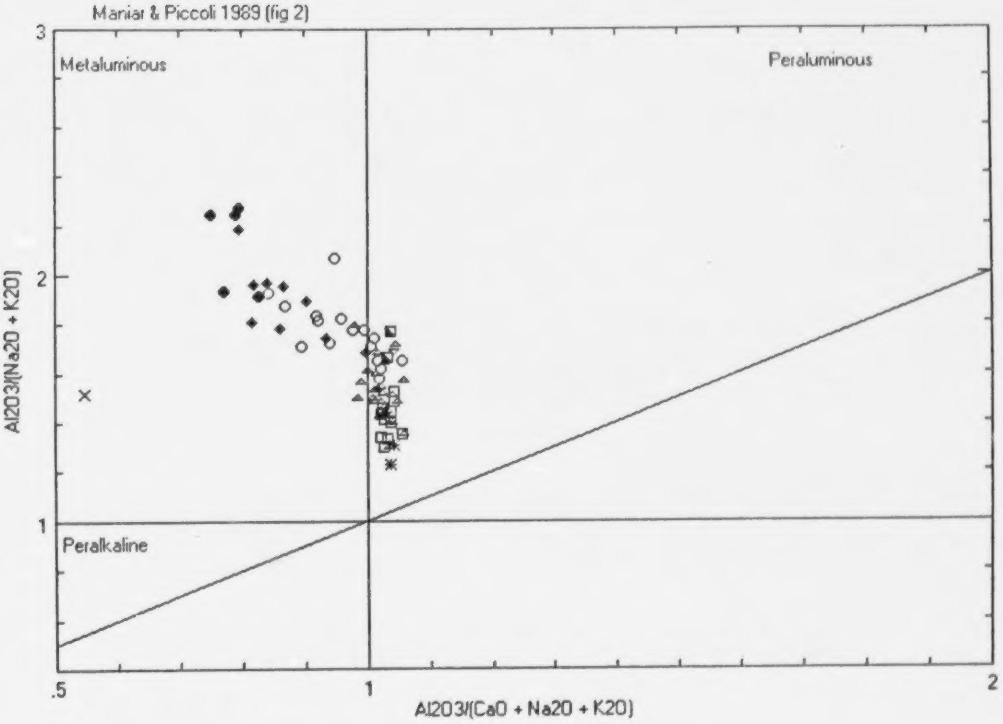

Figure 3.10 Shand's Index for the type-Nûk gneisses

All of the type-Nûk gneisses of dioritic and quartz-dioritic composition are metaluminous in character (hence diopside normative), while all the granodioritic gneisses are weakly peraluminous in nature (hence corundum normative). The tonalitic gneisses are divided almost equally between the two divisions; and approximately 90% of the trondhjemitic gneisses are weakly peraluminous with the few metaluminous samples falling close to the boundary of the two groups. The particular trend displayed by the type-Nûk gneiss, from metaluminous to peraluminous rocks, is indicative of hornblende fractionation (Zen, 1986). The fairly constant A/CNK ratio thereafter suggests that plagioclase may be the dominant fractionating phase.

Summary of Major Element Data

A summary of the mean, standard deviation, and range for each of the major and minor oxides of the type-Nûk gneisses are given in Table 3.2 by rock-type. The salient major and minor oxide variations *vs.* silica (by rock-type) are represented graphically in Figure 3.11. The major element Harker variation diagrams generally display the expected elemental trends associated with igneous differentiation-fractionation processes, however, the data show a fair degree of scatter. This scatter would be expected if the igneous precursors of the type-Nûk gneisses were not cogenetic, but were derived from widely differing source materials, for example. Alternatively, the scatter could have been caused by metamorphic differentiation (*e.g.*, Olsen, 1983) produced during the formation of the intensely deformed gneisses (Myers, 1978), or a combination of the two effects.

The presence of the 'Daly gap' argues against an origin of the tonalitic and trondhjemitic gneiss protoliths by fractional crystallization of dioritic melts.

The variation in the alumina saturation index (A/CNK) and A/NK suggests that hornblende fractionation played an important role in the

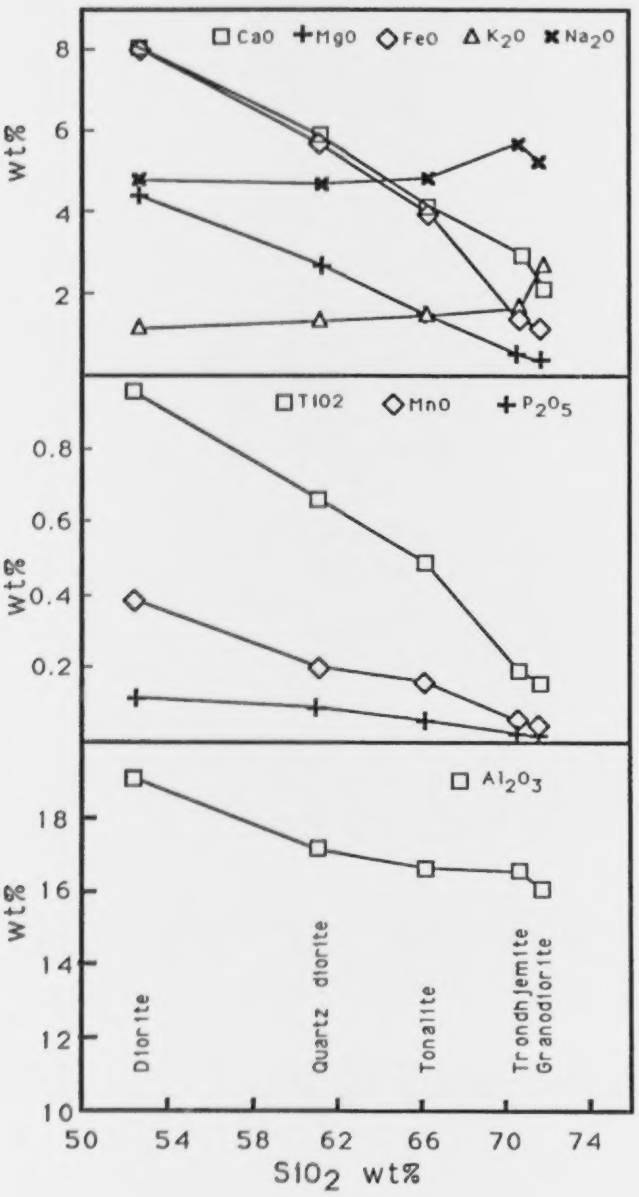

Figure 3.11 Mean major and minor element Harker diagrams by rock-type.

Table 3.2 Average major and minor oxide composition of the type-Nûk gneisses by rock-type.

	SiO_2	Al_2O_3	TiO_2	FeO*	MnO	CaO	MgO	K_2O	Na_2O	P_2O_5	Mg#	K_2O /Na_2O
Granodioritic gneisses (n = 10)												
Mean	71.6	16.1	0.163	1.01	0.020	2.32	0.34	2.65	5.16	0.046	0.36	0.518
1σ	0.9	0.5	0.046	0.26	0.003	0.31	0.14	0.34	0.32	0.017	0.08	0.090
Max	73.0	17.0	0.267	1.51	0.025	2.73	0.53	3.43	5.67	0.071	0.51	0.680
Min	70.3	15.3	0.091	0.56	0.014	1.76	0.10	2.35	4.45	0.018	0.24	0.414
Trondhjemitic gneisses (n = 29)												
Mean	70.7	16.6	0.200	1.36	0.022	2.90	0.48	1.59	5.60	0.058	0.39	0.286
1σ	1.6	0.7	0.064	0.39	0.006	0.58	0.17	0.36	0.40	0.024	0.05	0.077
Max	74.7	18.0	0.380	2.53	0.039	4.45	0.83	2.11	6.70	0.108	0.57	0.458
Min	67.4	14.8	0.125	0.68	0.012	1.68	0.26	0.89	4.54	0.007	0.31	0.174
Tonalitic gneisses (n = 15)												
Mean	66.2	16.7	0.500	3.82	0.062	4.24	1.48	1.44	4.87	0.166	0.41	0.297
1σ	2.1	0.5	0.117	0.95	0.025	0.78	0.45	0.30	0.35	0.053	0.04	0.067
Max	69.8	17.8	0.725	5.51	0.121	5.73	2.17	1.89	5.43	0.274	0.46	0.430
Min	63.5	15.8	0.334	2.29	0.025	3.13	0.70	0.91	4.07	0.083	0.35	0.187
Quartz dioritic gneisses (n = 10)												
Mean	61.0	17.2	0.664	5.65	0.096	5.87	2.70	1.36	4.69	0.210	0.46	0.294
1σ	0.9	1.3	0.130	1.04	0.028	0.74	0.72	0.28	0.69	0.052	0.05	0.068
Max	62.8	20.0	0.877	7.29	0.130	7.51	3.75	1.66	6.23	0.289	0.54	0.410
Min	59.8	16.1	0.401	3.43	0.039	4.48	1.07	0.82	4.00	0.138	0.36	0.196
Gabbroic/Dioritic gneisses (n = 4)												
Mean	52.4	19.0	0.962	8.10	0.115	8.12	4.40	1.19	4.78	0.385	0.49	0.255
1σ	0.6	0.3	0.112	0.41	0.009	0.57	0.63	0.20	0.49	0.106	0.01	0.061
Max	51.8	19.4	1.080	8.59	0.129	8.75	5.05	1.47	5.48	0.550	0.52	0.342
Min	50.7	18.6	0.787	7.65	0.103	7.26	3.55	0.93	4.30	0.286	0.46	0.170

evolution of the less silica-rich samples, while plagioclase would appear to have exerted a more significant control in the trondhjemitic and granodioritic gneiss protoliths.

3.2.2.2 Trace Element Chemistry

Trace element data for the samples studied, as determined by X-ray fluorescence (XRF), instrumental neutron activation analysis (INAA), and mass spectrometry isotope dilution (MSID) are listed in Appendix 4. Variation diagrams of selected trace elements *vs.* silica are displayed in Figures 3.12 to 3.16.

The transitional metals, especially Zn, V, Co and Sc, show good negative correlations with increasing silica content as expected of the compatible elements. The Ni and Cr data show more scatter than do Zn, V, Co and Sc. However, the negative inverse relationship with silica is still readily apparent. The rather uniform minimum concentration of Ni (*ca.* 8 ppm) determined for many of the samples in the 65 - 78% silica range is believed to be due to Ni impurities in the Rh X-ray tube used for excitation in the XRF analyses (see Appendix 2).

There is generally a large degree of scatter in the silica *vs.* large ion lithophile (LILE) data (*e.g.*, Rb, Ba, Sr, Cs, U, Th, and REE) and the high field strength elements (HFSE) (*e.g.*, Zr, Hf, Ta and Nb). Plotting the trace element data against MgO or TiO_2 as opposed to SiO_2 makes no obvious difference to the scatter on the LILE plots. One might expect that the HFSE would show less scatter and an improvement in correlation when plotted against TiO_2, another HFSE that is considered relatively immobile. However, any improvement in correlation is insignificant. This lack of correlation argues against a possible cogenetic origin for the type-Nûk gneisses.

Even within a particular gneissic composition-type the scatter of many trace elements is often significant, for example: the Cr content of the quartz-dioritic gneisses, the Th content of the gneisses of tonalitic and

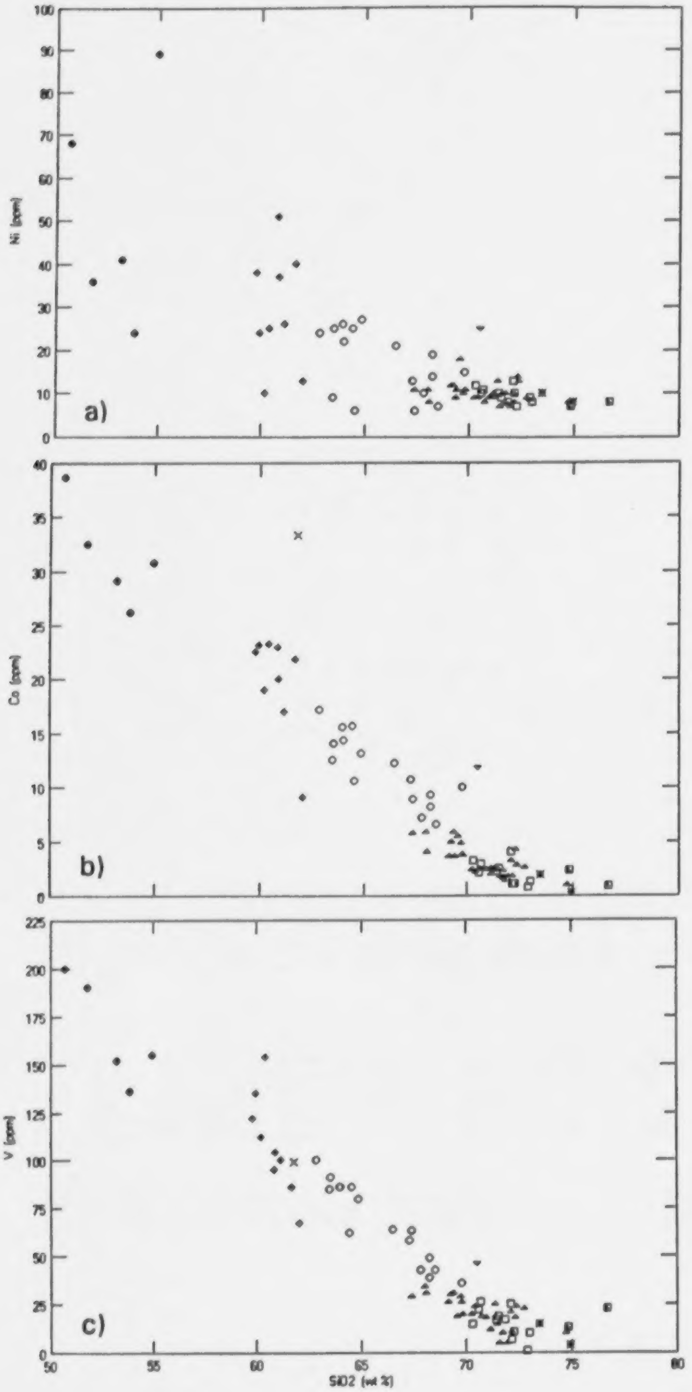

Figure 3.12 Harker diagrams of Ni, Co and V.

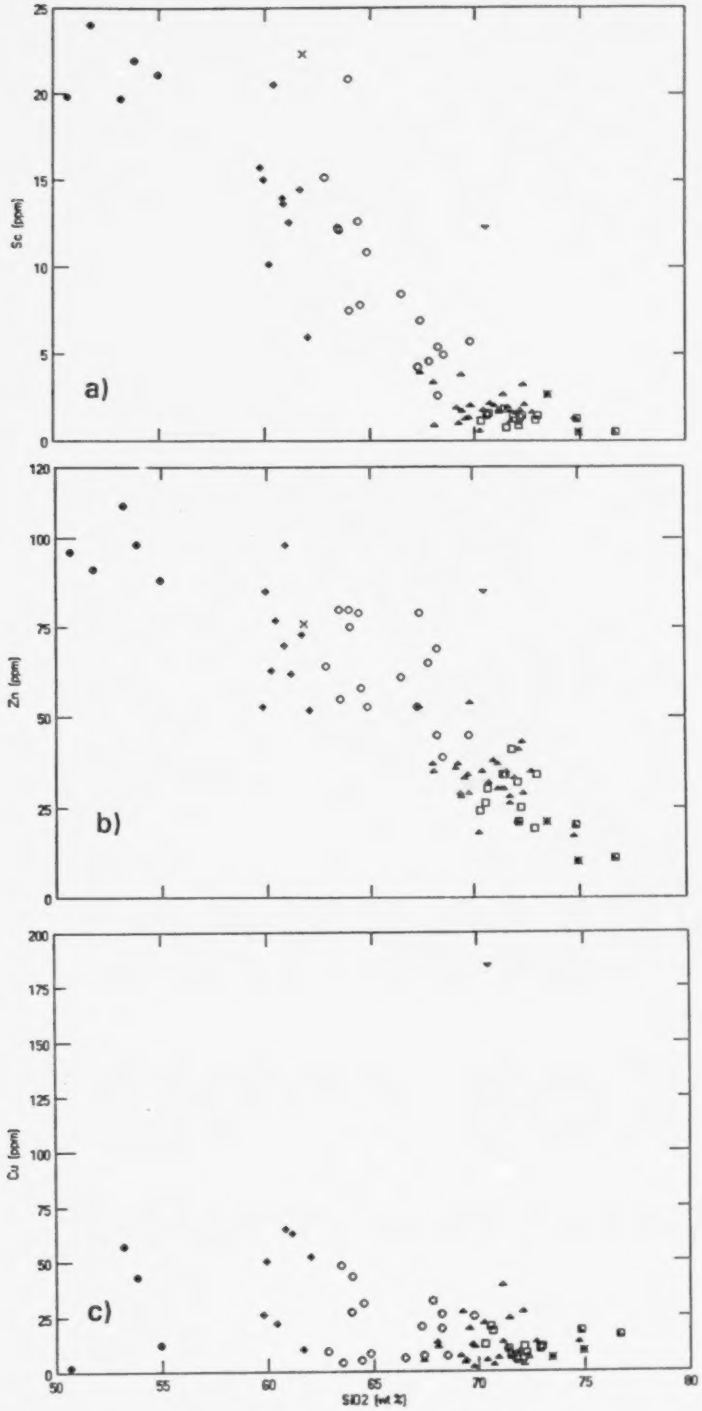

Figure 3.13 Harker diagrams of Sc, Zn and Cu.

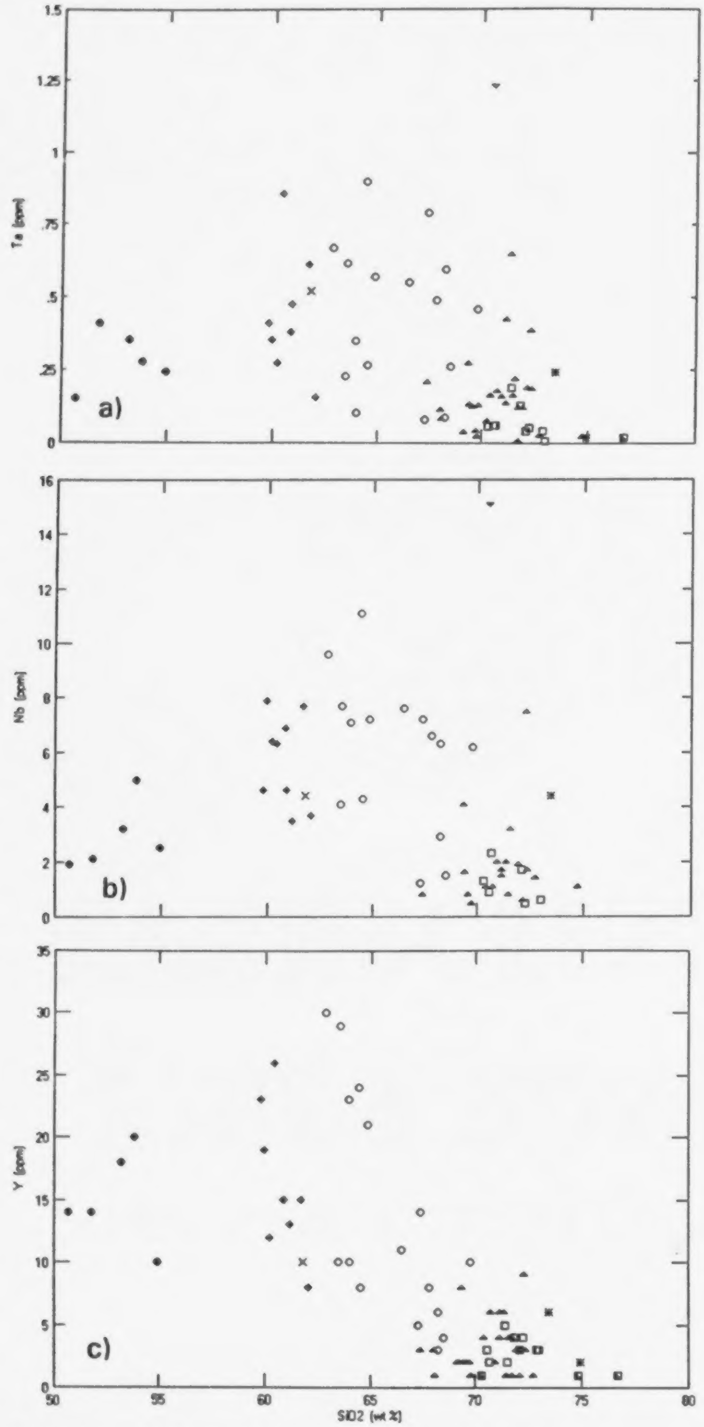

Figure 3.14 Harker diagrams of Ta, Nb and Y.

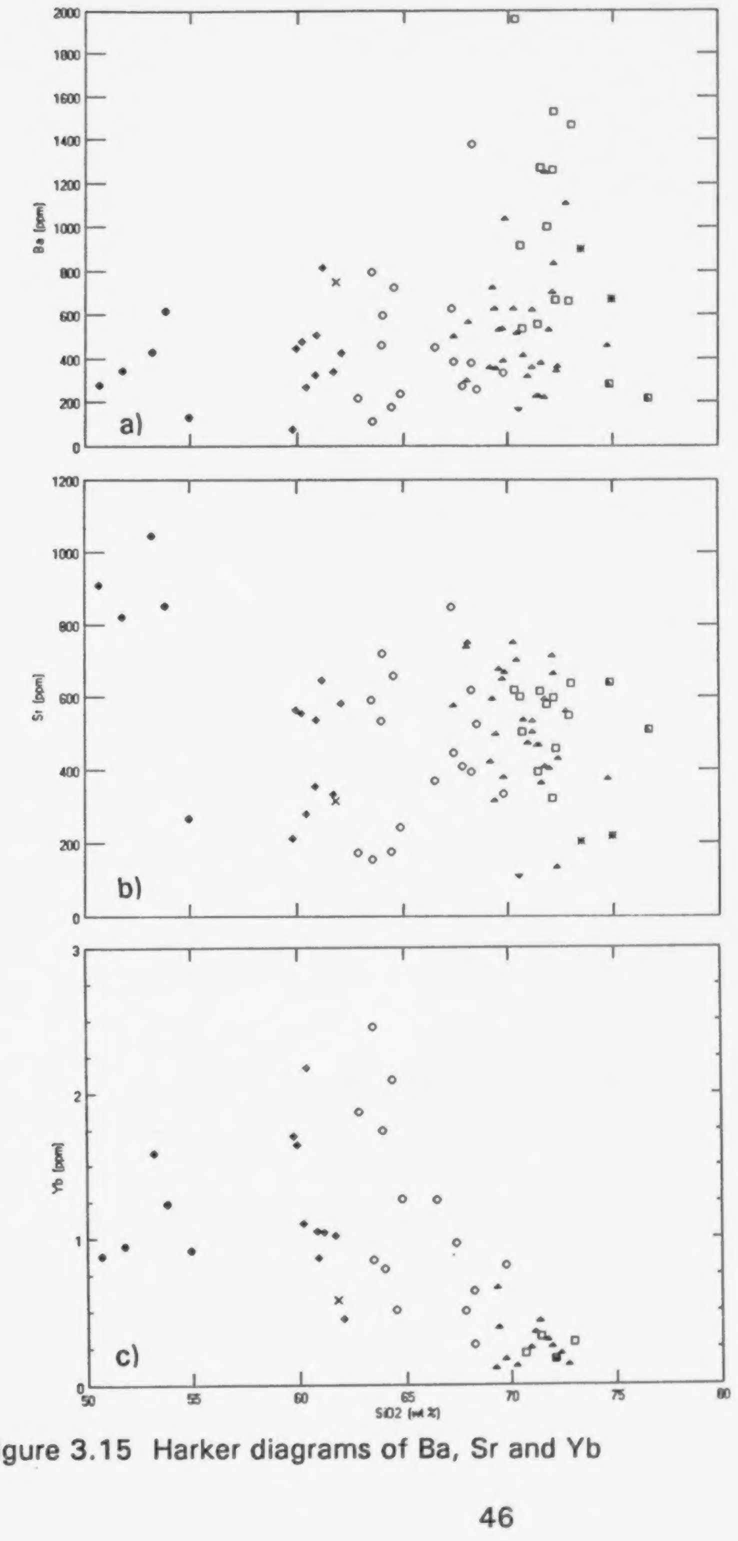

Figure 3.15 Harker diagrams of Ba, Sr and Yb

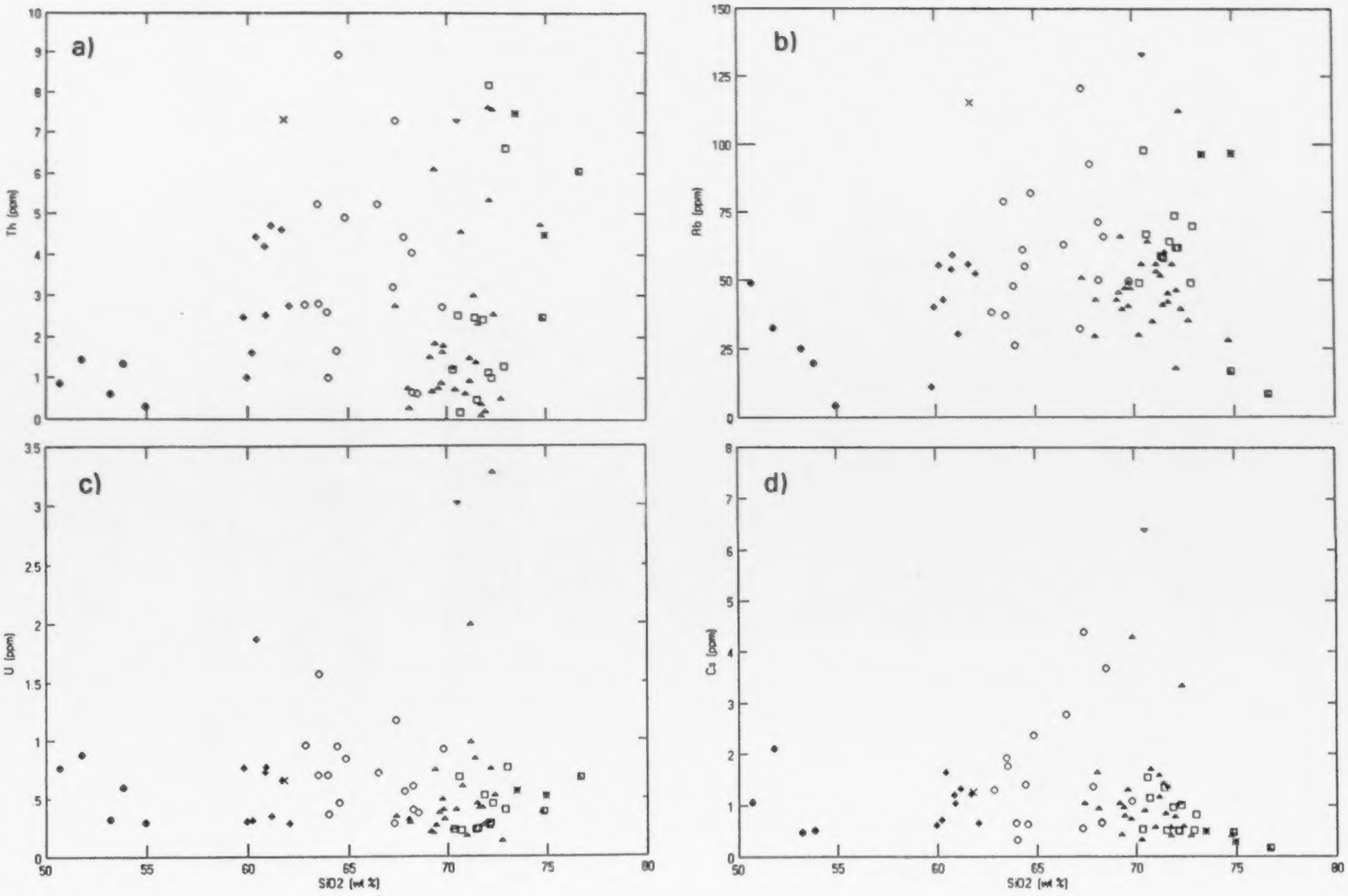

Figure 3.16 Type-Nûk gneiss Th, U, Rb and Cs Harker diagrams.

trondhjemitic composition, the Y content of the quartz-dioritic and tonalitic gneisses, and the Ba and Sr content of each compositional group. This again suggests that in many instances even gneisses of similar major element composition are not likely cogenetic.

As with the major oxides, sample G87-143 displays anomalous concentrations of many trace elements in comparison to other Nûk gneisses. In comparison to equivalent type-Nûk gneisses it contains about double the concentration of the HFS elements Zr, Hf, Nb and Ta; has an extremely elevated Y level (53 ppm) and a high Th (9.3 ppm) concentration. Given: a) the renowned immobile nature of the HFSE, b) the field relations of the sample location, and c) the fact that the augen-gneiss sub-unit of the Amîtsoq gneisses have very high levels of Zr (and presumably Hf also) Nb, and Y (Lambert and Holland, (1976); McGregor, 1979), it is considered likely that sample G87-143 is in fact a mylonitized Amîtsoq gneiss. However, not all the major element features of G87-143 are similar to the augen gneiss group. A number of the LIL elements *e.g.*, U, Th, Cs, Pb and Rb, are also elevated in G87-143.

Under the major element geochemistry section it was noted that sample G87-152 has a low K content. In addition, the sample displays low Rb, Th, U, and Cs values in comparison to the other dioritic gneisses. The resultant high K/Rb (1120), K/U (15460), and K/Th (14460) ratios are considered hallmarks of depleted granulites (see Rudnick *et al.*, 1985; Rudnick and Presper, 1990; and Chapter 4). These ratios are significantly greater than those found in any of the other type-Nûk gneisses, or the average upper continental crust (Taylor and McLennan, 1985). The low Rb/Sr ratio (0.015) of G87-152 even falls below that proposed for the average lower continental crust (0.023). Considering also the major element data, it appears most likely that this rock may have undergone depletion of the LILE during a granulite-facies metamorphic event.

The type-Nûk gneisses contain very low levels of uranium. In all cases U < 3.3 ppm. With the exception of two samples (one being the mylonite sample (G87-143) and the other G87-142 which came from < 20 m distance from G87-143) no sample contains more than 2 ppm U, and slightly over 90% of the samples contain < 1 ppm U. Thorium varies between *c.* 0.1 and 8.9 ppm. A wide range of Th/U ratios are found (Figure 3.17) varying between about 0.25 and 33. From Figure 3.18 it can be seen that the majority of the samples deviate significantly from the average crustal Th/U ratio of *c.* 3.8 (Taylor and McLennan, 1985).

K/U ratios for the gneisses vary from *c.* 4500 to 30,000 with a mean value of approximately 23,000 that is over twice the generally accepted crustal value of 10,000. K/Th ratios show a similar range to K/U ratios, *i.e.*, 4500 to 30,000, with a mean value of about 5000 which is significantly greater than either the upper or lower crust estimates (*ca.* 2600, Taylor and McLennan, 1985). To ascertain whether the gneisses have experienced loss or gain of K, Th, and/or U (or a combination thereof) sample data have been plotted on a Th/U *vs* La/Th diagram (after Rudnick *et al.*, 1985) in Figure 3.18. Because most of the gneisses contain < 2 ppm U, the fact that a number of samples plot to the right of the typical field for igneous rocks and have Th/U ratios < 3, suggests that for these samples Th loss has occurred. This would also result in elevated K/Th ratios. Those samples that plot above the igneous field have undergone an increase in Th/U ratio as a result of either a loss in U and/or gain in Th. The fact that the samples are not shifted to significantly lower La/Th ratios suggests that Th gain has not been significant and that U loss is largely responsible for the elevated Th/U ratios (as supported by the elevated Th/U ratios). The above assumes that the gneiss protoliths had Th/U ratios typical of igneous rocks. As all the samples have elevated K/Th ratios (over typical crustal values), it would seem likely that those samples with Th/U ratios greater than 3.8 must also have undergone an increase in K. The lower than average U, Th, and K values for

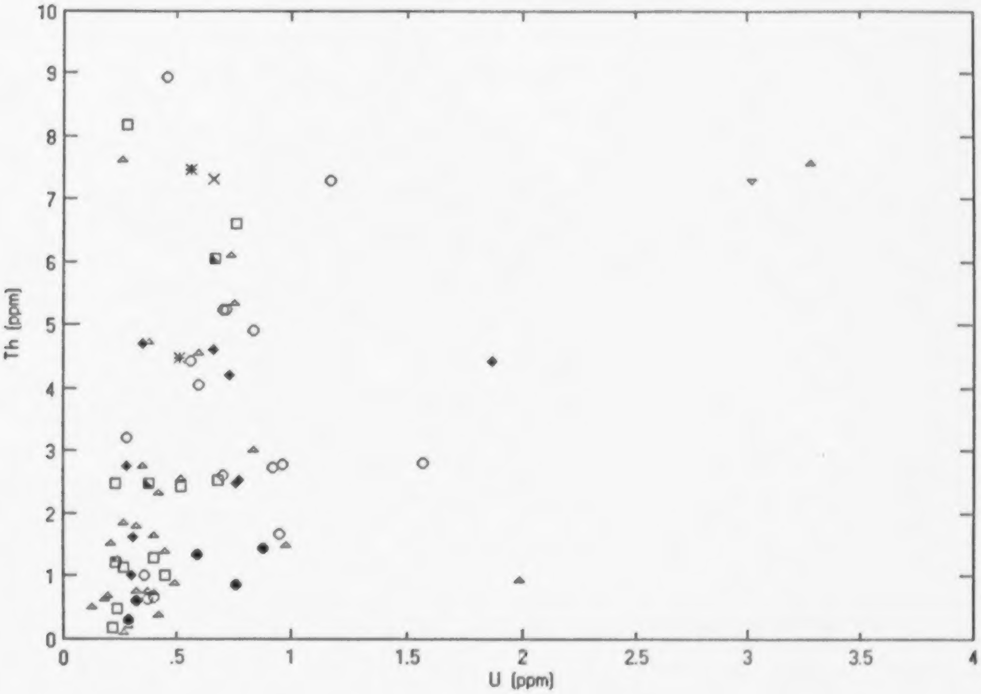

Figure 3.17 Uranium *vs* thorium for the type-Nûk gneisses

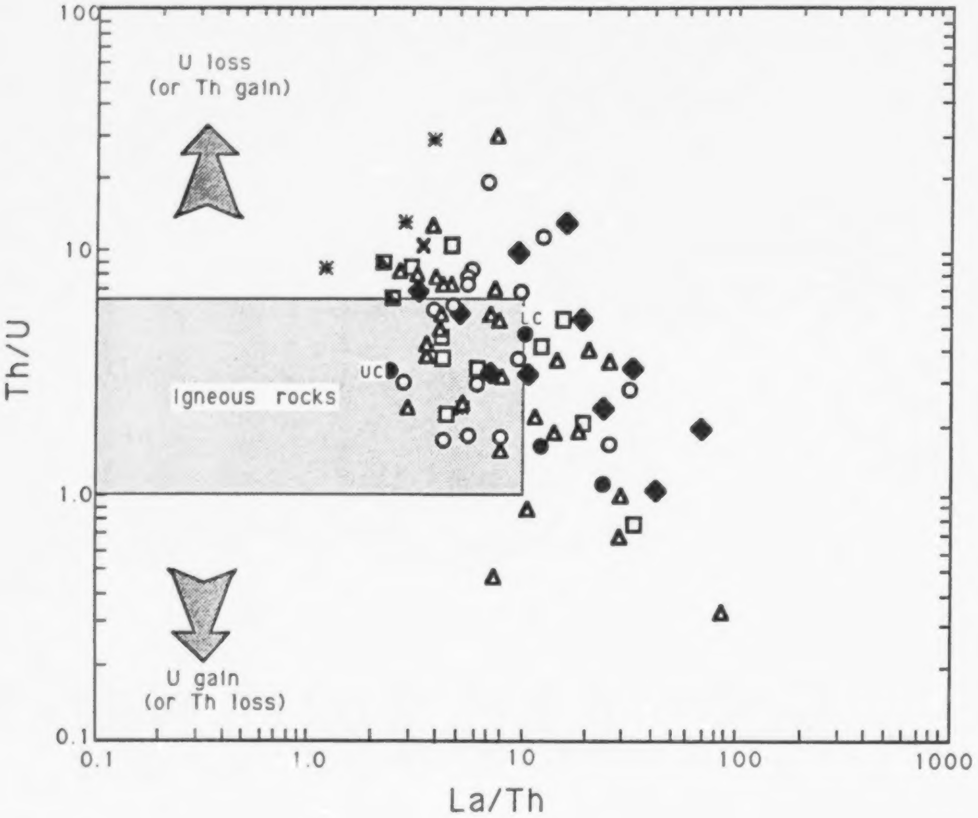

Figure 3.18 Th/U *vs* La/Th for the type-Nûk gneisses

(UC - upper crust, LC - lower crust, Taylor and McLennan, 1985) the type-Nûk gneisses results in a heat production that is about a quarter of that for average upper continental crust at present (Table 3.3).

Ahrens (1954) noted that in most instances the major, minor, and in particular trace elements of samples taken from the same population display a log-normal distribution. Consequently, log transformation of the U, Th, and K data was performed and the median value for each element calculated for comparison with the arithmetic mean of each element. The results of this exercise are listed in Table 3.3.

As expected the K_2O, Th, and U median values are less than the corresponding arithmetic means for the individual elements. This is a consequence of the data being positively skewed. That the type-Nûk gneisses are depleted in the heat producing elements in comparison to average upper crustal values is readily apparent. This is a fairly ubiquitous feature of Archaean grey gneisses of the North Atlantic Craton (Bowes, 1972). It is interesting that the median Th/U ratio agrees so well with the average crustal Th/U ratio. Elevated K/Th and K/U ratios are characteristic of many granulite-facies rocks. However, if the type-Nûk gneisses had undergone granulite-facies metamorphism one would also expect the gneisses to display elevated K/Rb ratios. The average K/Rb ratio for the type-Nûk gneisses is 294 (range: 117 - 619) *vs* the average upper crustal value of *ca.* 250 (Figure 3.19). Although slightly elevated, this mean value does not suggest that the gneisses underwent granulite-facies metamorphism. However, on a K *vs* Rb plot the data more closely resemble the Archaean granulite-trend (Jahn and Zhang, 1984) *vs* the 'main trend' (Shaw, 1968).

The gneisses have a mean Rb/Sr ratio of 0.127 (range: 0.025 to 0.82, excluding G87-152 [0.015]) *vs.* 0.32 for the upper crustal and 0.023 for lower crust. This ratio suggests some depletion in Rb compared to average continental crust. The values for the tonalitic, trondhjemitic and granodioritic type-Nûk gneisses fall within the typical range for rocks of these compositions (Peterman, 1979).

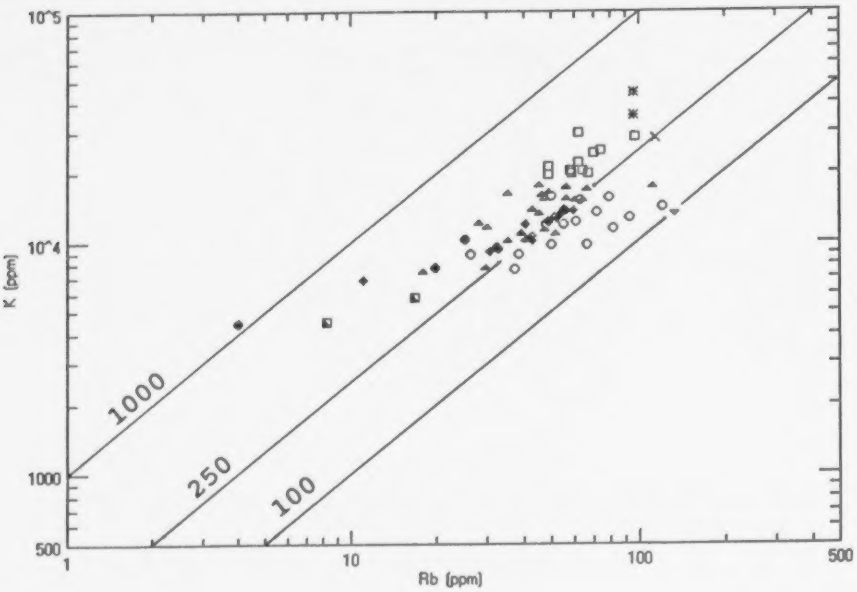

Figure 3.19 Rb *vs* K for the type-Nûk gneisses

Table 3.3. Comparison of the mean and median values of the major heat producing elements of the type-Nûk gneisses with average crustal values.

	Arithmetic mean	Median	Average upper crust	Average lower crust
K_2O (%)	1.65	1.54	3.37	0.34
Th (ppm)	2.78	1.82	10.7	1.06
U (ppm)	0.59	0.48	2.8	0.28
Th/U	4.7	3.8	3.8	3.8
K/Th	4930	7020	2620	2640
K/U	23200	26600	10000	10000
μW m^{-3}	0.49	0.38	1.80	0.19

(average upper and lower crustal values from Taylor and McLennan, 1985; heat production present day assuming rock ρ = 2.8 gcm^{-3}).

Compared to the Ikkattoq gneisses, the type-Nûk gneisses generally have much smaller Rb/Sr, largely reflecting the dominance of gneisses of granodioritic composition in the former, and tonalitic and trondhjemitic in the latter.

The gneisses have a mean Ba/Rb ratio of 13.2 (range: 2.9 to 40.2) *vs.* 4.9 of average upper continental crust, and 28.3 for the lower crust, again slightly elevated over average continental crust, but not as depleted as postulated average lower continental crust.

The mean Zr/Hf ratio *ca.* 36 is close to the crustal mean of *c.* 33 (Taylor and McLennan, 1985).

The dioritic, quartz dioritic, and most of the tonalitic gneisses show an increase in Nb with increasing silica while the trondhjemitic and granodioritic gneisses are depleted. Normalized 'spidergrams' (Appendix 6) demonstrate that compared to primitive mantle or MORB the type-Nûk gneisses show depletions in Nb, Ta, and Ti. This raises questions as to the role phases such as rutile, ilmenite, *etc.* play as sinks for many of the HFSE during partial melting for example (Tatsumi *et al.*, 1986; Ryerson and Watson, 1987).

Rare Earth Elements.

A distinctive geochemical feature of many Archaean granitoid gneisses is their depletion in the heavy rare earth elements (HREE) compared to post-Archaean granitoids (*e.g.*, Glikson, 1979; Jahn *et al.*, 1981; Pride and Muecke, 1980, *etc.*). Coupled with this depletion is the significant increase in the (La_N/Yb_N) ratio of Archaean gneisses. That is the chondrite normalized ratio of La to Yb. Following Jahn *et al.*, 1981, Martin (1986) using a large data set (over 600 samples), showed that when plotted in (La_N/Yb_N) *vs* Yb_N space, Archaean and post-Archaean granitoids formed two fields with only minor overlap. It was concluded that the elevated (La_N/Yb_N) ratio and low Yb content of the Archaean granitoids indicated that garnet and/or hornblende played a major role in the genesis of these Archaean rocks (as previously suggested by O'Nions and Pankhurst, 1978, for example).

The (La_N/Yb_N) *vs* Yb_N data for the type-Nûk gneisses (by rock-type) are plotted in Figure 3.20 together with the fields for Archaean and post-Archaean granitoids. It can be seen that TTG Nûk gneisses are typical Archaean grey gneisses in this regard. A large number of the gneisses have (La_N/Yb_N) ratios >20, reaching over 100 for some of the trondhjemitic gneisses. It is important to note that this diagram does not give a full picture of the HREE depletion/ LREE fractionation of many of the gneisses. A number of samples (predominantly tonalitic and granodioritic in composition) are not plotted on the diagram because the Yb concentration of these samples was below the detection limit of the INAA scheme. This implies that the concentration of Yb is low and the (La_N/Yb_N) ratio correspondingly high. The dioritic gneisses do not show the extreme REE fractionation

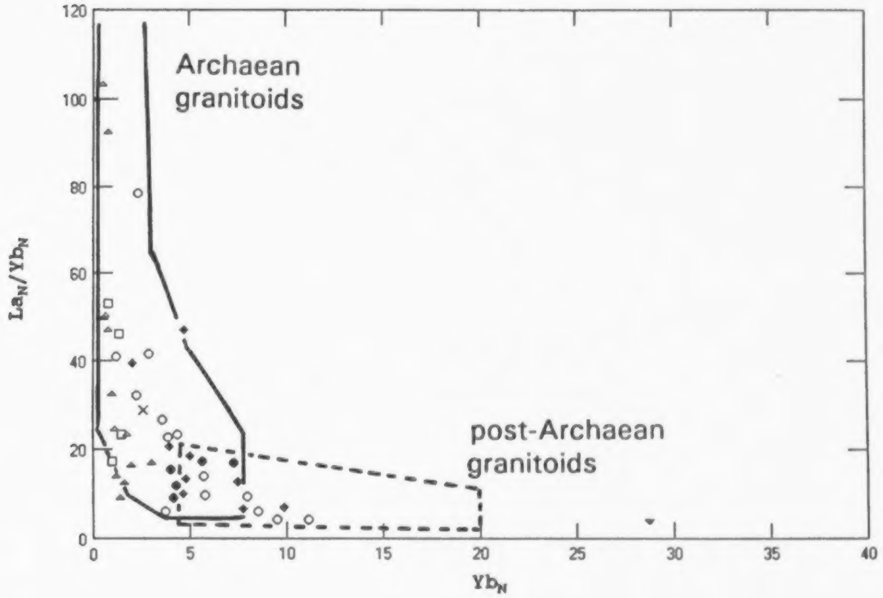

Figure 3.20 Yb_N *vs* La_N/Yb_N for the type-Nûk gneisses.

displayed by the granodioritic, trondhjemitic and some of the tonalitic gneisses, whilethose of quartz-diorite composition largely overlap the tonalites. The implied HREE depletion with increasing silica content is supported by the inverse relationship shown by Y with increasing SiO_2 (Figure 3.14c). Using Y as an indicator of the HREE additional plots of Y *vs* TiO_2, MnO, and CaO for the quartz-dioritic, tonalitic, trondhjemitic and granodioritic gneisses (Figure 3.21) show a positive correlation, but with non-zero intercepts (*c*. 0.1% for TiO_2 and *c*. 2 % for CaO). According to Tarney *et al*., (1979) the Y - Ti relationship suggests that two mineral phases, possibly garnet, and ilmenite (or rutile), removed Y (and the HREE) and Ti, respectively during fractionation of the protolith magmas (or were residual phases during partial melting of a basaltic source). Alternatively, fractionation of hornblende could be responsible for the observed pattern especially given the strong corr-elation between Y and MnO (excluding the dioritic gneisses and G87-59). The negative relationship displayed by Y with SiO_2 also suggests that hornblende dominated the fractionation process (Frey *et al*., 1978). Essentially identical patterns are observed with Yb in place of Y.

Some of the tonalites show extremely elevated (La_N/Yb_N) ratios, while others display fairly low values (Figure 3.20). This indicates that there is a play between the influence of potential residual mineral phases, such as garnet and hornblende, on the REE composition of initial melts generated by the partial melting of basic crust, and those minerals that are involved in the melt fractionation process (*e.g.* hornblende).

All the granodioritic and most of the trondhjemitic gneisses show positive Sr and Eu anomalies on spidergrams or chondrite normalized REE plots (Appendix 6), while the tonalites generally have no Sr anomaly, and a negative Eu anomaly. This suggests that plagioclase may have played an important role in the genesis of the tonalites, either by crystallizing out, leaving a tonalitic magma, or by not melting significantly during partial

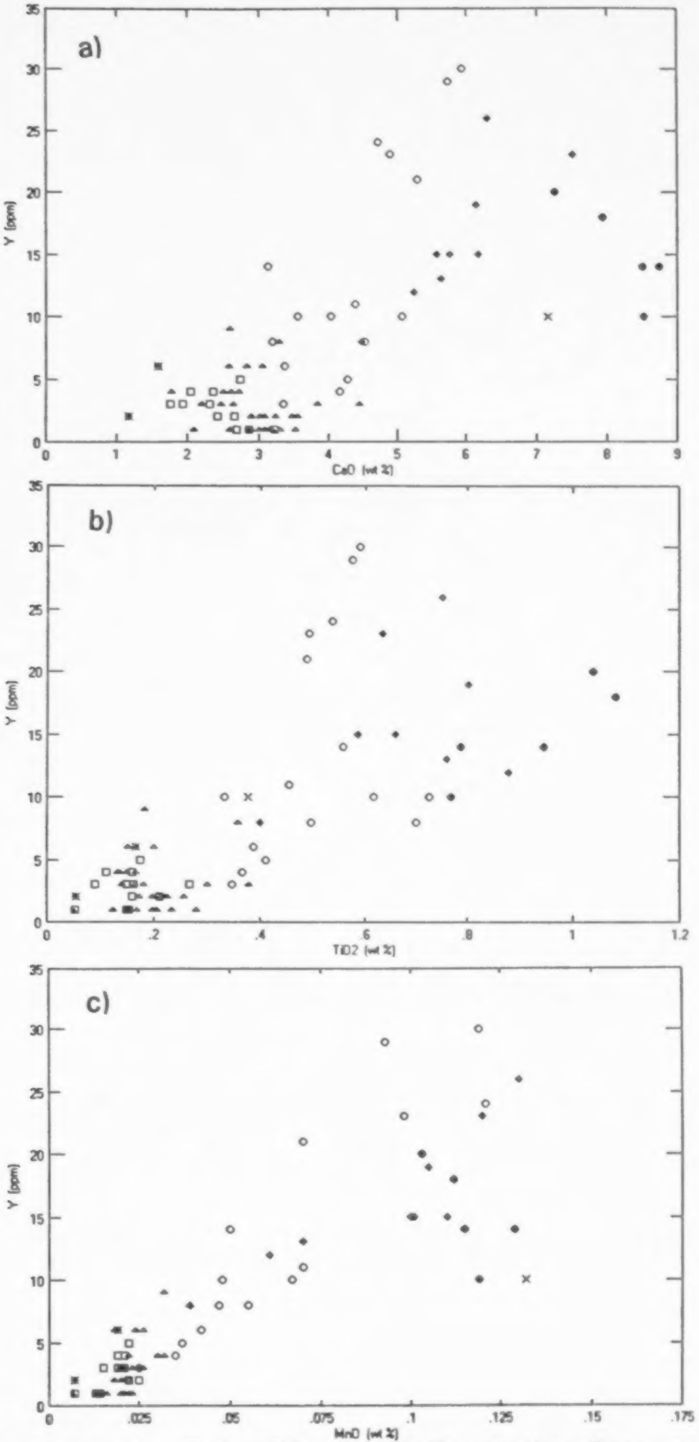

Figure 3.21 Y *vs* CaO, TiO_2 and MnO variation diagrams.

melting of a mafic source. The higher Sr and Eu^{2+} in the granodiorites and trondhjemites (and lower ferromagnesian minerals/elements) implies that either hornblende (without plagioclase) fractionated out leaving a melt enriched in Sr and Eu^{2+} and/or hornblende was not significantly involved in the partial melting of possible mafic precursors.

3.2.3 Geochronology and Isotope Geology

3.2.3.1 Zircon geochronology

In an attempt to answer the question of whether the type-Nûk gneisses were part of a single, protracted period of magmatic activity or the product of episodic magmatism, zircons were separated from a number of samples and analyzed by U-Pb 'small sample' techniques and/or by the high resolution ion microprobe using the SHRIMP at the Australian National University in Canberra, Australia.

Ion microprobe analyses.

Both unpicked, non-magmatic, sized fractions and picked zircons from various non-magnetic size fractions were mounted in epoxy, polished and analyzed using the ion microprobe. For details of the method and typical operating conditions see Compston *et al.*, (1984). Williams and Claesson (1987) describe refinements to the calibration and data processing procedures.

Results

U-Pb ion microprobe results for the concordant analyses are listed in Table 3.4 and shown graphically in Figures 3.22 to 3.25.

Table 3.4 Ion microprobe data for zircons separated from gneisses G87-17 an G87-85.

Grain Spot	U (ppm)	Th	Th/U	Radio' ^{206}Pb	^{204}Pb (ppb)	^{206}Pb*/^{238}U	± 1 σ	^{207}Pb*/^{235}U	± 1 σ	^{207}Pb*/ ^{206}Pb*	^{207}Pb/^{206}Pb (Ma)	± 1 σ
G87-17												
1-1	65	52	0.80	49	27	0.6141	0.0189	18.76	0.67	0.22155	2992	23
2-1	88	91	1.03	69	23	0.6039	0.0183	18.86	0.66	0.22644	3027	23
3-1	82	44	0.54	58	19	0.6072	0.0182	18.68	0.61	0.22318	3004	17
4-1	120	128	1.07	90	34	0.5750	0.0170	17.45	0.58	0.22013	2982	20
5-1	70	59	0.84	51	15	0.5804	0.0178	17.42	0.62	0.21768	2964	25
6-1	65	58	0.89	50	22	0.6082	0.0185	18.54	0.65	0.22108	2989	23
7-2	52	31	0.60	37	13	0.5965	0.0188	18.52	0.68	0.22523	3019	24
8-1	46	26	0.57	30	18	0.5512	0.0175	17.11	0.64	0.22512	3018	25
9-1	58	31	0.53	40	27	0.5851	0.0185	18.63	0.68	0.23097	3059	24
10-1	76	43	0.57	55	21	0.6142	0.0183	18.29	0.60	0.21601	2951	17
11-1	51	33	0.65	37	6	0.5994	0.0188	18.32	0.66	0.22172	2993	24
11-2	100	56	0.56	74	52	0.6234	0.0183	19.30	0.61	0.22450	3013	14
12-1	28	17	0.61	20	6	0.5944	0.0193	18.09	0.70	0.22070	2986	28
13-1	36	22	0.61	26	9	0.5902	0.0188	18.26	0.68	0.22431	3012	26
14-1	42	29	0.69	32	11	0.6269	0.0197	19.19	0.70	0.22200	2995	24
G87-85												
9-1	93	105	1.13	72	7	0.5737	0.0103	18.36	0.43	0.23211	3067	20
10-1	102	94	0.92	73	18	0.5549	0.0098	17.59	0.38	0.22991	3051	16
11-1	73	14	0.19	47	19	0.5856	0.0113	18.56	0.46	0.22987	3051	21
12-1	116	108	0.93	84	38	0.5673	0.0099	17.48	0.37	0.22347	3006	17
24-1	115	102	0.89	81	0	0.5541	0.0071	17.41	0.25	0.22788	3037	8
25-1	109	87	0.80	78	0	0.5682	0.0073	17.73	0.25	0.22631	3026	8
26-1	217	213	0.98	172	6	0.6173	0.0072	19.14	0.24	0.22488	3016	6
27-1	155	163	1.05	120	7	0.5980	0.0073	18.55	0.25	0.22498	3017	7
28-1	89	64	0.72	63	3	0.5805	0.0077	17.54	0.27	0.21914	2974	10
29-2	164	200	1.22	126	8	0.5734	0.0070	17.57	0.24	0.22224	2997	8

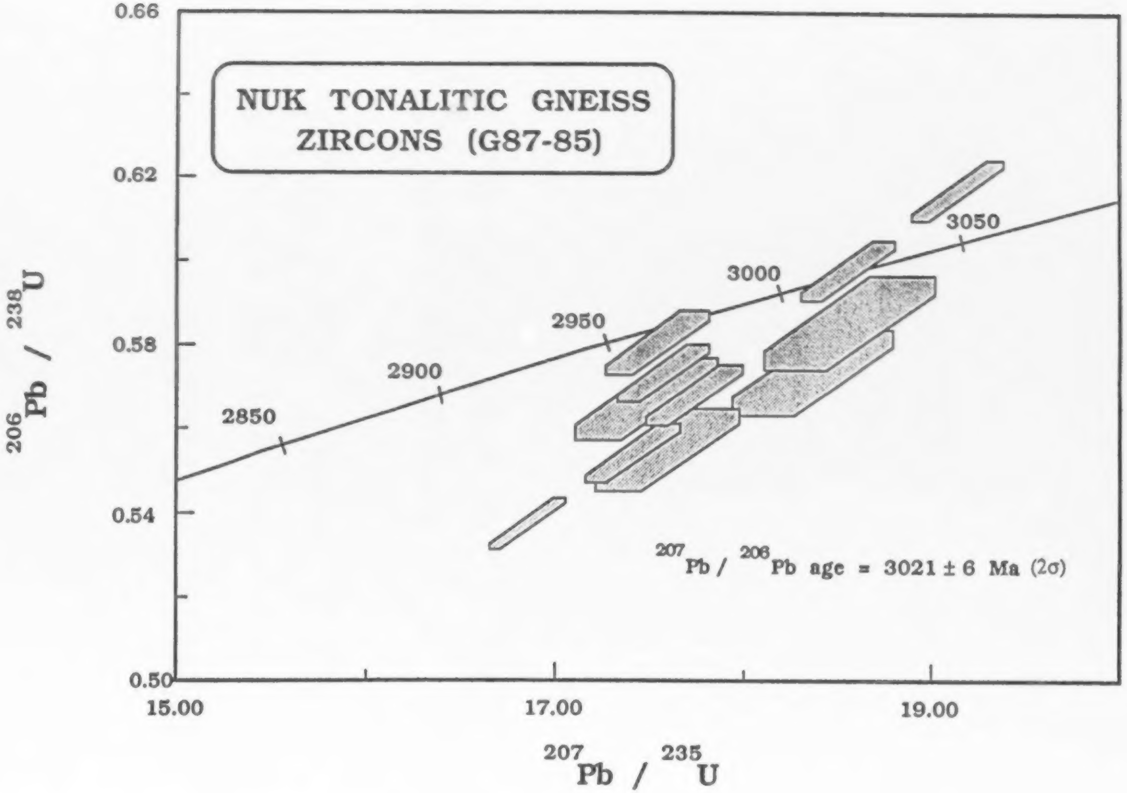

Figure 3.22 SHRIMP U-Pb results for zircons from G87-85.

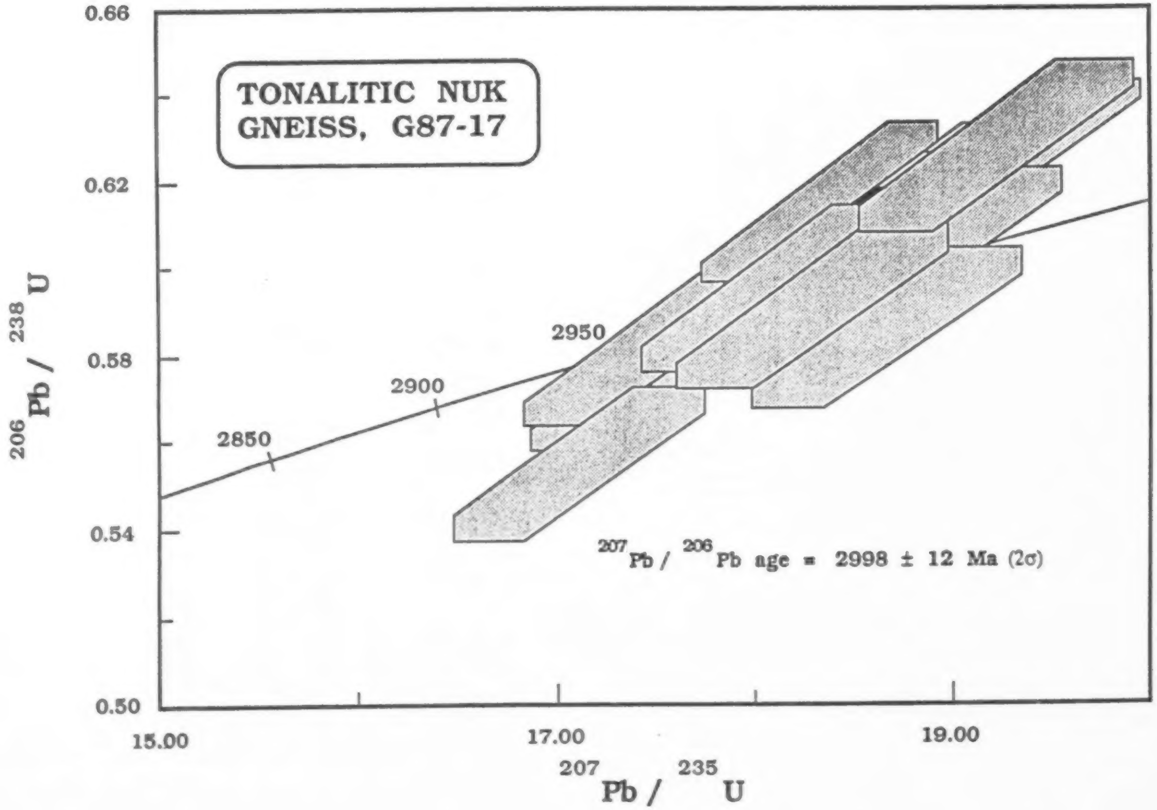

Figure 3.23 SHRIMP U-Pb results for zircons from G87-17.

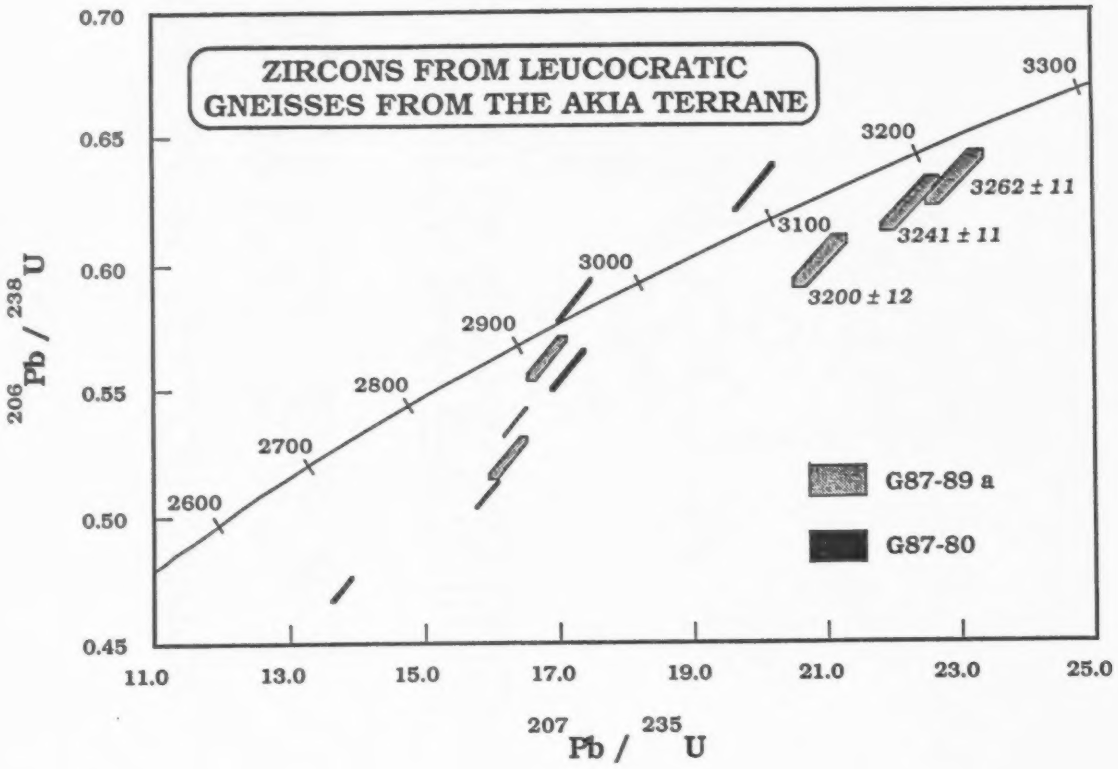

Figure 3.24 SHRIMP U-Pb results for zircons from G87-89a and G87-80.

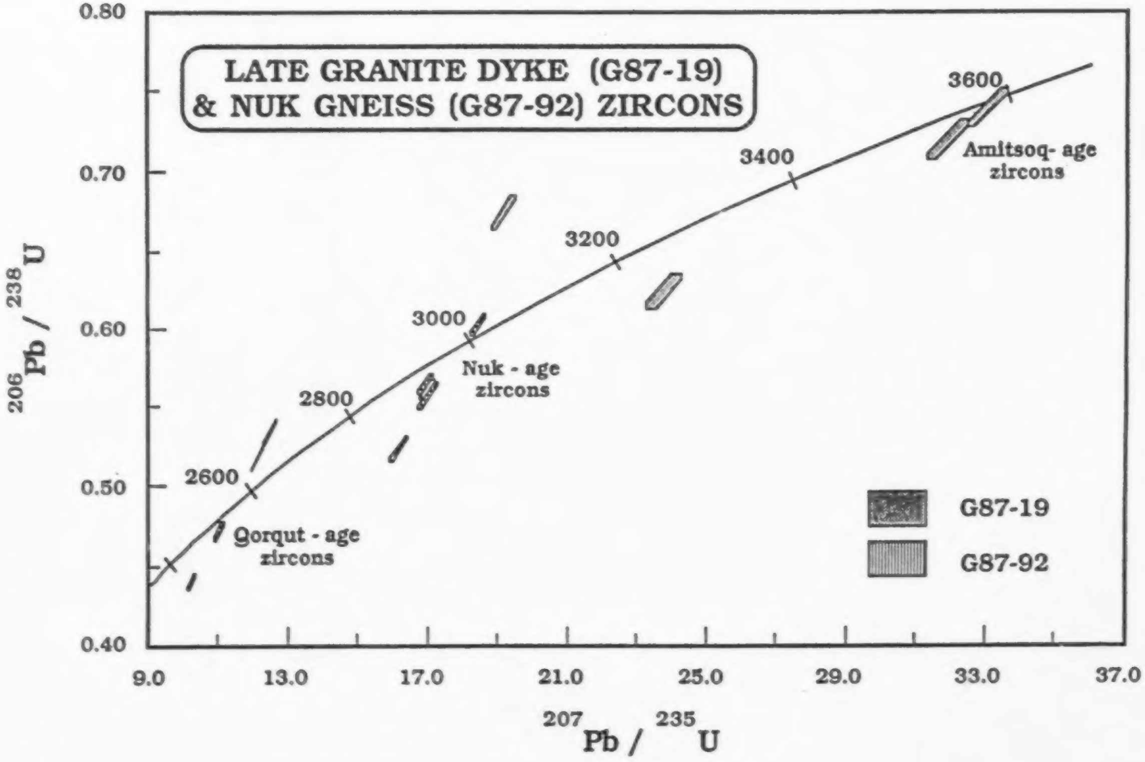

Figure 3.25 SHRIMP U-Pb results for zircons from G87-92.

As can be seen zircons separated from the tonalitic gneisses G87-85 and G87-17, gave essentially concordant dates of 3021 ± 6 Ma (2σ) and 2998 ± 12 Ma (2σ), respectively. These samples were picked prior to mounting and analysis. These dates are taken to represent the intrusive ages of the igneous protoliths of the gneisses. The greater size of the error polygons in G87-17 compared to G87-85, are in large part a consequence of the low U content of the selected zircons, which tend to give the most concordant results because of the reduced metamictization.

Figure 3.24 shows the ion probe results of a selection of zircons separated from the granodioritic and trondhjemitic samples G87-80 and G87-89a. These zircons were from bulk, non-magnetic, sized fractions that had not been picked. The lack of concordancy is readily apparent. The data points for G87-80 scatter about a line that intersects the Concordia at approximately 3000 Ma. A few zircon analyses from sample G87-89a (collected from an area mapped by McGregor as Amîtsoq gneiss) are discordant with minimum ^{207}Pb-^{206}Pb dates of between *c.* 2970 and 3040 Ma. A number of other zircons, also discordant, give minimum ^{207}Pb-^{206}Pb ages of *c.* 3250 Ma. Given the exceedingly radiogenic whole-rock Pb isotopic composition of G87-89a (compared to the renowned unradiogenic whole-rock Amîtsoq Pb) it is considered unlikely that these discordant zircons are Amîtsoq zircons that suffered severe Pb loss around 2550 Ma (age of the Qorqut granite intrusion) or *c.* 3000 Ma (approximate age of the intrusion of the precursors of the type-Nûk gneisses). More likely is the possibility that they represent remnants of younger, non-Amîtsoq gneiss felsic crust some 3250 - 3400(?) Ma old.

Results of the analyses of zircons separated from the tonalitic gneiss G87-92, are shown in Figure 3.25, and are interpreted in a manner similar to that for G87-80. A discordia of the majority of data points of G87-92 intersects the Concordia again at approximately 3000 Ma.

However, there is also evidence of zircon growth at *c*. 2580 Ma, the age of the Qorqut granite.

Small/single zircon analyses.

A number of zircon sub-samples were picked from the least magnetic sized fractions and analyzed by chemical techniques. A set of six samples were processed using a modified version of Krogh's (1973) column technique. Because of the generally high and inconsistent Pb blanks obtained when employing this approach, the author investigated the applicability of the single bead method of Manton (1988) to Archaean zircon U-Pb analyses. A dramatic reduction in the Pb blank resulted. A full description of the method utilized for this study is listed in Appendix 3 (see also Duke and Baadsgaard, 1993).

Using the single bead procedure U-Pb analyses were performed on zircons separated from *c*. 20 type-Nûk gneisses. Zircons were selected on the basis of their clarity, and where possible, those containing inclusions and/or cracks were excluded. In most instances the picked samples were also abraded (Krogh, 1982).

For the most part, the zircons were of high quality, euhedral in form, and invariably a distinctive hyacinth colour (Figures 3.26 to 3.31). Some samples displayed a wide variety of zircon morphologies, *e.g.*, sample G87-5 (Figure 3.29a). A number of samples (*e.g.,* G87-5, G87-149, and G87-112) had zircons that displayed obvious cores and rims (*e.g.*, Figure 3.31). The cores were always much lighter in colour than the rims, which were usually dark red to brown in colour (Figure 3.31b). On the basis of colour, subsamples of the light pink coloured and dark red zircons were picked and analyzed as representative of the cores and rims, respectively. Where applicable these samples are identified (c - cores, r - rims). In all cases the darker 'overgrowth gave younger dates compared to the assumed 'core' material.

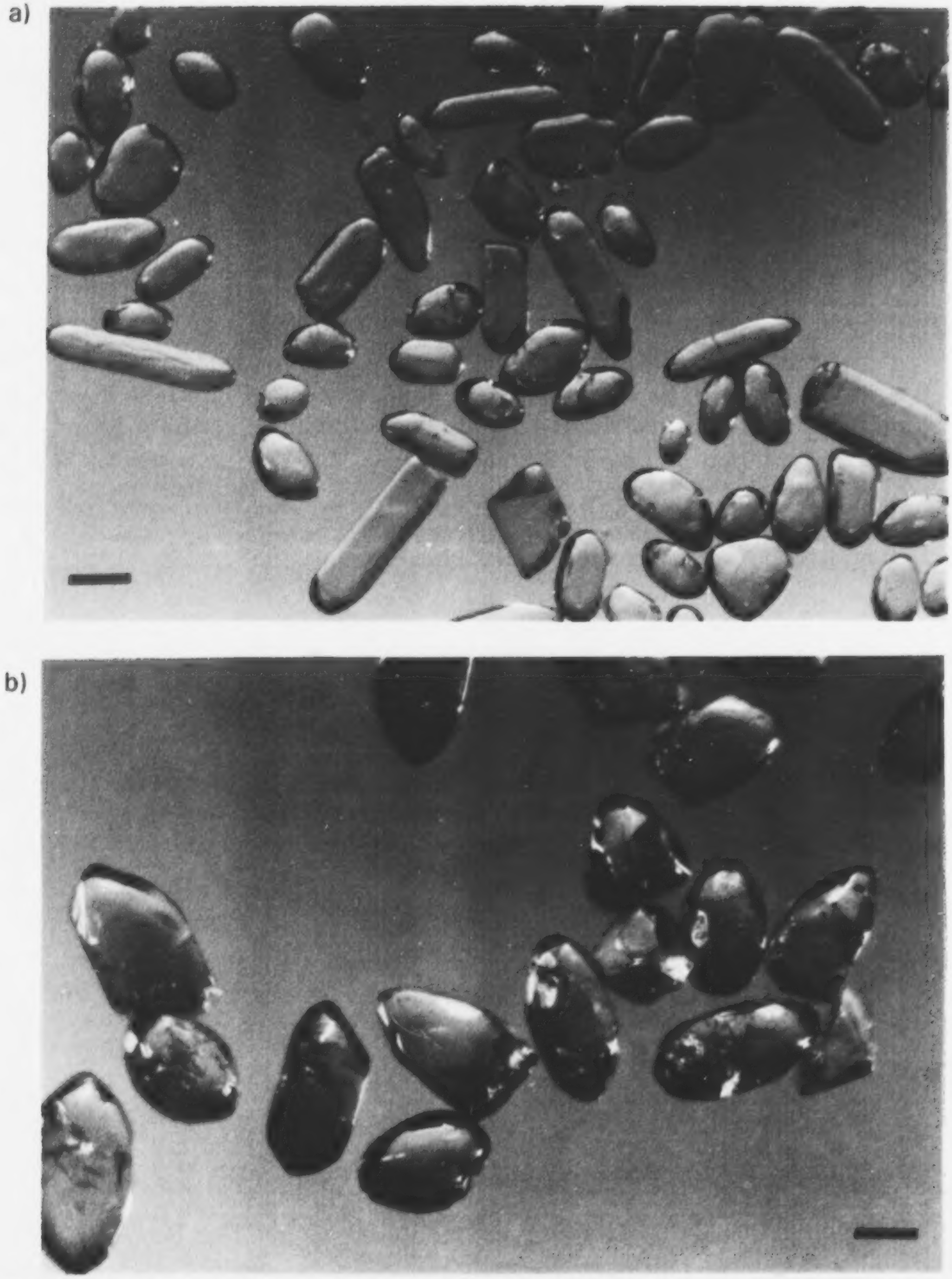

Figure 3.26 Type-Nûk gneiss picked and abraded zircons. a) G87-18 b) G87-2 (oblique lighting, scale 100 μm).

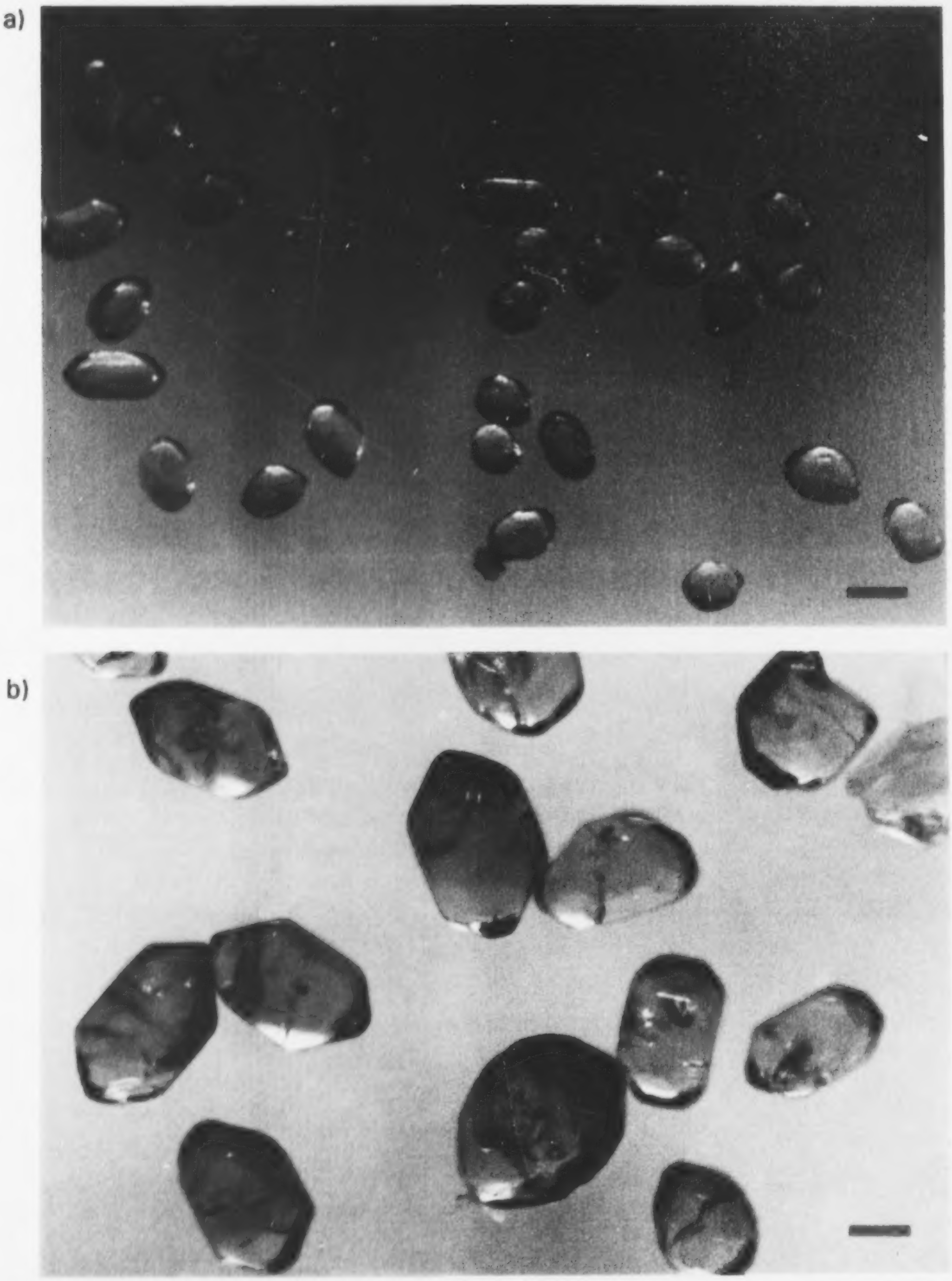

Figure 3.27 Type-Nûk gneiss picked and abraded zircons. a) G87-34
b) G87-94 (oblique lighting, scale 100 μm).

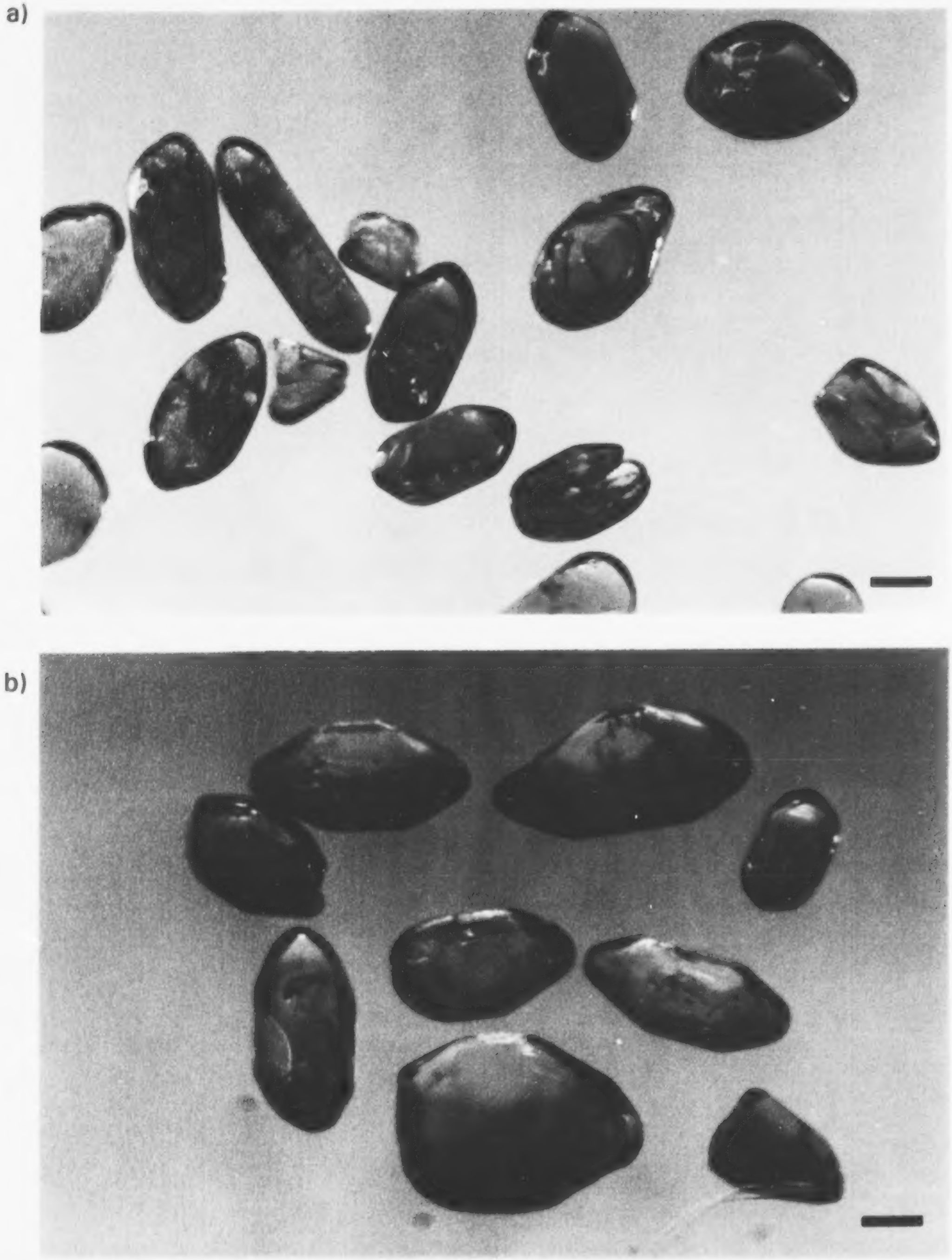

Figure 3.28 Type-Nûk gneiss picked and abraded zircons. a) G87-103 b) G87-111 (oblique lighting, scale 100 μm).

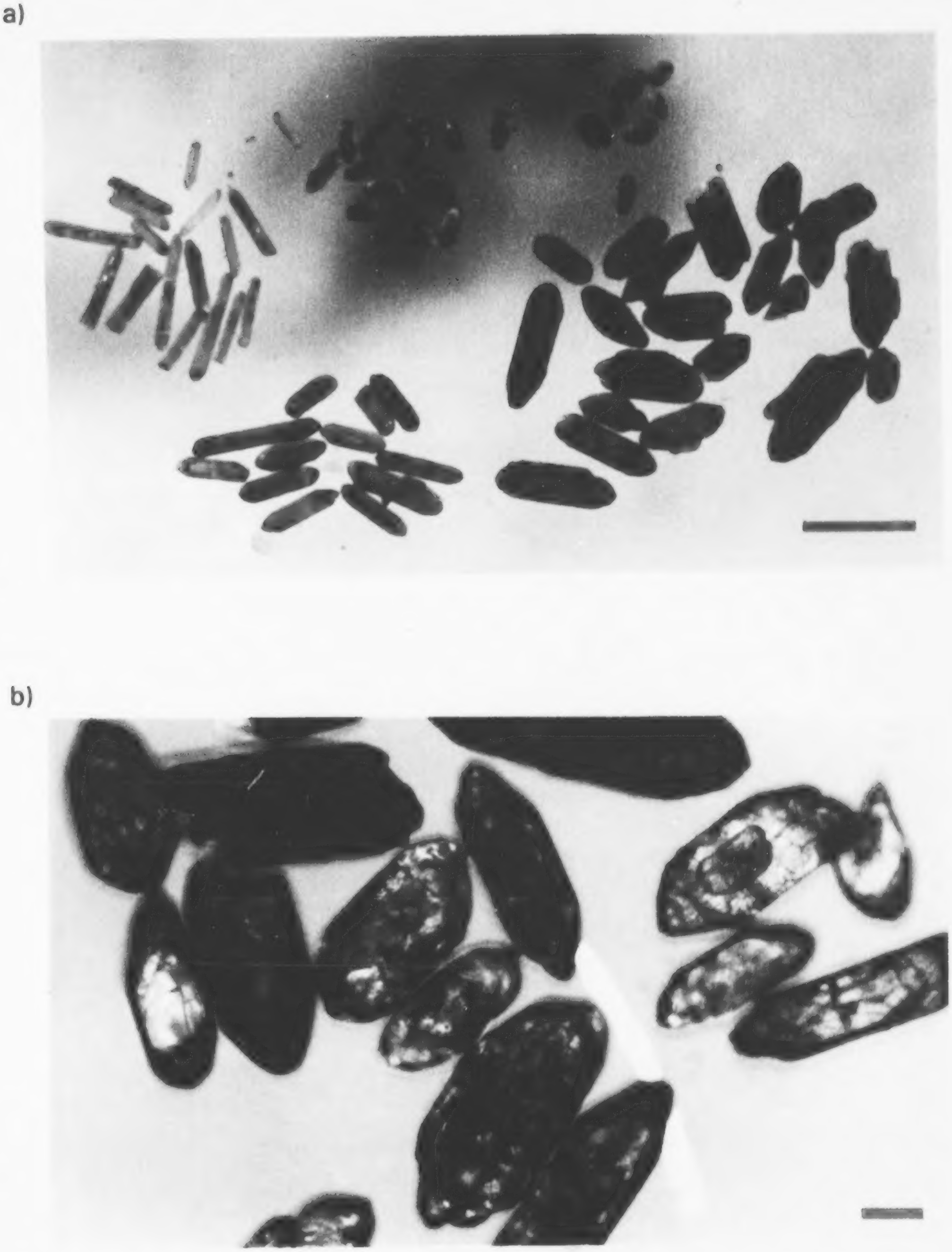

Figure 3.29 Zircons from G87-5 a) example of multiple zircon populations - oblique light, scale = 0.5 mm, b) example of a core in a zircon from one of the populations of (a) - crossed polars, scale = 100 μm.

a)

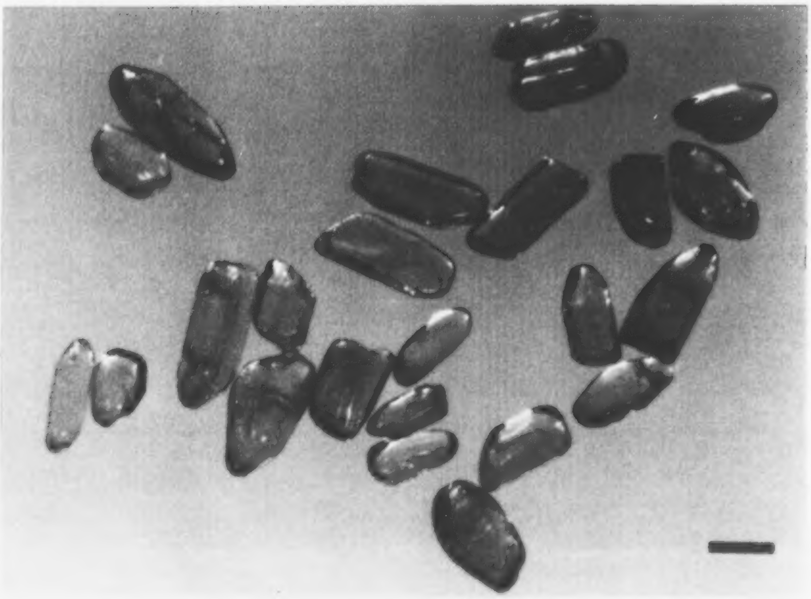

b)

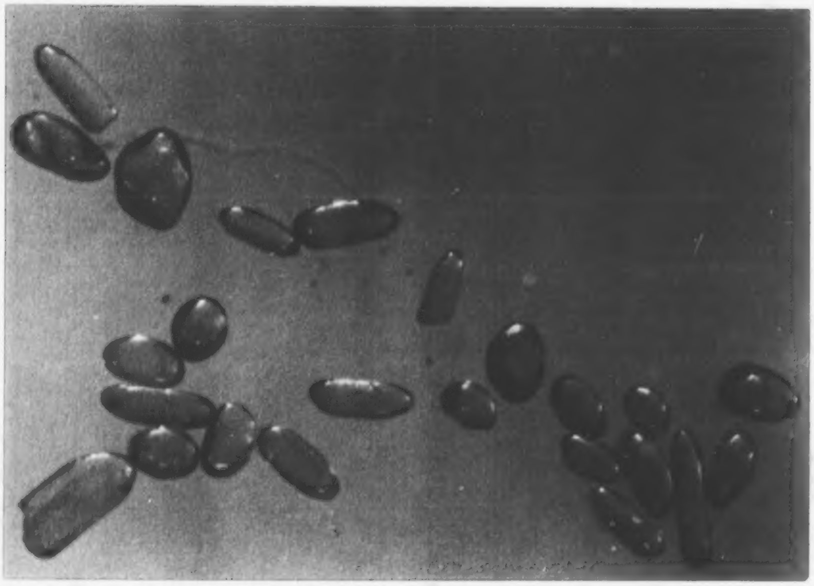

Figure 3.30 Type-Nûk gneiss picked and abraded zircons. a) G87-16 b) G87-90 (oblique lighting, scale 100 μm).

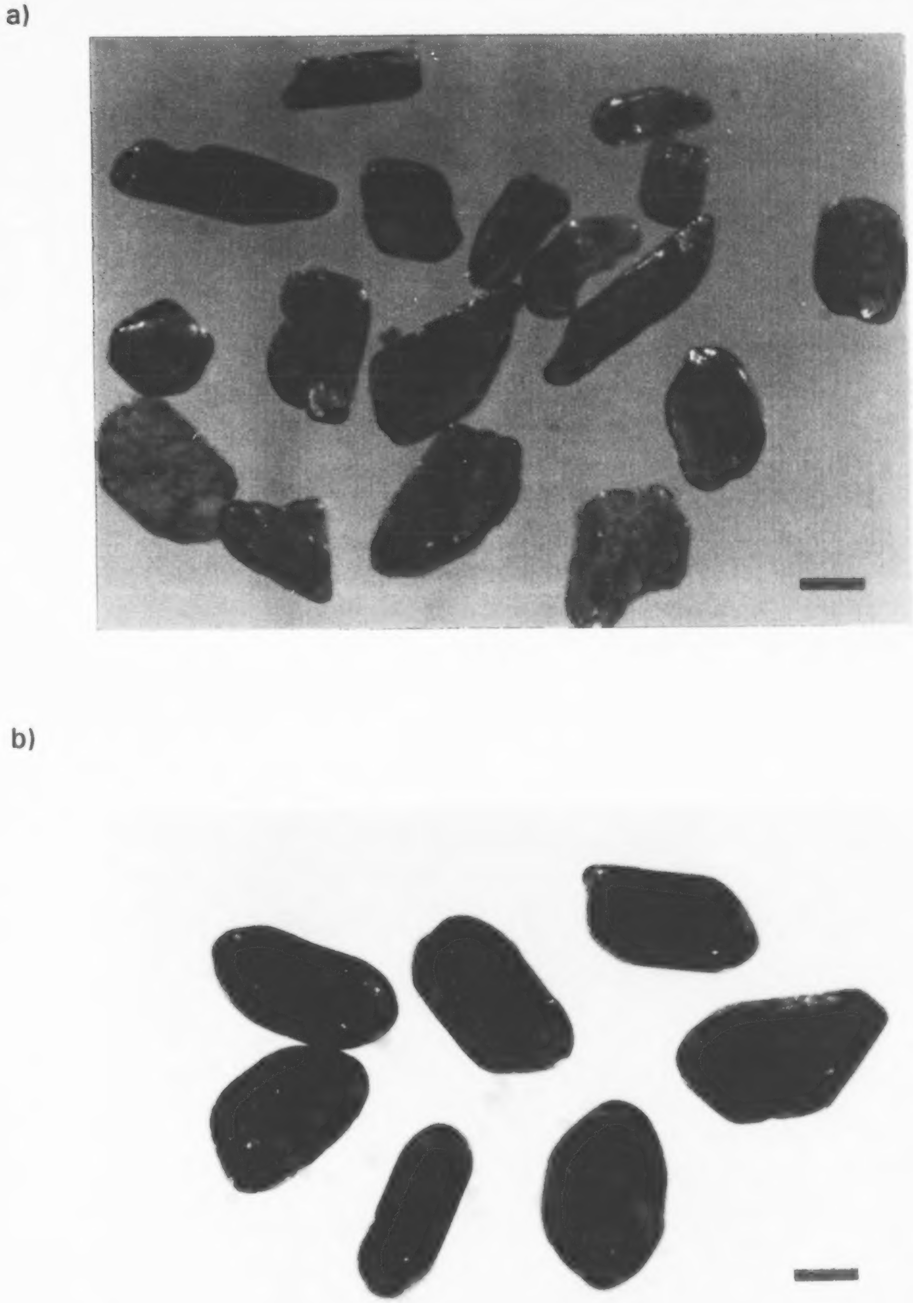

Figure 3.31 Two zircon populations from type-Nûk gneiss G87-149 a) anhedral, fractured, pink 'core' zircons b) euhedral, equant, high-U dark metamorphic zircons (oblique lighting, scale 100 μm).

Results.

Table 3.5 lists the blank-corrected data for the chemically-analyzed zircons of this study, together with calculated dates, U, Th and Pb concentrations for each sample. Common lead corrections were applied according to the SK-model (Stacey and Kramers, 1975). The Th concentrations are only considered reliable for those samples that are concordant, or almost so, as they were back calculated given the age of the zircon sample and its blank and common Pb corrected ^{208}Pb/^{204}Pb ratio. Given the uncertainty in the mass of zircon and spike used, the element ratios are more accurate compared to the element concentrations.

The data are also plotted on conventional Concordia diagrams in Figures 3.32 to 3.33.

U-Pb Zircon Ages

In the following description discordant results are assigned a *minimum* discordancy based on extrapolation from the origin, through the ^{206}Pb/^{238}U - ^{207}Pb/^{235}U data, to the Concordia. Results are grouped by rock-type, not to imply that the dioritic gneisses represent the oldest component of the type-Nûk gneisses, for example, but to provide a simple means to group data.

Uncertainties in the ^{207}Pb-^{206}Pb ages are calculated using a programme written by Dr. H. Baadsgaard that sums the *determinant* errors and so maximizes the measurement uncertainty.

Dioritic gneisses

G87-39: From the island of Tartunguaq, south of Nuuk

- two zircon populations separated on the basis of colour (pink and red grains). These zircons showed no evidence of a core/rim relationship. The results are slightly discordant with ^{207}Pb-^{206}Pb dates of 2922 and 2962 Ma, respectively.

Table 3.5 Results of conventional U-Pb zircon analyses.

		Concentration						Atomic Ratios*			Apparent Age (Ma)		
ID	Mass	U	Th	Pb	Com Pb	Th/	^{206}Pb	^{206}Pb	^{207}Pb	^{207}Pb	^{206}Pb	^{207}Pb	^{207}Pb
G87-	(ug)	------	(ppm)	------		U	^{204}Pb	^{238}U	^{235}U	^{206}Pb	^{238}U	^{235}U	^{206}Pb
149c>100	117	339	286	254	0.27	0.844	8140	0.5929	18.635	0.22796	3001	3023	3038
149r>100	149	1704	13	1038	0.22	0.007	49436	0.5798	17.550	0.21953	2948	2965	2977
113	65	121	51	82	0.15	0.422	5145	0.5830	17.794	0.22137	2961	2979	2991
90	74	246	132	169	0.16	0.537	9976	0.5833	17.734	0.22049	2962	2975	2984
16	130	201	168	147	0.20	0.835	6634	0.5838	17.830	0.22149	2964	2981	2992
12	105	633	325	373	0.22	0.512	15918	0.4973	14.505	0.21156	2602	2783	2918
24	108	81	58	57	1.14	0.709	475	0.5745	16.921	0.21360	2926	2930	2933
17>100	146	72	43	52	1.21	0.595	415	0.6015	18.517	0.22329	3036	3017	3005
118<100	100	84	54	58	1.11	0.643	501	0.5763	17.235	0.21690	2934	2948	2958
18 <100	120	78	46	54	0.16	0.586	584	0.5825	17.467	0.21749	2959	2961	2962
111 >100	79	118	45	79	1.03	0.379	769	0.5877	17.981	0.22188	2980	2989	2994
4	17	204	65	142	1.25	0.316	1138	0.6167	19.057	0.22412	3097	3045	3011
21	49	159	94	110	2.42	0.589	439	0.5807	17.476	0.21827	2952	2961	2968
39pink	25	291	75	183	2.23	0.257	849	0.5673	16.591	0.21212	2897	2912	2922
39 red	84	695	198	446	0.31	0.284	14390	0.5740	17.210	0.21744	2924	2947	2962
112c>100	100	105	59	73	0.59	0.588	1163	0.5824	17.837	0.22213	2959	2981	2996
112r>100	185	336	71	208	0.36	0.210	5898	0.5615	16.893	0.21819	2873	2929	2967
94 >100	170	132	82	91	1.46	0.622	584	0.5693	17.509	0.22306	2905	2963	3003
103>100	113	257	101	164	0.27	0.391	5795	0.5546	16.954	0.22172	2844	2932	2993
5	65	389	1228	382	0.71	3.159	3207	0.5201	15.188	0.21180	2700	2827	2919
27	162	622	80	321	9.40	0.128	316	0.4479	17.495	0.28327	2386	2962	3381
114	31	297	83	170	1.12	0.277	1612	0.5205	14.047	0.19573	2701	2753	2791

* - corrected for blank, spike and common lead

Th concentration data calculated assuming concordancy

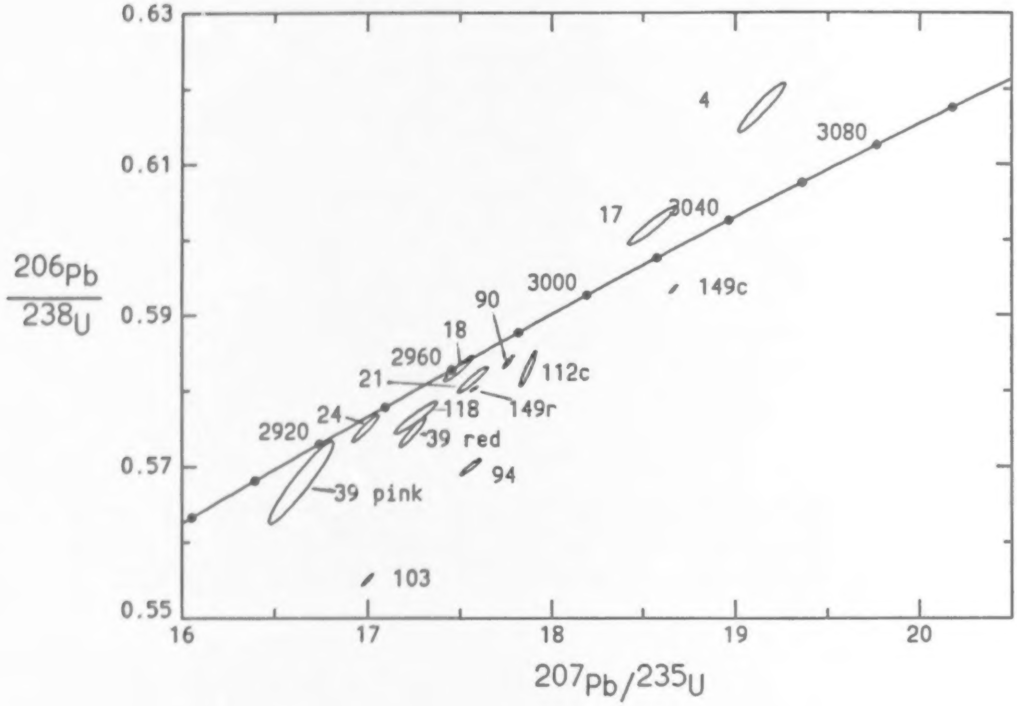

Figure 3.32 U-Pb concordia diagram of zircon analyses.

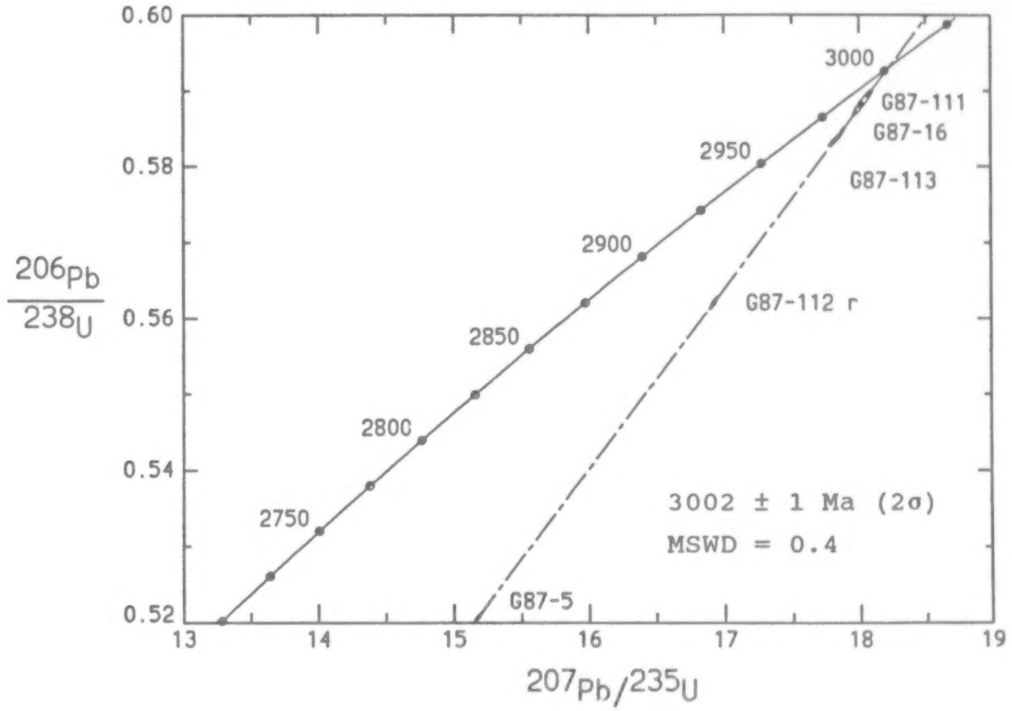

Figure 3.33 U-Pb concordia diagram for samples G87-5, G87-16, G87-111, G87-112 and G87-113.

Quartz dioritic gneisses

G87-16, 17, and 18 Airport road

- G87-16: minimum of 1.15% discordant, ^{207}Pb-^{206}Pb age of 2992 Ma
- G87-17: reverse discordant, ^{207}Pb-^{206}Pb age of 3005 Ma which agrees well with the SHRIMP age of 2998 ± 12 Ma (2σ)
- G87-18: essentially concordant, 2962 Ma (0.15% discordancy) taken as age of intrusion of igneous precursors (cut by G87-19).

G87-118 southern Sadelø

- G87-118: a minimum of 1.0% discordant at 2958 Ma

G87-112 Nuuk promontory

- G87-112: pink 'core' zircon, slightly discordant (minimum 1.57%) with a ^{207}Pb-^{206}Pb age of 2996 Ma; red 'rim' zircon, minimum 4.0% discordant with a ^{207}Pb-^{206}Pb age of 2967 Ma

(*n.b.*, G87-113 (2991 Ma) intrudes G87-112, and both are cut by a granitic (*s.l.*) dyke G87-114 (2791 Ma)

G87-149 southern Bjørneøen

- G87-149 core and rim zircons

  cores: pink, irregular, sugary looking; minimum discordancy of 1.5%), ^{207}Pb-^{206}Pb age 3038 Ma; rims: red, euhedral, high U, minimum discordancy 1.2%, ^{207}Pb-^{206}Pb age 2977 Ma

Tonalitic gneisses

G87-90 Airport road quarry

- G87-90: slightly discordant (0.94%) ^{207}Pb-^{206}Pb age of 2984 Ma

G87-21 Airport road

- G87-21: almost concordant result (minimum 0.70%) ^{207}Pb-^{206}Pb age of 2968 Ma

G87-24 Town road

- G87-24: essentially a concordant result (minimum of 0.26% discordancy), low U, Th and Pb, ^{207}Pb-^{206}Pb age 2933 Ma

Trondhjemitic gneisses

G87-4 from Airport (mapped as Amîtsoq gneiss), reverse discordant ^{207}Pb-^{206}Pb age 3011 Ma

G87-12 N end of runway, turbid grains, excellent ^{206}Pb-^{204}Pb ratio, however, very discordant (minimum of 13%) hence a minimum ^{207}Pb-^{206}Pb age of 2918 Ma.

G87-103 and G87-111 Marina

- G87-103: discordant (≥ 6.2%) with a ^{207}Pb-^{206}Pb age of 2993 Ma
- G87-111: slightly discordant result (≥ 0.6%), ^{207}Pb-^{206}Pb age of 2994 Ma

Granodioritic gneisses

- G87-94: discordant (≥4.05%), maximum ^{207}Pb-^{206}Pb age of 3003 Ma
- G87-5 at airport (mapped as Amîtsoq gneiss) minimum of 5 populations (Figure 3.30a) - picked clearest for analysis. Highly discordant (≥9.2%) ^{207}Pb-^{206}Pb age of 2919 Ma

As noted by Baadsgaard and McGregor (1981) the oldest ages determined on the type-Nûk gneisses were for samples from Bjørneøen *vs* the straight belt that passes through the Nuuk townsite and towards the northeast. Where cross-cutting relationships are discernable on an outcrop scale (*e.g.*, G87-112, -113, and -114) the zircon geochronology supports the temporal-compositional relationship of early intermediate gneisses, intruded by more felsic tonalitic/trondhjemitic gneisses, that are all cut by the late granitic (*s.l.*) sheets. However, on a larger scale (*i.e.*, kms) there is no evidence to suggest that the intermediate gneisses are always older than the tonalitic gneisses, which in turn are always older than the trondhjemitic gneisses. On the contrary, it would appear that the quartz diorite-tonalite-trondhjemite-granodiorite sequence is repeated many times throughout the region. This would seem to indicate multiple "TTG intrusive 'cycles'" *vs.* a prolonged period of intermediate magmatism, followed at a later date by tonalitic magmatism, and at an even later date by trondhjemitic or granodioritic magmatism. The dioritic and quartz dioritic gneisses are not restricted to > 3000 Ma and the trondhjemitic gneisses to < 2950 Ma, for example.

Metamorphic Zircons.

Zircons separated from samples G87-149 and G87-112 (both quartz-dioritic gneisses, the former from southern Bjørneøen, the latter from one of the promontories in the Nuuk townsite) both displayed dark red coloured rims, interpreted as metamorphic overgrowths, on pink coloured cores. In addition, each of the samples yielded two zircon populations one pink, the other dark red, interpreted as magmatic and metamorphic zircon, respectively. The core zircons were generally anhedral, irregular, and 'fractured' (Figure 3.31a) while the metamorphic zircons were well facetted, euhedral, and had a small aspect ratio (Figure 3.31b). U-Pb zircon analyses of these metamorphic zircons gave discordant results of between 1.3 and 4%. The ^{207}Pb-^{206}Pb minimum ages were 2977 and 2967 Ma, respectively for G87-149 (r) and G87-112 (r). Assuming that they were both generated by the same metamorphic event, a line regressed through the two points gave a Concordia intercept age of 2981 ± 1 Ma (2σ), in reasonable agreement with the minimum ^{207}Pb-^{206}Pb age of G87-149(r) suggesting a metamorphic event at that time.

However, Figure 3.33 shows that samples G87-111, G87-16, G87-113, G87-112r, and G87-5 all lie on a discordia with a Concordia upper intercept age of 3002 ± 1 Ma (2σ) and a MSWD of 0.4.

U-Th-Pb Zircon data

As would be predicted, those samples that had the lowest U and Th concentrations tended to give more concordant results. Where 'core' and 'rim' zircon populations occur, the 'rim' material (accepted as being of metamorphic origin, see Chapter 4) always has a higher concentration of U than the core material. The reasons and implications of this are discussed in Chapter 4.

Discussion of the U-Pb Zircon results.

The range of combined SHRIMP and conventional U-Pb ages for the type-Nûk gneisses, determined as part of this study, span about 120 Ma (2920 - 3040 Ma). Baadsgaard and McGregor, (1981) reported a greater range (2890 - 3065 Ma) based on the analysis of bulk, sized, zircon samples.

Of particular importance is the 2981 ± 1 Ma (2σ) Concordia intercept age for the two metamorphic zircon samples G87-112r and G87-149r. This age agrees extremely well with the bulk zircon U-Pb result of 2982 ± 7 Ma (2σ) obtained for the Taserssuaq tonalite (Garde *et al.*, 1985) at the northwest head of Godthåbsfjord (and a less precise Rb-Sr age of 2980 ± 50 Ma (2σ) obtained for a large granodioritic body from the east coast of Bjørneøen). The Taserssuaq tonalite crops out over an area > 2000 km^2, and McGregor *et al.*, 1986, postulated that this batholith may have been responsible for the granulite-facies metamorphism of the Nordlandet gneisses. As shown in Chapter 4, SHRIMP and conventional U-Pb analyses of zircons from Nordlandet clearly indicate that the peak of granulite-facies metamorphism peak was at 3014 ± 7 Ma (2σ). This is significantly older than the 2982 Ma metamorphism of the type-Nûk gneisses.

An alternative interpretation is inferred by the extreme linearity of the discordia which includes G87-112 r (and G87-5, -16, -111, and -113). It would appear that there was a metamorphic event at about 3002 Ma (possibly related to or accompanying intrusion of type-Nûk gneiss precursors). Given the MSWD of 0.4 for the fit of this discordia the probability that the analyses line-up in this manner by 'chance' is vanishingly small. Therefore this second interpretation must be preferred over the 'chance' agreement between the discordia intercept age of 2981 Ma for G87-149 r and G87-112 r and the age of the Taserssuaq tonalite. Morphologically, some of the other zircon samples suggest a metamorphic origin (*e.g.*, G87-5 and possibly G87-111 - Figures 3.30 and 3.28). Although G87-5 showed examples of cores (Figure 3.30 b) no such evidence was found for the other samples.

Baadsgaard and McGregor (1981) suggested the range in ages they obtained for the type-Nûk gneisses was due to Pb loss induced by strong metamorphism at *ca.* 2850 Ma, *ca.* 2660 Ma, and at *ca.* 2500 Ma, the time of emplacement of the Qorqut granite. Given the data reported here it is suggested that a metamorphic event at 3002 Ma, and the severe ductile deformation that produced the straight belt that runs through Nuuk townsite at *ca.* 2530 Ma, were likely two major causes of Pb loss.

Recognizing that at least some of the type-Nûk gneiss zircons have suffered some Pb loss, a histogram of the combined SHRIMP and conventional ^{207}Pb-^{206}Pb zircon ages was generated in an attempt to answer the question of whether the type-Nûk magmatism was of a prolonged or episodic nature. The resulting histogram is shown in Figure 3.34a.
The obvious metamorphic 'rim' zircons have not been included in this diagram. Although the data are few, they indicate a 'normal' grouping of ages around 3000 Ma, a lull at about 2950 Ma, and possibly a minor increase in magmatism around 2920 Ma. However, Figure 3.34b shows the effect of simply shifting the histogram interval by 10 Ma. A major portion of the results still cluster about 3000 Ma, but a second minor period of activity at 2960 Ma is indicated. Clearly, more high precision U-Pb zircon analyses will be required to determine the validity of either of these distributions.

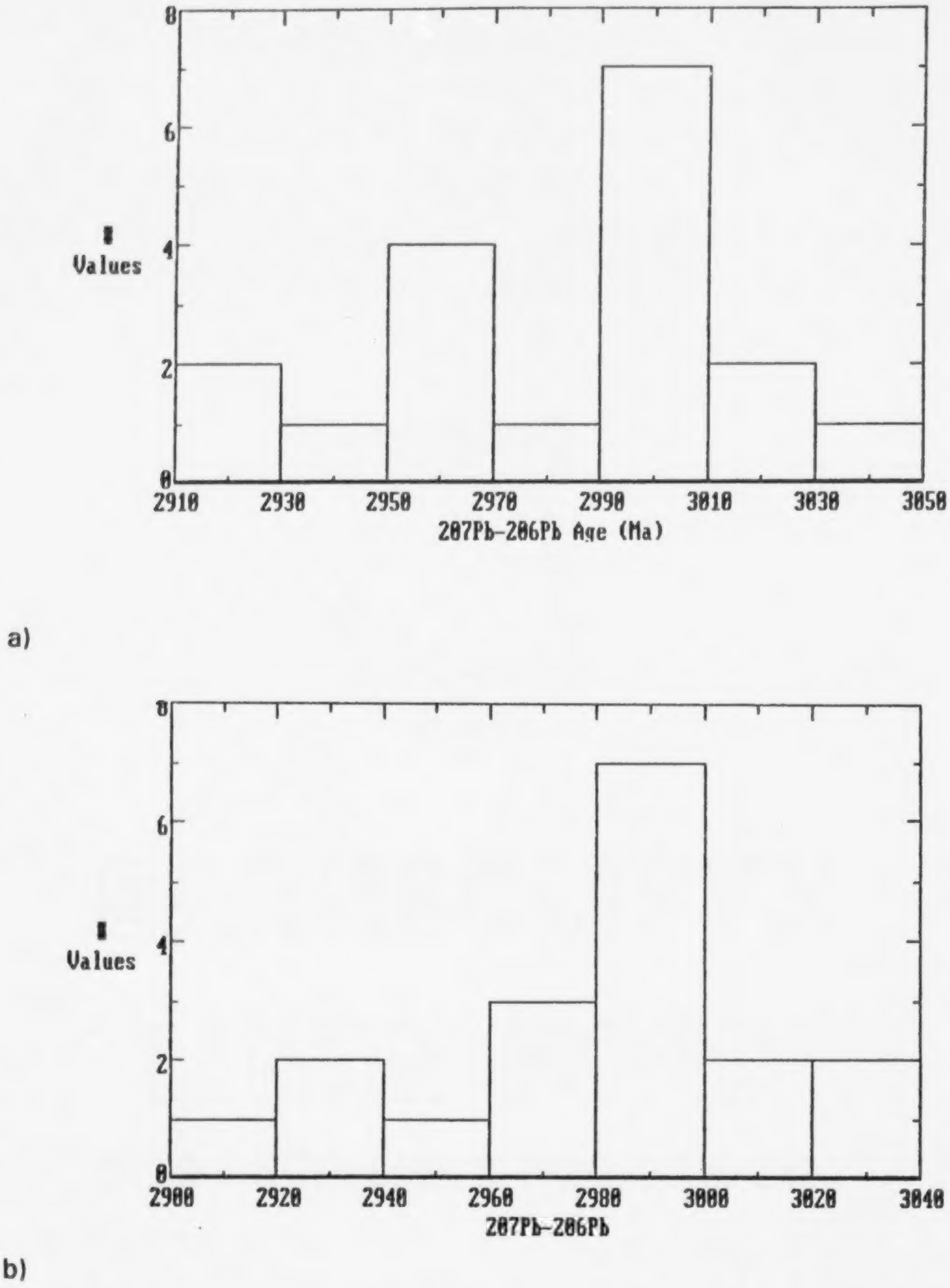

Figure 3.34 Histograms of ^{207}Pb-^{206}Pb zircon ages of analyzed type-Nûk gneisses.

3.2.3.2 Whole-Rock Isotopic Data

With a few exceptions all the samples studied as part of this thesis were analyzed isotopically for their common Pb composition. Rubidium-Sr and Sm-Nd radiometric analyses were also performed on the vast majority of the samples. A full description of the chemical separation procedures and mass spectrometric analyses are given in Appendix 2. Analyses were performed with the aim of determining both age and tracer information.

Rubidium-Strontium

The Rb and Sr concentrations of the majority of samples were determined by MSID. Excellent agreement was found between the MSID and XRF Rb and Sr content (see Appendix 2). Consequently, the $^{87}Rb/^{86}Sr$ ratios of those samples which were not analyzed by MSID for their Rb and Sr content were calculated from the combined Rb and Sr XRF data and the $^{87}Sr/^{86}Sr$ measurement of those samples. Where utilized such data are identified.

Conventional Rb-Sr isochron diagrams for the type-Nûk gneisses are presented in Figures 3.35 and 3.36. In Figure 3.35 only those samples that were analyzed by TIMS for both Sr isotopic composition and the $^{87}Rb/^{86}Sr$ ratio are plotted. These data (n=43) give an errorchron age of 3143 ± 130 Ma (2σ) (regression Model I, York, 1969) with an initial $^{87}Sr/^{86}Sr$ ratio of 0.7017. Applying York's Model III regression analysis (where the scatter in data is not assumed to be only analytical) gives an 'age' of 3115 ± 120 Ma (2σ), $^{87}Sr/^{86}Sr_{initial} = 0.7018 \pm 0.0006$. Removal of samples from areas mapped as being 'Amîtsoq gneisses' gave an errorchron 'age' of 3069 ± 140 Ma (2σ), $^{87}Sr/^{86}Sr_{initial} = 0.7019_5 \pm 0.0004_0$ (2σ) (Model I, York, 1969), not shown. York's Model III regression for this smaller data set (n=30) gives an errorchron age of 2960 ± 130 Ma (2σ), $^{87}Sr/^{86}Sr_{initial} = 0.7023 \pm 0.0005$ (2σ).

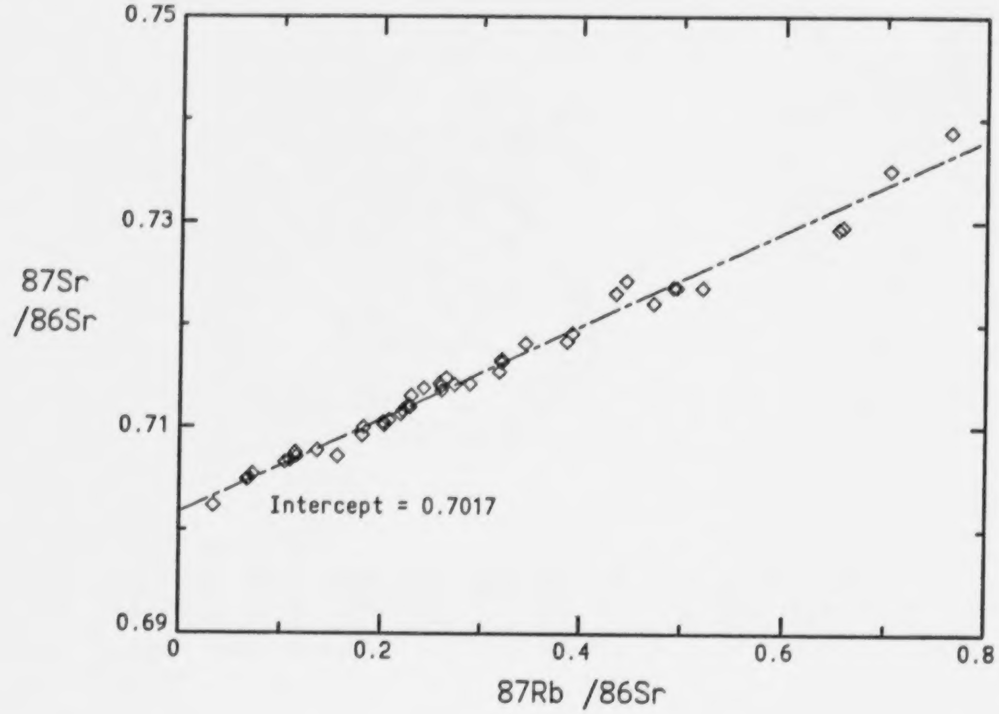

Figure 3.35 Type-Nûk gneiss Rb-Sr scatterchron for whole-rock data determined solely by TIMS.

The Rb-Sr results for all the samples based on the XRF determined $^{87}Rb/^{86}Sr$ and TIMS $^{87}Sr/^{86}Sr$ determinations are plotted in Figure 3.36. Regression analysis of these data gives a Model I errorchron age of 3004 ± 87 Ma (2σ), $^{87}Sr/^{86}Sr_{initial} = 0.7017_7 \pm 0.00025$. (Model III: 2988 ± 57 Ma (2σ), $^{87}Sr/^{86}Sr_{initial} = 0.7017_4 \pm 0.0003_9$). Excluding the radiogenic sample G87-142 from the regression analysis has an insignificant effect on the ages and initial ratios determined by either model. As explained below the results based on the Model III regression are preferred.

These ages and initial ratios are identical within error to those determined previously by Pankhurst *et al.*, (1973) for type-Nûk gneisses from the islands of Bjørneøen and Sadelø. They reported a Rb-Sr age of 2970 ± 50 Ma (2σ) [recalculated from published age by this author using $^{87}\lambda_{Rb} = 1.42 \times 10^{-11}\ a^{-1}$] with a $^{87}Sr/^{86}Sr_{initial} = 0.7026 \pm 0.0004$ (2σ). Agreement is also found between the errorchron results of this study and the Rb-Sr isochron (3076 ± 27 Ma (2σ), MSWD = 0.55, $^{87}Sr/^{86}Sr_{initial} = 0.70205 \pm 0.00009$) reported by Baadsgaard and McGregor (1981) for a suite of dioritic to granodioritic type-Nûk gneisses from southern Bjørneøen. Their Rb-Sr analyses of whole-rocks from the Nuuk townsite gave evidence of open-system behaviour, scattering about a reference isochron of 2840 Ma. A wide belt of intense ductile deformation runs through the Nuuk peninsula and townsite with a NNE-SSW trend ('straight belt' McGregor *et al.*, 1991). Given the obvious deformational effects it would seem most probable that the Rb-Sr isotope systematics (and possibly the Pb-Pb and Sm-Nd) of the these samples were disturbed. In comparison, the type-Nûk gneisses on southeastern Bjørneøen are largely removed from the effects of the straight belt deformation, display clear cross-cutting relationships, and at most only reached medium amphibolite-facies grade. The scatter of the Rb-Sr results of this study is in all likelihood due to the inclusion of samples from both the straight-belt and areas of lower deformation as well as the inclusion of possibly older samples.

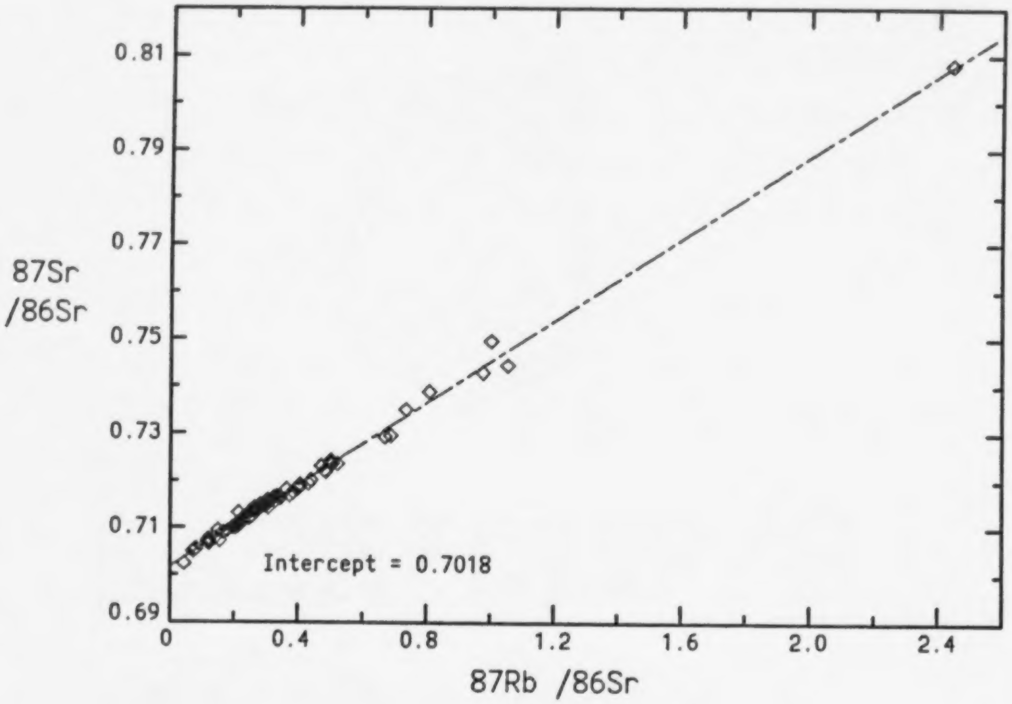

Figure 3.36 Type-Nûk gneiss whole-rock Rb-Sr scatterchron for whole-rock data determined by TIMS and XRF.

Taylor *et al.*, (1980) reported a Rb-Sr isochron age of 2980 ± 50 Ma (2σ) with $^{87}Sr/^{86}Sr_{initial}$ = 0.7022 ± 0.0003 for a samples of a single, large, granodioritic gneiss body from the east coast of Bjørneøen. On the basis of intrusive relationships and the homogeneous nature of the granodiorite, the granodiorite is not considered to be representative of the oldest type-Nûk gneiss components.

One might be tempted to suggest that the decrease in the age and increase in the $^{87}Sr/^{86}Sr_{initial}$ value, brought about by excluding the supposed 'Amîtsoq gneisses' from the Rb-Sr regression, were real and indicated that the Akia terrane 'Amîtsoq gneisses' are older than the remaining type-Nûk gneisses. Based on other data (*e.g.*, ion microprobe results) this is believed to be the case, however, the uncertainty in the Rb-Sr data does not permit that conclusion.

Plotting the $^{87}Sr/^{86}Sr_{initial}$ value on a time *vs* $^{87}Sr/^{86}Sr$ diagram demonstrates two points. Firstly, the type-Nûk gneisses could not have been derived by the partial or complete melting of early Archaean Amîtsoq-like material (*n.b.* the terrane model in its present form also negates this possibility). Secondly, the various initial Sr data all plot well above the $^{87}Sr/^{86}Sr$ linear mantle growth-line, constrained by BABI and the present day variation of oceanic basalts. The data fit and tend to support the suggestion of Faure and Powell (1972) that Sr evolution in the mantle has been non-linear and is best represented by a series of evolution curves (Figure 3.37). The flattening of these curves implies that Rb was depleted relative to Sr fairly early in the Earth's history with a concomitant reduction in Rb/Sr ratio. Extraction of a significant proportion of the present day continental crust early in the Earth's history would produce this effect. In a Sr-isotopic study of Labrador and West Greenland Hurst (1978) concluded that Rb was depleted early in the evolution of the mantle beneath the North Atlantic Craton mantle. Glikson supported this conclusion on the basis of an apparent secular decrease in Rb/Sr ratio from the Amîtsoq gneisses to the Nûk gneisses (*s.l.*). Model Sr ages, based on 'Uniform Reservoir' parameters $^{87}Sr/^{86}Sr = 0.7045$, $^{87}Rb/^{86}Sr = 0.0827$ (DePaolo, 1988), were calculated for each sample analyzed. Open-system behaviour was indicated by the wide range of model ages (see Figure 3.38b) and suggests significant changes in Rb/Sr and/or $^{87}Sr/^{86}Sr$ ratios following crystallization of the igneous precursors and/or metamorphic equilibration. This implies that for the analysis of the Nûk gneiss data the assumptions of York's Model III regression analysis are more appropriate than those of Model I, and should be used. Given the preceding discussion regarding the possibility that linear mantle growth curves are in all likelihood not applicable to the sub-North Atlantic Craton mantle, the significance of Sr-model ages is debatable.

Figure 3.37 shows that a rock derived from depleted mantle A2 at 3.0 Ga with a Rb/Sr ratio of 0.15 would give a T_{Sr} model age based on the linear growth of $^{87}Sr/^{86}Sr$ in the mantle from BABI to a present day value of 0.702 at least 200 Ma older than the extraction age (M1). With decreasing Rb/Sr ratios the error in the model age (*e.g.*, M2) would increase as the angle of intersection between the mantle and sample growth curve decreased. Figure 3.38 shows such a relationship for the type-Nûk gneisses. This effect is not unique to a variably depleted mantle and would occur with a linearly evolving mantle also, and emphasises the need for caution when interpreting Sr-model ages (or similarly Nd-model ages, *e.g.*, Arndt and Goldstein, 1987).

Lead-Lead

Whole-rock Pb data for the type-Nûk gneisses are plotted on a $^{206}Pb/^{204}Pb$ - $^{207}Pb/^{204}Pb$ diagram displayed in Figure 3.39, together with Pb analyses of known Amîtsoq gneisses collected as part of this study. Regression of the type-Nûk gneiss data gives an errorchron age of 2947 ± 110 Ma (2σ) [Model I], while York's Model III regression gives an errorchron 'age' of 3035 ± 100 Ma (2σ).

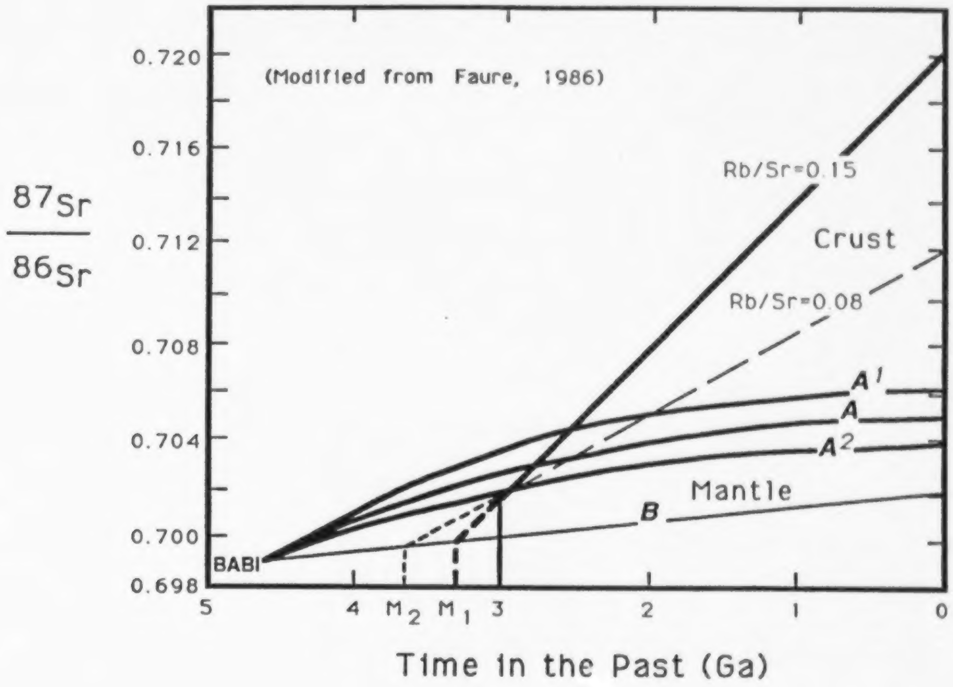

Figure 3.37 Strontium evolution diagram

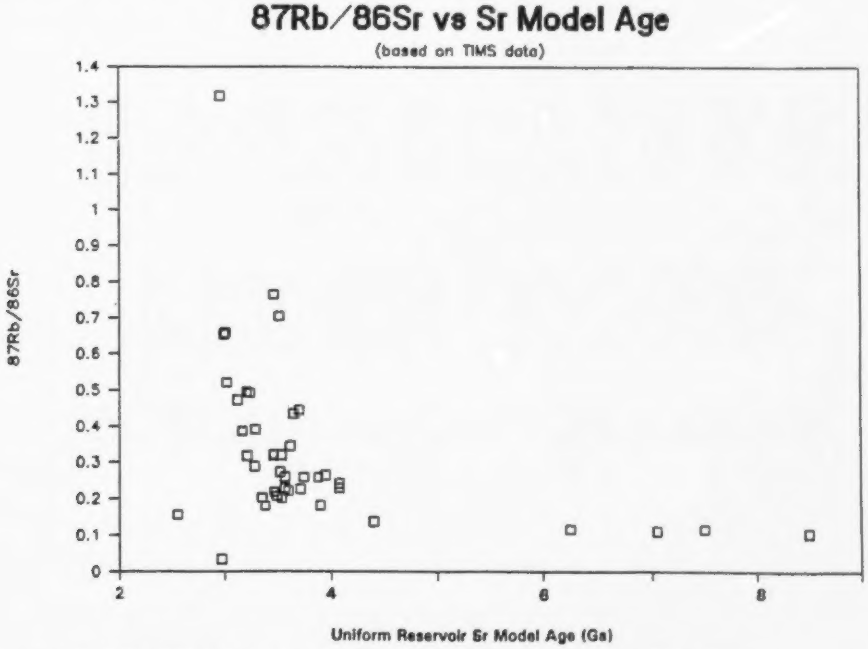

Figure 3.38 Effect of variable ^{87}Rb/^{86}Sr on Sr model ages.

Table 3.6 lists the mean literature Pb isotopic composition of Amîtsoq gneisses (data from Black *et al.*, (1971), Griffin *et al.*, (1980), and Baadsgaard (1976)). Comparison of these values with the Pb-isotopic analyses of the type-Nûk gneisses, and known Amîtsoq gneisses, determined in this study show that none of the type-Nûk gneisses overlap the literature Amîtsoq gneiss mean values. In fact, many of the samples collected from areas mapped as Amîtsoq gneisses by McGregor (*i.e.*, the Akia 'Amîtsoq gneisses') show quite radiogenic Pb compositions (*e.g.* G87-2, G87-89B, G87-151, *etc.*).

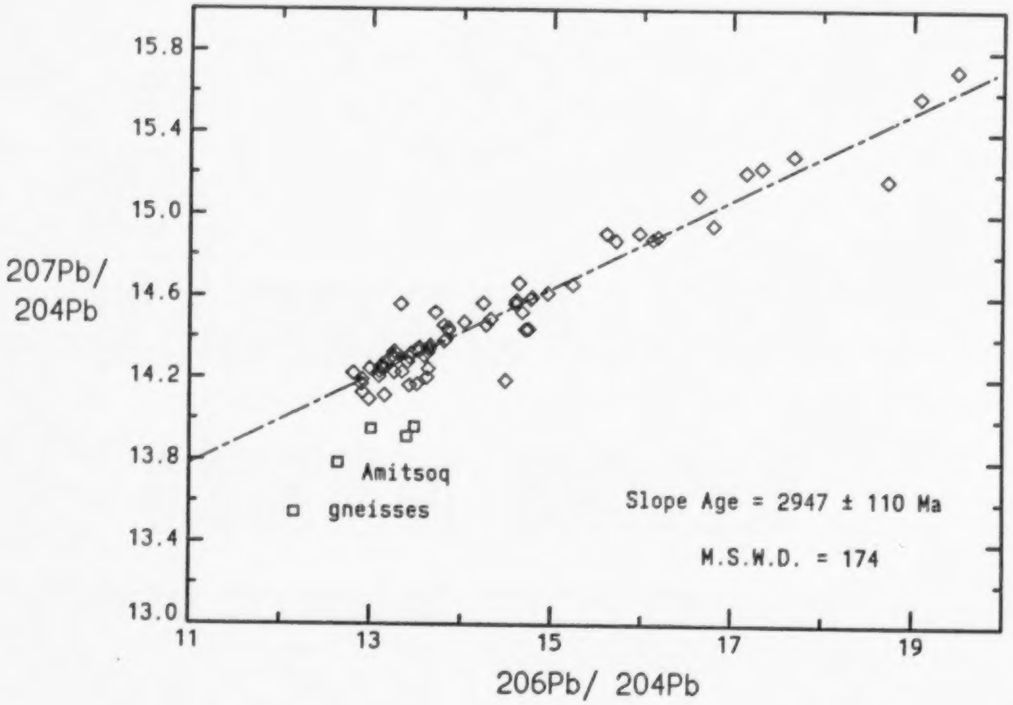

Figure 3.39 Pb-Pb isochron for type-Nûk gneisses (type-Nûk gneisses open diamonds, for comparison Amîtsoq gneisses - open boxes).

Table 3.6 Whole-rock Pb isotopic composition of Amîtsoq gneisses.

GGU #	Ref.	^{206}Pb /^{204}Pb	^{207}Pb /^{204}Pb	^{208}Pb /^{204}Pb
201402	A	12.229	13.361	32.086
201403	A	12.313	13.408	32.247
201404	A	12.090	13.315	31.627
201405	A	12.351	13.410	32.263
201406	A	12.071	13.315	31.884
221131	A	11.929	13.306	31.748
110869	B	13.89	13.52	31.39
110999	B	11.73	13.16	31.34
155817	B	12.73	13.37	31.79
155818	B	11.91	13.23	31.52
155819	B	12.31	13.44	32.03
155820	B	11.82	13.22	31.82
86431	C	11.96	13.29	32.32
86439	C	13.07	13.69	38.02
86596	C	13.37	13.78	33.01
86597	C	12.24	13.39	31.88
110819	C	12.71	13.71	34.23
110822	C	11.81	13.31	33.02
110823	C	13.39	13.77	33.38
110869	C	11.73	13.23	31.32
110870	C	11.95	13.34	31.67
110927	C	12.59	13.71	32.94
110969	C	12.93	13.49	31.87
110999	C	11.83	13.29	31.53
125519	C	11.51	13.14	31.37
125522	C	11.89	13.30	32.04
125523	C	11.83	13.23	31.64
125526	C	12.61	13.68	33.90
125540	C	11.85	13.27	31.78
Mean	:	**12.30**	**13.40**	**32.33**
(1σ, n=30)	:	**0.58**	**0.18**	**1.31**
A - Griffin *et el.* (1980) [n = 6]				
		12.16	13.35	31.98
		0.15	0.04	0.24
B - Baadsgaard *et al.* (1976) [n = 6]				
		12.40	13.32	31.65
		0.75	0.13	0.25
C - Black *et al.* (1971) [n = 17]				
		12.31	13.45	32.70
		0.59	0.22	1.59

Samarium-Neodymium

Sm-Nd data for the type-Nûk gneisses and an amphibolite band (dyke?), G87-6, are presented on a conventional Sm-Nd isochron diagram in Figure 3.40. Sample G87-144 (not plotted) was excluded from the regression analysis because it fell so far off the regression line. The fitted errorchron has a slope age of 2786 ± 120 Ma (2σ), and a $^{143}Nd/^{144}Nd_{initial}$ = 0.50889 ± 8, corresponding to an ϵ_{CHUR} = -2.6, suggesting involvement of older continental crust.

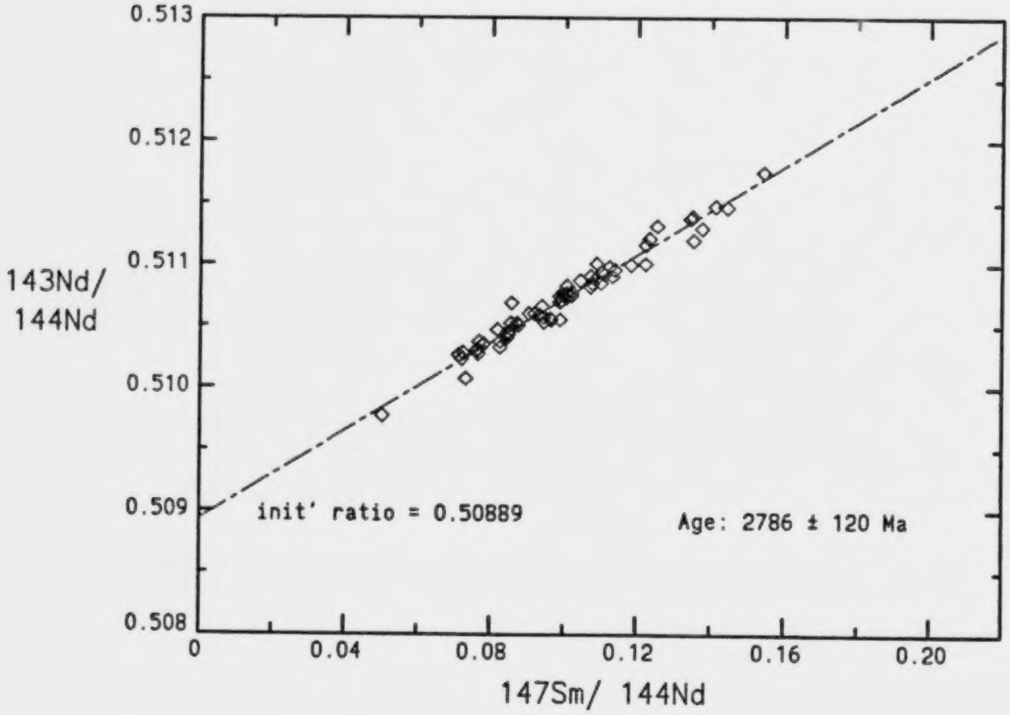

Figure 3.40 Type-Nûk gneiss whole-rock Sm-Nd errorchron.

Table 3.7 lists the Sm-Nd data for the type-Nûk gneisses and related parameters and model ages; model parameters and references are given in the table. The author prefers the T_{DM2} ages as there is ample evidence to suggest that the early Archaean mantle, at least of beneath the North Atlantic Craton, was significantly depleted (Hamilton *et al.*, 1983; Baadsgaard *et al.*, 1986; Moorbath and Taylor, 1986; Jacobsen and Dymek, 1988; Collerson *et al.*, 1991). Those samples collected as Akia terrane 'Amîtsoq gneisses' are marked with an asterisk. As can be seen the T_{DM2} model ages show quite a wide range, from 2.9 to 3.8 Ga. Some of the samples that give early Archaean T_{DM2} model ages also have early Archaean Sr T_{DM} ages. However, early Archaean Sr T_{DM} ages are found for samples that give *c.* 3.1 Ga T_{DM2} model ages and *vice versa*.

Using the precise U-Pb zircon dates for a number of the type-Nûk gneisses samples, Nd $\epsilon_{(T)}$ values were calculated and are plotted on a time *vs* $\epsilon_{(T)}$ diagram in Figure 3.41. The trajectory for the Amîtsoq gneisses was calculated from analyses of Amîtsoq gneisses performed as part of this study. Sample G87-17 plots well above the T_{DM2} evolutionary curve. Apparently in contradiction to the earlier statement by the author regarding his preference for this particular evolutionary curve, the majority of the positive ϵ values plot closer to T_{DM1} than T_{DM2}. However, excepting G87-17, most of the samples seem shifted to negative ϵ values, which could be interpreted as indicating involvement of older continental crust. Only sample G87-112 gives any suggestion of having a retarded Pb-isotopic composition, but its $^{207}Pb/^{204}Pb$ ratio does not overlap that of the mean literature $^{207}Pb/^{204}Pb$ value of the Amîtsoq gneisses at the 2σ level. Two alternatives to contamination by Amîtsoq-like crust come to mind. Firstly, the Akia terrane 'Amîtsoq gneisses' could in fact be *c.* 3.2 - *c.*3.4 Ga in age (as suggested by the SHRIMP analyses of G87-89A) and never experienced the severe U- and Th-loss of the Amîtsoq gneisses, and hence have 'normal'

G87	^{143}Nd/ ^{144}Nd	^{147}Sm/ ^{144}Nd	f Sm/Nd	$\epsilon_{Nd}(0)$	$T_{(CHUR)}$ (Ga)	$T_{(DM1)}$ (Ga)	$T_{(DM2)}$ (Ga)
1*	0.510371	0.0824	-0.581	-44.2	3.00	3.11	3.22
2*	0.511315	0.1253	-0.363	-25.8	2.81	2.99	3.17
3*	0.510910	0.1072	-0.455	-33.7	2.92	3.06	3.20
4*	0.510571	0.0945	-0.520	-40.3	3.06	3.17	3.29
5*	0.510399	0.0844	-0.571	-43.6	3.02	3.12	3.24
10*	0.510870	0.1043 0.1066	-0.470	-34.4	2.90	3.04	3.17
12	0.510281	0.0724	-0.632	-45.9	2.87	2.98	3.09
13	0.510693	0.0987	-0.498	-37.9	3.00	3.12	3.25
15	0.510352	0.0780	-0.604	-44.6	2.92	3.02	3.14
16	0.510751	0.0997	-0.493	-36.8	2.95	3.07	3.20
17	0.510685	0.0856	-0.565	-38.1	2.66	2.80	2.93
18	0.510658 0.510673	0.0939	-0.522	-38.6	2.92	3.04	3.17
20	0.510273	0.0765	-0.611	-46.1	2.98	3.08	3.19
21	0.510523	0.0855 0.0852	-0.565	-41.2	2.88	3.00	3.12
22	0.510600	0.0918	-0.533	-39.7	2.94	3.06	3.18
24	0.510502	0.0875	-0.555	-41.6	2.96	3.07	3.19
34	0.510728	0.1005	-0.489	-37.2	3.01	3.13	3.26
35	0.510467	0.0818	-0.584	-42.3	2.86	2.98	3.10
36	0.510747	0.1020	-0.481	-36.9	3.02	3.14	3.27
39	0.511162	0.1223	-0.378	-28.8	3.00	3.16	3.31
43*	0.511476	0.1412	-0.282	-22.6	3.17	3.34	3.52
57	0.510985	0.1124	-0.428	-32.2	2.97	3.11	3.26
58	0.510451	0.0847	-0.569	-42.6	2.96	3.07	3.18
59	0.510742	0.0987	-0.498	-37.0	2.93	3.06	3.19
60	0.510071	0.0731	-0.628	-50.0	3.14	3.23	3.33
80	0.510847	0.1076	-0.453	-34.9	3.04	3.17	3.31
85	0.510368	0.0768	-0.610	-44.2	2.87	2.98	3.09
86	0.511198	0.1352	-0.312	-28.1	3.54	3.65	3.79
87*	0.510530	0.0945	-0.519	-41.1	3.12	3.22	3.34
88*	0.510886	0.1085	-0.448	-34.1	3.01	3.14	3.28
89A*	0.510592	0.0932	-0.526	-39.9	2.99	3.11	3.23
89B*	0.511213	0.1233	-0.373	-27.8	2.94	3.10	3.27
90	0.511296	0.1376	-0.300	-26.1	3.43	2.11	3.71
91	0.510822	0.1072	-0.455	-35.4	3.07	3.19	3.33
92	0.510295	0.0761	-0.613	-45.7	2.94	3.05	3.16
93	0.510325	0.0825	-0.581	-45.1	3.07	3.16	3.27
94	0.510262	0.0712	-0.638	-46.3	2.87	2.97	3.08
103	0.510777	0.1020	-0.481	-36.3	2.98	3.10	3.23
111	0.510521	0.0871	-0.557	-41.3	2.93	3.04	3.16
112	0.510562	0.0962	-0.511	-40.5	3.13	3.23	3.35
113	0.510232	0.0720	-0.634	-46.9	2.92	3.02	3.13
116	0.509771	0.0503	-0.744	-55.9	2.97	3.05	3.14
118	0.510853	0.1020	-0.441	-34.8	3.12	3.24	3.37
120	0.510432	0.0848	-0.569	-43.0	2.99	3.09	3.21
121	0.510767	0.1006	-0.488	-36.5	2.95	3.08	3.21
122	0.510598	0.0904	-0.540	-39.8	2.91	3.03	3.15
123	0.511392	0.1350	-0.313	-24.3	3.06	3.23	3.41
124	0.510703	0.0993	-0.495	-37.7	3.01	3.13	3.25
127	0.510308	0.0763	-0.612	-45.4	2.93	3.04	3.15
142	0.511012	0.1088	-0.446	-31.7	2.80	2.96	3.11
145*	0.511000	0.1182 0.1180	-0.399	-31.9	3.16	3.28	3.43
146*	0.510942	0.1104	-0.438	-33.0	2.98	3.11	3.26
148	0.510959	0.1138	-0.421	-32.7	3.07	3.20	3.34
149	0.511008	0.1221	-0.379	-31.8	3.31	3.42	3.56
151*	0.511466	0.1444	-0.265	-22.8	3.39	3.53	3.71
152*	0.511375	0.1345	-0.316	-24.6	3.07	3.24	3.42
154*	0.510906	0.1132	-0.424	-33.8	3.14	3.26	3.40
964	0.510824	0.1007	-0.488	-35.4	2.86	3.00	3.13
965	0.511750	0.1542	-0.215	-17.3	3.16	3.38	3.60
966	0.510698	0.0989	-0.497	-37.8	3.00	3.12	3.25
968	0.510549	0.0964	-0.510	-40.7	3.15	3.25	3.37
969	0.510550	0.0989	-0.497	-40.7	3.23	3.33	3.44
970	0.510922	0.1110	-0.436	-33.4	3.03	3.16	3.30

* - samples of Akia terrane 'Amitsoq gneisses'

Model age parameters:

	143Nd/144Nd	147Sm/144Nd	
CHUR:	0.512638	0.1967	(Jacobsen and Wasserburg, 1980)
DM2 :	0.513163	0.2136	(Goldstein *et al.*,1984)
DM1 :	$\epsilon = 0.25t^2 - 3t + 8.5$		(DePaolo, 1981)

Table 3.7 Type-Nûk gneiss whole-rock Sm-Nd data

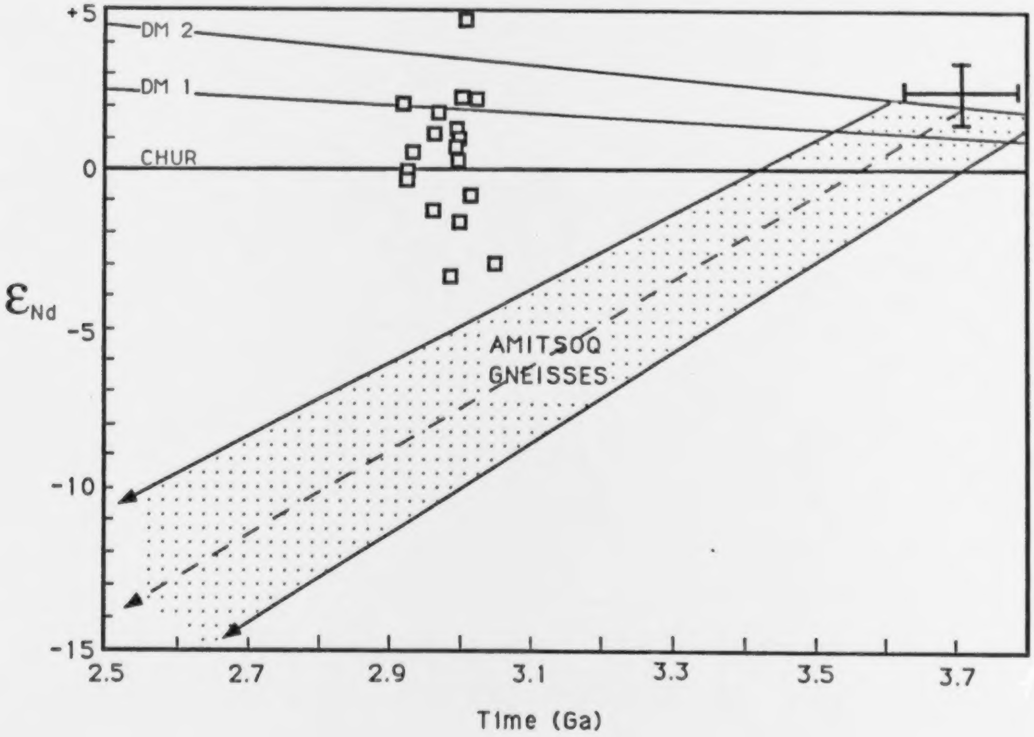

Figure 3.41 Nd evolution diagram showing the type-Nûk gneisses and the trajectory of the Amîtsoq gneisses. (DM parameters given in Table 3.7; error bar: Amîtsoq gneisses Sm-Nd data from Moorbath and Taylor, 1986).

crustal Pb compositions. Such crust would evolve along a path essentially parallel to that drawn for the Amîtsoq gneisses of the Akulleq terrane, but shifted up some 6 ϵ-units, *i.e.*, passing through the data points of Figure 3.41. Alternatively, the severe ductile deformation associated with the straight-belt has disturbed the Sm-Nd systematics so that they are unreliable. However, sample G87-149 from southern Bjørneøen, displays an ϵ value of -3 but comes from an area of low deformation.

An ϵ_{Nd} *vs* ϵ_{Sr} diagram for the type-Nûk gneisses at 3.0 Ga is displayed in Figure 3.42. ϵ_{Nd} values range from about +5 to -5, while with two exceptions ϵ_{Sr} values are all positive. The ϵ_{Nd} values appear to be evenly distributed about CHUR. This is not interpreted to mean that the source region of the type-Nûk gneisses had CHUR Sm-Nd characteristics, but like Figure 3.41, indicates possible contamination with older crust *c.* $\geq$ 3.2 Ga.

3.2.3.3 Comparison with Amîtsoq gneisses

Four Amîtsoq gneisses, collected from the Akulleq terrane, were chemically and isotopically analyzed to compare with the type-Nûk gneisses and possible 'Amîtsoq gneisses' from the Akia terrane. In addition, the chemical data were compared with Amîtsoq gneiss chemical analyses reported in the literature (*e.g.*, Lambert and Holland, 1976; McGregor, 1979; Nutman and Bridgwater 1986).

The whole-rock chemical and isotopic data for the samples are listed in Appendix 4 and Table 3.8, respectively. Chondrite normalized REE plots and 'spidergrams' are provided in Appendix 6.

Isotopic Results

A single U-Pb zircon determination of one of the samples (G87-140) gave a discordant result (-2.9%) with a ^{207}Pb-^{206}Pb minimum age of 3524 Ma (Figure 3.43) confirming its field identification.

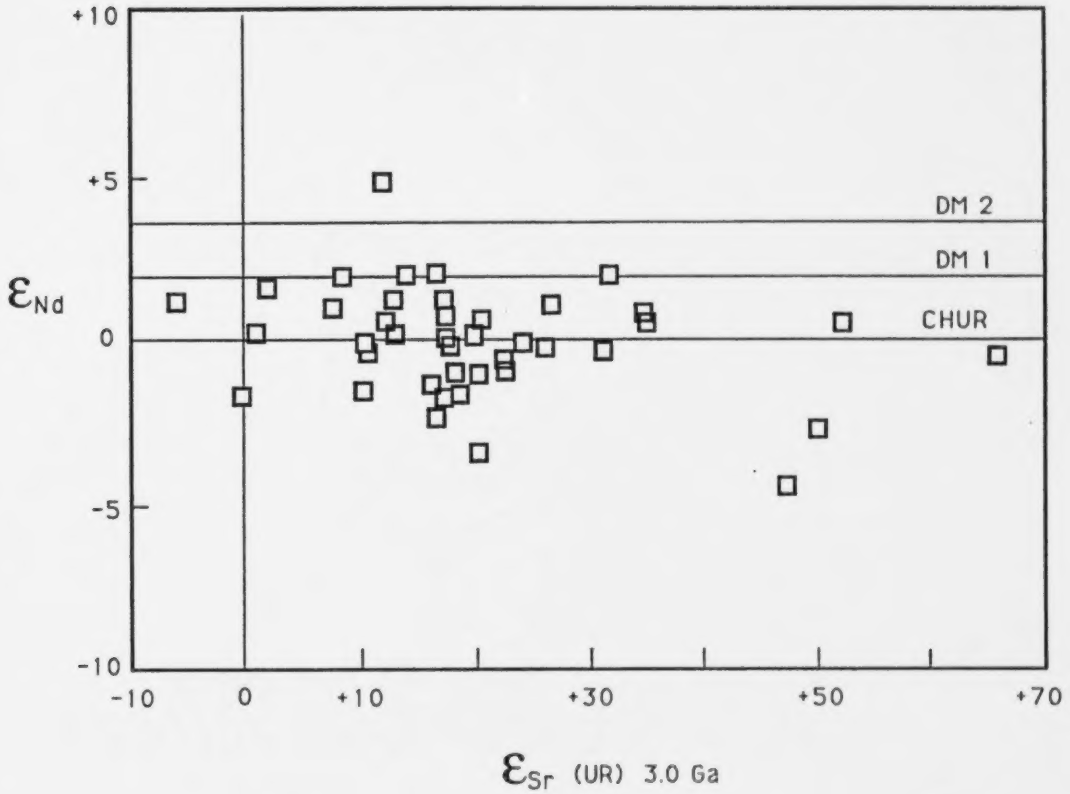

Figure 3.42 ϵ_{Nd} *vs* ϵ_{Sr} diagram for the type-Nûk gneisses at 3.0 Ga.

Compared to the type-Nûk gneisses the unradiogenic nature of the Amîtsoq gneiss whole-rock Pb is apparent from Table 3.8. Sample G87-140, with a $^{206}Pb/^{204}Pb$ ratio of 12.159, is particularly unradiogenic. The results of this study agree well with the mean literature values reported earlier (Table 3.6) and confirm the potential of using the unradiogenic Pb composition of the Amîtsoq gneisses as a tracer for crustal contamination.

The T_{DM2} model ages of the analyzed Amîtsoq gneisses are indicative of an early Archaean age. Note the excellent agreement between the T_{DM2} model age for G87-140 (3.51 Ga) and the U-Pb ^{207}Pb-^{206}Pb minimum age of 3.524 Ma (Table 3.8).

The $^{87}Sr/^{86}Sr$ ratio was only measured in two samples, and both measurements were fairly radiogenic.

Chemical Results

On the basis of chemical data reported in the literature, and the few analyses of Amîtsoq gneisses performed as part of this study, the salient chemical differences between the type-Nûk gneisses and the Amîtsoq gneisses are as follows. For similar rock-types the Amîtsoq gneisses are generally enriched in Y, Nb, Pb and Rb, and depleted in Sr and Ba compared to the type-Nûk gneisses. The increase in Sr and Ba in the *c*. 3.0 Ga type-Nûk gneisses *vs c*. 3.6 Ga Amîtsoq gneisses is the reverse of the general trend for these elements in Archaean high-grade gneisses world-wide (Glikson, 1979). As a consequence of the above enrichments/depletions the Rb/Sr ratios for the type-Nûk gneiss TTG-suite are invariably much lower than their Amîtsoq gneiss counterparts (by at least a factor of two). This has potential ramifications with regards to Rb-Sr isotopic studies. Based on Rb-Sr isotopic analyses of rocks from Labrador and west Greenland, Hurst (1978) deduced that the mantle beneath the North Atlantic Craton had a mean Rb/Sr ratio of 0.014, indicating Rb depletion early in the history of

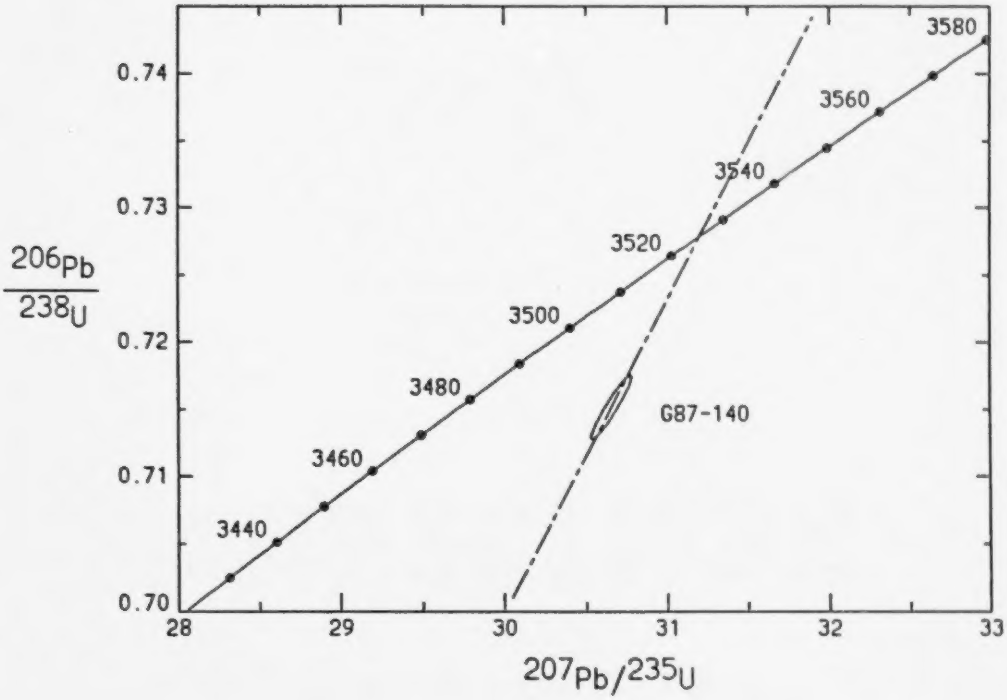

Figure 3.43 U-Pb concordia diagram for Amîtsoq gneisses sample G87-140.

Table 3.8 Isotopic data for analyzed Amîtsoq gneisses

G87	$^{206}Pb/^{204}Pb$	$^{207}Pb/^{204}Pb$	$^{208}Pb/^{204}Pb$	Pb (ppm)	U (ppm)	Th (ppm)	Th/U
25	13.481	13.961	34.948	24	0.79	0.60	0.76
64	13.004	13.951	33.391	21	0.53	3.86	7.28
78	12.641	13.784	33.829	25	0.53	5.17	9.75
140	12.159	13.544	34.981	23	0.49	9.34	19.1

G87	$^{147}Sm/^{144}Nd$	$^{143}Nd/^{144}Nd$	Sm (ppm)	Nd (ppm)	f Sm/Nd	$\epsilon_{Nd(0)}$	T_{CHUR} (Ga)	T_{DM1} (Ga)	T_{DM2} (Ga)	ϵNd (3.6 Ga)
25	0.0882	0.51011	1.73	11.85	-0.552	-49.3	3.52	3.58	3.68	+1.2
64	0.0855	0.50990	1.07	7.53	-0.565	-53.3	3.72	3.76	3.84	-1.7
78	0.0944	0.51022	2.33	14.88	-0.520	-47.2	3.57	3.64	3.73	+0.35
140	0.1085	0.51064	9.69	54.0	-0.449	-38.9	3.42	3.51	3.62	+2.1

$^{143}Nd/^{144}Nd_{CHUR}$ = 0.512636, $^{147}Sm/^{144}Nd_{CHUR}$ = 0.1967, ^{147}Sm $\lambda = 6.54 \times 10^{-12}$ a^{-1}

T_{CHUR} = model age based on a chondritic reservoir

$T_{DM\ 1}$ = model age based on derivation from a progressively depleting mantle reservoir (DePaolo, 1981)

$T_{DM\ 2}$ = model age based on a depleted mantle that evolved in a linear manner from a chondritic source at 4.5 Ga (current values: $^{143}Nd/^{144}Nd$ = 0.513163, $^{147}Sm/^{144}Nd$ = 0.2136, Goldstein et al., 1984)

G87	$^{87}Sr/^{86}Sr$	$^{87}Rb/^{86}Sr$ (meas)	$^{87}Rb/^{86}Sr$ (calc)	Rb (ppm)	Sr (ppm)	T_{UR} (meas)	T_{UR} (calc)	T_{DM} (meas)	T_{DM} (calc)
25	0.72375	---	0.296	42	412	----	6.10	----	5.86
64	---	---	---	51	515	----	----	----	----
78	0.72501	---	0.446	60	390	----	3.87	----	3.89
140	0.78073	1.364	1.357	93.37	199.4	4.07	4.09	4.09	4.10

$^{87}Rb/^{86}Sr$ calc : ratio calculated from XRF Rb-Sr data and measured $^{87}Sr/^{86}Sr$ ratio

^{87}Rb $\lambda = 1.42 \times 10^{-11}$ a^{-1}

**** - unrealistic model ages because sample $^{87}Rb/^{86}Sr$ ratio close to that of UR and DM

T_{UR} = model age based on a uniform reservoir: $^{87}Sr/^{86}Sr_{UR}$ = 0.7045, $^{87}Rb/^{86}Sr_{UR}$ = 0.0827

T_{DM} = model age based on derivation from depleted mantle reservoir: $^{87}Sr/^{86}Sr_{DM}$ = 0.7026, $^{87}Rb/^{86}Sr_{DM}$ = 0.052

the source region of the gneiss precursors, possibly relating to the extraction of large amounts of continental crust from the mantle of the region. The reduction in the chemical Rb/Sr ratio from the Amîtsoq to the type-Nûk gneisses agrees with this conclusion and indicates that the source region of the type-Nûk gneiss precursors was likely quite depleted.

3.2.4 Summary

Chemical results of this study, which was not designed to collect samples on the basis of rock-type, show that the amphibolite-facies type-Nûk gneisses are dominantly tonalitic and trondhjemitic in composition, with slightly smaller proportion of granodioritic gneisses, with minor dioritic and quartz-dioritic gneisses. In this regard the type-Nûk gneisses are typical of most Archaean high-grade gneiss TTG-suites.

In comparison to the Amîtsoq gneisses the type-Nûk gneisses are depleted in Y, Nb, and Pb, and enriched in Sr and Ba. On average the type-Nûk TTG gneisses contain less Rb than their Amîtsoq gneiss counterparts. The Rb content of the dioritic gneisses is more variable. A consequence of the low Rb and high Sr contents of the type-Nûk gneisses *vs* the Amîtsoq gneisses is the much lower Rb/Sr ratio observed for type-Nûk gneisses compared to the Amîtsoq gneisses (or Ikkattoq gneisses).

Given the effects of the 3002 Ma metamorphic event, the intrusion of the Taserssuaq tonalite (and possibly the large granodioritic type-Nûk gneiss intrusions) at *ca.* 2982 Ma, and the formation of the straight-belt at *ca.* 2500 Ma on zircon ages, it would not be surprising to find that one or more of the Rb-Sr, Pb-Pb, and Sm-Nd whole-rock systems was disturbed. That the data show scatter well outside that due to analytical uncertainty is in all probability due largely to open system behaviour. In fact, it is quite remarkable that the errorchron 'ages' agree so well, and that a weighted mean of the 'ages' of the three systems gives an 'age' of *c.* 2940 that agrees fairly well with the U-Pb zircon ages.

CHAPTER 4

Nordlandet Granulites

4.1 Introduction

Prior to this study the relationship between the granulites of Nordlandet peninsula and the type-Nûk gneisses was uncertain. A geochronological study of the granulites was undertaken to clarify the situation. Furthermore, chemical analyses of the Nordlandet granulites were performed to assist in determining their relationship, if any, to the type-Nûk gneisses, and to provide geochemical data on this important rock-type and to help elucidate their mode of formation.

The Nordlandet peninsula, in the north-western part of the Akia terrane, is an extensive granulite terrane some 4000 km^2 in area. The peninsula is separated from the amphibolite-facies rocks of the type-Nûk gneisses by the western arm of Godthåbsfjord (Figure 1). Statements as to the relationship between the granulites and the type-Nûk gneisses vary. McGregor *et al.*, (1986) stated that the granulites are:

> "..not included within the Nûk gneisses because their relations to the type Nûk gneisses across the fjord are uncertain." p.124.

Whereas in regard to the same granulites, Riciputi, Valley and McGregor (1990) stated that:

> "Although separated by the western arm of Godthabsfjord, the granulites are believed continuous with the westernmost terrane in the amphibolite facies belt.....which contains the type Nûk gneisses." p.172.

And Nutman *et al.*, (1989) stated:

> "The Akia terrane is dominated by the amphibolite facies type Nûk gneisses of Nuuk town and southwestern Godthabsfjord and what are probably their equivalents at granulite facies to the west on Akia" p.577.

This uncertainty arises in part because: a) the western arm of Godthåbsfjord separates the two areas, b) the fjord follows the Ataneq fault, a major

Proterozoic fault, and c) prior to this study no zircon U-Pb dating had been performed on the granulites. The only age determined for the granulites (3000 ± 70 Ma, Taylor *et al.*, 1980; and data in Black *et al.*, 1971) although contemporaneous with the accepted age of the type-Nûk gneisses was assumed to date the granulite metamorphic event.

4.1.1 Previous Work

The Nordlandet peninsula is separated by the western arm of Godthåbsfjord from the amphibolite-facies rocks of the type-Nûk gneisses. Macdonald (1974) reported some preliminary findings following systematic mapping of part of the area while Reed (1980) carried out a petrographic study of the rocks of the region. The greater portion of the area consists of dioritic to quartz-dioritic gneisses which were metamorphosed to granulite-facies grade. However, few geochemical data have been published on the granulites to date.

Taylor *et al.*, (1980) reported a Pb-Pb whole-rock age of 3000 ± 70 Ma for the granulites which was interpreted to be the age of granulite-facies metamorphism. Others assumed that in all likelihood the age of the granulite precursors was probably not significantly older than the metamorphic age hence the origin of the idea that the precursors of the Nordlandet granulites were probably contemporaneous with those of the type-Nûk gneisses (*e.g.*, McGregor *et al.*, 1986; Nutman *et al.*, 1989).

James (1975), reporting on rocks from Bjørneøen and the eastern coast of Nordlandet, described mylonitic shear zones from Nordlandet that display a similar orientation and sense to steeply dipping, NNE-SSW trending shear zones from central Bjørneøen (*i.e.*, the straight belt). He deduced that the structural evidence was consistent with a steep, west-verging thrust.

4.1.2 Description of the Granulites

The Nordlandet granulites are predominantly of igneous origin. However, metasedimentary enclaves occur and are more abundant on the western side of the peninsula. Macdonald (1974) reported that granulites of dioritic and quartz dioritic composition dominate the area, though minor amounts of apparently younger tonalitic and trondhjemitic rocks, metamorphosed to granulite-facies grade also occur. He also reported a supracrustal suite composed of amphibolites, pelitic metasediments, and minor skarns which on the basis of field relations was considered older than the dioritic granulites.

Using a variety of geothermometers and geobarometers applied largely to metasedimentary rocks, Riciputi *et al.* (1990) determined the conditions of granulite-facies metamorphism in the region to have been $800 \pm 50°$ C, 7.9 ± 1.0 kb (0.79 GPa). They estimated that f_{H2O} and f_{CO2} were low, suggesting that peak metamorphism was fluid absent *i.e.*, there was no pervasive CO_2-rich fluid during granulite-facies metamorphism.

As part of this study fourteen samples were collected from the eastern side of the Nordlandet peninsula by the author. A description of the samples and their field locations are given in Appendix 1. One of these samples, G87-68, is a late granite sheet that cuts and locally caused retrogression of the intruded granulite. A sample of the retrogressed granulite (G87-69) was collected close to the contact of G87-68 with the aim of examining the isotopic and chemical effects of retrogression. On the basis of their mineralogy the remaining samples were considered granulites or retrogressed granulites.

On Nordlandet there are a number of shear zones that invariably are only a few cm wide. Mineralogically, the shear zones commonly display retrogression to epidote amphibolite-facies. G87-133 is a sample taken from such a shear zone (which trends 020° 80° E, and appears to be sinistral with the east side up). Samples G87-131, and G87-130 were taken approximately 1 m and 2.5 m, respectively from G87-133. These two samples showed no evidence of retrogression in either hand specimen or thin-section. G87-128, another fresh granulite, was collected *c*. 30 m from G87-133. Because of its white colour in hand specimen (*vs.* the greasy-looking brown to green coloured dioritic granulites), sample G87-129 was interpreted in the field as a retrogressed granulite. Thin-section examination and major-oxide chemical analyses, show that the sample is retrogressed and trondhjemitic in composition (*i.e.*, a retrogressed enderbite). However, the LILE depletion displayed by the sample demonstrates that the retrogression was isochemical in nature. Similarly, in the field sample G87-136, a coarse grained rock with purple coloured quartz, was also considered to have undergone retrogression. Thin-section examination showed this to be the case (no residual orthopyroxene was observed). As with G87-129 the low LILE content, very high K/Rb ratio and extremely low Rb/Sr ratio of the sample suggests that it had almost certainly experienced granulite-facies grade metamorphism and underwent isochemical retrogression. Major element analysis suggests the rock is a metamorphosed tonalite (*i.e.*, again a retrogressed enderbite). Samples G87-135 and G87-139 were taken from small shear zones (a few cms wide) again to examine the effects of shearing and possible geochemical and isotopic effects. The shear zone samples G87-133 and G87-139 are composed of fine grained, foliated plagioclase + hornblende + epidote + quartz + biotite (Nutman *et al.*, 1989; and this study). Using plagioclase-hornblende geothermobarometry Nutman *et al.*, (1989) determined that this new mineral assemblage equilibrated at *c.* 550°C and *c*. 5.5 kb (0.55 GPa) (*i.e.*, epidote amphibolite facies grade).

In addition to the samples collected by the author, Lee Riciputi generously supplied powdered aliquots of a number of samples that were collected from west central Nordlandet (see Riciputi *et al.*, 1990). A number of these samples were isotopically analyzed by the author (here designated LR-nnnnnn).

On the eastern side of the Nordlandet peninsula the granulites are predominantly dioritic to quartz dioritic in composition (that is, norites and quartz norites) while on the western side ultramafic and paragneisses are more abundant.

All of the Nordlandet samples collected by the author were analyzed by XRF, INAA and MSID, and the majority had whole-rock Sm-Nd, Rb-Sr, and Pb-Pb analyses performed on them. Two of these fourteen samples were specifically collected with U-Pb zircon dating in mind (G87-67 and G87-70). Samples supplied by L. Riciputi invariably were analyzed for their common Pb isotopic composition and Sm-Nd systematics; a number were also analyzed by INAA for elemental data.

4.2 Geochemistry

The major and trace element results for the granulite samples collected by the author are given in Appendix 4. On the basis of their major element composition and the Debon and Le Fort (1982) igneous rock classification scheme (Figure 4.1), the majority of the granulite samples may be classified as norites (G87-128, 130, 131) or quartz norites (G87-67, 70, 135, 137, 138, 139), while G87-136 and G87-129 are enderbites (of tonalitic and trondhjemitic parentage, respectively). G87-69 and G87-133 were likely quartz norites prior to retrogression. Unless otherwise identified in the following geochemical diagrams the norites are represented by filled circles, the quartz norites by filled diamonds, the enderbites by an open circle and triangle (tonalitic and trondhjemitic, respectively), the severely retrogressed sample G87-133 by a filled, inverted triangle, and the granitic sheet by an asterisk (see Figure 4.1).

Mineralogically, the norites and quartz-norites are fairly straight forward, containing orthopyroxene + clinopyroxene + plagioclase + quartz ± magnetite ± ilmenite ± amphibole ± biotite ± apatite. When present, the amphibole and biotite invariably replace the pyroxenes, with hornblende

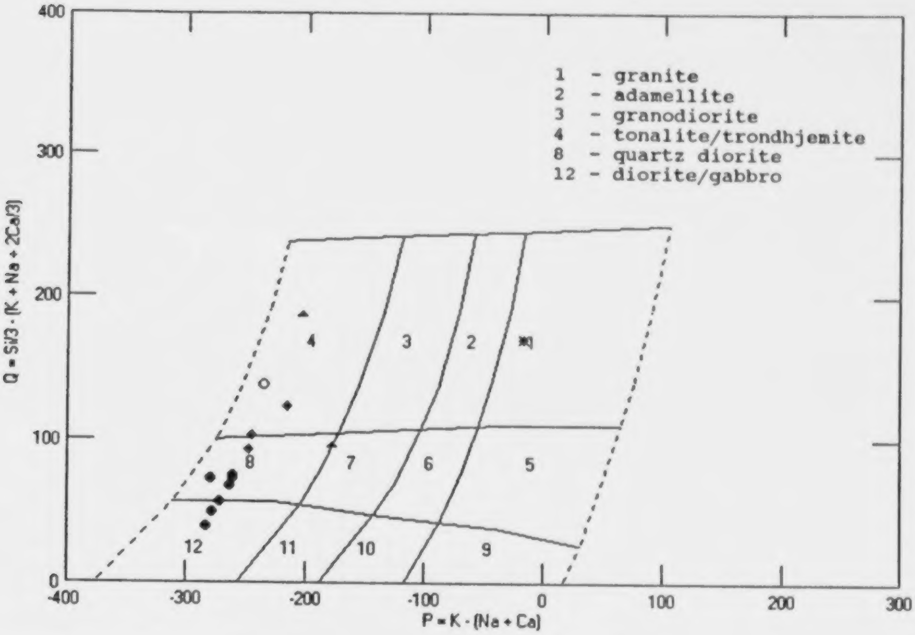

Figure 4.1 Igneous protolith classification of the Nordlandet granulites (according to Debon and Le Fort, 1982; fields as in Figure 3.3)

commonly rimming hypersthene. The presence of a weak penetrative foliation suggests that the granulites formed predominantly by static recrystallization. The granulites display a granoblastic texture.

Shaw (1972) proposed a discriminant function (DF) to identify the parentage of granulites based on the analysis of six major oxides. However, the reliability of the function has been called into question by a number of workers (Paterson (1983) and references therein). The positive values determined for all the granulites collected by the author are indicative of an igneous parentage. Similarly, the fact that all but the trondhjemitic gneiss are metaluminous (diopside normative) suggests an igneous source for the granulites (Figure 4.2). On a TiO_2 *vs* SiO_2 diagram all of the analyzed Nordlandet samples fall in the orthogneiss field defined by Tarney (1976). Using the P_2O_5/TiO_2 *vs* MgO/CaO discrimination diagram for distinguishing ortho- and paragneisses from high-grade complexes (Werner, 1987) all the Nordlandet samples plot in the field indicative of a magmatic origin. Given the agreement of all these indicators it seems most probable that the precursors of the granulites were igneous in nature.

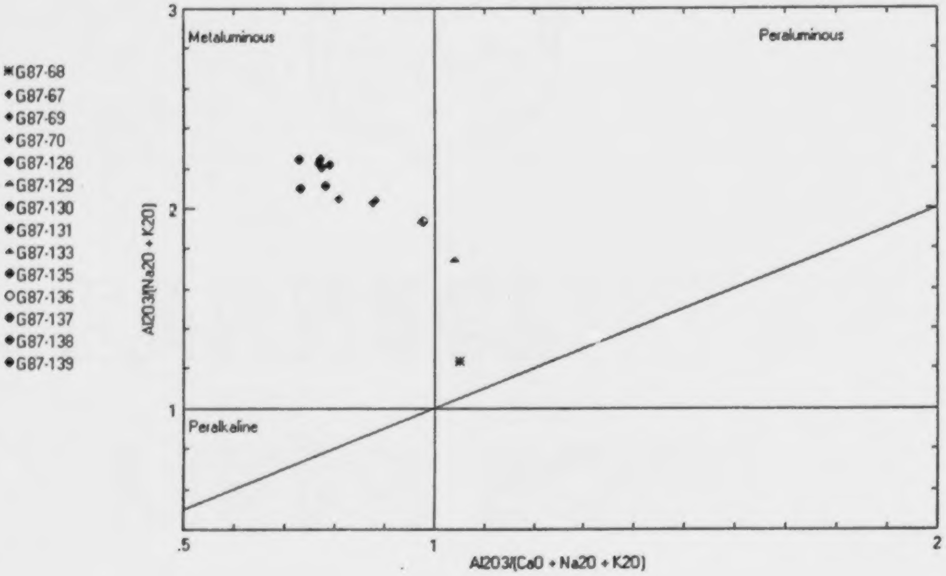

Figure 4.2 Shand's Index for the Nordlandet granulites.

4.2.1 Major Element Chemistry

Harker variation diagrams for the granulites and the late, cross-cutting granite sheet are graphically presented in Figures 4.3 to 4.5.

The silica content of the granulites ranges from *c*. 54 to *c*. 73 wt %, but the majority of samples are dioritic to quartz dioritic in composition (ranging from *c*. 54 to *c*. 61% SiO_2). The Al_2O_3 data show a fair degree of scatter, while TiO_2, FeO*, MgO, CaO, Na_2O and P_2O_5 show a high degree of linearity with varying SiO_2 content. On the basis of these and a number of the trace element Harker diagrams a strong case can be made suggesting that the patterns are representative of igneous differentiation-fractionation processes.

Plotted on an AFM triangular diagram (Figure 4.6) the samples are seen to be calc-alkaline in character and suggest a trondhjemitic trend. However, the data for the more sodic rock-types are too few in number to be definitive. On a Na-K-Ca triangular diagram (Figure 4.7) the depletion in K is readily apparent, and the enderbitic samples show no suggestion of becoming appreciably enriched in K.

Because of the low levels of K_2O, further discussion regarding the K content of the granulites will be left until the section entitled 'Trace Element Geochemistry'.

In the following description of the granulites (unless explicitly stated) any mention of the term 'granulite' implies fresh material with little or no evidence of retrogression.

4.2.2 Trace Element Chemistry

Like the majority of the major elements, silica variation diagrams of many the trace elements display strong correlations with silica content, *e.g.*, Ba, Cr, Co, Hf, Ni, Sc, V, Zn, and Zr (Figures 4.8 and 4.9).

LILE (K, Rb, Cs, U, Th)

The LILE content of granulites are of particular interest with regard to

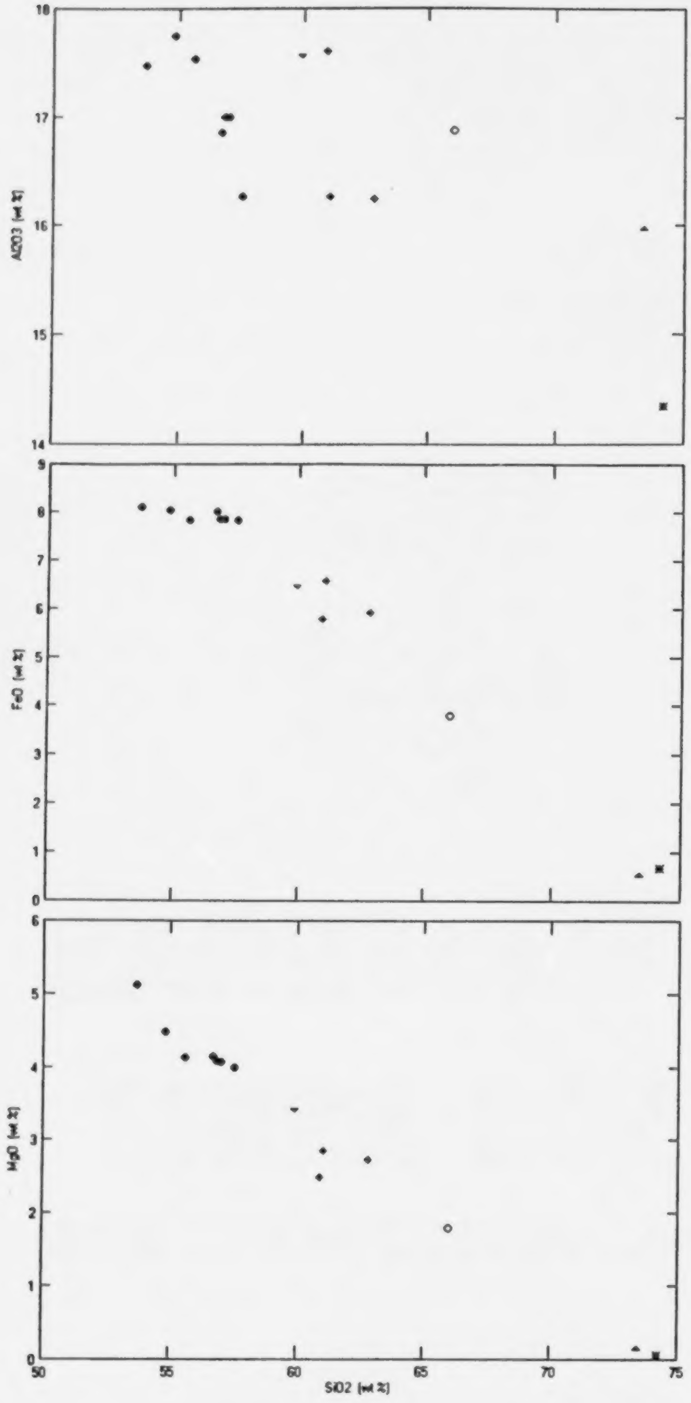

Figure 4.3 Harker diagrams for Al_2O_3, FeO^*, and MgO.

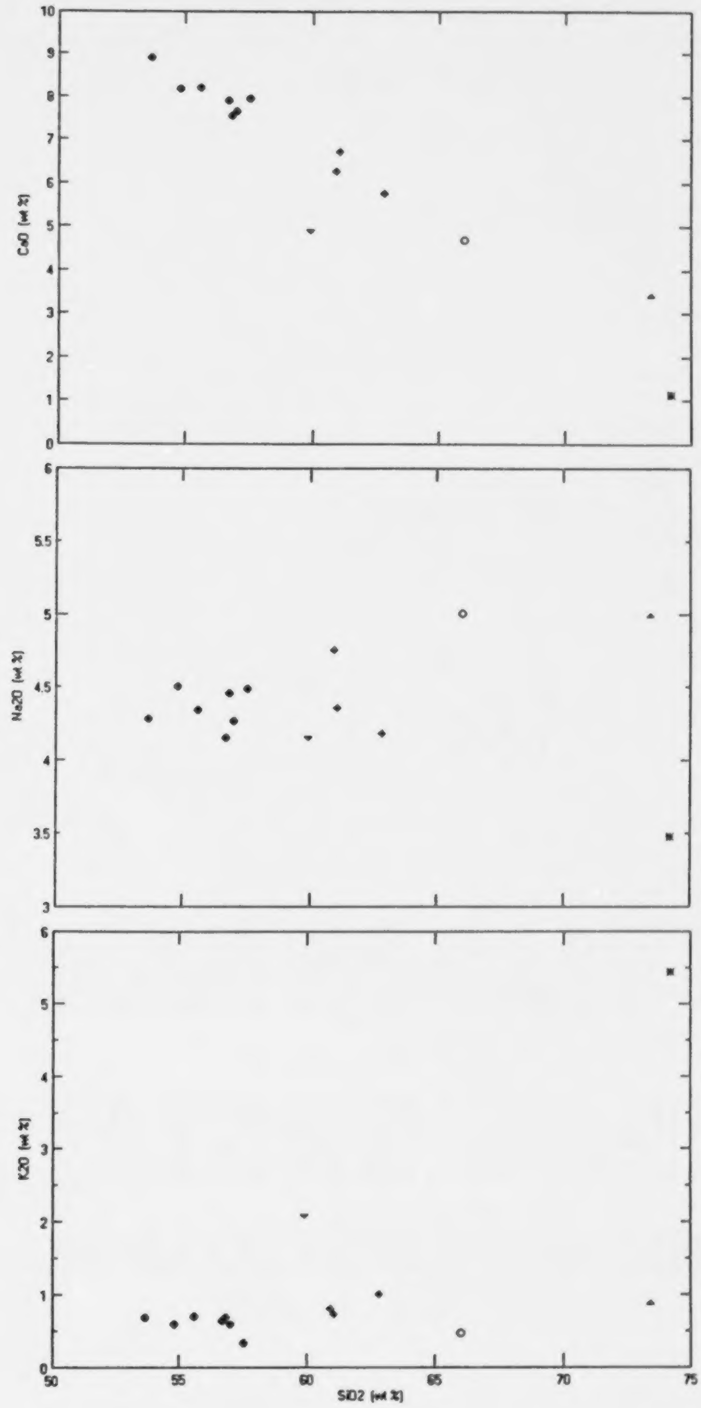

Figure 4.4 Harker diagrams for CaO, Na_2O, and K_2O.

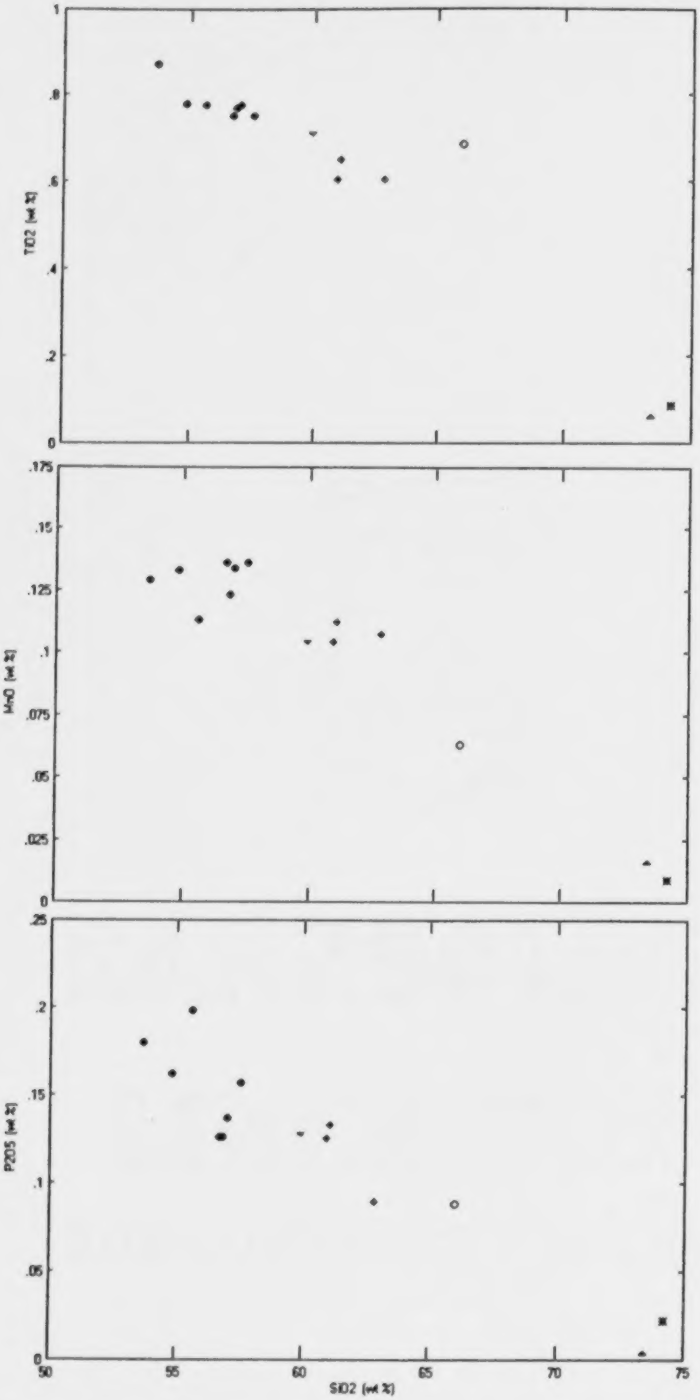

Figure 4.5 Harker diagrams for TiO_2, MnO, and P_2O_5.

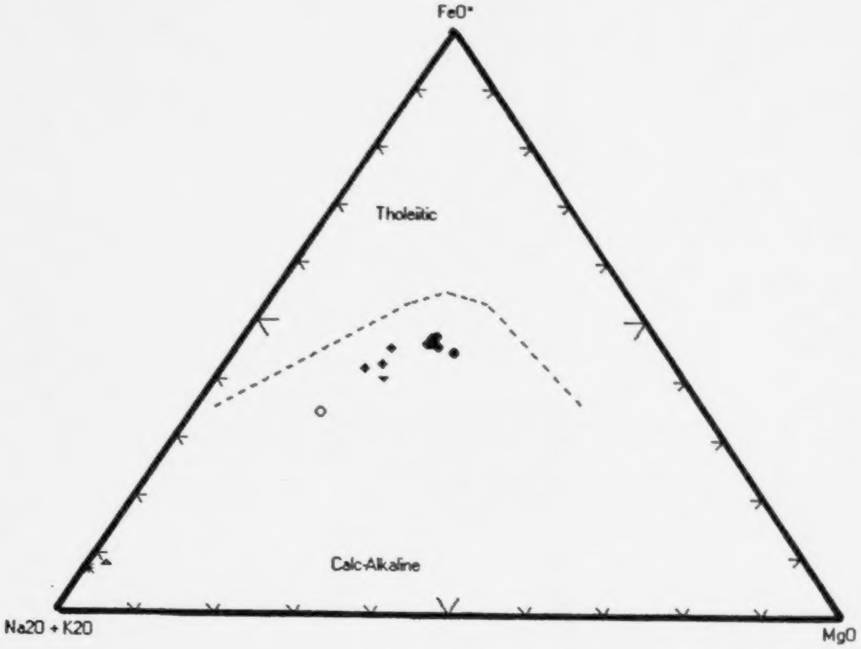

Figure 4.6 AFM plot of the Nordlandet granulites.

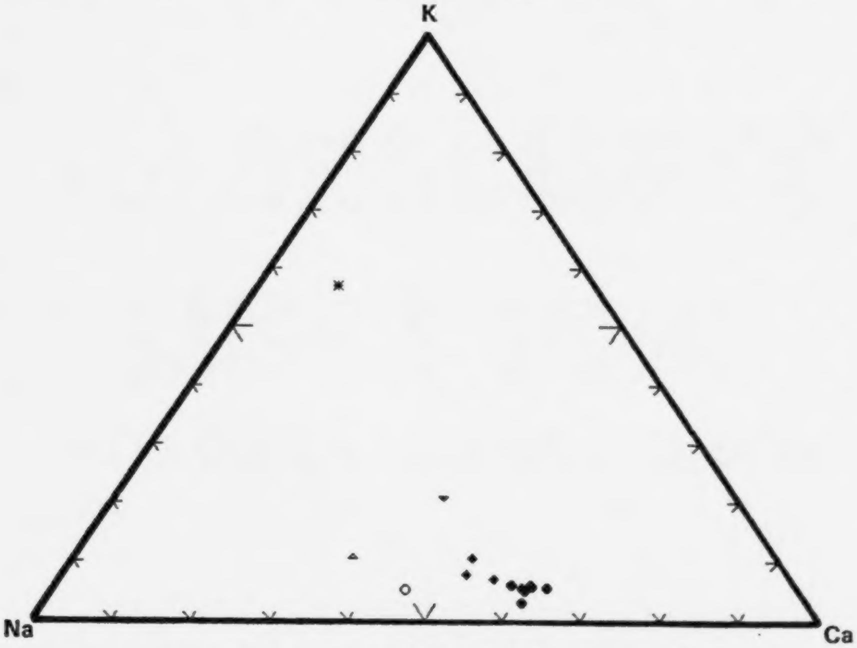

Figure 4.7 Na-K-Ca ternary diagram of the Nordlandet granulites.

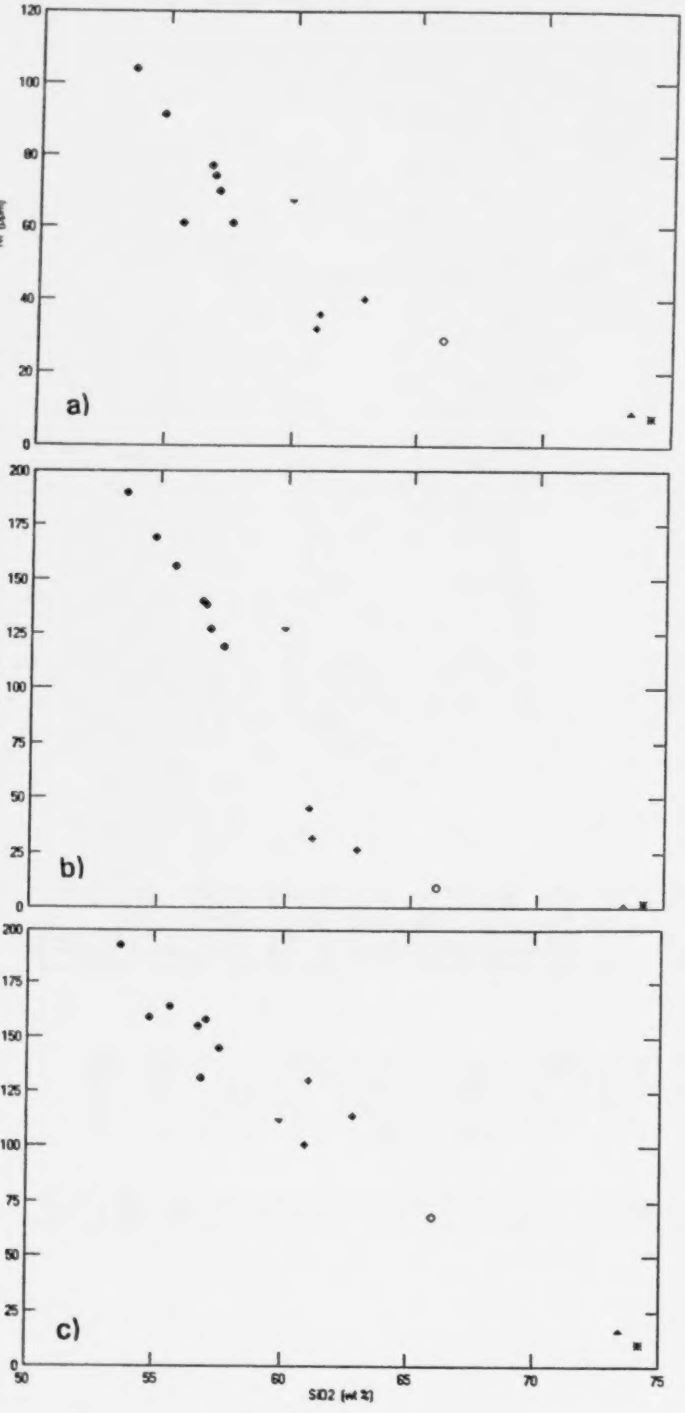

Figure 4.8 Harker diagrams of Ni, Cr, and V.

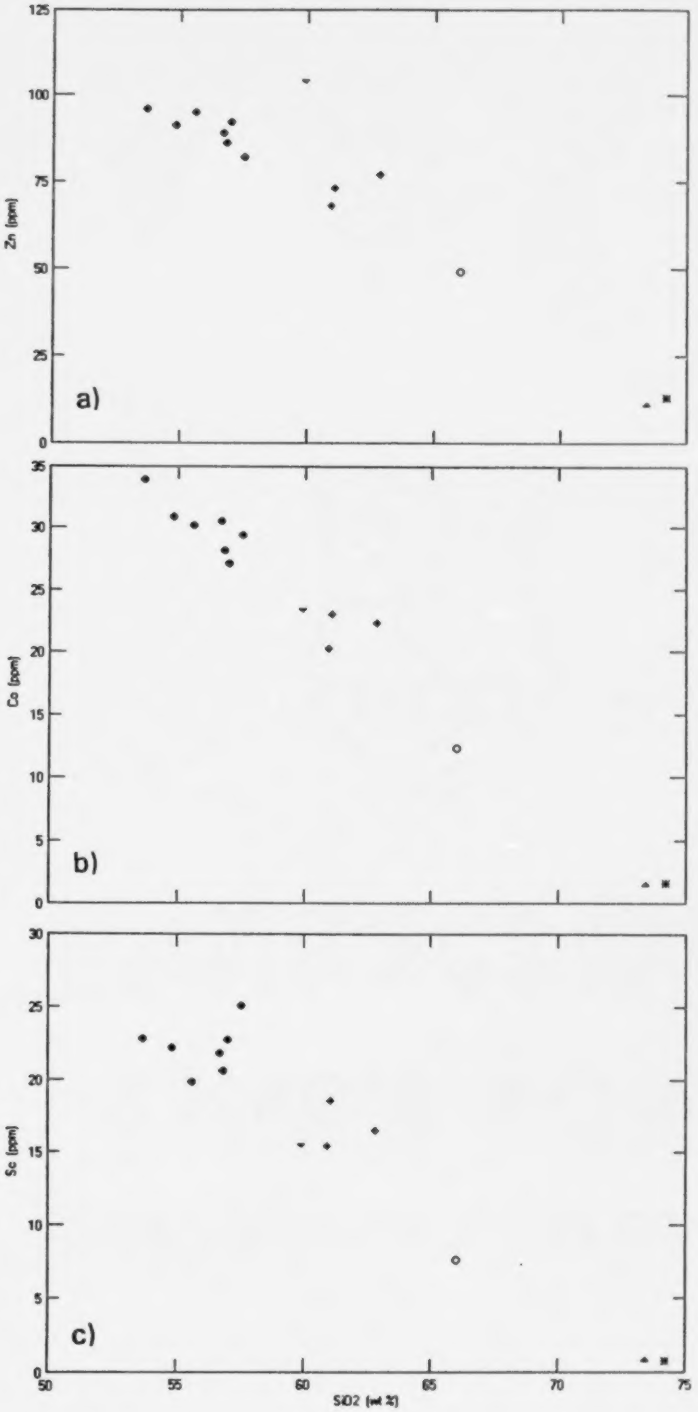

Figure 4.9 Harker diagrams of Zn, Co, and Sc.

understanding possible mechanisms of granulite formation.

The K_2O content of the granulites is uniformly low and less than 0.9%. Those samples that have undergone extensive retrogression (G87-133 and G87-69) show significantly elevated potash levels.

Similarly, Rb levels in the granulites are extremely low, ranging from 9.0 ppm down to a remarkable 0.284 ppm, again with the retrogressed gneisses displaying greatly elevated concentrations. The data are displayed on a K *vs* Rb plot (Figure 4.10) and mimic the Precambrian granulite trend observed by other workers (Jahn and Zhang, 1984; Rudnick, *et al.*, 1985) as opposed to Shaw's (1968) main trend (MT). All the granulites show elevated K/Rb ratios far in excess of the average upper continental crustal value of 252, and with one exception in excess of the lower crustal average of 533 (Taylor and McLennan, 1985). Rudnick and Presper (1990) recently compiled and synthesised geochemical data for intermediate and high pressure granulites of all ages. Only one sample is recorded as having a K/Rb ratio > 5000, and that being between 6000 and 7000. Special note is therefore made of samples G87-138 and G87-136. With an elevated K/Rb ratio of 11100 sample G87-138 (a quartz-norite) is unique amongst granulites! Even though Rb contamination would reduce the K/Rb ratio, to ensure that the MSID determination of the Rb concentration was reliable the analysis was repeated using a 1 g sample aliquot. The Rb concentration was slightly *lower* than the previous determination, resulting in an increase in the K/Rb ratio. For an enderbite sample G87-136 (of tonalitic parentage) also has an extremely high K/Rb ratio (5130).

Figure 4.11 demonstrates the inverse relationship between K/Rb and K content, and that Rb depletion relative to K is responsible for the extreme ratios (Rudnick *et al.*, 1985). That K is depleted is shown by the lower K/Sr ratios of the granulites ($\leq$ 31) compared to average upper crustal value (51), or the retrogressed granulites of this study (61 and 40).

The effect of Rb depletion on the Rb/Sr ratio is discussed more fully

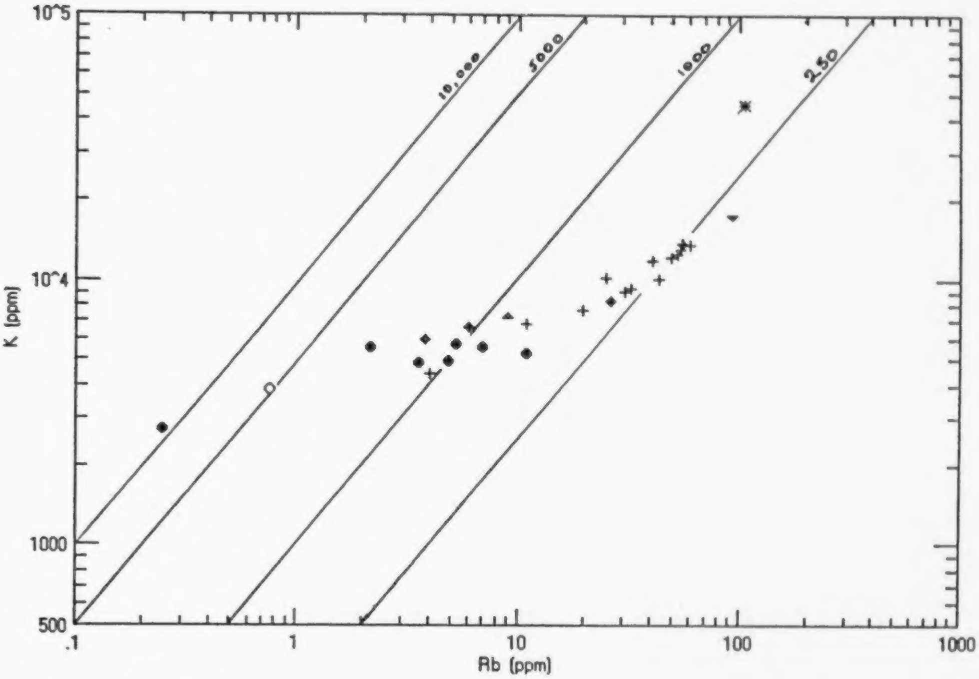

Figure 4.10 Rb *vs*. K of the Nordlandet granulites together with the amphibolite-facies type-Nûk dioritic gneisses (+) for comparison.

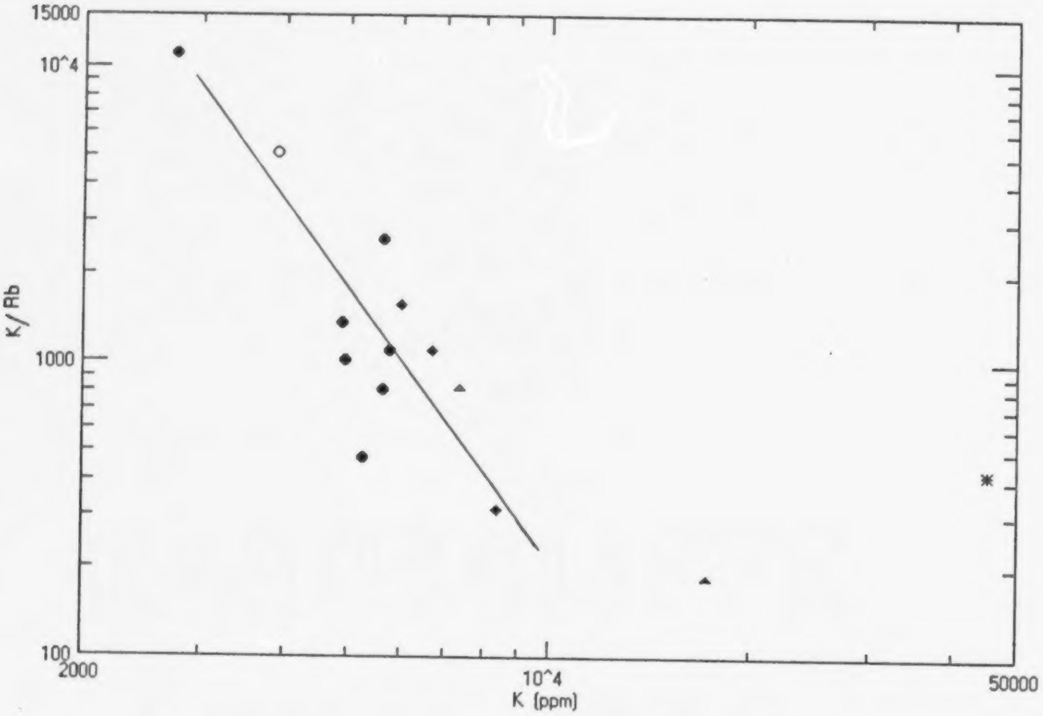

Figure 4.11 K *vs.* K/Rb of the Nordlandet granulites.

under the Rb-Sr whole-rock isotopic section. It is sufficient to mention that Rb/Sr ratios reach very low values (0.001), almost two orders of magnitude less than the median value for Archaean granulites (Figure 4.11).

Cesium was below the detection limit of the INAA scheme utilized for the majority of the samples analyzed (*c.* 0.1 - 0.2 ppm) and was only quantified in three of the fourteen granulite samples analyzed (fresh and retrogressed), two of which were from shear zones. Sample G87-129, an enderbite of trondhjemitic parentage, has about 54 ppb Cs (determined by extending the count time for gamma-ray spectrometry by a factor of five). The resultant Rb/Cs ratio of 167 compares with 30.3 and 53 for average upper and lower continental crust, respectively.

As with many other Archaean granulites the Nordlandet granulites are characterized by low concentrations of U and Th (see Table 4. in the isotopic section of this chapter). Unfortunately, the Th content of some of the granulites was below the detection limit of the INAA scheme employed. With the exception of G87-129 (trondhjemitic in composition) all the granulites have Th/U ratios $\leq$ 1.8, which is much lower than the crustal average of 3.8. Similarly, the Th/U ratios of the Nordlandet granulites are *significantly* lower than either the mean (13.9) or median (7.6) value for Archaean granulite terrains (Rudnick and Presper, 1990). Compared with the median Th and U concentrations of 3.4 and 0.4 ppm, respectively for Archaean granulites (Rudnick and Presper, 1990) the Nordlandet granulites, although depleted in both Th and U, appear to be preferentially depleted in Th.

The K/U ratios for the granulites are, with the exception of G87-128, far greater than the assumed crustal value of 10,000 (Figure 4.13). However, all the samples fall below the mean K/U ratio for Archaean granulites (58500) reported by Rudnick and Presper (1990), and most are close to, or below the median value (39400). With a maximum K/U ratio of 44800 the Nordlandet granulites fall well below ratios determined for the

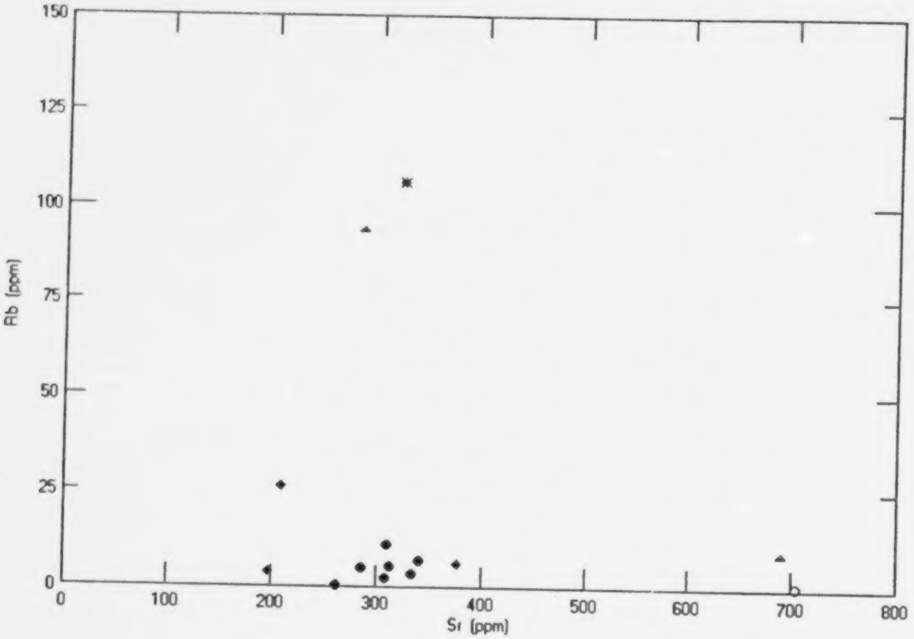

Figure 4.12 Sr *vs* Rb variation diagram for the Nordlandet granulites.

Scourian granulites (many of which are > 100,000). The retrogressed granulites from Nordlandet also have elevated K/U ratios and are indistinguishable from the fresh granulites. Unlike the K/Rb ratios there is no relationship between K/U and K content (Figure 4.13).

For those samples where Th was determined the K/Th ratio varies between 17000 and 29000. It can confidently be assumed that for those samples where Th was below the detection limit of the INAA scheme that the K/Th ratio is equally as high, if not higher, than these values. The measured values are again in excess of the crustal average of *c.* 2630, show no correlation with K content (excluding the granitic sample G87-68), and are also high in the retrogressed granulites. Compared with other intermediate- and high-pressure granulites, only the Scourian granulites consistently show higher K/Th ratios than the Nordlandet granulites (Rudnick and Presper, 1990).

On the basis of the reduced Th/U ratios and greater increase in K/Th ratios *vs* K/U ratios compared to crustal averages, it is concluded that the Nordlandet granulites are more severely depleted in Th than they are in U. This conclusion is affirmed when one examines a Th/U *vs* La/Th plot of the available Nordlandet granulite data (Figure 4.15). The norites and quartz norites in particular are shifted to low Th/U ratios and increased La/Th values, a combination most readily explained by preferential Th loss.

Rare Earth Elements (REE)

The majority of the Nordlandet granulites have Sm/Nd ratios greater than the 0.19 median (mean = 0.19 also) value reported for Archaean granulites by Rudnick and Presper (1990). Excluding the two enderbites, G87-136 (0.193) and G87-129 (0.096), and the sheared, retrogressed granulite G87-133 (0.182), the mean Sm/Nd ratio for the remaining granulites is 0.224 ± 0.017 (n = 11). Thus compared to the majority of

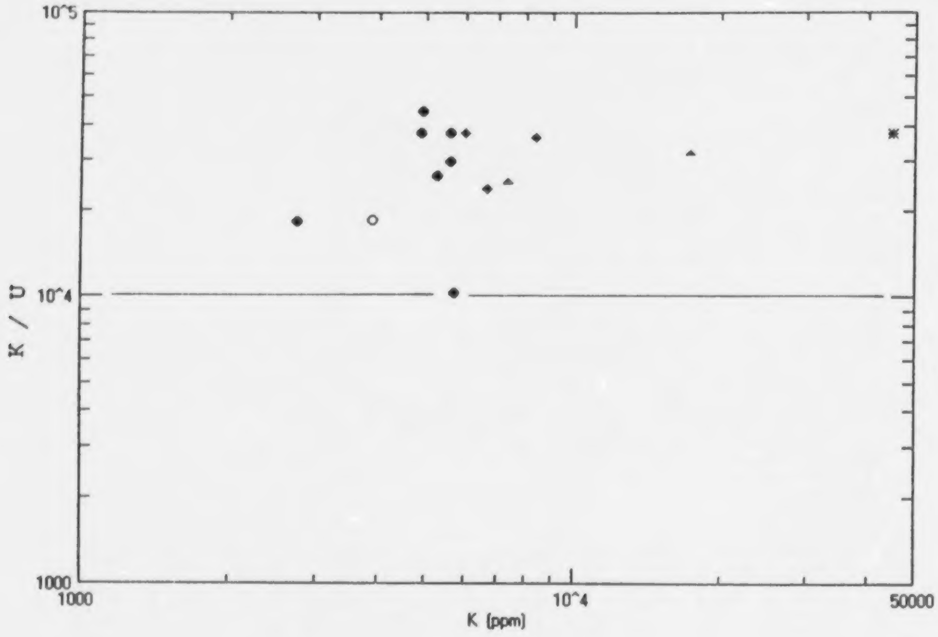

Figure 4.13 K *vs* K/U for the Nordlandet granulites.

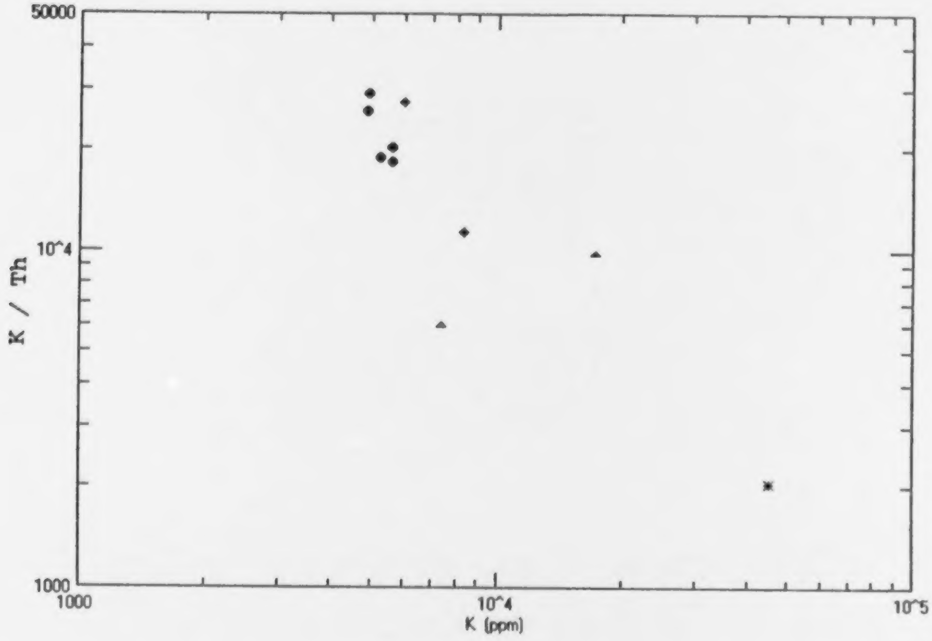

Figure 4.14 K *vs* K/Th for the Nordlandet granulites.

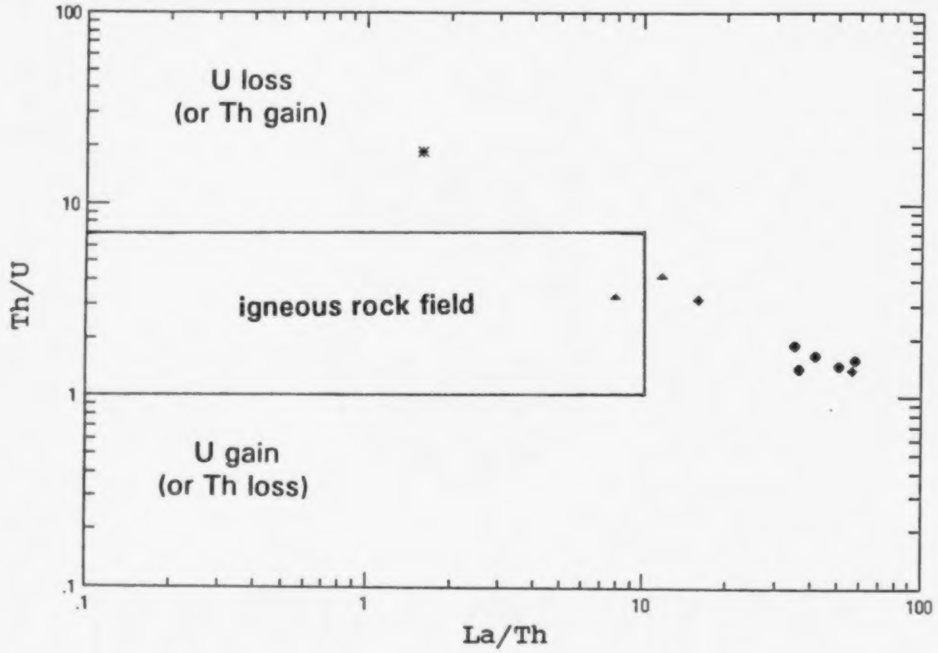

Figure 4.15 Th/U *vs* La/Th for the Nordlandet granulites.

other Archaean granulite terrains the Nordlandet granulites have a flatter LREE pattern. This could be due to the more mafic nature of the Nordlandet granulite protoliths (compared to 'average' Archaean granulites) and/or that the granulites suffered LREE depletion *via* removal of a partial melt phase.

Chondrite normalized REE patterns for the average of the dioritic, and quartz dioritic granulites, the two enderbites, and the average Scourian granulite are plotted in Figure 4.16. The SiO_2 content of the samples are also shown. The dioritic to quartz dioritic granulites have very similar REE patterns and abundances. They are not depleted in the HREE and show only slight LREE enrichment as expressed by the (La_N/Yb_N) ratios a little over 6. From both averages a slight positive Eu anomaly is apparent (Eu/Eu* *c.* 1.1). The patterns are in many ways very similar to the Scourian granulite, but the latter is significantly more LREE enriched (La_N/Yb_N *c.*15) than the dioritic

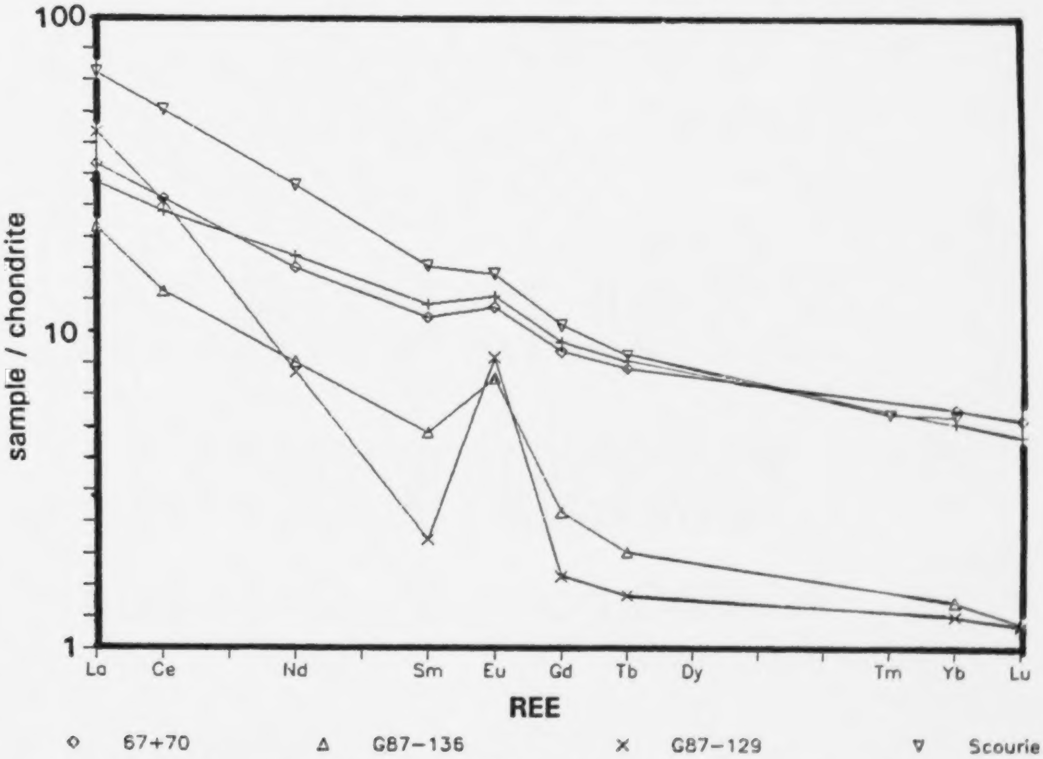

Figure 4.16. Chondrite normalized REE plot of the Nordlandet granulites together with the average Scourian granulite.

gneisses. In comparison to the dioritic granulites the tonalitic sample G87-136 shows significant depletion in the HREE, greater LREE fractionation (La_N/Yb_N = 14) and a distinctly more positive Eu anomaly (Eu/Eu* = 1.7). The trondhjemitic granulite has an even greater positive Eu anomaly (*c.* 4), and LREE fractionation than the other granulites (La_N/Yb_N *c.*35).

Weaver and Tarney (1980a) argued that if LILE depletion in granulites was due to their removal *via* a partial melt this would be reflected in a decrease in the Ba/Sr ratio of the residual granulites as Ba partitions more readily into the melt phase compared to Sr. The fresh Nordlandet granulites have a median Ba/Sr ratio of 0.73 (range 0.44 to 1.25), while the median Ba/Sr for the dioritic type-Nûk gneisses is 0.64. This, coupled with the fact that the dioritic Nûk gneisses do not show the depletion in LILE that the granulites display, is considered fairly strong evidence against depletion of the LILE *via* a partial melt phase.

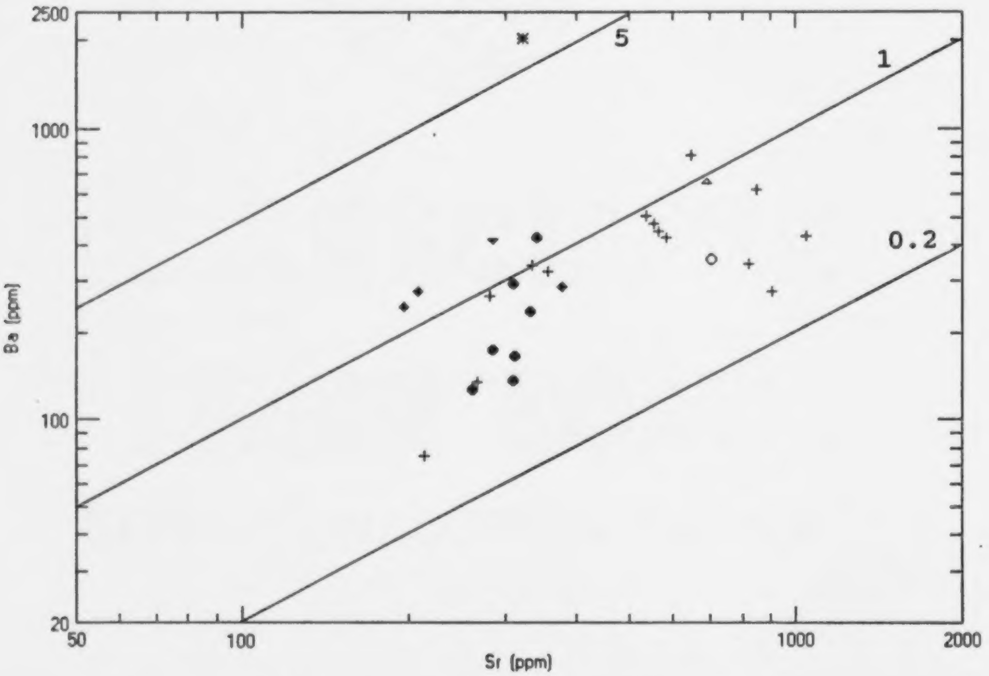

Figure 4.17 Sr *vs* Ba for the Nordlandet granulites and dioritic type-Nûk gneisses (+).

Geochemical Effects of Retrogression

Rehydration of the Nordlandet granulites was accomplished by one of two mechanisms, namely:

- expulsion of hydrous fluids from granitic magmas producing retrogressed aureoles
- generation of shear zones that acted as conduits for fluids.

Both mechanisms resulted in a significant increase in the alkali metals K, Rb and Cs, and the actinides U and Th in the retrogressed granulites.

4.3 Geochronology and isotope systematics

4.3.1 Zircon geochronology

Samples G87-67 and G87-70 were processed and zircons separated for U-Pb geochronology. Both samples were extremely fertile and produced a large fraction of high quality, non-magnetic zircons, many of which were >100 mesh size. Examination of the sized bulk, non-magnetic zircons quickly showed that there were two zircon populations, one light pink in colour, and the other a slightly darker red colour. In many instances zircons displayed readily identifiable cores and rims. As with a number of the type-Nûk gneiss zircon populations, the cores were light pink in colour, and the rims darker. The light pink coloured zircons, in addition to forming cores, occurred as large, broken, irregular fragments; while the darker zircons were generally euhedral and displayed with low aspect ratios (Figures 4.18 and 4.19).

Zircon overgrowths on pre-existing zircons are accepted as morphological evidence for the metamorphic growth of zircon. As mentioned by Heaman and Parrish (1991), in their review of U-Pb geochronology of accessory minerals, such overgrowths are particularly common, though not restricted to, granulite-facies rocks. In addition to rims on pre-existing zircons, a distinct metamorphic zircon population may also form. Heaman

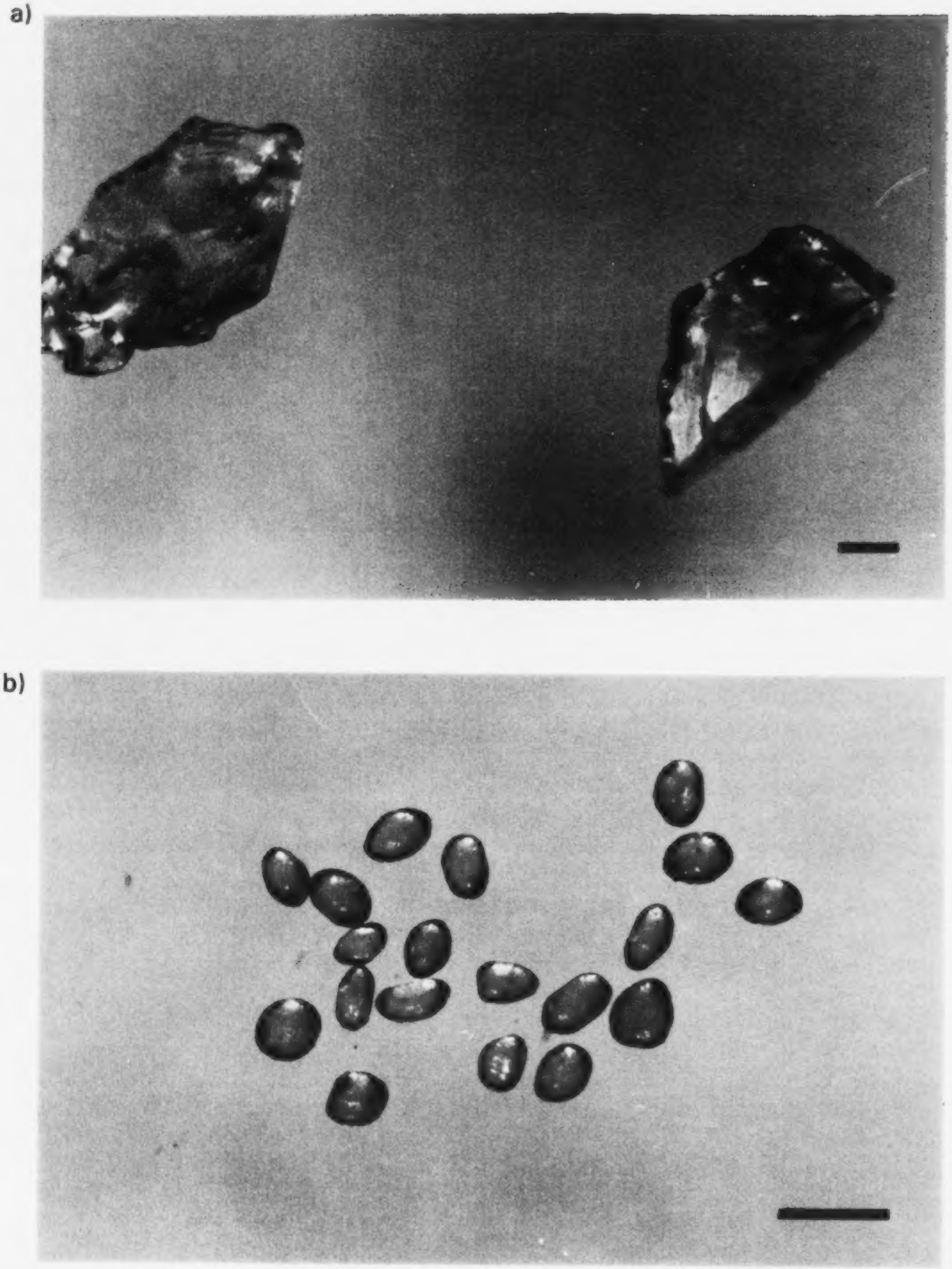

Figure 4.18 Zircons from the Nordlandet granulite G87-70. a) irregular fragments (scale = 100 μm), b) abraded and picked (scale = 0.5 mm).

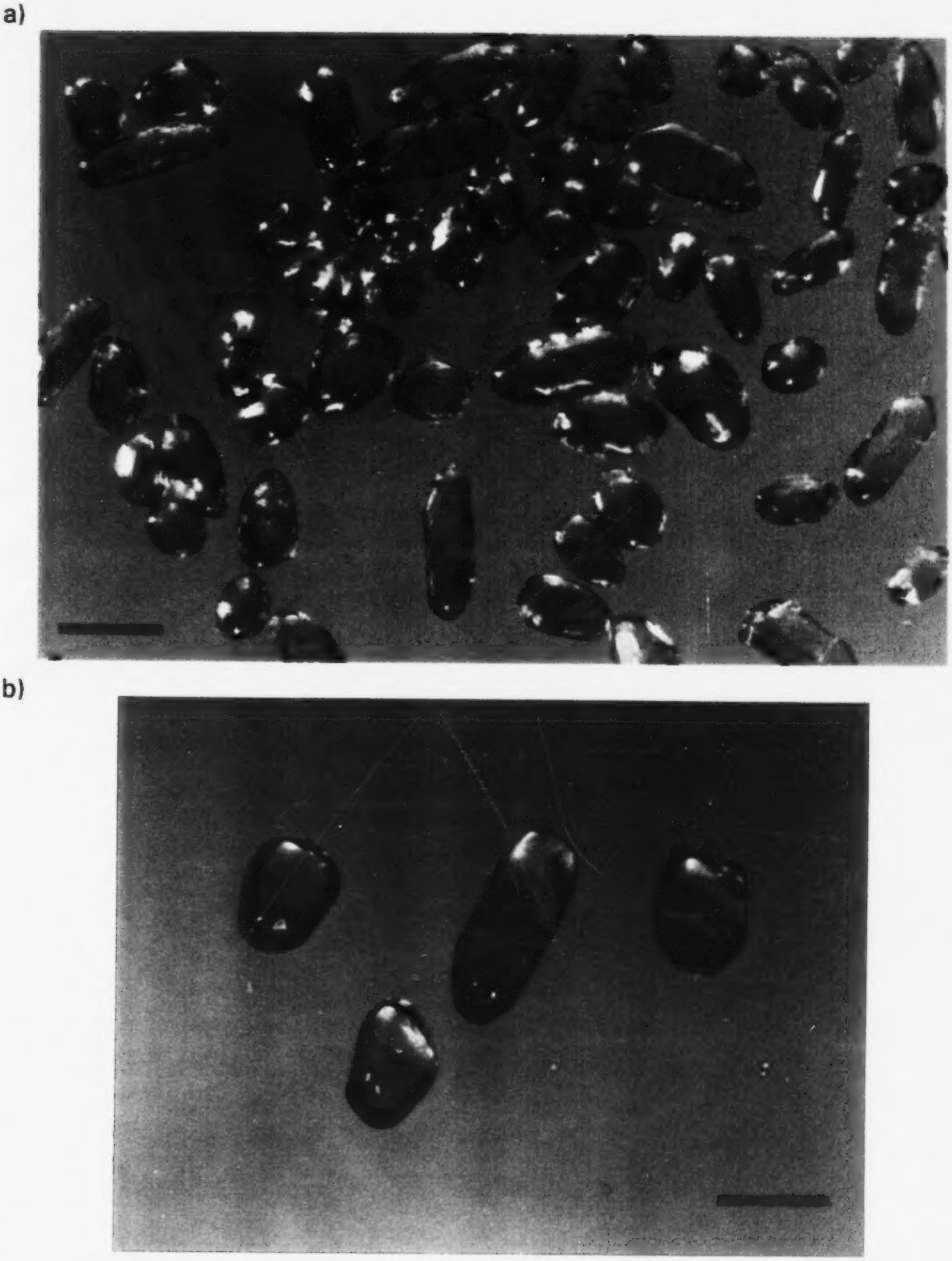

Figure 4.19 Zircons from the Nordlandet granulites a) G87-70, abraded b) G87-67, abraded and picked (oblique lighting, scale = 0.5 mm).

and Parrish (1991) suggest that a general indicator of the metamorphic origin of zircons is their equant, multifaceted, and relatively round morphology (*vs.* the generally more needle-like, orthogonal, by-pyramidal magmatic zircons with a high aspect ratios). They cite an example in which the igneous zircons are large, clear, anhedral fragments while the metamorphic zircons are predominantly clear, multifaceted, equant grains. This description perfectly describes the zircon populations from the Nordlandet granulites (and to a lesser degree from the type-Nûk gneiss, G87-149). The U content of the igneous and metamorphic zircons described by Heaman and Parrish were essentially the same, but, the Th content of the metamorphic zircons was less than that of the igneous ones.

4.3.1.1 Ion microprobe U-Pb analyses

Various sized fractions of the least magnetic (≥ 1.8 A, 0.5° slope) zircons from G87-67 and -70 were mounted in epoxy resin and polished for SHRIMP U-Pb analyses. The ion probe data are presented in Table 4.1 and shown graphically in Figure 4.20 in the more familiar Concordia diagram.

Combined core analyses from both samples gave an age of 3193 ± 7 Ma (2σ), while analyses of rims from G87-70 gave an age of 3014 ± 7 Ma (2σ).

4.3.1.2 Small sample U-Pb analyses

For the chemical U-Pb zircon analyses aliquots of the non-magnetic, >100 mesh, pink and red zircons were generally abraded, before final picking under alcohol, and weighing and cleaning. The U-Pb results are listed in Table 4 and shown graphically in a Concordia diagram in Figure 4.21.

Pink core-material zircons from G87-67 gave a slightly discordant (minimum of 0.9%) ^{207}Pb-^{206}Pb age of 3174 Ma, while one aliquot of similarly prepared 'core' zircons from G87-70 gave a concordant age of 3153 Ma, and a second aliquot from the same sample gave a slightly

Table 4.1 Ion microprobe data for G87-67 and G87-70

Grain	U	Th	Th/U	Radiogenic	204Pb	206Pb*	±1σ	207Pb*	±1σ	207Pb/	207/206
Spot	(ppm)			206Pb (ppm)	(ppb)	/238U		/235U		206Pb	Age Ma (±1σ)
Cores (G87-67)											
1-1	121	122	1.01	97	27	0.6081	0.0181	21.42	0.71	0.25544	3219 ± 18
1-2	90	90	1.00	75	31	0.6328	0.0187	21.92	0.71	0.25125	3193 ± 16
2-2	184	63	0.34	134	28	0.6297	0.0182	21.86	0.65	0.25178	3196 ± 8
3-1	57	61	1.07	49	29	0.6421	0.0202	22.06	0.83	0.24920	3180 ± 27
4-1	44	37	0.84	35	26	0.6332	0.0202	21.40	0.80	0.24517	3154 ± 26
5-1	116	46	0.40	88	20	0.6496	0.0192	22.59	0.71	0.25224	3199 ± 12
6-1	50	47	0.94	41	24	0.6403	0.0199	21.93	0.79	0.24843	3175 ± 24
Cores (G87-70)											
1-1	48	30	0.63	38	35	0.6561	0.0201	22.52	0.76	0.24896	3178 ± 18
2-1	121	99	0.82	102	56	0.6653	0.0195	23.05	0.72	0.25128	3193 ± 13
4-1	35	16	0.46	27	28	0.6390	0.0219	22.23	0.90	0.25226	3199 ± 29
7-1	42	33	0.79	34	42	0.6480	0.0200	22.69	0.80	0.25392	3209 ± 21
8-1	122	46	0.38	95	24	0.6732	0.0195	23.10	0.70	0.24884	3177 ± 9
9-1	91	50	0.55	75	18	0.6865	0.0202	24.16	0.76	0.25524	3217 ± 12
10-1	61	14	0.23	47	34	0.6834	0.0204	23.49	0.75	0.24936	3181 ± 13
11-1	80	22	0.28	60	25	0.6585	0.0165	22.67	0.71	0.24967	3183 ± 12
12-1	337	271	0.80	291	33	0.6830	0.0195	23.55	0.70	0.25004	3185 ± 8
13-1	78	23	0.29	60	10	0.6717	0.0199	23.33	0.74	0.25196	3197 ± 12
14-1	105	83	0.79	90	19	0.6719	0.0197	23.96	0.75	0.25860	3238 ± 13
Rims (G87-70)											
3-1	132	45	0.34	87	36	0.5825	0.0169	17.86	0.55	0.22241	2998 ± 11
4-2	716	115	0.16	479	56	0.6132	0.0173	19.10	0.55	0.22588	3023 ± 4
5-2	486	86	0.18	315	33	0.5943	0.0169	18.11	0.52	0.22097	2988 ± 5
6-1	768	128	0.17	497	36	0.5935	0.0168	18.23	0.52	0.22279	3001 ± 4
7-2	548	158	0.29	381	60	0.6190	0.0175	19.50	0.56	0.22848	3041 ± 5

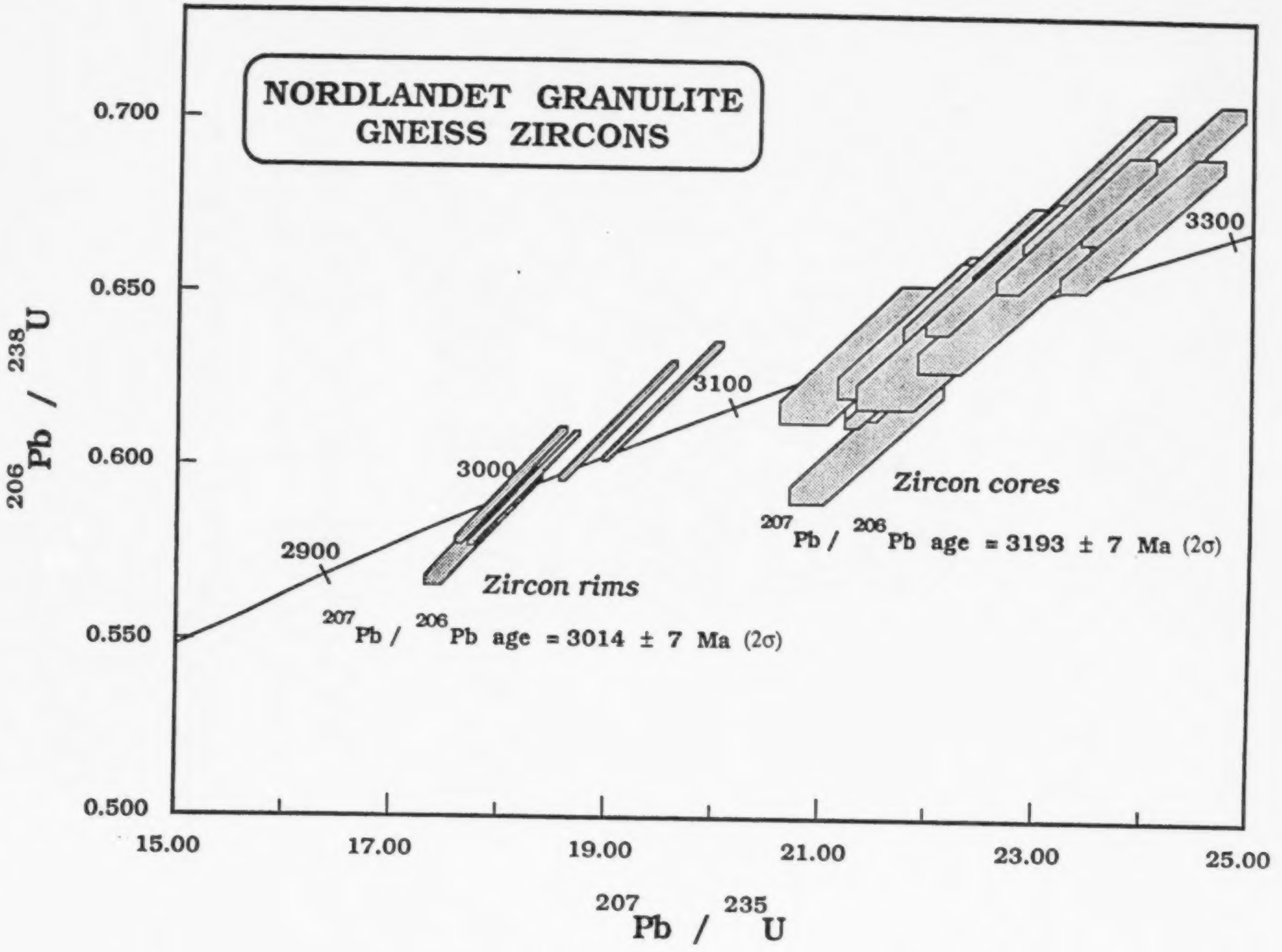

Figure 4.20 SHRIMP U-Pb results of zircons from G87-67 and G87-70.

Table 4.2 Conventional U-Pb zircon results for G87-67 and G87-70.

		Concentration						Atomic Ratios*			Apparent Age (Ma)		
ID	Mass	U	Th	Pb	Com Pb	Th/	^{206}Pb	^{206}Pb	^{207}Pb	^{207}Pb	^{206}Pb	^{207}Pb	^{207}Pb
G87-	(ug)	------		(ppm)	------	U	^{204}Pb	^{238}U	^{235}U	^{206}Pb	^{238}U	^{235}U	^{206}Pb
67c >100	141	82	59	64	0.22	0.723	2523	0.6304	21.587	0.24837	3151	3165	3174
70c >100	152	64	19	46	0.25	0.295	1771	0.6305	21.295	0.24497	3152	3152	3153
70r >100	122	898	122	569	0.28	0.136	20459	0.5835	18.044	0.22427	2963	2992	3012

* - corrected for blank, spike, and common Pb
c - core material
r - rim material
Th concentration data calculated on the assumption of near concordancy

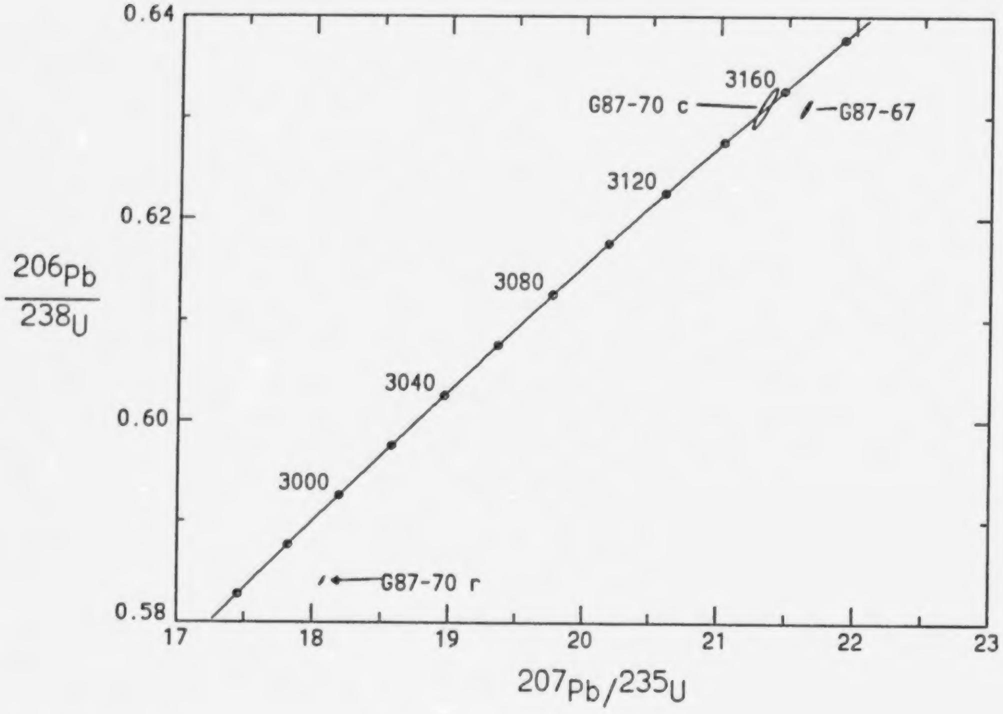

Figure 4.21 Concordia plot of conventional U-Pb zircon analyses from G87-67 and G87-70.

discordant (minimum of 0.4%) ^{207}Pb-^{206}Pb age of 3143 Ma. Analysis of an aliquot of the 'rim' material zircon from G87-70 gave a discordant ^{207}Pb-^{206}Pb age of 3012 Ma (minimum degree of discordancy = 2.0%). It is interesting to compare the U and Th concentration data, together with the Th/U ratios, of the Nordlandet zircons determined by conventional chemical and purely instrumental SHRIMP analyses with the zircon analyses from the type-Nûk gneisses G87-112 and G87-149. Samples G87-112 and G87-149 also display rims and cores, even though they have apparently only been metamorphosed to upper amphibolite-facies grade. The comparison shows that in each of the three examples the U content of the metamorphic zircons is greater than the magmatic ones. The increase is between a factor of 3 and 14. Thorium shows variable behaviour. In some instances there is an increase in Th from the magmatic to metamorphic zircons, while others show a decrease. In all cases, however, the Th/U ratio **decreases** from the magmatic to metamorphic zircons. In regard to these data certain questions come to mind, including:

- where does the U incorporated in the metamorphic zircons come from?
- why was U incorporated in metamorphic zircons (either as rims on preexisting zircons, or as a separate zircon population) instead of being removed (particularly in the case of the Nordlandet granulite sample)?
- given the similar ionic radii and identical charge of U and Th why was Th not incorporated by the metamorphic zircons to the same extent as U?

Unfortunately the metamorphic reactions that give rise to zircon generation are poorly understood. Breakdown or recrystallization of Fe-Ti oxides, clinopyroxene, hornblende, or even existing crystals of zircon may release Zr during recrystallization. It is important to note that many of the zircons forming cores in the Nordlandet granulites show evidence of corrosion and may record the existence of a melt or fluid phase. In the case of the granulites, it is possible that a felsic melt fraction was produced during granulite-facies metamorphism. In the initial stages of its formation this melt may not have been able to escape because it amounted to less than the critical melt fraction and originally remained trapped or enclosed in the protolith. This would give both the opportunity for the residue to equilibrate with the melt phase, and time for the melt phase to begin to possibly corrode existing zircons. As temperatures and/or pressures began to decrease a new generation of zircons began to crystallize forming rims around pre-existing zircons, as well as separate population of metamorphic zircons. Given the extreme depletion of the LILE in the granulites, if originally present, the melt phase must have escaped from the norites and quartz norites.

The U-Pb results show that the amphibolite-facies type-Nûk gneisses are **not** lower-grade equivalents of the Nordlandet granulites. The granulites being *ca*. 150 Ma older than the type-Nûk gneisses. Prior to this study there were no known *c.* 3.2 Ga ages on high-grade gneisses of the region.

4.3.2 Whole-Rock Isotope Systematics

4.3.2.1 Lead-Lead

Whole-rock lead isotopic data for granulites (plus a plagioclase separate) from the Nordlandet peninsula, are given in Table 4.2 together with available whole-rock U and Th concentration data. In addition to the samples collected by the author, there are analyses of a number of samples (supplied by Lee Riciputi) that were collected from west-central Nordlandet.

The $^{207}Pb/^{204}Pb$ and $^{206}Pb/^{204}Pb$ data for *just* the dioritic gneisses (that show little or no retrogression) and the plagioclase separate from G87-67 are plotted in Figure 4.22. An errorchron fitted to the data gives an age of 3029 ± 46 Ma (2σ), MSWD = 29.0 (n=16). This age is within error of the

Table 4.3 Pb-Pb data for the Nordlandet granulites.

ID	$^{206}Pb/^{204}Pb$	$^{207}Pb/^{204}Pb$	$^{208}Pb/^{204}Pb$	U (ppm)	Th (ppm)	Description
G87-67 Plag	12.905	14.236	32.676	na	na	plagioclase
G87-67	13.263	14.302	32.843	0.16	bd	dioritic gneiss
G87-70	13.529	14.410	33.103	0.28	0.39	dioritic gneiss
G87-128	14.390	14.614	33.272	0.37	0.80	dioritic gneiss
G87-129	13.167	14.306	33.244	0.28	1.12	trondhjemitic gn.
G87-130	12.951	14.247	32.926	0.11	0.17	dioritic gneiss
G87-131	13.120	14.290	32.848	0.16	bd	dioritic gneiss
G87-135	12.876	14.173	33.559	0.14	bd	dioritic gneiss
G87-136	13.005	14.257	32.972	0.13	bd	tonalitic gneiss
G87-137	13.067	14.268	33.388	0.12	0.31	dioritic gneiss
G87-138	12.690	14.175	32.586	0.09	bd	dioritic gneiss
G87-139	13.277	14.268	33.640	0.18	bd	dioritic gneiss
LR-341901	13.534	14.421	32.930	na	na	dioritic gneiss
LR-341904	14.076	14.569	33.531	na	na	dioritic gneiss
LR-341918	13.390	14.400	33.346	na	na	dioritic gneiss
LR-341919	13.341	14.390	32.891	na	na	dioritic gneiss
LR-341938	27.002	17.432	40.499	1.16	2.65	dioritic gneiss
LR-341939	13.970	14.503	33.777	na	na	dioritic gneiss
LR-341971	24.744	16.839	36.323	na	na	cpx-rich gneiss
LR-341976	13.034	14.328	34.566	na	na	granitic gneiss

na - not analyzed, bd - below detection limit, U and Th determined by INAA/DNC.

presumed age of granulite-facies metamorphism based on the ion microprobe analyses of zircon rims (3014 ± 7 Ma, 2σ), the slightly discordant conventional zircon analysis which gave a $^{207}Pb/^{206}Pb$ age of 3012 Ma, and the Pb-Pb age of 3000 ± 70 Ma (2σ) determined by Taylor *et al.*, (1980) on granulites from western Nordlandet. The effect of sample 341938, with its extremely radiogenic Pb, on the regression analysis is apparent when the data are processed excluding this sample. The resultant age of 3325 ± 210 Ma (2σ), MSWD = 20.2 (n=15) does not overlap the errorchron age described above at the 95% confidence level. In fact, the 'age' more closely approximates the presumed age of protolith formation (3193 ± 7 Ma) as opposed to the metamorphic event.

Including the trondhjemitic (G87-129), tonalitic (187-136), granitic (LR-341976), and clinopyroxene-rich (ultrabasic ?) (LR-341971) gneisses with all of the other granulites of dioritic composition gives an errorchron age of 3005 ± 36 Ma, (2σ) [MSWD = 31.0, (n=20)]. The radiogenic cpx-rich sample, supports an age of metamorphism close to 3 Ga in agreement with sample LR-341938.

It may be questionable to include rocks of such diverse composition to determine an isochron. Field relations suggest that tonalitic and trondhjemitic gneisses are younger than the dioritic gneisses, and the granitic gneisses still younger. The ultramafic and supracrustal gneisses appear to be older than the dioritic gneisses. However, as demonstrated by their depletion in the LILE, the enderbites (G87-129, -136) underwent granulite-facies metamorphism. If Pb homogenization took place during the granulite-facies metamorphism, then the history of the rocks prior to that time should have no effect on the Pb-Pb isochron age of granulite-facies metamorphism.

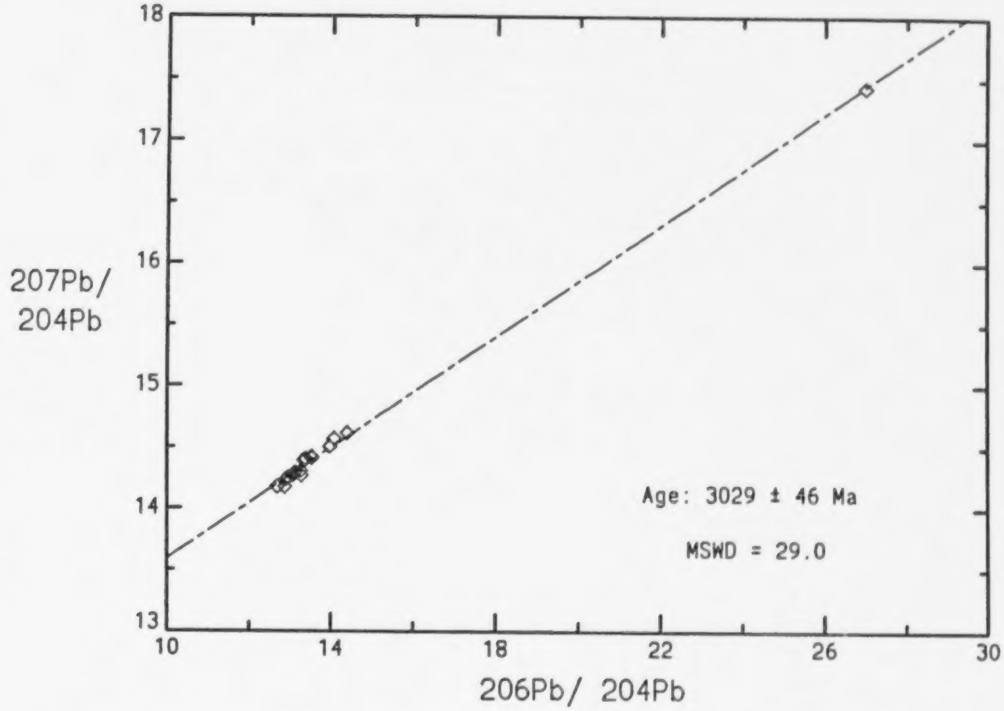

Figure 4.22 $^{207}Pb/^{204}Pb$ vs $^{206}Pb/^{204}Pb$ plot for the Nordlandet dioritic granulites.

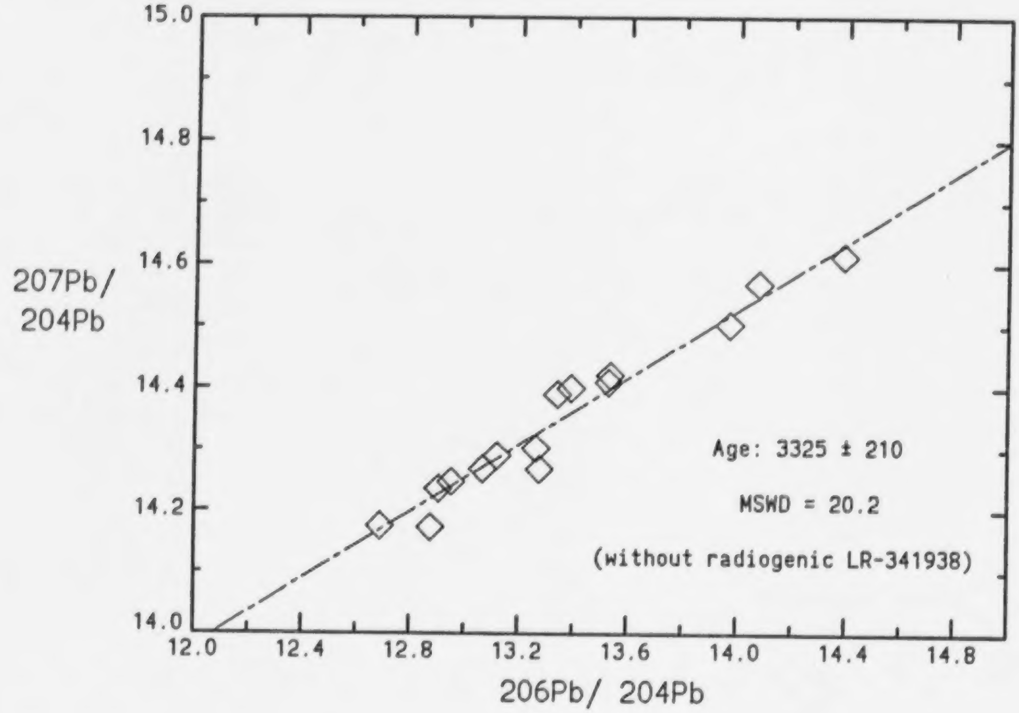

Figure 4.23 $^{207}Pb/^{204}Pb$ vs $^{206}Pb/^{204}Pb$ plot of the Nordlandet dioritic granulites. (same as Figure 4.22 but without sample LR-341938)

4.3.2.2 Rubidium-Strontium

For the same reason that the majority of the granulites display unradiogenic Pb compositions, the Sr isotopic composition of the granulites is invariably most unradiogenic. Dioritic sample G87-138 is unique in its extreme LILE depletion. As a result the sample has a very low $^{87}Sr/^{86}Sr$ ratio (0.70148), as well as a Pb signature not unlike the much older Amîtsoq gneisses. Taking the date of granulite-facies metamorphism as 3.0 Ga then the enderbite G87-136 (with a measured $^{87}Sr/^{86}Sr$ ratio of 0.70192 and $^{87}Rb/^{86}Sr$ ratio 0.0031) had a $^{87}Sr/^{86}Sr_{in}$ of 0.70018. This value almost falls within the 95 % confidence limits of the source evolution of tonalites and trondhjemites (Peterman, 1979). This does not take into consideration the Sr evolution from the time of protolith formation to granulite-facies metamorphism. Similar to the U-Th-Pb isotopic system, the Rb-Sr system has undergone at least a two-stage history - from protolith formation until the time of granulite-facies metamorphism and from cessation of granulite facies metamorphism until the present. Tonalitic type-Nûk gneisses show a wide range in $^{87}Rb/^{86}Sr$ from *c.* 0.104 to 0.704. If it is assumed that the initial $^{87}Rb/^{86}Sr$ of the igneous precursor of G87-136 was also in this range (and probably at the lower end of the range as the higher values give initial Sr ratios < BABI), one can calculate that the initial $^{87}Sr/^{86}Sr$ ratio was *c.* 0.7000. Peterman (1979) showed that it would be difficult to discriminate between granitoid rocks derived by partial melting of low $^{87}Rb/^{86}Sr$ source rocks soon after the formation of the source rocks and granitoid rocks produced directly by the partial melting of mafic oceanic crust. Both would have low $^{87}Sr/^{86}Sr_{initial}$ ratios. Similarly, because the time between the protolith formation and granulite-facies event was so short, it is not possible to use the mantle-like $^{87}Sr/^{86}Sr_{in}$ ratio calculated for G87-136 to discriminate between a mode of origin by a two-stage mantle derivation, or a three-stage history involving partial melting of low Rb/Sr dioritic (?) lower crustal material during granulite facies metamorphism. If the LILE were lost by partial melting of the precursors of the norites and quartz norites, then it is difficult to imagine that the enderbitic gneisses G87-136 and G87-129 are the products, because they also show extreme LILE depletion. Consequently, little age information can be extracted from the Rb-Sr system.

Those samples that suffered noticeable retrogression are readily identified on the basis of their higher concentrations of Rb and U, increased Rb/Sr ratio, and more radiogenic $^{87}Sr/^{86}Sr$, compared to the fresh granulites.

4.3.2.3 Samarium-Neodymium

Whole-rock Sm-Nd isotopic data were determined for the majority of the granulite samples collected by the author and samples supplied by Lee Riciputi from west-central Nordlandet. The measured Sm, Nd concentration data and $^{143}Nd/^{144}Nd$ and $^{147}Sm/^{144}Nd$ ratios are presented in Table 4 together with the parameters associated with Sm-Nd isotopic systematics.

The $^{143}Nd/^{144}Nd$ and $^{147}Sm/^{144}Nd$ data are plotted in a conventional isochron diagram in Figures 4.24 and 4.25. In Figure 4.24 only those granulites that showed no obvious signs of retrogression are plotted, while in Figure 4.25 all the samples are plotted. The fresh granulites give a very imprecise age 2957 ± 140 Ma (2σ) with a fairly low MSWD (2.99). The uncertainty largely being due to the restricted range of the variables. Model ages (T_{CHUR} and T_{DM2}) calculated on the basis on the basis of the 0.50876 $^{143}Nd/^{144}Nd$ initial ratio are 2985 Ma and 3120 Ma, respectively. Due to the large uncertainty associated with the regression, the significance, if any, of the 2.96 Ga date is uncertain, though it is within error of the assumed age of the granulite-facies metamorphism. Samarium-Nd mineral analyses of plagioclase feldspar, clinopyroxene, orthopyroxene, and apatite separated from G87-67 displayed a large amount of scatter and indicated an age significantly younger than either the age of protolith formation or age of the granulite-facies event. A similar disparity was found by Humphries and Cliff (1982) who determined a Sm-Nd mineral isochron date of 2.49 Ga for the

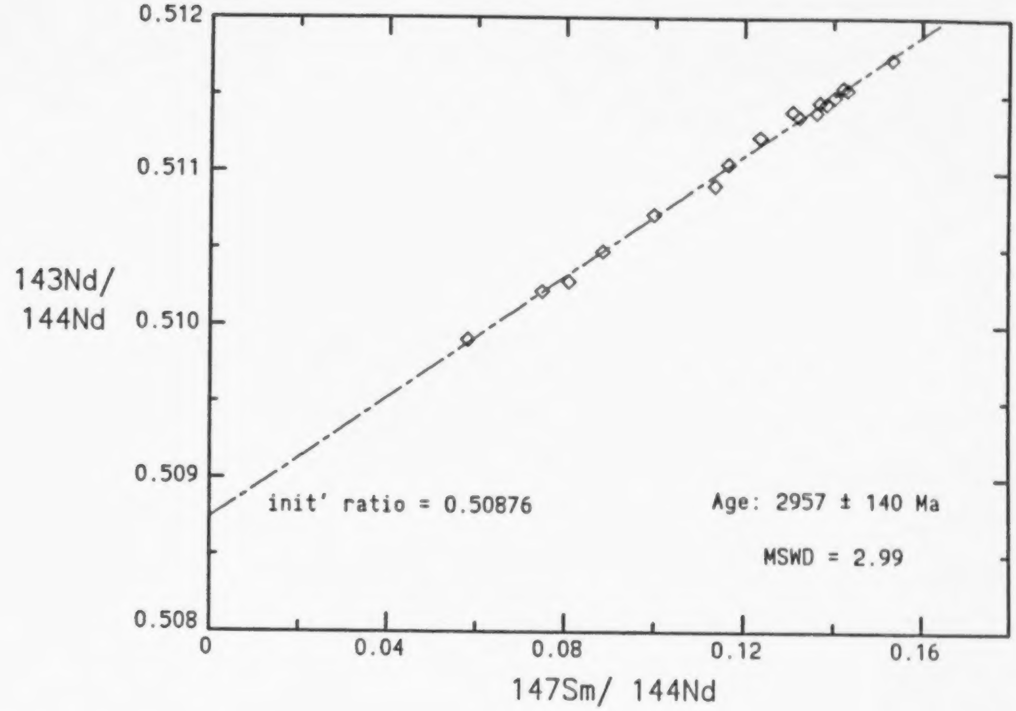

Figure 4.24 Sm-Nd whole-rock isochron plot of fresh granulites.

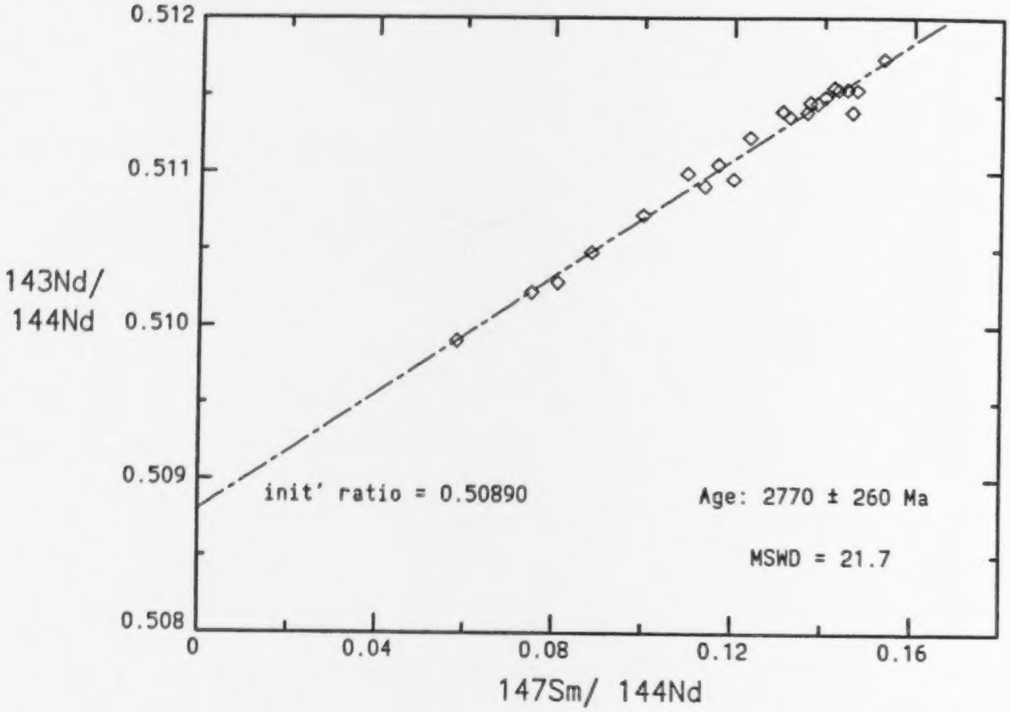

Figure 4.25 Mixed whole-rock Sm-Nd isochron plot.

Scourian granulites; a date that is significantly younger than the time when granulite-facies metamorphism ceased (2.68 ± 0.06 Ga, Chapman and Moorbath, 1978) or the presumed age of protolith formation (*c.* 2.92 Ga) (Hamilton *et al.*, 1976; Whitehouse and Moorbath. 1986). Humphries and Cliff (1982) explained this as a result of re-equilibration of the REE on a grain-size scale after the peak of granulite-facies metamorphism. This may equally apply to the Nordlandet granulites.

All the analyzed granulites (retrogressed and fresh) are plotted in Figure 4.25 and give an errorchron age of 2770 ± 260 Ma (2σ) [MSWD 21.7]. The initial ratio of 0.50890 corresponds to an ϵ_{CHUR} of -2.6.

Most of the granulites have Sm-Nd model ages greatly in excess of their conventional and ion microprobe U-Pb zircon ages. In an attempt to explain this difference it was considered worthwhile to speculate on the isotopic consequences of the formation and removal of a partial melt during granulite-facies metamorphism. Assuming that the precursors of the Nordlandet granulites were originally quartz-dioritic to tonalitic in composition then partial melting of such rock-types would result in Nd partitioning preferentially into the melt over Sm. This would cause the Sm/Nd ratio of the residue to increase. Consequently, the Sm-Nd system will have a '2-stage' history. On an ϵ_{Nd} *vs* T diagram the trajectory of the protolith will decrease to a lower slope in ϵ-T space to compliment the partial melt fraction. Therefore, calculation of a 'T_{DM} age' involves extrapolation back along the second-stage Sm/Nd ratio for a residuum resulting in intersection with the DM curve at an older age than would have been achieved if the rocks had only a 'single-stage' history (excluding partial melting of the source of the dioritic rocks). It can be assumed that model ages for the partial melt fraction will give erroneous results too because a) DM mantle was not its immediate source and b) it too will have suffered a 2 stage history and the trajectory will be overly steep, giving an excessively young age Arndt and Goldstein (1987). Graphic analysis of this idea failed to

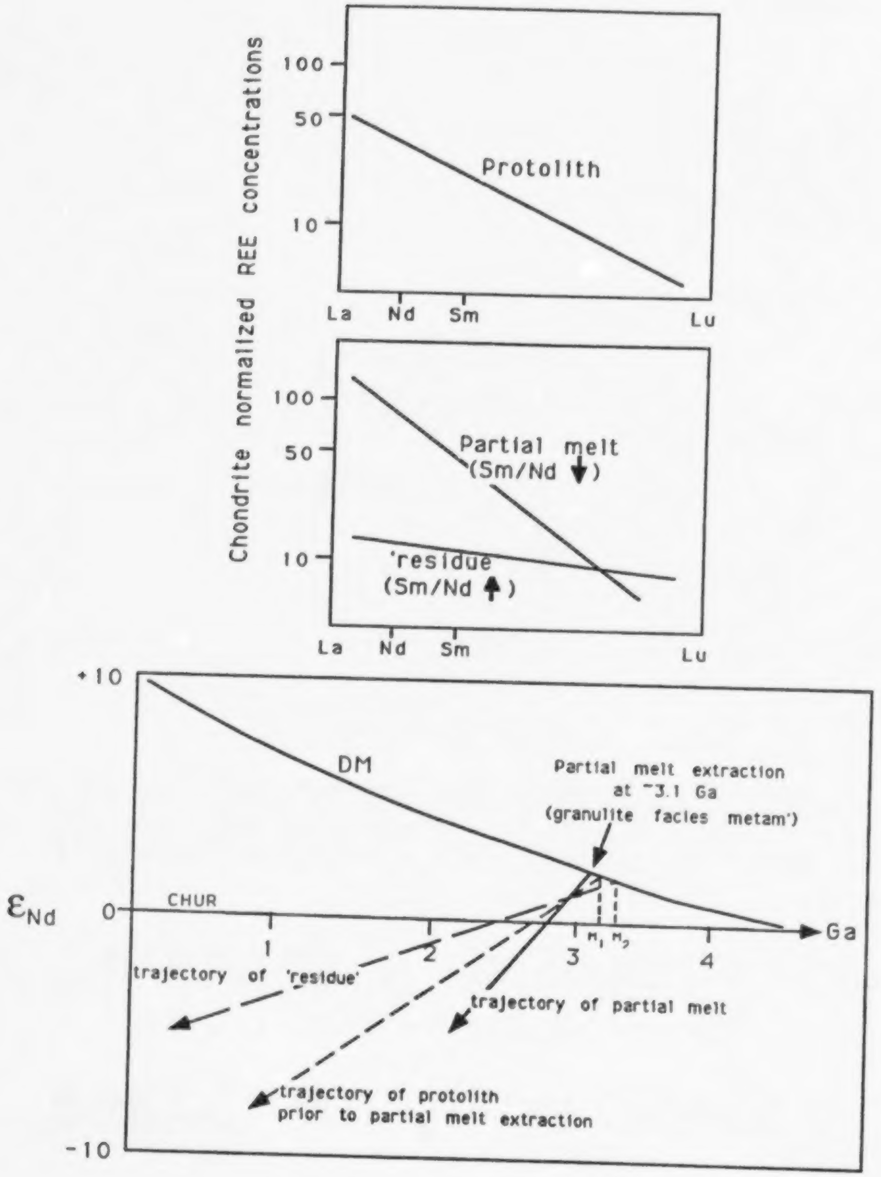
Chondrite normalized REE concentrations
100
50
10
Protolith
La
Nd
Sm
Lu
100
50
10
Partial melt
(Sm/Nd ↓)
'residue
(Sm/Nd ↑)
La
Nd
Sm
Lu
+10
0
-10
ε_{Nd}
DM
CHUR
Partial melt extraction
at ~3.1 Ga
(granulite facies metam')
1
2
3
4
M_1
M_2
Ga
trajectory of 'residue'
trajectory of partial melt
trajectory of protolith
prior to partial melt extraction

Figure 4.26 The effect of partial melt extraction on Nd model ages.

produce model ages greater than about 100 Ma older than the U-Pb age of *c*.3.2 Ga, interpreted as the age of the protolith. Nelson and DePaolo (1985) suggested that the maximum error in a Model age due to fractionation of the f Sm/Nd was equal to the change in f Sm/Nd * difference in age between the protolith and the fractionating event. They suggested a delta f Sm/Nd of 0.2 as a reasonable upper limit, and given the difference in the protolith and granulite-facies event as 200 Ma, the maximum error would be about 40 Ma.

A number of Sm-Nd studies in granulite-facies rocks have shown REE mobility (*e.g.*, DePaolo *et al.*, (1982), Black and McCulloch (1987), Whitehouse (1988)). Consequently, Sm-Nd models ages from granulites should be treated with caution, and the few 3.5 Ga ages calculated here may have no geological implication for the involvement of older crust.

4.4 Discussion

4.4.1 Origin of Granulites

In recent years the origin and geochemical character of granulites has increasingly become of interest. The geochemical and isotopic characterization of the deeper parts of the Earth's continental crust is fundamental to our understanding of the formation and evolution of the crust as a whole. In comparison to the upper continental crust the composition of the lower crust is poorly known (Taylor and McLennan, 1985). As a result neither the bulk composition of the continental crust, nor models of crust-mantle evolution which depend upon a knowledge of this bulk crust composition, are well constrained. This lack of knowledge is in part a consequence of the relative rarity of exposed lower crustal rocks.

On the basis of the high temperatures and pressures commonly displayed by granulites (*e.g.*, > 0.6 Gpa and > 700°C as determined by geothermometry and geobarometry) they are widely considered to be representative of the lower crust. As such, determination of the chemical and isotopic composition of granulite facies rocks, and their variability, is essential to an understanding of crustal evolution. Samples of granulite-facies xenoliths (transported to the surface by volcanic eruptions) and exposed granulite terrains (commonly found in Archaean cratons) are currently the only means by which we may sample, and hence chemically characterize, the lower crust. Rudnick and Presper (1990) reported that although there is an overlap in composition between granulite terrains and granulite xenoliths, the latter have a median composition that is more mafic than the former. Also, in comparing post-Archaean and Archaean granulite terrains they found that Archaean granulites are more felsic than the post-Archaean ones. This variability only serves to exacerbate the difficulty of characterizing the lower crust.

A ubiquitous feature of granulites is that all have undergone some degree of dehydration. Furthermore, a common geochemical characteristic of many granulites (though by no means universal) is their depletion in LILE (*e.g.*, K, Rb, Th and U). This effect was predicted and then described by Heier (1965), and Heier and Adams (1965), respectively. With such LILE depletion comes a concomitant increase in K/Rb, K/U, and K/Th ratios, and a reduction in the Rb/Sr ratio, for example. The cause (or causes) of the LILE depletion (or lack thereof) and the resultant geochemical signatures is controversial, and is inextricably linked to the formation or origin of granulites. The controversy surrounding the origin of granulites was highlighted when Moorbath (1984) mimicked and extended H.H. Read's famous comment about granites when he stated 'there most certainly are granulites and granulites'. Similarly, Harley (1989) emphasised the problem in the title of his paper 'The **origins** of granulites: a metamorphic perspective' (this author's emphasis). Although a large percentage of granulites fall within a fairly tight P-T regime (*i.e.*, 800° ± 50°C and 0.75 ± 0.1 Gpa) Harley (1989) reported in a thorough survey of more than 90 granulite terranes that over 50 % fell outside the above mentioned range.

This, he concluded, was a reflection of the diversity of their modes of origin.

Commonly cited modes of granulite formation (and in some cases LILE depletion), include:

a). partial melting of rocks and the selective removal of H_2O and the LILE in the melt (although Fyfe, 1973 is commonly cited, Lambert (1969) proposed the mechanism)

b). dehydration by fluxing CO_2-rich fluids through rocks

c). recrystallization of already dry rocks.

d). crystallization of magmas under granulite-facies conditions.

Opinion is shifting more and more towards a mode of granulite formation driven by magmatic processes, with partial melt production being touted as the main mechanism of dehydration (*e.g.*, Valley (1992), Clemens (1992)). Magmas could also act as a source of CO_2 for dehydration (Frost and Frost, 1989).

4.4.2 Depletion Of LILE

There are numerous examples of granulite facies rocks that are severely depleted in the heat producing elements (U, Th, and K) and related LIL elements. The cause(s) of this common (though not universal) depletion has been a centre of the debate regarding granulite formation.

The mode of formation and LILE depletion of the granulite facies rocks of the Scourian complex in the northwest highlands of Scotland have been a source of much debate. Some workers argue that pervasive flooding by an externally derived fluid induced the dehydration of the rocks (*e.g.*, Tarney and Weaver, 1987) while others suggest that the generation and extraction of a partial melt phase was the controlling mechanism (Pride and Muecke, 1980; Rollinson and Windley, 1980a,b).

In an attempt to elucidate the mechanism(s) of granulite formation Cohen *et al.*, (1988) carried out a detailed isotopic study of a granulite-facies ultrabasic-basic sequence from the Scourian complex, NW. Scotland.

They were able to demonstrate that the ultrabasic lithology showed little or no LILE depletion, while the enclosing grey gneisses immediately adjacent to the ultrabasics, were highly depleted in LILE. They concluded that partial melting may have been the principal mechanism by which U and Th (and by inference other LIL elements) were depleted because of the high solidus lithologies (*i.e.*, the ultrabasics). Riciputi interpreted sample 341971, a clinopyroxene-rich granulite from west central Nordlandet, as possibly being an ultramafic pod (L. Riciputi, written comm, 1990). The Pb-isotopic composition of this sample is extremely radiogenic in comparison to all but one of the other granulites analyzed (Table 4.3). If Riciputi's interpretation regarding the protolith of LR-341971 is correct then it could be argued in the same manner put forward by Cohen *et al.*, (*ibid.)* for the Scourian granulites, that formation and removal of a partial melt fraction resulted in the depletion of LIL elements in the Nordlandet granulites. A problem with this hypothesis however, is the even more radiogenic character of dioritic granulite LR-341938, compared to LR-341971. It is also strange that this dioritic gneiss, although depleted in Rb and Cs, is enriched in U and Th compared to the other dioritic granulites (Table 4.3).

In an attempt to assess the possible role of a partial melt on the depletion of the LILE the median chemical composition of the amphibolite-facies type-Nûk dioritic gneisses are compared with the those of dioritic composition from Nordlandet in Table 4.4. Ratios of the 'immobile' trace HFSE in the granulites to those in the amphibolite-facies rocks indicate a fairly constant value at *c.* 0.6. A similar value is obtained for Ba, Sr, and Pb. In comparison ratios for Rb(0.16), K (0.49), Th (0.18), and U (0.32) indicate a decoupling of the LILE. Also apparent is the preferential depletion of Rb over K, and Th over U. These data suggest that LILE depletion was not effected by partial melt extraction, but that selective transport by metamorphic fluids was responsible. This scenario is the same as deduced for the Scourian granulites by Weaver and Tarney (1980a) and requires low H_2O activity fluids.

4.5 Conclusions

SHRIMP and single zircon U-Pb analyses, determined as part of this study, have shown that the age of the protoliths of the dioritic granulites from the eastern side of Nordlandet is 3193 ± 20 Ma (2σ). Consequently, the protoliths of the Nordlandet granulites are $\geq$ 125 Ma older than the igneous precursors of the type-Nûk gneisses. These data settle any debate as to whether the two suites are contemporaneous in nature.

Ion microprobe and conventional U-Pb small sample zircon analyses of metamorphic zircon rims and metamorphic zircons give an age of peak granulite-facies metamorphism at 3012 ± 7 Ma. Consequently, there may well be a genetic link between the granulite-facies metamorphism and the intrusion of large volumes of the precursors of the type-Nûk gneisses. As suggested by McGregor *et al.*, (1986) the intrusion of large volumes of tonalitic, trondhjemitic, and granodioritic magmas into the lower to middle crust would significantly raise the geothermal gradient and could easily promote dehydration of existing crust.

A number of parallels can be drawn between the Scourian granulites and those from Nordlandet. In both cases there was an extensive period of time between protolith formation and granulite-facies metamorphism. In both cases Sm-Nd mineral isochrons gave ages significantly younger than the protolith of granulite-facies metamorphic event (Scourian 2.48 Ga *vs* 2.92 Ga; 2.82 Ga *vs* 3.19 Ga) Scourian event Humphries and Cliff, 1982. This indicates that small scale requilibration of the REE occurred for a period of *c.* 400 Ma during cooling and excavation of the complex.

Furthermore, granulite facies rocks from the Lewisian of the NW Highlands of Scotland, and in particular the Scourian complex, show extreme LILE depletion, to such a degree many researchers consider them

Table 4.4 Comparison of granulite and amphibolite-facies dioritic and quartz-dioritic gneisses from the Akia terrane.

	Nordlandet granulites	type-Nûk dioritic gneisses
	(n=9)	(n=8)
	mean 1σ	mean 1σ
SiO_2	56.5 ± 2.0	57.4 ± 3.6
Al_2O_3	17.2 ± 0.5	17.8 ± 1.2
TiO_2	0.76 ± 0.07	0.82 ± 0.17
Fe_2O_3	2.13 ± 0.20	1.87 ± 0.35
FeO*	5.74 ± 0.53	5.06 ± 0.94
MnO	0.13 ± 0.01	0.11 ± 0.02
CaO	7.80 ± 0.71	6.79 ± 1.09
MgO	4.06 ± 0.68	3.34 ± 0.80
K_2O	0.62 ± 0.13	1.26 ± 0.29
Na_2O	4.40 ± 0.17	4.75 ± 0.52
P_2O_5	0.15 ± 0.02	0.29 ± 0.13
Mg#	0.483 ± 0.025	0.467 ± 0.028

	Median	Median	Granulite /Amphibolite
Ni	63	27	2.33
Cr	109	36	3.03
Sc	21	17	1.24
V	146	136	1.07
Ba	216	344	0.63
Rb	5	32	0.16
Sr	298	541	0.55
Zr	86	133	0.65
Hf	1.7	3.1	0.55
Y	12	18	0.67
Nb	3.4	4.7	0.72
Cu	9	37	0.24
Zn	85	82	1.04
Pb	9	14	0.64
La	10	27	0.37
Ce	21	58	0.36
Nd	11	28	0.39
Sm	2.4	5.3	0.45
Eu	0.99	1.04	0.95
Tb	0.40	0.60	0.67
Yb	1.10	1.36	0.81
Lu	0.166	0.165	1.01
Ta	0.23	0.38	0.61
Th	0.29	1.6	0.18
U	0.19	0.6	0.32

major oxides in wt %, trace element concentrations in parts per million (ppm) geochemically unrepresentative granulites and make no attempt to explain their geochemistry. However, the LILE depletion demonstrated by the Nordlandet granulites show that the Scourian granulites are not unique in their extreme LILE depletion. The K/Rb ratios of the Nordlandet granulites are the largest on record for granulites, and the granulites have been depleted in Th to a greater extent than U. Elemental data suggest that LILE depletion of the granulites was due to a metamorphic fluid rather than removal *via* a partial melt.

Chapter 5.

Late Granite Sheets.

5.1 Introduction

Throughout the Akia and Akulleq terranes the dioritic-tonalitic-trondhjemitic-granodioritic gneisses are intruded by late, cross-cutting sheets and dykes of granitic (*s.l.*) composition. Generally, these intrusions do not display the gneissose texture characteristic of the host rocks. In some instances only a slight lineation can be seen in the sheets as indicated by the orientation of biotite, for example.

As part of this study samples from seven granitic sheets/dykes were collected for geochemical and isotopic study - five from the Akia terrane and two from the Akulleq terrane. It was reasoned that if the sheets were the products of the partial melting of existing felsic crust at depth they would inherit the isotopic signature of these source rocks (Moorbath *et al.*, 1981). With its characteristic unradiogenic Pb composition, it was predicted that it might be possible to detect the sub-surface presence of early Archaean Amîtsoq gneisses from the isotopic composition of the granitic sheets (as suggested by Taylor *et al.*, 1980, 1984).

As the terrane model for the region developed, the possible significance of the granite sheets has increased. They are now considered to have been generated during terrane assembly, and thus may provide geochronological information with which to delimit that process (*i.e.*, the date of its initiation, completion, *etc.*). The following is a summary of the geochemical, isotopic, and geochronological study of the granite sheets.

5.2 Classification

Based on their field relations and/or major element composition, the samples collected by the author have been divided into one of four categories, namely sheets that:

a) intrude type-Nûk gneisses which are subdivided into:

i) those of granitic (*s.s.*) composition (G87-19, -61)

ii) those of trondhjemitic composition (G87-114, -115)

b) intrude known Amîtsoq gneisses (in the Akulleq terrane) (G87-27, -141)

c) intrude and cause retrogression of the Nordlandet granulites (G87-68).

Using the normative feldspar granitoid classification scheme (O'Connor, 1965) four of the 'granite' sheets fall in the granite field, namely, G87-19, -61, -68, and -141. Samples G87-114 and G87-115 plot in O'Connor's tonalite field. However, their low ferromagnesian content (particularly G87-115) makes this designation incorrect. They are shifted towards the anorthite apex of the ternary diagram (and consequently into the tonalite field) because of their high CaO content (Figure 5.1 and Table 5.1). Following Barker (1979) these two samples are 'calcic trondhjemites' and employing his modifications to the O'Connor classification (shifting the tonalite-trondhjemite boundary from $Ab_{75}An_{25}$ to $Ab_{70}An_{30}$) the samples in fact, are classified as trondhjemites. Sample G87-27 plots well into the trondhjemite field, and compares very well with Barker's definition of trondhjemite based on the major element composition (Barker, 1979). Employing the igneous classification scheme devised by Debon and Le Fort (1982) samples G87-61, 68, and 61 plot in the granite (*s.s.*) field, G87-19 in the adamellite field, while G87-114, 115, and G87-27 fall in the tonalite-trondhjemite field (Figure 5.2). On the basis of the normative quartz, alkali and plagioclase feldspar content (mesonorm calculation) and the ternary QAP diagram G87-19, -61, -68, and -141 plot in the granite field (monzogranite), G87-114 and -115 in the tonalite-trondhjemite field, and G87-27 in the granodiorite field (Figure 5.3) (but close to the boundary with the tonalite-trondhjemite field). That is, in essential agreement with the other classification schemes. On the basis of the above information samples G87-19, - 61, -68, and -141 are considered granitic (*s.s.*) in composition, and G87-27, -114, and -115 trondhjemitic. In the remainder of this thesis usage of the term 'granitic' or 'granite' sheets will be utilized when referring

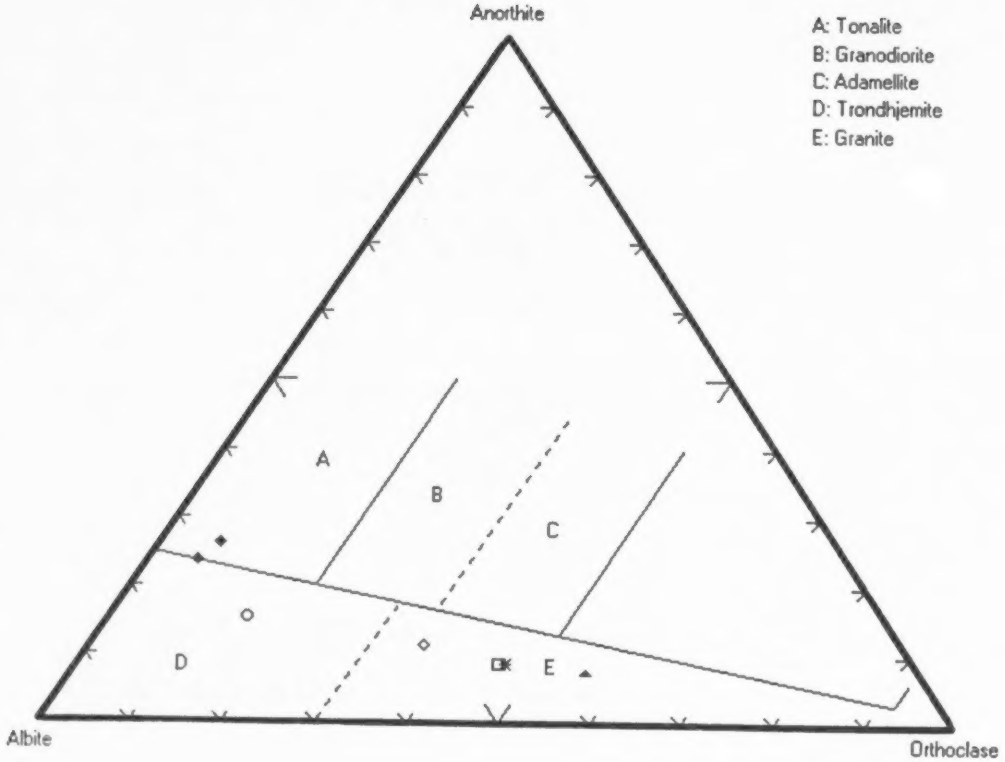

Figure 5.1 Normative feldspar granitoid classification of the granite sheets (after O'Connor, 1965)

Table 5.1 Elemental data for the granitic sheets.

G87-	19	114	115	27	61	141	68	MM
SiO2	73.46	74.85	76.70	71.42	74.95	70.76	74.20	76.5
TiO2	0.17	0.15	0.05	0.14	0.05	0.10	0.09	0.1
Al2O3	14.64	14.75	14.10	16.45	14.13	15.84	14.35	12.9
Fe2O3	0.34	0.27	0.10	0.34	0.11	0.27	0.22	-
FeO	0.78	0.62	0.24	0.79	0.25	0.63	0.50	1.1
MnO	0.02	0.01	0.01	0.02	0.01	0.01	0.01	-
MgO	0.25	0.29	0.08	0.42	0.01	0.21	0.06	0.1
CaO	1.58	3.22	2.86	2.30	1.17	1.10	1.13	0.7
Na2O	4.01	4.62	4.78	5.71	3.49	3.18	3.48	3.8
K2O	4.22	0.69	0.55	1.86	5.31	7.36	5.44	4.7
P2O5	0.04	0.01	0.00	0.04	0.00	0.02	0.02	-
Mg#	28.6	37.8	29.5	40.6	5.0	29.4	13.2	-
Cr	2.6	3.6	-	1.2	-	-	1.9	-
Ni	10	7	8	11	8	8	8	-
Co	1.92	2.28	0.93	1.75	0.35	1.10	1.62	-
Sc	2.65	4.24	0.52	1.59	0.51	1.05	0.74	-
V	15	13	23	2	4	14	10	-
Cu	6	18	16	9	9	8	39	-
Pb	22	16	15	38	30	44	26	-
Zn	21	20	11	31	10	20	13	-
Rb	96.25	16.81	8.21	59.72	96.41	173	106	-
Cs	0.48	0.47	0.17	0.98	0.29	1.99	0.16	-
Ba	900	286	219	223	673	2132	2024	-
Sr	204.0	640.6	510.7	421.4	217.6	248	322	-
Ta	0.24	-	0.02	0.23	0.02	0.30	-	-
Nb	4.4	0.5	0.5	3.1	1.1	4.0	1.0	-
Hf	2.93	3.09	5.42	2.60	1.98	0.85	3.10	-
Zr	101	113	161	100	49	43	98	-
Y	6	1	1	5	2	4	4	-
Th	7.48	2.48	6.05	3.93	4.48	1.70	22.0	-
U	0.56	0.38	0.67	0.48	0.51	0.48	1.20	-
La	20.6	5.99	13.6	14.2	5.27	3.69	35.4	-
Ce	34.1	10.6	26.5	27.3	9.06	6.47	61.2	-
Nd	12.18	4.43	10.61	9.49	3.25	2.63	19.72	-
Sm	2.14	0.61	1.48	1.60	0.52	0.49	2.64	-
Eu	0.55	0.57	0.61	0.45	0.40	0.77	0.48	-
Tb	0.24	-	0.10	0.15	-	0.10	0.16	-
Yb	-	-	-	0.18	-	-	0.16	-
Lu	-	-	-	-	-	-	0.02	-
K/Rb	364	343	553	259	458	353	426	-
Rb/Sr	0.472	0.026	0.016	0.142	0.443	0.698	0.329	-
Ba/Sr	4.41	0.45	0.43	0.53	3.09	8.60	6.29	-
Th/U	13.4	6.53	9.03	8.19	8.78	3.54	18.3	-
K/Th	4679	2323	751	3935	9847	35960	2053	-
K/U	62500	15160	6780	32220	86500	127400	37630	-

MM - minimum melt composition (White and Chappell, 1977)
oxides - weight %, trace elements - parts per million (ppm)

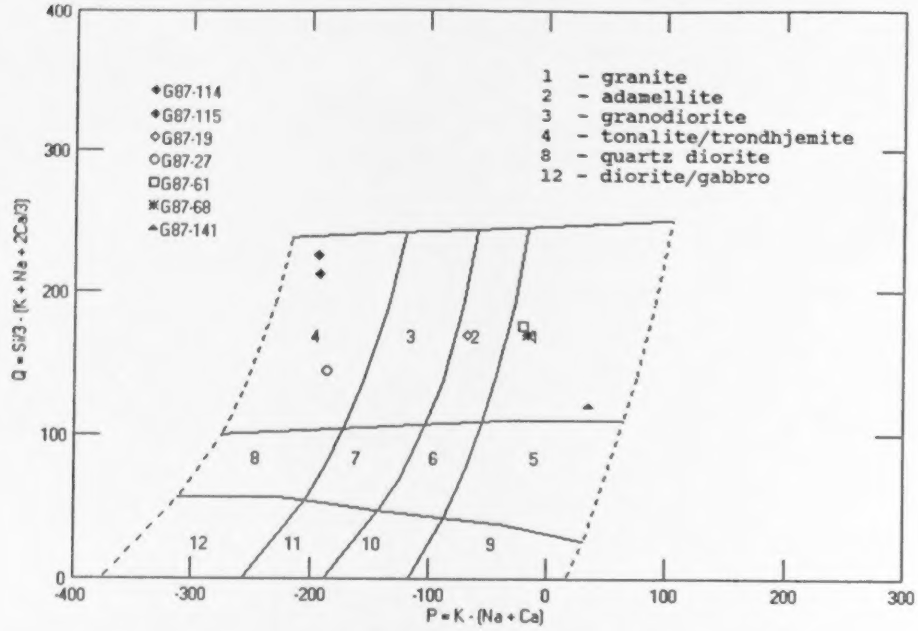

Figure 5.2 Granite sheet classification after DeBon and Le Fort (1982).

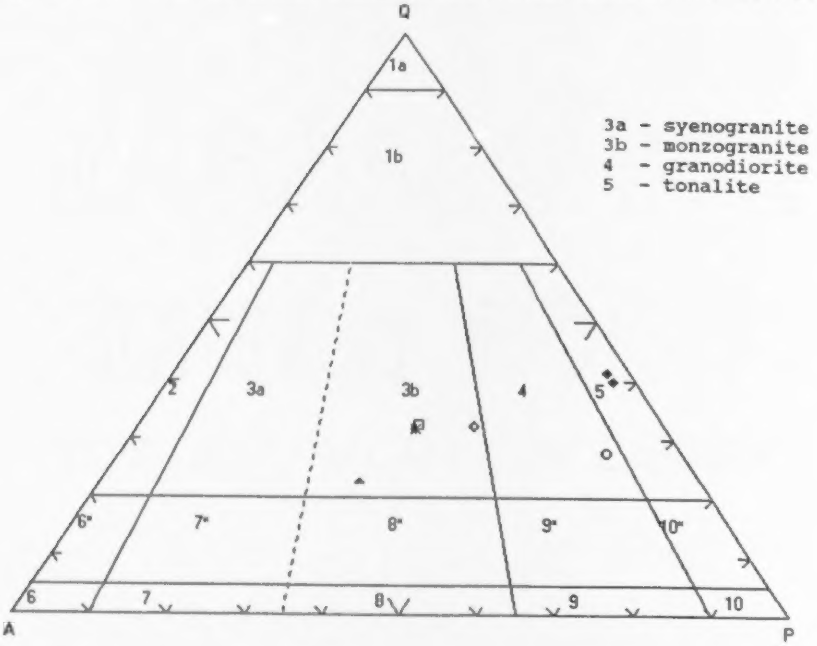

Figure 5.3 Normative Q-A-P plot of the granite sheets.

to the sheets collectively, 'granitic (*s.s.*) sheets' will be used when specifically referring to the samples G87-19, -61, -68, and -141, and 'trondhjemitic sheets' when referring to G87-27, -114, and -115. As shown below (and in Table 5.1) the distinction between the two groups is particularly apparent when one examines the Rb/Sr and Ba/Sr ratios.

5.3 Geochemistry

5.3.1 Major element composition

The silica content of the granite sheets ranges from 70.8 to 76.7 wt %, there being no obvious difference between the silica content of the two groups.

Compared to the trondhjemitic sheets the granitic (*s.s.*) sheets are readily identified by their elevated K_2O and lower CaO content. In some cases the K_2O content of the granitic (*s.s.*) sheets is more than a factor-of-ten greater than that of trondhjemitic sheets G87-114 and -115.

The major element composition of the granitic (*s.s.*) sheets (Table 5.1) closely resembles the minimum melt composition reported by White and Chappell (1977) and suggests these rocks were generated by partial melting of pre-existing crustal material.

When plotted on a Na-K-Ca ternary diagram the granitic (*s.s.*) sheets plot in, or close to, the field for samples of the Qorqut granite (taken from McGregor, 1979) (Figure 5.4). Available petrological, geochemical, and isotopic evidence unequivocally supports a crustal anatexis origin for this granite complex (*e.g.*, Moorbath *et al.*, 1981). On the H_2O saturated pseudo-ternary Or-Ab-Qtz system the granitic (*s.s.*) sheets plot close to the 'granite minimum' (Tuttle and Bowen, 1958). The shift of samples towards the albite apex is indicative of increased P_{H2O} (Luth *et al.*, 1964). The fact that the trondhjemitic sheets plot well away from the granite minimum suggests they formed at greater temperatures than required to produce a minimum melt. Sample G87-141 is a little unusual with its high K_2O content which causes it

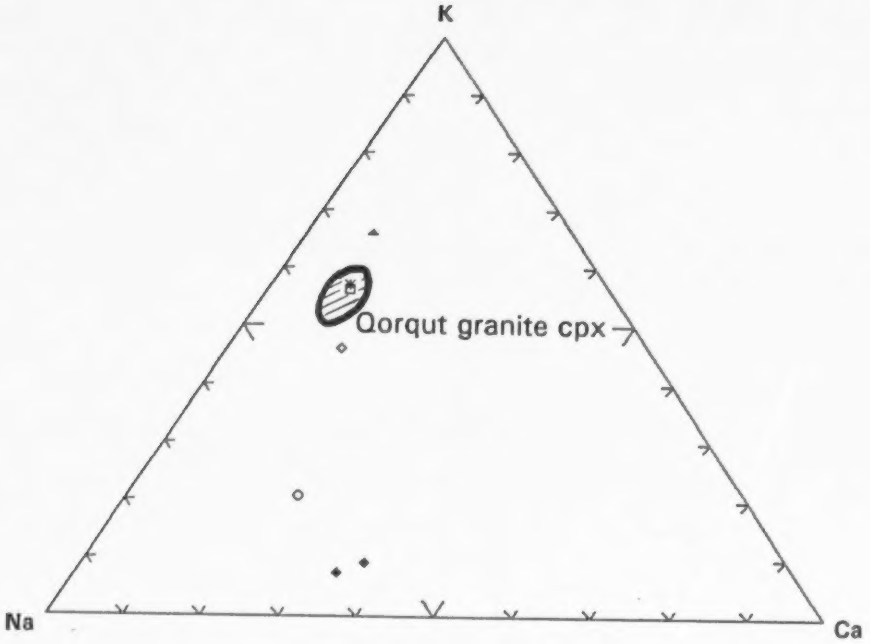

Figure 5.4 Na-K-Ca diagram of the granite sheets

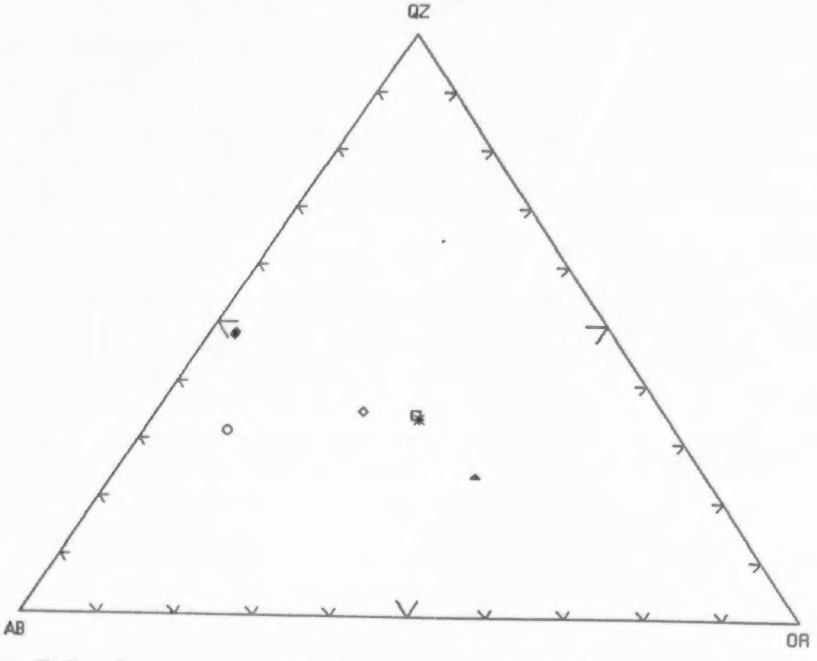

Figure 5.5 Granite sheets plotted on the pseudo-ternary Q-Ab-Or system.

to be shifted towards the orthoclase apex of the ternary diagram.

5.3.2 Trace element chemistry

As expected, the granitic sheets contain very low levels of the transitional elements Cr, Ni, Co, Sc, and V (Table 5.1). In comparison to the type-Nûk gneisses the granitic (*s.s.*) sheets and G87-27 are enriched in the alkalies. The trondhjemites G87-114 and -115 have low alkali contents (excepting Na). A number of the granitic sheets have Rb/Cs ratios that range between average upper and lower crustal values (30.3 and 53, respectively), while others have exceedingly high values (200 - 660). The ratios for the trondhjemitic sheets are all low. The highest value is for the granitic (*s.s.*) sheet, G87-68, that intrudes and locally causes retrogression of the intruded Nordlandet granulite. This is likely a reflection of the trace element content of the source material. Increased depletion of Cs relative to Rb is common in intermediate- to high-pressure granulites (Rudnick and Prepser, 1990).

Again, Pb and Ba concentrations in the granitic sheets are higher than in the type-Nûk gneisses, and as found with the gneisses, show a strong positive correlation with increasing K-content suggestive of K-feldspar control.

All of the granitic sheets have K/Rb ratios falling between the values for average upper (252) and lower (533) continental crust (Taylor and McLennan, 1985), or very close to them. The Rb/Sr ratios of the granitic (*s.s.*) sheets are much greater than found in the trondhjemitic sheets (Table 5.1); this is also the case for Ba/Sr, and is again likely a reflection of K-feldspar control.

With the exception of the G87-141 (a granitic (*s.s.*) sheet that intrudes known Amîtsoq gneiss) the sheets have Th/U ratios $\geq$ 6.5 (range 6.5 - 18.3), which are significantly higher than the crustal average (3.8) due either to Th enrichment and/or U loss. The K/U ratios for the sheets are, with the exception of G87-114 and -115, far greater than the assumed crustal value of 10,000. A number of the granitic (*s.s.*) sheets have ratios significantly greater than 58500, the average value for Archaean granulites (Rudnick and Presper, 1990) - *e.g.*, G87-141 has a ratio of 127400! Sample G87-141 also has a K/Th ratio (at *ca*. 36000) significantly greater than the suggested crustal average of *ca*. 2630, while the remaining samples are within a factor of 2 to 4 of this average.

Unlike granulites, the granitic sheets show a strong positive correlation between K/U and K, indicative of a mineralogical control *i.e.*, K fixed in K-feldspar (Figure 5.6). Although there is more scatter in the data, a similar relationship and interpretation is indicated by K/Th *vs* K (Figure 5.7).

Given the similar chemical behaviour of U and Th during magmatic processes and the elevated Th/U ratios for all the samples (excepting G87-141) the extreme K/U ratios must reflect source rock composition. As for G87-141 it intrudes Amîtsoq gneisses of the Akulleq terrane and as stated earlier the Amîtsoq gneisses at the mouth of Ameralik fjord underwent granulite-facies metamorphism at *ca*. 3.6 Ga which left the gneisses extremely impoverished in U and Th. Partial melting of such a source would produce a granitic melt enriched in K, but still relatively poor in U and Th because of their extreme depletion in the source material. Consequently, the very high K/U and K/Th ratios observed in G87-141 would result.

5.4 Geochronology and Isotope systematics

5.4.1 Uranium-lead zircon analyses

Zircons were separated from three of the seven granitic samples. One sample (G87-19) was analyzed using the SHRIMP, the other two (G87-114 and G87-27) were analyzed using the single-bead method described in Appendix 3 and TIMS.

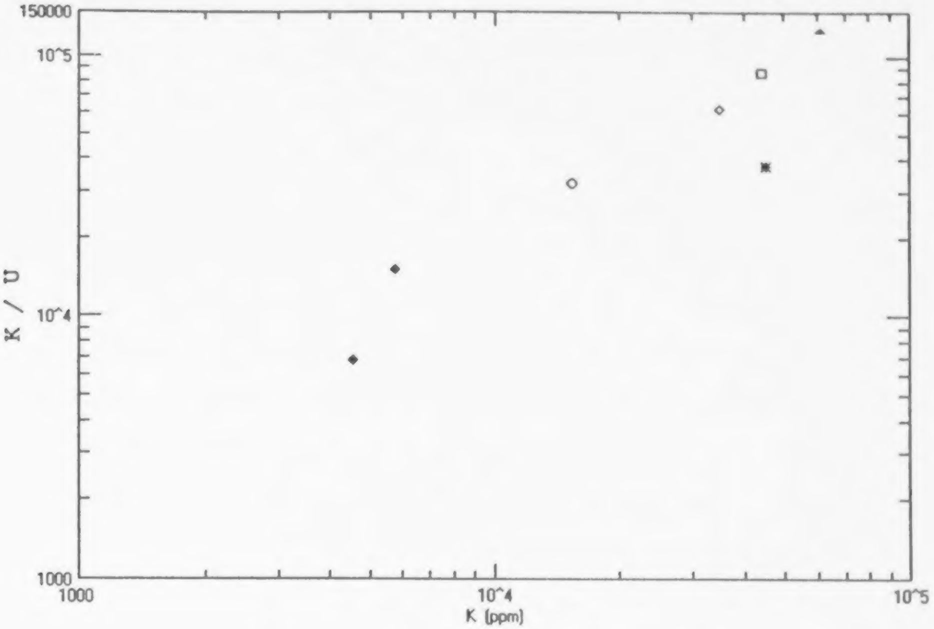

Figure 5.6 K *vs* K/U ratio of the granite sheets

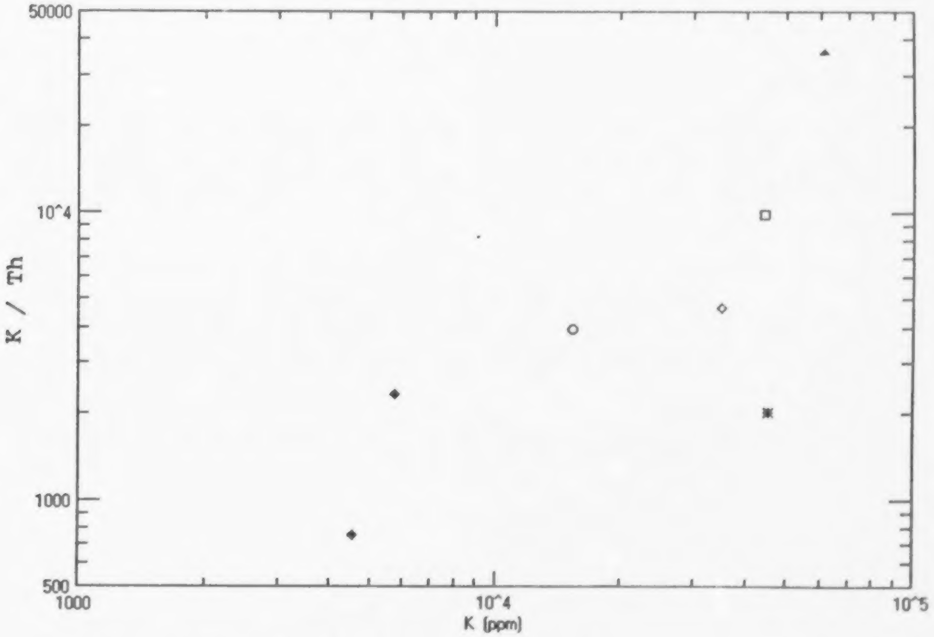

Figure 5.7 K *vs* K/Th ratio of the granite sheets

5.4.1.1 Ion Microprobe results

The ion microprobe analyses of a bulk, non-magnetic zircon aliquot from G87-19 were of a reconnaissant nature only. Analyses showed a mixed-age zircon population (Figure 5.8) with some Qorqut-aged zircons (*ca.* 2.5 Ga), inherited early Archaean Amîtsoq-aged zircons (*ca.* 3.6 Ga) and Nûk-aged zircons (*ca.* 3.0 Ga). In addition, a single discordant analysis fell on a discordia joining 3.6 Ga and 2.5 Ga. This is possibly an inherited Amîtsoq-aged zircon that suffered Pb-loss during the partial melting event that produced the granitoid. Alternatively, it is possible that this represents an example of a fourth zircon population, aged *ca.* 3.2 - 3.4 Ga (compare with the U-Pb zircon results for the type-Nûk gneisses).

The results suggest that sample G87-19 is part of the Qorqut granite complex (Moorbath *et al.*, 1981) and like the Qorqut granite was generated by the partial melting of a mixed source comprised of Amîtsoq and Nûk gneisses.

5.4.1.2 Conventional U-Pb zircon results

Sample G87-114 was picked from the least magnetic zircon fraction (≥ 1.8 A, 0.5°) but was not abraded. The sample of G87-27 used for analysis was a large non-magnetic, 'polished' *bulk* sample weighing 162.4 μg. The results of the conventional U-Pb analyses of these samples are shown in Figure 5.9 and Table 3.5. As can be seen G87-27 is particularly discordant (minimum discordancy of 35%) and has a ^{207}Pb-^{206}Pb age of 3.38 Ga. The trondhjemitic sheet shows a small degree of discordancy (minimum of 3.9 %), and gives a minimum ^{207}Pb-^{206}Pb age of 2791 Ma.

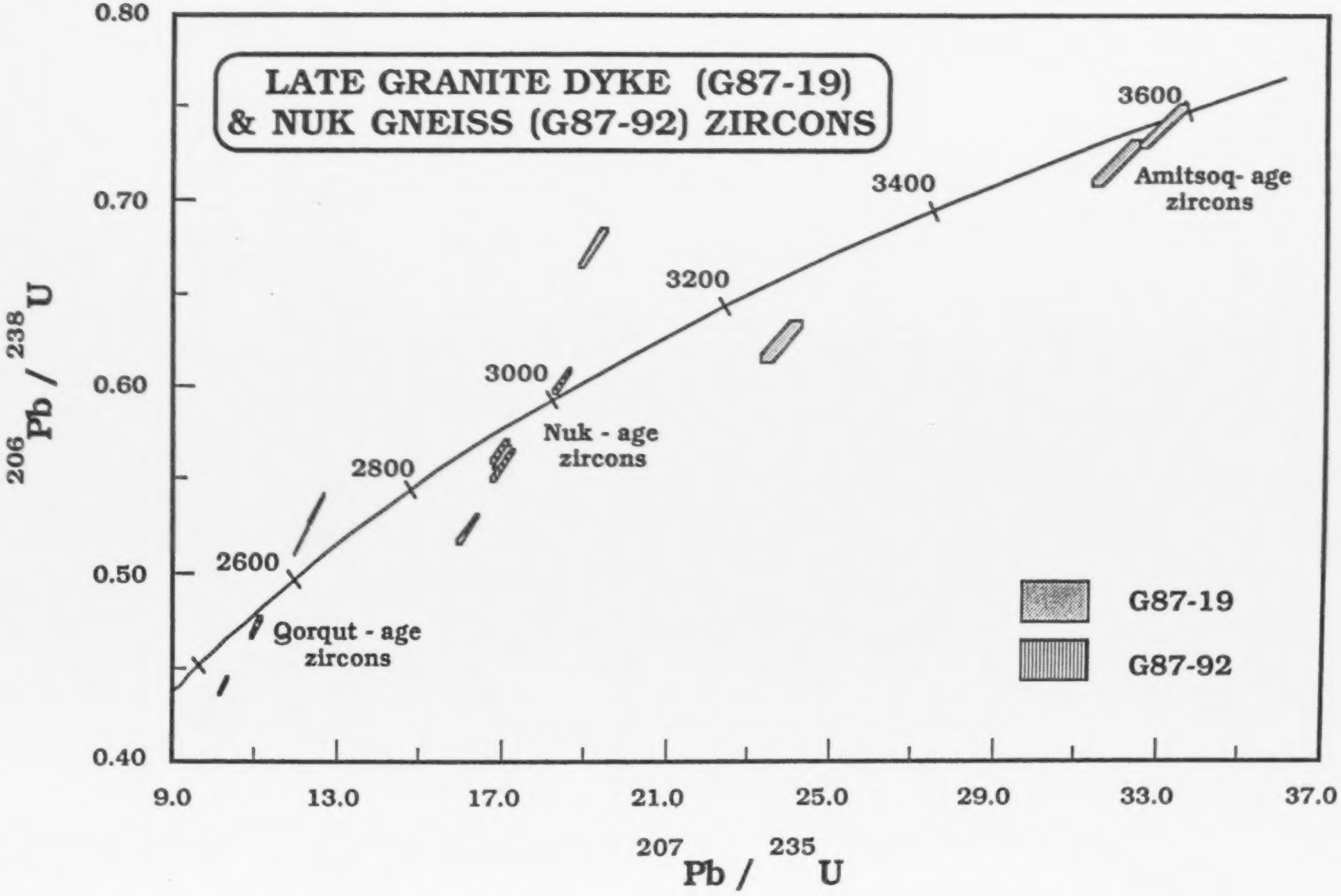

Figure 5.8 U-Pb Concordia plot of SHRIMP analyses of G87-19

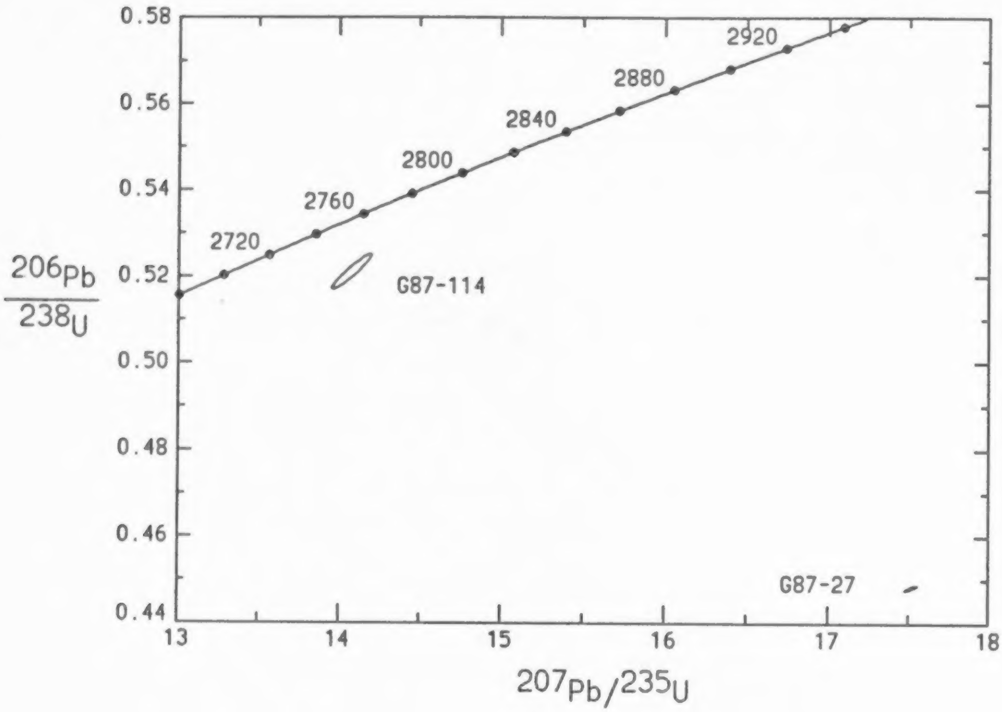

Figure 5.9 U-Pb concordia diagram for samples G87-114 and G87-27.

5.4.2 Whole-rock isotopic analyses

5.4.2.1 Lead-Lead

Whole-rock common-lead results for the granitic sheets, together with their Pb, Th and U concentration data (determined by XRF, DNC, and INAA, respectively), are listed in Table 5.2. When plotted on a $^{207}Pb/^{204}Pb$ - $^{206}Pb/^{204}Pb$ or $^{208}Pb/^{204}Pb$ - $^{206}Pb/^{204}Pb$ diagram (not shown) the data show a high degree of scatter indicating different (and possibly mixed) sources and ages.

As discussed in Chapter 3 the Amîtsoq gneisses are characterized by extremely unradiogenic Pb compositions, and very low U and Th concentrations. Consequently, any rocks derived by partial melting of such source material would inherit this depleted signature. Depending upon the enrichment of U, Th and Pb in the partial melt (controlled by the degree of partial melting, concentration of U, Th and Pb in the source rock, the accessory minerals present, *etc.*) and the age of the melting event, the Pb isotopic composition of granitoid rocks could retain a time integrated unradiogenic Pb isotopic signature.

Samples G87-27 and G87-141 intrude known Amîtsoq gneisses (from the Akulleq terrane) and have $^{206}Pb/^{204}Pb$ and $^{207}Pb/^{204}Pb$ ratios significantly less than 13.0 and 14.0, respectively, that are indistinguishable from typical Amîtsoq gneisses (mean $^{206}Pb/^{204}Pb = 12.30 \pm 0.58$, $^{207}Pb/^{204}Pb = 13.40 \pm 0.18$, 1σ, $n=30$, see Chapter 3). However, of sixty-nine type-Nûk gneiss whole-rock Pb isotopic measurements (determined in the course of this study) only six samples have $^{206}Pb/^{204}Pb$ ratios < 13 (and of those most are only barely so), and none of the sixty-nine samples have $^{207}Pb/^{204}Pb$ ratios < 14. Thus, the Pb isotopes suggest that these two granitic (*s.s.*) sheets were derived solely, or in large part, by anatexis of Amîtsoq gneiss-like crust.

Where a crustal melt is derived from a mixed source (*e.g.* Amîtsoq and type-Nûk gneisses) the situation will not be so clear cut. The unradiogenic Pb signature derived from the Amîtsoq gneiss source component will likely

Table 5.2 Isotopic data for the granite sheets.

G87	206Pb 204Pb	207Pb 204Pb	208Pb 204Pb	Pb (ppm)	U (ppm)	Th (ppm)
19	13.566	14.301	34.374	22	0.56	7.48
27	12.476	13.673	33.324	38	0.48	3.93
61	13.297	14.207	33.298	30	0.51	4.48
68	14.254	14.583	44.764	26	1.20	22.0
114	13.279	14.188	33.739	16	0.38	2.48
115	13.857	14.307	34.606	15	0.67	6.05
141	12.313	13.448	32.643	44	0.48	1.70

G87	147Sm 144Nd	143Nd 144Nd	Sm (ppm)	Nd (ppm)	f Sm/Nd	$\epsilon_{Nd(0)}$	T_{CHUR} (Ga)	T_{DM1} (Ga)	T_{DM2} (Ga)	ϵNd (2.8 Ga)
19	0.1061	0.51083	2.14	12.18	-0.460	-35.2	3.01	3.14	3.28	-2.6
27	0.1016	0.51032	1.60	9.49	-0.483	-45.2	3.68	3.74	3.83	-11.0
61	0.0963	0.51066	0.52	3.25	-0.510	-38.6	2.98	3.10	3.23	-2.4
68	0.0809	0.51028	2.64	19.72	-0.588	-46.0	3.08	3.18	3.28	-4.3
114	0.0833	0.51056	0.61	4.43	-0.576	-40.5	2.77	2.90	3.02	0.36
115	0.0843	0.51043	1.48	10.61	-0.571	-43.0	2.97	3.08	3.20	-2.5
141	0.1135	0.51085	0.49	2.63	-0.423	-34.8	3.24	3.36	3.49	-4.9

$^{143}Nd/^{144}Nd_{CHUR} = 0.512636$, $^{147}Sm/^{144}Nd_{CHUR} = 0.1967$, $^{147}Sm\ \lambda = 6.54 \times 10^{-12}\ a^{-1}$

T_{CHUR} = model age based on a chondritic reservoir
T_{DM1} = model age based on derivation from a progressively depleting mantle reservoir (DePaolo, 1981)
T_{DM2} = model age based on a depleted mantle that evolved in a linear manner from a chondritic source at 4.5 Ga
(current values: $^{143}Nd/^{144}Nd = 0.513163$, $^{147}Sm/^{144}Nd = 0.2136$, Goldstein *et al.*, 1984)

G87	^{87}Sr ^{86}Sr	$^{87}Rb/^{86}Sr$ (meas)	$^{87}Rb/^{86}Sr$ (calc)	Rb (ppm)	Sr (ppm)	T_{UR} (meas)	T_{UR} (calc)	T_{DM} (meas)	T_{DM} (calc)
19	0.76165	1.373	1.413	96.25	204.0	3.06	2.96	3.08	2.99
27	0.72512	---	0.436	64	426	----	4.00	----	4.02
61	0.76024	1.288	1.321	96.41	217.6	3.19	3.10	3.20	3.13
68	0.74169	---	0.956	106	322	----	2.94	----	2.98
114	0.70748	0.0759	0.0918	16.81	640.6	****	****	****	****
115	0.70553	0.0465	0.0617	8.21	510.7	****	****	****	****
141	0.79431	---	2.036	173	248	----	3.17	----	3.18

$^{87}Rb/^{86}Sr$ calc : ratio calculated from XRF Rb-Sr data and measured $^{87}Sr/^{86}Sr$ ratio
$^{87}Rb\ \lambda = 1.42 \times 10^{-11}\ a^{-1}$
**** - unrealistic model ages because sample $^{87}Rb/^{86}Sr$ ratio close to that of UR and DM

T_{UR} = model age based on a uniform reservoir: $^{87}Sr/^{86}Sr_{UR} = 0.7045$, $^{87}Rb/^{86}Sr_{UR} = 0.0827$
T_{DM} = model age based on derivation from depleted mantle reservoir: $^{87}Sr/^{86}Sr_{DM} = 0.7026$, $^{87}Rb/^{86}Sr_{DM} = 0.052$

be 'diluted', particularly as the type-Nûk gneiss component increases. The ion microprobe data for G87-19 clearly shows a mixed Amîtsoq and Nûk gneiss source for this sheet, and that it is probably genetically linked to the Qorqut granite. Using Pb isotopic data Moorbath *et al.*, (1981) estimated that the relative proportions of Amîtsoq and Nûk gneiss contributing to the formation of the Qorqut granite *ca*. 40 and 60 %, respectively; while Collerson *et al.*, (1989) calculated contributions of 53 and 47 %, respectively based on a few Sm-Nd data. It would therefore be feasible to produce the Pb isotopic composition determined for G87-19 by mixing Amîtsoq and Nûk gneiss Pb in about equal amounts.

Sample G87-68, a granite sheet (*s.s.*) from Nordlandet, has a particularly radiogenic $^{208}Pb/^{204}Pb$ ratio (44.764), and elevated $^{206}Pb/^{204}Pb$ and $^{207}Pb/^{204}Pb$ ratios compared to the other granitic sheets. This is readily explained by the sample's elevated Th concentration and high Th/U ratio. On the basis of the Nordlandet granulite Th/U, K/Th, and La/Th data for example (see Chapter 4), it was concluded that the granulites were preferentially depleted in Th compared to U. If the depletion was caused by removal of the LILE in a fluid or partial melt phase then this phase would have had a Th/U ratio > 3.8, be enriched in both Th and U (plus other LILE), and would over time, develop radiogenic Sr and Pb compositions relative to the residuum. If LILE depletion was effected by extraction in a partial melt one would expect that the U and Th concentration data and Pb isotopic characteristics of G87-68 would strongly resemble the solidified melt. This suggests that there may be a genetic link between the granite sheet, G87-68 and granulite-facies metamorphism. Alternatively, it may be possible to produce a geochemical and isotopic characteristics of G87-68 by a very small degree of partial melting (O'Nions and McKenzie, 1988) of the already depleted granulite sometime after granulite-facies metamorphism.

5.4.2.2 Rubidium-Strontium

During partial melting Rb preferentially partitions into the melt compared to Sr. Consequently, the time integrated $^{87}Sr/^{86}Sr$ ratio of the continental crust is far greater than that of the mantle, or low Rb/Sr lower continental crust. As a result granitoids derived by partial melting of continental crust (particularly ancient continental crust) generally have Sr isotopic compositions considerably more radiogenic than those derived by partial melting of oceanic crust or the mantle wedge.

Rb-Sr isotopic data for the granite sheets are presented in Table 5.2, together with various model ages. High precision $^{87}Rb/^{86}Sr$ ratios, determined *via* mass spectrometry isotope dilution, were determined for four of the seven samples. For the other samples less precise $^{87}Rb/^{86}Sr$ ratios were calculated on the basis of the Rb and Sr concentrations determined by XRF and their $^{87}Sr/^{86}Sr$ ratio determined by TIMS.

The granitic (*s.s.*) sheets show elevated $^{87}Rb/^{86}Sr$ and $87Sr/^{86}Sr$ ratios suggesting involvement of a source with an elevated Rb/Sr ratio, *e.g.*, continental crust. The trondhjemitic sheets, however, have Rb-Sr characteristics very similar to the type-Nûk gneiss trondhjemites.

Uniform reservoir and depleted mantle model ages were calculated for the granitic sheets based on both the measured and calculated $^{87}Rb/^{86}Sr$ ratios. Given the uncertainty in the measured parameters (particularly for the XRF calculated $^{87}Rb/^{86}Sr$ ratios) the differences between the two models are negligible. With model ages of *ca*. 4 Ga it is again clear that G87-27 was derived from early Archaean Amîtsoq-like material with little or no contribution from younger other sources. At *ca*. 3.2 Ga the model ages for G87-141, are much younger than expected if this sample was also derived largely from Amîtsoq gneiss material, and suggests either a significant contribution from younger material and/or the $^{87}Rb/^{86}Sr$ ratio calculated from XRF data it is unreliable. As the model ages for those samples in which the $^{87}Rb/^{86}Sr$ ratio was both measured and calculated agree within 0.1 Ma it is not felt that the $^{87}Rb/^{86}Sr$ ratio for G87-141 is likely to be significantly in error. Model ages for G87-61 suggests Nûk-like material was the major contributor to this sheet, with minor if any contribution from Amîtsoq-aged material. Sample G87-68, which intrudes the Nordlandet granulites, gives a model age of *ca.* 3.0 Ga, much younger than the protolith age of the granulites (*ca.* 3.2 Ga) and with no indication of contamination by early Archaean crust. For the trondhjemitic sheets (G87-114 and -115) the model Sr ages are meaningless as their $^{87}Rb/^{86}Sr$ ratios are equal or less than those of the model reservoirs.

5.4.2.3 Samarium - Neodymium

Measured whole-rock $^{143}Nd/^{144}Nd$, and $^{147}Sm/^{144}Nd$ ratios, together with Sm and Nd concentration data for the granitic sheets and various model parameters, are listed in Table 5.2.

The influence of significantly older, LREE-enriched, continental crust on the isotopic systematics of a number of the granitic sheets is apparent from the Sm-Nd model ages which greatly exceed the interpreted formation age of the sheets. As explained in Chapter 3, depleted mantle model Nd ages (T_{DM2}) based on the linearly changing DM of Goldstein *et al.*, (1984) are preferred over DePaolo's continuously varying DM (DePaolo, 1981) or the chondritic uniform reservoir Jacobsen and Wasserburg (1979) on the basis of $\epsilon Nd(t)$ values determined for the early Archaean Amîtsoq gneisses and Isua supracrustals.

Samples G87-27 and G87-141, sheets which appear to have been derived by anatexis of Amîtsoq-like material at depth, have T_{DM2} model ages indicative of such a source (3.83 and 3.49 Ga, respectively). T_{DM2} model ages for G87-19, -61, -68, -115 suggest a predominantly type-Nûk gneiss source, possibly with an early Archaean component. The T_{DM2} model age for G87-114 shows no evidence of an Amîtsoq-like source. Epsilon$_{CHUR}$ values for the granitic sheets calculated for an age of 2.8 Ga (with the exception of

G87-19 which is calculated to 2.53 Ga based on the SHRIMP data) and are plotted on an ϵ *vs* time diagram in Figure 5.10 together with the evolutionary field for Amîtsoq gneisses and trend for type-Nûk gneisses. Clearly, G87-27 is a partial melt of Amîtsoq gneiss crust, while G87-141 would appear to be a mixture of Amîtsoq and Nûk gneiss material. G87-68 which intrudes the Nordlandet granulites, which might at first sight appear to be a mixture of Amîtsoq and Nûk material is interpreted as being derived solely from the granulites (protolith age of *ca*. 3.2 Ga). On the basis of the ϵ-time plot it would appear that there was little or no early Archaean crustal contribution to samples G87-61 and -115, and that they were derived predominantly from pre-existing Nûk gneisses. At -5.75 the $\epsilon_{(2.53Ga)}$ value for

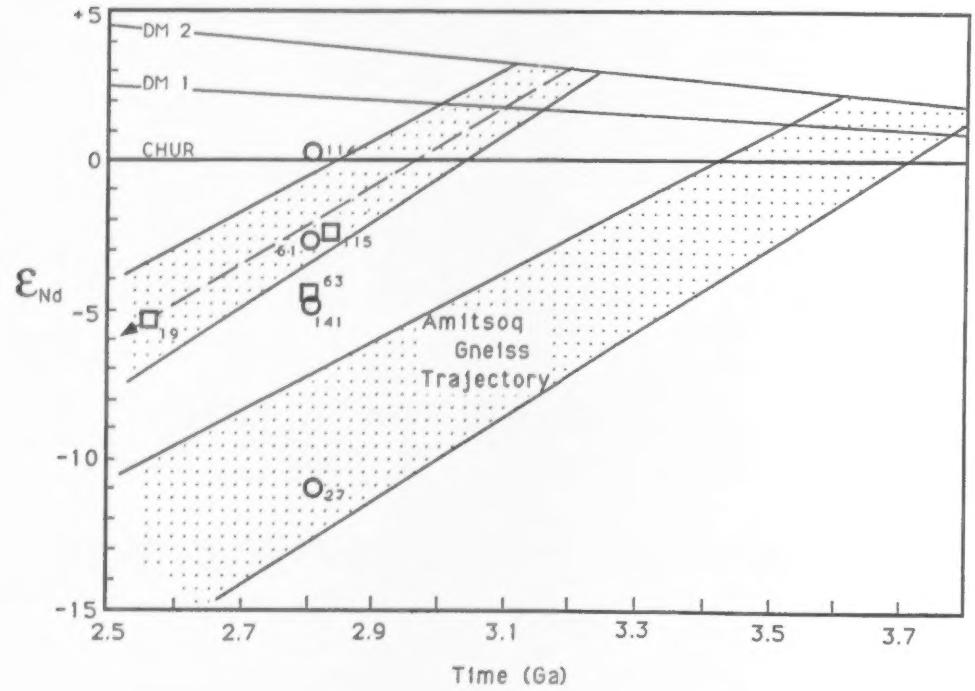

Figure 5.10 Nd evolution diagram related to the origin of the granite sheets.

G87-19 falls on the type-Nûk gneiss trajectory with no suggestion of an Amîtsoq gneiss component. As the ion microprobe zircon results indicate involvement of Amîtsoq gneiss in the genesis of G87-19, it must be assumed that the contribution was minor. This conclusion may equally apply to samples G87-61 and G87-115. The ϵ_{Nd} value for G87-114 at 2.8 Ga suggests a more juvenile source with the possibility of some crustal contamination.

5.5 Conclusions

On the basis of their major element chemistry, and whole-rock Rb-Sr, Sm-Nd, and Pb-Pb isotopic systematics, the granitic (*s.s.*) sheets (G87-19, 61, 68, and 141) and trondhjemitic sheet (G87-27) are considered to be partial melts of pre-existing gneisses. The influence of Amîtsoq-like source material on the isotopic systematics of G87-27 and -141 is obvious. However, the Pb-isotopic compositions, Nd model ages, and Sr model ages of the remaining granitic (*s.s*) sheets, do not give an unequivocal answer as to whether these sheets were derived solely from pre-existing type-Nûk gneiss-like material, or whether Amîtsoq gneiss crust was involved in their genesis. As demonstrated in Chapter 4, Nd model ages of partial melts will invariably give ages younger than the actual time of partial melting because of the reduced Sm/Nd ratio of the melt. It is clear from the SHRIMP zircon analyses of G87-19 that early Archaean crust was involved in the origin of that sample. The similarity of the Pb-isotopic composition of G87-19 and G87-61, and their model Nd and Sr ages indicates that Amîtsoq-like material was likely involved in the genesis of G87-61 too.

If, as is believed, Amîtsoq gneisses do not occur in the Akia terrane then any isotopic evidence of their presence implies involvement after amalgamation of the Akia and Akulleq terranes. Precise U-Pb zircon age determinations, on G87-61 for example, would help define the timing of the docking of the two terranes.

CHAPTER 6

Origin of the type-Nûk gneisses

6.1 Review of the origin of Archaean granitoids

Since the 1970's a large body of geochemical evidence has amassed suggesting that Archaean tonalitic and trondhjemitic magmas originated by partial melting of basic crust (*e.g.*, Arth and Hanson, (1972); Arth and Barker (1976); O'Nions and Pankhurst (1978); Jahn *et al.*, (1981)). The extreme HREE and Y depletion displayed by many Archaean gneisses initially led many workers to suggest residual garnet was the cause of the depletion. Measurement of HREE partition coefficients between hornblende and dacitic liquid (Arth and Barker, 1976) prompted consideration of depletion by residual hornblende in partial melting and fractional crystallization models. REE data for Archaean acid sodic rocks are therefore widely interpreted in terms of the partial melting of source materials such as eclogite, basic granulite and amphibolite. Rudnick and Taylor (1986) showed that amphibole alone is incapable of producing the fractionated LREE patterns, and depleted HREE commonly observed in Archaean tonalites and concluded that some garnet is required.

Early experimental partial melting studies of basalt, or its metamorphosed equivalent (*e.g.*, amphibolite, basic granulite, or eclogite) performed by Green and Ringwood (1968), Lambert and Wyllie (1972), and Helz (1976) indicated that partial melting of such starting materials could produce melts that were broadly tonalitic in composition. The number of experimental studies into the origin of Archaean Na-rich granitoids blossomed in the late 1980's and early 1990's (Beard and Lofgren (1989, 1991), Rushmer (1991), Rapp *et al.*, (1991), Winther and Newton (1991), Wolf and Wyllie, 1991). Some of these and earlier studies did not use starting materials representative of Archaean basic crust, *i.e.*, they were generally enriched in K_2O compared to suggested examples of Archaean basic crust, and hence may not be applicable to Archaean granitoid genesis.

Where remedied in later studies melts of tonalitic composition were invariably produced. Trondhjemitic melts were also generated in a number of experiments. It is important to note that a number of the melts identified by Rapp *et al.* (1991) as being tonalitic in composition are actually trondhjemitic, and similarly some identified as trondhjemitic were in fact tonalitic! The mistakes appear to have been caused by dependence on the O'Connor (1965) normative feldspar classification scheme with little regard or no regard to the overall bulk chemistry.

6.2 Possible modes of formation of the type-Nûk gneisses

Two commonly cited models for the origin of TTG-suites include: a) the partial melting of a mafic source material rich in hornblende and/or garnet (*e.g.*, Weaver and Tarney, 1980), and b) the fractional crystallization of wet basaltic or dioritic magma (*e.g.*, Barker and Arth, 1976; Jahn *et al.*, 1988). It would seem probable to the author that models involving some combination of partial melting with subsequent fractional crystallization would be most realistic. The presence of the Daly gap would seem to preclude fractional crystallization of a basaltic or dioritic magma as the source of the Nûk gneiss precursors. A number of experimental studies have demonstrated that melts of tonalitic composition can be produced by the partial melting of basaltic crust (*e.g.*, Rapp *et al.*, 1991; Winther and Newton, 1991). Various degrees of HREE depletion could have been produced depending upon the partial melting conditions. On the basis of REE modelling, Rudnick and Taylor (1986) argued that residual amphibole in the source would be incapable of producing the fractionated REE patterns commonly observed in Archaean tonalitic and trondhjemitic gneisses and that some garnet would have been necessary. The major and trace element contents of the trondhjemitic and granodioritic gneisses are consistent with them having been produced from tonalitic melts predominantly by hornblende fractionation. Removal of hornblende would deplete the melt in the HREE, Y, and ferromagnesian elements, and enrich it in the LREE. As hornblende has a negative Eu anomaly the melt would also develop an increasingly positive Eu anomaly as hornblende crystallized out. Fractionation of hornblende would also cause a significant decrease in the normative diopside content of the melt and an increase in the alumina saturation index (Cawthorn and Brown, 1976; Zen, 1986) unless compensated for by the crystallization of a phase such as plagioclase. The strong correlation of Y and Yb with CaO and MnO, coupled with the fact that there is a shift from metaluminous tonalitic gneisses to weakly peraluminous trondhjemitic and granodioritic gneisses suggests plagioclase fractionation was not as significant as hornblende.

Thus, it is concluded that the precursors of the type-Nûk gneiss TTG-suite were derived by a combination of partial melting of mafic crust and subsequent hornblende, and later plagioclase, fractional crystallization. Garnet is believed to have been the main phase responsible for imparting the depleted HREE character of the gneisses and implies that the depth of formation of the melts was at least 25 km.

6.3 Summary

A straightforward model for producing the type-Nûk gneiss TTG-suite therefore includes: a) the initial partial melting of low K tholeiitic basic crust to produce a tonalitic magma (*e.g.*, Rapp *et al.*, 1991; Winther and Newton, 1991), b) fractional crystallization of hornblende to produce high-Sr trondhjemitic melts, while fractional crystallization of both hornblende and plagioclase will produce a low-Sr trondhjemitic suites (more like the Amîtsoq gneisses), c) continued crystallization of plagioclase would lead to the production of melts of granodioritic composition. The absence of rocks of intermediate compositions (in the silica range 56-61%) argues against generation of the TTG-suite by fractional crystallization of a dioritic melt.

Chapter 7.

Summary and Conclusions.

The type-Nûk gneisses of the Akia terrane are largely made up of tonalitic, trondhjemitic, and granodioritic orthogneisses with subordinate amounts of dioritic and quartz dioritic rocks. Whole-rock dating methods all gave errorchrons (Rb-Sr: 2960 ± 130 Ma, Pb-Pb: 3035 ± 100 Ma, and Sm-Nd: 2786 ± 120 Ma, all uncertainties 2σ). The scatter of results is considered to be largely due to open system behaviour promoted by intense ductile deformation that occurs in belts, up to *ca.* 4 km wide, which affected the some but not all samples. Combining the whole-rock Rb-Sr, Pb-Pb and Sm-Nd results gives a weighted mean age of 2940 ± 66 Ma (2σ). Given the scatter of whole-rock analyses, this mean age agrees remarkably well with the majority of the U-Pb zircon results for the type-Nûk gneisses determined by SHRIMP and conventional small zircon techniques. It is, however, slightly younger and outside the uncertainty range of the older U-Pb zircon results.

Conventional U-Pb zircon analyses, generally employing samples weighing ≤ 120 µg, gave results with a range of ages (2920 - 3040 Ma) commensurate with the 2890 - 3065 Ma range determined by Baadsgaard and McGregor (1981) using bulk, sized, zircon fractions from samples of type-Nûk gneisses. SHRIMP analyses of two, least magnetic and picked type-Nûk gneiss samples gave concordant ages of 2998 ± 12 Ma (2σ) and 3021 ± 6 Ma (2σ). A histogram of ^{207}Pb-^{206}Pb zircon ages appears to suggest the presence of two distinct periods of intrusion of the type-Nûk gneiss precursors. Initially, a main event that peaked at *ca.* 3.00 Ga, followed by a hiatus, then some minor magmatism at *ca.* 2.96 Ma. This conclusion may be of limited validity due to the small size of the data set.

A Concordia intercept age, determined on metamorphic zircons for both the Nuuk townsite and southern Bjørneøen, gave an age of 2981 ± 2 Ma (2σ), which agrees remarkably well with the age determined for the Taserssuaq tonalite by bulk zircon analysis (2982 ± 7 Ma (2σ), Garde *et al.*, 1985). McGregor, *et al.*, 1986 postulated that the Taserssuaq tonalite, some 2200 km^2 in area, was possibly the heat source for the granulite facies metamorphism on Nordlandet. SHRIMP U-Pb zircon analyses gave what has been interpreted as the time of peak metamorphism on Nordlandet. At 3014 ± 7 Ma (2σ) this is significantly older than the age of the Taserssuaq tonalite. A number of U-Pb zircon analyses (in most instances from apparently unrelated samples) from type-Nûk gneisses lie on a discordia with an age of 3002 ± 1 Ma (2σ) and excellent MSWD. The fact that one of the zircon samples was obviously of metamorphic origin indicates there was certainly a period of metamorphism at that time which was likely associated with the intrusion of large volumes of the precursors of the type-Nûk gneiss. This event, together with the effect of the emplacement of the Taserssauq tonalite, and the severe ductile deformation associated with the formation of the straight belt, likely were responsible for Pb loss from many of the type-Nûk gneisses zircons and the open system behaviour of the Rb-Sr system (and possibly Sm-Nd and Pb-Pb).

Given their isotopic and trace element variation it is concluded that the type-Nûk gneisses are not derived from single cogenetic precursors.

The samples collected from areas within the Akia terrane mapped as Amîtsoq gneisses show no consistent geochronologic or isotopic evidence of being early Archaean in origin. In particular, the characteristic unradiogenic Pb isotopic signature of the Amîtsoq gneisses is not evident in any of the analyses of the supposed 'Amîtsoq gneisses' of the Akia terrane. On the contrary, many of these gneisses show Pb isotopic compositions more radiogenic than the bulk of the type-Nûk gneisses. Similarly, the trace element characteristics of these gneisses do not resemble known Amîtsoq gneisses. Data from the literature, plus the small number of analyses of known Amîtsoq gneisses performed as part of this study, show that for comparable rock compositions the supposed 'Amîtsoq gneisses' of the Akia terrane are poorer in Y, Pb and Nb, and richer in Ba and Sr than their

Amîtsoq gneisses 'equivalents'. The isotopic systematics of the late-granitic (*s.l.*) sheets, which intrude known Amîtsoq gneisses of the Akulleq terrane, clearly indicate derivation from Amîtsoq gneiss material. Thus, the designation of rocks within the Akia terrane as 'Amîtsoq gneisses' is considered erroneous. Disproving the existence of Amîtsoq gneisses within the Akia terrane strengthens the terrane model argument.

However, this is not to suggest that the Akia terrane has no grey gneiss components older than the type-Nûk gneisses. On the contrary, the Sr and Nd isotopic data for some of the Akia 'Amîtsoq gneisses' and type-Nûk gneisses do suggest the involvement an older crustal component in their genesis. SHRIMP zircon analyses of a sample of Akia 'Amîtsoq gneiss' gave an indication of a crustal component *ca*. 3250 - 3400(?) Ma. At the completion of this study Dr. Allan Nutman determined a ^{207}Pb-^{206}Pb SHRIMP age of 3235 ± 9 Ma (2σ) (*unpub. data*) for zircons separated from a dioritic gneiss collected from an area of the Akia terrane close to the Nuuk airport that had been mapped as 'Amîtsoq gneiss'. Consequently, the isotopic systematics of many of the Akia 'Amîtsoq gneisses' can be explained by their having a protolith age of *ca*. 3.25 Ga.

The existence of *ca*. 3.25 Ga crust is supported by the *ca*. 3.2 Ga age determined for the precursors of the Nordlandet granulites. The exact relationship between the granulites and the *ca*. 3.2 Ga 'Amîtsoq gneisses' of the Akia terrane is at present not known. Estimates, based on geobarometry, suggest that the exposed rock groups on either side of the Ataneq fault could represent a difference in level of exposure of up to 10 kms.

Uranium-Pb ion microprobe analyses of zircons from Nordlandet, and some samples from the Nuuk peninsula, demonstrate the presence of previously unrecognized *c*. 3.20-3.25 Ga old intermediate-to-felsic crust in the Akia terrane specifically, and the Godthåbsfjord area in general. The absence of gneissic crust of a similar age from either the Akulleq or

Tasiusarsuaq terranes lends support to the terrane model for the Godthåbfjord area.

Recently, Schiøtte *et al.*, (1989, 1990) reported ion microprobe and conventional small zircon U-Pb results, respectively for zircons separated from rocks of the Saglek and Hopedale blocks of the Archaean Nain Province, Labrador. An almost concordant ^{207}Pb-^{206}Pb age of 3219 ± 3 Ma (2σ), was reported for zircon separated from a mafic granulite of the Saglek block (referred to as the Parkavik gneiss), which they suggested might be broadly correlated with the Lister gneiss (3235 ± 8 Ma (2σ)) from further north. They proposed a correlation with the Maggo gneiss of the Hopedale block on the basis of an ion microprobe ^{207}Pb-^{206}Pb age of 3258 ± 24 Ma (2σ) determined from igneous-looking zircons separated from the 'Weekes metasediment'. The zircons were considered detrital in nature and as being derived from early phases of the Maggo gneiss. They concluded that the Lister, Maggo and Parkavik gneisses from Labrador and the type-Nûk gneisses of the Akia terrane belong to the same terrane (Schiøtte *et al.*, (1990). At that time there was no published evidence for *c.* 3.2 Ga crust in the Akia terrane as the SHRIMP U-Pb zircon results from Nordlandet were not published until late 1990 (Duke *et al.*, 1990). Consequently, Schiøtte *et al.*, (1990) put forward SHRIMP data for two zircons from a supracrustal from the island of Simiuta with a ^{207}Pb-^{206}Pb age of 3227 ± 8 Ma (2σ) (Schiøtte *et al.*, 1988). Being fairly discordant the zircons were originally interpreted as being Amîtsoq grains that had suffered early Pb loss. However, Schiøtte *et al.*, (1990) reinterpreted the results (as the analyses became less discordant given a revision of the SHRIMP standardization procedure) suggesting that they were derived from a Greenlandic equivalent to the 3235 Ma Lister gneiss. A major flaw in this argument is the fact that the island of Simiuta is part of the **Akulleq** terrane, and not the Akia terrane, which they were attempting to show a correlation. However, given the evidence from this study of *c.* 3.2 Ga gneisses in the Akia terrane the author is in general agreement with the hypothesis of correlation between the middle Archaean of Labrador and the Akia terrane of southern West Greenland. The middle Archaean chronology of geological events for the Saglek and Hopedale blocks is very similar to that proposed for the Akia terrane here. The main differences between the two histories relates to the timing of the Hopedale dykes and basic dykes of the Saglek block *vs.* those found in the Akia 'Amîtsoq gneisses'. It is interesting to note that as the dykes that intrude the Akia 'Amîtsoq gneisses' were confused with the Ameralik dykes of the Akulleq terrane the basic dykes of the Saglek block were previously correlated with the main Saglek dykes.

Origin of the type-Nûk gneisses

Since the 1970's a large body of geochemical evidence has amassed suggesting that Archaean tonalitic and trondhjemitic magmas originated by partial melting of basic oceanic crust (*e.g.*, O'Nions and Pankhurst, 1978; Arth and Barker, 1976). The extreme HREE and Y depletion displayed by many Archaean gneisses initially led many workers to suggest residual garnet in the source was the cause of the depletion. Measurement of HREE partition coefficients between hornblende and dacitic liquid (Arth and Barker, 1976) prompted consideration of depletion by residual hornblende in partial melting and fractional crystallization models. Rudnick and Taylor (1986) showed that amphibole alone is incapable of producing the fractionated LREE patterns and depleted HREE observed in Archaean tonalites and concluded that some garnet is required.

In the late 1980's many experimental petrologists turned their attention to the generation of low K, Archaean tonalitic and trondhjemitic magmas. Melting experiments of low K tholeiite under a wide variety of conditions resulted in the generation of tonalitic or trondhjemitic melts. One may confidently assume that the production of the rock-types of the TTG-suite therefore involves partial melting of low K tholeiitic oceanic crust to produce a tonalitic magma (*e.g.*, Rapp *et al.*, 1991; Winther and Newton, 1991). Fractional crystallization of hornblende from such a magma will produce a high Sr content trondhjemite, while fractional crystallization of both hornblende and plagioclase will produce a low Sr trondhjemite. Further crystallization of plagioclase will lead to the production of rocks of granodioritic composition. The absence of rocks of intermediate composition, in the silica range 56-61%, suggests that fractional crystallization from a melt more basic than tonalite is improbable. Similarly, major oxide variations within the tonalite-trondhjemitic-granodioritic gneisses appears more continuous than when the dioritic and quartz dioritic gneisses are included.

The development of the terrane model for the Godthåbsfjord region signalled the demise of the Taylor *et al.*, (1980) crustal contamination model based on the Nûk gneisses. The main principle of the model was that the type-Nûk gneisses suffered variable amounts of early Archaean, Amîtsoq gneiss crustal contamination during intrusion. Proving the absence of Akia 'Amîtsoq gneisses' demonstrates that any contamination of the type-Nûk gneisses that might have occurred had to have done so *after* the juxtaposition of the Akia and Akulleq terranes. Assembly of these two terranes is inferred to have occurred about 2750 Ma. Consequently, the various isotopic systems would have had some 250 Ma to evolve prior to contamination. McGregor *et al.*, (1986) stated that the sample base utilized in Taylor's study was of a mixed-aged and included some post-2800 Ma gneisses that were likely partial melts of Amîtsoq gneiss material.

In demonstrating the absence of early Archaean gneisses from the Akia terrane this study has verified the integrity of the terrane, and as such lends support to the terrane model for southern West Greenland. Whether the similarities between these Archaean terranes and those of Phanerozoic and Proterozoic age, can be extended to the driving mechanism, *i.e.,* plate-tectonics, is still a matter for conjecture. However, more and more evidence suggests that some form of plate-tectonic process, albeit of a rudimentary nature, must have operated in the Archaean. Differences between mid- to early-Archaean and modern plate-tectonic processes are probably related to the greater heat generation in the early- and mid-Archaean. This likely manifested itself as either a) rapidly moving young plates, showing an increased rate of subduction (probably at shallower angles than occur today) and direct melting of the subducting slab *vs* present-day mantle wedge, or b) greater ridge length, hence smaller plates than at present, moving more slowly than in (a).

The existence of distinctive terranes in the Archaean is strong evidence for some form of Archaean plate-tectonic process (Nisbet, 1987).

The exact relationship between the granulites of Nordlandet and the amphibolite-facies type-Nûk gneisses and Akia terrane 'Amîtsoq gneisses' is unclear. At the north of Godthåbsfjord there appears to be a prograde amphibolite- to granulite-facies grade boundary. However, the Taserssuaq tonalite, dated by a U-Pb zircon Concordia intercept at 2982 ± 7 Ma, and the effects of retrogression and later deformation have largely obscured the original prograde boundary. Sample G87-152, from northwestern Sadelø, has granulite-facies geochemical characteristics.

As a consequence of this study a refined Archaean chronology of the Akia terrane is proposed and is reported in Table 7.1.

Table 7.1. **The Archaean Geochronology of the Akia Terrane.**

2.53 Ga Qorqut granite complex formation NNE-SSW trending straight-belt formation with associated intense ductile deformation spanning the period of Qorqut granite complex formation.

2.66 Ga Intrusion of the Qarusuk dykes.

ca. 2.75 Ga Amalgamation of the Akia and Akulleq terranes (continent-continent collision) with associated granite sheet intrusion.

2.98 Ga Intrusion of the Taserssuaq tonalite (and large granodioritic bodies, such as are found on eastern Bjørneøen) with associated metamorphism of earlier Nûk gneisses (*e.g.*, southern Bjørneøen) and related zircon growth and Pb-loss of pre-existing zircons.

3.06 - 2.94 Ga intrusion of type-Nûk gneiss precursors - early phases accompanied thrusting and interleaving of the type-Nûk gneiss precursors and the 'Malene' supracrustals. The deformation declined somewhat by the time the 2.98 Ga Taserssuaq tonalite and similar bodies were intruded. Possible relationship between magma intrusion and the 3.01-3.02 Ga granulite-facies metamorphism on Nordlandet.

ca. 3.1 Ga (?) Formation - deposition of 'Malene' supracrustal precursors, *i.e.*, tholeiitic basic crust (pillow lavas, pyroclastics, *etc*.), anorthosites, and deposition of sediments.

ca. 3.15 Ga (?) intrusion of basic dykes (mistakenly identified as older Ameralik dykes of the Akulleq terrane).

3.20-3.25 Ga intrusion of the precursors of the Akia terrane 'Amîtsoq gneisses' and voluminous Nordlandet dioritic equivalents (?).

pre-3.25 Ga Formation - deposition of supracrustal sequence of pelitic metasediments, ultrabasic and basic rocks, gabbro-anorthosites, and minor skarns occurring on Nordlandet.

BIBLIOGRAPHY.

Aherns, L.H. (1954) The log-normal distribution of the elements. *Geochim. et Cosmochim. Acta.*, **6**, 121-131.

Allaart, J.H. (1976) The pre-3760 m.y. old supracrustal rocks of the Isua area, central West Greenland, and the associated occurrence of quartz-banded ironstone, **in**: *The Early History of the Earth*, B.F. Windley. ed., 177-189. J. Wiley and Sons, London.

Andersen, T. and Knutsen, A.B. (1962) Anion-exchange study I. Adsorption of some elements in HBr-solutions. *Acta Chemica Scand.* **16**, 849-854.

Anderson, R.N., DeLong, S.E. and Schwarz, W.M. (1978) Thermal model for subduction with dehydration in the downgoing slab. *J. Geol.*, **86**, 731-739.

Arculus, R.J. and Ruff, L.J. (1990) Genesis of continental crust: evidence from island arcs, granulites, and exospheric processes. **in** D. Vielzeuf and Ph. Vidal (eds), *Granulites and Crustal Evolution*, 7-23.

Arkani-Hamed, J. and Jolly, W.T. (1989) Generation of Archean Tonalites. *Geology*, **17**, 307-310.

Arndt, N.T. and Goldstein, S.L. (1987) Use and abuse of crust-formation ages. *Geology*, **15**, 893-895.

Arth, J.G. and Hanson, G.N. (1972) Quartz diorites derived by partial melting of eclogite or amphibolite at mantle depths. *Contrib. Mineral. Petrol.*, **37**, 161-174.

Arth, J.G. and Barker, F. (1976) Rare-earth partitioning between hornblende and dacitic liquid and implications for the genesis of trondhjemitic-tonalitic magmas. *Geology*, **4**, 534-536.

Arth, J.G., Barker, F., Peterman, Z.E., and Friedman, I. (1978) Geochemistry of the gabbro-diorite-tonalite-trondhjemite suite of southwest Finland and its implications for the origin of tonalitic-trondhjemitic magmas. *J. Pet.*, **19**, 289-316.

Arth, J.G. (1979) Some trace elements in trondhjemites - their implications to magma genesis and paleotectonic setting. **in** Trondhjemites, Dacites and Related Rocks. **ed.** Barker, F., 123-132. Elsevier, Amsterdam.

Ashwal, L.D., Jacobsen, S.B., Myers, J.S., Kalsbeek, F., and Goldstein, S.J. (1989) Sm-Nd age of the Fiskenaesset Anorthosite Complex, West Greenland. *Earth Planet. Sci. Lett.*, **91**, 261-270.

Baadsgaard, H. (1973) U-Th-Pb dates on zircons from the early Precambrian Amîtsoq gneisses, Godthaab district, West Greenland. *Earth Planet. Sci. Lett.*, **19**, 245-259.

Baadsgaard, H. (1976) Further U-Pb dates on zircons from the early Precambrian rocks of the Godthaabsfjord area, West Greenland. *Earth Planet. Sci. Lett.*, 33, 261-267.

Baadsgaard, H., Lambert, R. St. J., and Krupicka, J. (1976) Mineral isotopic age relationships in the polymetamorphic Amîtsoq gneisses , Godthaab District, West Greenland. *Geochim. et Cosmochim. Acta.*, **40**, 513-527.

Baadsgaard, H., and McGregor, V.R. (1981) The U-Th-Pb systematics of zircons from the type-Nûk gneisses, Godthabsfjord, West Greenland. *Geochim. et Cosmochim. Acta.*, **45**, 1099-1109.

Baadsgaard, H., Nutman, A.P., Bridgwater, D., Rosing, M., McGregor, V.R., and Allaart, J.H. (1984) The zircon geochronology of the Akilia association and Isua supracrustal belt, West Greenland. *Earth Planet. Sci. Lett.*, **68**, 221-228.

Baadsgaard, H., Nutman, A.P., and Bridgwater, D. (1986) Geo-chronology and isotopic variation of the early Archaean Amîtsoq gneisses of the Isukasia area, southern West Greenland. *Geochim. et Cosmochim. Acta.*, **50**, 2173-2183.

Barbey, P. and Cuney, M. (1982) K, Rb, Sr, Ba, U and Th geochemistry of the Lapland granulites (Fennoscandia). LIL fractionation controlling factors. *Contrib. Mineral. Petrol.*, **81**, 304-316.

Barker and Peterman (1974) Bimodal tholeiitic-dacitic magmatism and the early Precambrian crust. *Precamb. Res.*, **1**, 1-12.

Barker, F. and Arth, J.G. (1976) Generation of trondhjemitic-tonalitic liquids and Archean bimodal trondhjemite-basalt suites. *Geology*, **4**, 596 - 600.

Barker, F. (1979) Trondhjemite: definition, environment and hypothesis of origin. **in** Trondhjemites, Dacites and Related Rocks. **ed.** Barker, F., 1-12, Elsevier, Amsterdam.

Barker, F., Arth, J.G., and Hudson, T. (1981) Tonalites in crustal evolution. *Phil. Trans. R. Soc. Lond.*, **A301**, 293-303.

Beach, A. and Tarney, J. (1978) Major and trace element patterns established during retrogressive metamorphism of granulite facies gneisses, NW Scotland. *Precamb. Res.*, **7**, 325-348.

Beard, J.S., and Lofgren, G.E. (1989) Effects of water on the composition of partial melts of greenstone and amphibolite. *Science*, **244**, 195-197.

Beard, J.S., and Lofgren, G.E. (1991) Dehydration melting and water-saturated melting of basaltic and andesitic greenstones and amphibolites. *J. Petrol.*, **32**, 365-401.

Bergerioux, C., Kennedy, G., and Zikovsky, L. (1979) Use of the semi-absolute method in neutron activation analysis. *J. Radioanal. Chem.*, **50**, 229-234.

Bickle, M.J. (1978) Heat loss from the Earth: a constraint on Archaean tectonics from the relation between geothermal gradients and the rate of plate production. *Earth Planet. Sci. Lett.*, **40**, 301-315.

Black, L. P., Gale, N.H., Moorbath, S., Pankhurst, P.J., and McGregor, V.R. (1971) Isotopic dating of very early Precambrian amphibolite gneisses from the Godthaab district, West Greenland. *Earth Planet. Sci. Lett.*, **12**, 245-259.

Black, L.P., Williams, I.S., and Compston, W. (1986) Four zircon ages from one rock: The history of a 3930 Ma-old granulite from Mount Sones, Enderby Land, Antarctica. *Contrib. Mineral. Petrol.*, **94**, 427-437.

Black, L.P. and McCulloch, M.T. (1987) Evidence for isotopic equilibration of Sm-Nd whole-rock systems in early Archean crust of Enderby Land, Antarctica. *Earth Planet. Sci. Lett.*, **82**, 15-24.

Black, L.P. (1988) Isotopic resetting of U-Pb zircon and Rb-Sr and Sm-Nd whole-rock systems in Enderby Land, Antarctica: Implications for interpretation of isotopic data from polymetamorphic and multiply deformed terrains. *Precamb. Res.*, **38**, 355-365.

Bowes, D.R. (1972) Geochemistry of Precambrian crystalline basement rocks, north-west Highlands of Scotland. *24th Int. Geol. Cong.*, 97-103.

Bowring, S.A., Williams, I.S., and Compston, W. (1989a) 3.96 Ga gneisses from the Slave Province, N.W.T. Canada. *Geology*, **17**, 971-975.

Bowring, S.A., King, J.E., Housh, T.B., Isachsen, C.E., and Podosek, F.A. (1989b) Neodymium and lead isotope evidence for enriched early Archaean crust in North America. *Nature*, **340**, 222-225.

Bridgwater, D., McGregor, V.R., and Myers, J.S. (1974) A horizontal tectonic regime in the Archaean of Greenland and its implications for early crustal thickening. *Precambrian Res.*, **1**, 179-197.

Bridgwater, D., Watson, J. and Windley, B.F. (1973) The Archaean craton of the North Atlantic region. *Phil. Trans. R. Soc. London*, **A273**, 493.

Cambell, I.H. and Jarvis, G.T., (1984) Mantle convection and early crustal evolution. *Precambrian Res.*, **26**, 15-56.

Cameron, A.E., Smith, D.H., and Walker, R.L. (1969) Mass spectrometry of nanogram-size samples of lead. *Anal. Chem.*, **41**, 525-526.

Card, K.D. (1990) A review of the Superior Province of the Canadian Shield, a product of Archean accretion. *Precambrian Res.*, **48**, 99-156.

Cartwright, I. (1989) Processes of formation and retrogression of Scourian granulites. **in** *Fluid Movements - element transport and the composition of the deep crust*, (ed) Bridgwater, D., 95-110.

Cavell, P.A. (1986) The geochronology and petrogenesis of the Big Spruce Lake Alkaline Complex. Unpublished Ph.D. thesis. Univ. of Alberta. pp.448.

Cawthorn, R.G. and Brown, P.A. (1976) A model for the formation and crystallization of corundum-normative calc-alkaline magmas through amphibole fractionation, *J. Geol.*, **84**, 467-476.

Chadwick, B. and Coe, K. (1973) Field work on the Precambrian basement in the Buksefjorden region, southern West Greenland. *Rapp. Gronlands geol. Unders.* **55**, 32-37.

Chadwick, B., Coe, K., Gibbs, A.D., Sharpe, M. and Wells, P.R.A. (1974) Mapping of the Precambrian basement in the Buksefjorden region, southern West Greenland. *Rapp. Gronlands geol. Unders.* **65**, 54-60.

Chadwick, B. and Coe, K. (1975) A horizontal tectonic regime in the Archaean of Greenland and its implications for early crustal thickening - a comment. *Precambrian Res.*, **2**, 397-404.

Chadwick, B. (1981) Field relations, petrography and geochemistry of Archaean amphibolite dykes and Malene supracrustal amphibolites, northwest Buksefjorden, southern West Greenland. *Precambrian Res.*, **14**, 221-259.

Chapman, H.J. and Moorbath, S. (1978) Lead isotope measurements from oldest recognised Lewisian gneisses of north-west Scotland. *Nature*, **268**, 41-42.

Clemens, J.D. (1992) Partial melting and granulite genesis: a partisan overview. *Precambrian Res.*, **55**, 297-301.

Cohen, A.S., O'Nions R.K., and O'Hara, M.J. (1988) The timing and mechanism of depletion in Lewisian granulites. **in** *Workshop on the Growth of Continental Crust*. (ed) Ashwal, L.D., LPI Tech. Rep. 88-02. 48.

Collerson, K.D., and Bridgwater, D. (1979) Metamorphic development of earlyArchean tonalitic and trondhjemitic gneisses: Saglek area, Labrador. **in** Trondhjemites, Dacites and Related Rocks. **ed.** Barker, F., 205-273, Elsevier, Amsterdam.

Collerson, K.D., McCulloch, M.T., and Nutman, A.P. (1989) Sr and Nd isotope systematics of polymetamorphic Archean gneisses from southern West Greenland and northern Labrador. *Can. J. Earth Sci.*, **26**, 446-466.

Collerson, K.D., Cambell, L.M., Weaver, B.L. and Palacz, A. (1991) Evidence for extreme mantle fractionation in early Archean ultramafic rocks from northern Labrador. *Nature.*, **349**, 209-214.

Compston, W., Williams, I.S., and Meyer, C. (1984) U-Pb geo-chronology of zircons from Lunar Breccia 73217 using a sensitive high mass-resolution ion microprobe. **in** Proc. 14th Lunar Planet. Sci. Conf., *J. Geophys. Res.,* **89B**, 525-534.

Compston, W., Froude, D.O., Ireland, T.R., Kinny, P.D., Williams, I.S., Williams, I.R., and Myers, J.S. (1985) The age of a tiny part of) the Australian continent. *Nature*, **317**, 559-560.

Compston, W., Kinny, P.D., Williams, I.S. and Foster, J.J. (1986) The age and lead loss behaviour of zircons from the Isua supracrustal belt as determined by ion microprobe. *Earth Planet. Sci. Lett.*, **80**, 71-81.

Compton, P.N. (1978) Rare earth evidence for the origin of the Nûk gneisses, Buksefjorden region, southern West Greenland. Contrib. Mineral. Petrol., **66**, 283-293.

Currie, L.A. (1968) Limits for qualitative detection and quantitative determination - application to radiochemistry. *Anal. Chem.*, **40**, 586-593.

DeBon, F. and Le Fort, P (1982) A chemical mineralogical classification of common plutonic rocks and associations. *Trans. R. Soc. Lond.*, **73**, 135-149.

DePaolo, D.J. (1981) Neodymium isotopes in the Colorado Front Range and crust-mantle evolution in the Proterozoic. *Nature*, **291**, 193-196.

DePaolo, D.J., Manton, W.I., Grew, E.S., and Halpern, M. (1982) Sm-Nd, Rb-Sr and U-Th-Pb systematics of granulite facies rocks from Fyfe Hills, Enderby Land, Antarctica. *Nature*, **298**, 614-618.

DePaolo, D.J. (1983) Geochemical evolution of the crust and mantle. *Rev. Geophy. and Space Phys.*, **21**, 1347-1358.

DePaolo, D.J. (1988) Neodymium geochemistry - an introduction. Springer-Verlag, New York. pp.187

DeSoete, D., Gijbels, R., and Hoste, J. (1972) Neutron Activation Analysis. John Wiley and Sons, London. pp. 836.

Duke, M.J.M. (1983) Geochemistry of the Exshaw Shale of Alberta - an application of neutron activation analysis and related techniques. unpublished M.Sc. thesis, University of Alberta, Edmonton, Canada, pp.186.

Duke, M.J.M., Baadsgaard, H., Nutman, A.P., Compston, W., and McGregor, V.R. (1990) The geochronology of the Akia terrane, southern West Greenland. 7th *Int. Conf. on Geochronology, Cosmochhronology and Isotope Geology*. Geol. Soc. of Australia, **27**, p.19.

Duke, M.J.M. and Baadsgaard, H. (1993) Refinement of single bead ion exchange chromatography for U-Pb dating of small zircon samples. GAC/MAC Abstracts, Edmonton, Alberta, Canada. A24.

Ellis, D.J. (1992) Precambrian tectonics and the physiochemical evolution of the continental crust. II. Lithosphere delamination and ensialic orogeny. *Precambrian Res.*, **55**, 507-524.

Engel, A.E., Itson, S.P., Engel, C.G., Stickney, D.M., and Cray, Jr., E.J. (1974) Crustal evolution and global tectonics: a petrogenic view. *Geol. Soc. Am. Bull.*, **85**, 843-858.

Erdtmann, G. and Petri, H. (1986) Nuclear activation analysis: fundamentals and techniques. in Treatise on Analytical Chemistry, 2nd Ed, Pt.1, vol 14. Edited by Elving, P.J., John Wiley and Sons, New York.

Eugster, O., Tera, F., Burnett, D.S., and Wasserburg, G.J. (1970) Isotopic composition of gadolinium and neutron capture effects in some meteorites. *J. Geophys. Res.*, **75**, 2753-2768.

Faure, G., and Powell, J.L. (1972) *Strontium Isotope Geology*. Springer-Verlag, New York, pp.188.

Faure, G. (1986) *Principles of Isotope Geology*. 2nd edition, John Wiley and Sons, New York, pp.589.

Frey, F.A., Green, D.H., and Roy, S.D. (1978) Integrated models of basalt petrogenesis: a study of quartz-tholeiites to olivine melilites from southeastern Australia utilizing geochemical and experimental petrological data. *J. Petrol.*, **19**, 463-513.

Friend, C.R.L., Hall, R.P., and Hughes, D.J. (1981) The geochemistry of the Malene (Mid-Archaean) ultramafic-mafic amphibolite suite, southern West Greenland. *Spec. Publs. geol. Soc. Aust.*, **7**, 301-312.

Friend, C.R.L., Nutman, A.P., and McGregor, V.R. (1987) Late-Archaean tectonics in the Færinghaven - Tre Brødre area, south of Bukesfjorden, southern West Greenland. *J. Geol. Soc., Lon.*, **144**, 369-376.

Friend, C.R.L., Nutman, A.P., and McGregor, V.R. (1988) Late Archaean terrane accretion in the Godthåb region, southern West Greenland. *Nature*, **335**, 535-538.

Frost, B.R. and Frost, C.D. (1989) Magmas as a source of heat and fluids in granulite metamorphism. **in**: *Fluid Movements - Element Transport and the Composition of the Deep Crust* **ed.** Bridgwater, D., 1-18, Kluwer Academic Publishers.

Froude, D.O., Ireland, T.R., Kinny, P.D., Williams, I.S., and Compston, W. (1983) Ion microprobe identification of 4100 - 4200 Myr-old terrestrial zircons. *Nature*, **304**, 616-618.

Fyfe, W.S. (1973) The granulite facies, partial melting, and the Archean crust. *Phil. Trans. R. Soc. London*, **A273**, 457-461.

Gancarz, A.J. and Wasserburg, G.J. (1977) Initial Pb of the Amîtsoq gneisses, West Greenland, and implications for the age of the Earth. *Geochim. et Cosmochim. Acta.*, **41**, 1283-1301.

Garde, A.A. Larsen, O. and Nutman, A.P. (1985) Dating of the late Archaean crustal mobilisation north of Qugssuk, Godthåbsfjord, southern West Greenland. *Rapp. Grønlands. geol. Unders.*, **128**, 23-36.

Gill, J. (1981) Orogenic andesites and plate tectonics. Springer Verlag. pp. 389.

Gladney, E.S., Burns, C.E., and Roelaawts, I. (1983) 1982 Compilation of elemental concentrations in eleven United States Geological Survey rock standards. *Geostandards Newsletter*, **7**, 3-227.

Gladney, E.S. and Roelandts, I. (1988) 1987 Compilation of elemental concentration data for USGS BHVO-1, MAG-1, QLO-1, RGM-1, SCo-1, SDC-1, SGR-1 and STM-1. *Geostandards Newsletter*, **12**, 253-362.

Glikson, A.Y. (1979) Early Precambrian tonalite-trondhjemite sialic nuclei. *Earth Sci. Rev.*, **15**, 1-73.

Goldstein, S.L., O'Nions, R.K., and Hamilton, P.J. (1984) A Sm-Nd isotopic study of atmospheric dusts and particulates from major river systems *Earth Planet. Sci. Lett.*, **70**, 221-236.

Govindaraju, K. (1989) 1989 compilation of working values and sample description for 272 geostandards. *Geostandards Newsletter*, **13**, 1-113.

Govindaraju, K. (1987) 1987 compilation report on Ailsa Craig granite AC-E with the participation of 128 GIT-IWG laboratories. *Geostandards Newsletter*, **11**, 203-255.

Grant, N.K. and Hickman, M.H. (1984) Rb-Sr isotope systematics and contrasting histories of late Archean gneisses, West Greenland. *Geology*, **12**, 599-601.

Green, T.H. and Ringwood, A.E. (1968) Genesis of the calc-alkaline igneous rock suite. *Contr. Miner. Petrol.*, **18**, 105-162.

Griffin, W.L., McGregor, V.R., Nutman, A.P., Taylor, P.N., and Bridgwater, D. (1980) Early Archaean granulite-facies metamorphism south of Ameralik, West Greenland. *Earth planet. Sci Lett.,* **50**, 59-74.

Hamilton. P.J., O'Nions, R.K., Evensen, N.M., Bridgwater, D., and Allaart, J.H. (1978) Sm-Nd isotopic investigations of Isua supracrustals and implications for mantle evolution. *Nature*, **273**, 41-43.

Hamilton. P.J., Evensen, N.M., O'Nions, R.K., and Tarney, J. (1979) Sm-Nd systematics of Lewisian gneisses: implications for the origin of granulites. *Nature*, **277**, 25-28.

Hamilton. P.J., O'Nions, R.K., Bridgwater, D., and Nutman, A. (1983) Sm-Nd studies of Archaean metasediments and metavolcanics from West Greenland and their implications for the Earth's early history. *Earth Planet. Sci. Lett.*, **62**, 263-272.

Hargraves R.B. (1986) Faster spreading or greater ridge length in the Archean? *Geology*, **14**, 750-752.

Harland,W.B., Cox, A., Llewellyn, P.G., Pickton, C.A.G., Smith, A.G., and Walters, R. (1982) *A geological time scale*. Cambridge University Press.

Harley, S.L. (1989) The origins of granulites: a metamorphic perspective. *Geol. Mag.*, **126**, 215-247.

Hawkesworth, C.J., Hergt, J.M., McDermott, F., and Ellam, R.M. (1991) Destructive margin magmatism and the contributions from the mantle wedge and subducted crust. *Aust. J. Earth Sci.*, **38**, 577-594.

Heaman, L., Bowins, R., and Crocket, J. (1990) The chemical composition of igneous zircon suites: Implications for geochemical tracer studies. *Geochim. et Cosmochim. Acta.*, **54**, 1597-1607.

Heaman, L. and Parrish, R. (1991) U-Pb geochronology of accessory minerals. in Mineralogical Association of Canada Short course handbook on 'Application of radiogenic isotope systems to problems in geology'. *Ed*. Heaman, L. and Ludden, J.N., 59-102.

Heier, K.S. (1965) Metamorphism and the chemical differentiation of the crust. *Geol. Fören. Stockholm Förh.*, **87**, 49-256.

Heier, K.S. and Adams, J.A.S. (1965) Concentration of radioactive elements in deep crustal material. *Geochim. et Cosmochim. Acta.*, **29**, 53-61.

Heier, K. (1973) The movement of uranium during higher grade metamorphic processes. *Phil. Trans. R. Soc. Lond. A*, **291**, 413-421.

Hellman, P.L. and Green, T.H. (1979) The role of sphene as an accessory phase in the high-pressure partial melting of hydrous mafic components. *Earth Planet. Sci. Lett.*, **42**, 191-201.

Helz, R.T. (1976) Phase relations of basalts in their melting ranges at $PH_2O = 5$ kb. Part II. Melt composiawons. *J. Petrol.*, **17**, 139-193.

Herzberg, C.T., Fyfe, W.S., and Carr, M.J. (1983) Density constraints on the formation of the continental Moho and crust. *Contrib. Mineral. Petrol.*, **84**, 1-5.

Hoffman, P. (1988) United plates of America, the birth of a craton: Early Proterozoic assembly and growth of Laurentia. *Ann. Rev. Earth Planet. Sci.*, **16**, 543-603.

Holland, J.G. and Lambert, R.St.J. (1975) The chemistry and origin of the Lewisian gneisses of the Scottish mainland: the Scourie and Inver assemblages and sub-crustal accretion. *Precambrian Res.*, **2**, 161-188.

Hooper, P.R, and Johnson, D. (1987) Major and trace element analyses of rocks and minerals by automatic X-ray spectrometry. Internal report, Department of Geology, Washington State University, Pullman.

Humphries, F.J. and Cliff, R.A. (1982) Sm-Nd dating and cooling history of Scourian granulites, Sutherland. *Nature*, **295**, 515-517.

Hurst, R.W. (1978) Sr evolution in the West Greenland-Labrador craton: a model for early Rb depletion in the mantle. *Geochem. et Cosmochem. Acta*, **42**, 39-44.

Irvine, T.N. and Baragar, W.R.A. (1971) A guide to the chemical classification of the common volcanic rocks. *Can. J. Earth Sci.*, **8**, 523-548.

Jacobsen, S.B. and Wasserburg, G.J. (1980) Sm-Nd isotopic evolution of chondrites. *Earth Planet. Sci. Lett.*, **50**, 139-155.

Jacobsen, S.B. and Wasserburg, G.J. (1984) Sm-Nd isotopic evolution of chondrites ans achondrites II. *Earth Planet. Sci. Lett.*, **67**, 137-150.

Jacobsen, S.B. and Dymek, R.F. (1988) Nd and Sr systematics of clastic metasediments from Isua, West Greenland: identification of pre-3.8 Ga differentiated crustal components. *J. Geophy. Res.*, **93**, 338-354.

Jaffey, A.H., Flynn, K.F., Glendenin, L.E., Bentley, W.C., and Essling, A.M. (1971) Precision measurement of the half-lives and specific activities of U^{235} and U^{238}. *Phys. Rev.*, C, **4**, 1889-1906.

Jahn, B.-M., Glikson, A.Y., Peucat, J.J., and Hickman, A.H. (1981) REE geochemistry and isotopic data of Archaean silicic volcanics and granitoids from the Pilbara Block, Western Australia: implications for early crustal evolution. *Geochem. et Cosmochem. Acta*, **45**, 1633-1652.

Jahn, B.-M. and Zhang, Z. (1984) Archean granulite gneisses from eastern Hebei province, China: rare earth geochemistry and tectonic implications. *Contrib. Mineral. Petrol.*, **85**, 224-243.

Jahn, B.-M. (1990) Origin of granulites: geochemical constraints from Archean granulite facies rocks of the Sino-Korean craton, China. in D.Vielzeuf and Ph. Vidal (eds), *Granulites and Crustal Evolution*, 471-492.

James, P.R. (1975) Field mapping of Bjørneøen and the adjacent coast of Nordlandet, Godthåbsfjord, southern West Greenland. *Rapp. Grønlands. geol. Unders.*, **75**, 58-62.

Johnston, A.D. and Wyllie, P.J. (1988) Constraints on the origin of Archean trondhjemites based on phase relationships of Nûk gneiss with H_2O at 15 kbar. *Contrib. Mineral. Petrol.*, **100**, 35-46.

Kalsbeek, F. and Petersen, T.S. (1974) Estimation of the mode of (hornblende-) biotite gneisses and amphibolite with the help of chemical analyses. *Lithos*, **7**, 227-234.

Kalsbeek, F. and Pidgeon, R.T. (1980) The geological significance of Rb-Sr whole-rock isochrons of poly-metamorphic Archaean gneisses, Fiskenaesset area, southern West Greenland. *Earth Planet. Sci. Lett.*, **50**, 225.

Kinny, P.D. (1986) 3820 Ma zircons from a tonalitic Amîtsoq gneiss in the Godthåb district of southern West Greenland. *Earth Planet. Sci. Lett.*, **79**, 337-347.

Kramers, J.D. and Ridley, J.R. (1989) Can Archean granulites be direct crystallization products from a sialic magma layer? *Geology*, **17**, 442-225.

Kramers, J.D. (1991) Paradoxes of the mantle lithosphere underneath Archaean continents and models for its origin. *Schweiz. Mineral. Petrogr. Mitt.*, **71**, 175-186.

Krogh, T.E. (1973) A low contamination method for hydrothermal decomposition of zircon and extraction of U an Pb for isotopic age determinations. *Geochem. et Cosmochem. Acta*, **37**, 485-494.

Krogh, T.E. and Davis, G.L. (1975) The production and preparation of ^{205}Pb for use as a tracer for isotope dilution analyses. *Carnegie Inst. Washington, Yearbook*, 1974, 416-417.

Krogh, T.E. (1982) Improved accuracy of U-Pb ages by the creation of more concordant systems using an air abrasion technique. *Geochem. et Cosmochem. Acta*, **46**, 637-649.

Lambert, I.B. (1971) The composition and evolution of the deep continental crust. *Spec. Publ geol. Soc. Aust.*, **3**, 419-428.

Lambert, I.B. and Wyllie, P.J. (1974) Melting of tonalite and crystallization of andesite liquid with excess water to 30 kilobars. *J. Geol.*, **82**, 88-97.

Lambert, R. St. J. (1976) Archean thermal regimes, crustal and upper mantle temperatures, and a progressive evolutionary model for the Earth. in *The Early History of the Earth*. Ed. B. F. Windley., 363-373.

Lambert, R. St. J., and Holland, J.G. (1976) Amîtsoq gneiss geochemistry: preliminary observations.in *The Early History of the Earth*. Ed. B. F. Windley., 191-201.

Lambert, R. St. J., Chamberlain, V.E., and Holland, J.G. (1976) The geochemistry of Archean rocks. in *The Early History of the Earth*. Ed. B. F. Windley., 377-387.

Leake, B.E. (1990) Granite magmas: their sources, initiation and consequences of emplacement. *J. Geol. Soc., Lond.*, **147**, 579-589.

Lederer, C.M. and Shirley, V.S. (1978) Table of the Isotopes (7th ed.) John Wiley and Sons, New York.

Luth, W.C., Johns, R.H., and Tuttle, O.F. (1964) The granite system at pressures of 4 to 40 kilobars. *J. Geophys. Res.*, **69**, 759-773.

Macdonald, R. (1974) Investigations on the granulites of southern Nordland, Godthåbsfjord, Central West Greenland. *Grønl. Geol. Unders., Rapp.*, **65**, 44-49.

Manton, W.I. (1988) Separation of Pb from young zircons by single-bead ion exchange. *Chem. Geol. (Isotope Geosci. Sect.)*, **73**, 147-152.

Martin, H. (1986) Effect of steeper Archean geothermal gradient on geochemistry of subduction-zone magmas. *Geology*, **14**, 753-756.

Mattinson, J.M. (1972) Preparation of hydrofluoric, hydrochloric, and nitric acids at ultralow lead levels. *Anal. Chem.*, **44**, 1715-1716.

McGregor, V.R. (1973) The early Precambrian gneisses of the Godthåb district, West Greenland. *Phil. Trans. R. Soc. London*, **A273**, 343-358.

McGregor, V.R. and Mason, B. (1977) Petrogenesis and geochemistry of metabasaltic and metasedimentary enclaves in the Amîtsoq gneisses, West Greenland. *Am. Mineralogist.*, **62**, 887-904.

McGregor, V.R. (1979) Archaean gray gneisses and the origin of continental crust: Evidence from the Godthåb Region, West Greenland. in *Trondhjemites, Dacites and Related Rocks*. ed. Barker, F., 169-205, Elsevier, Amsterdam.

McGregor, V.R., Bridgwater, D, and Nutman, A.P. (1983) The Qârusuk dykes: Post-Nûk pre-Qôrqut granitoid magmatism in the Godthåb region, southern West Greenland. *Grønl. Geol. Unders., Rapp.*, **112**, 101-112.

McGregor, V.R., Nutman, A.P., and Friend, C.R.L. (1986) The Archean geology of the Godthåbsfjord region, southern West Greenland. in Early crustal genesis: the Worlds's oldest rocks. (ed) Ashwal, L.D., *LPI Tech. Rep. 86-04.*, 113-169.

McGregor, V.R., Friend, C.R.L. and Nutman, A.P. (1991) The late Archaean mobile belt through Godthåbsfjord, southern West Greenland: a continent-continent collision zone? *Bull. geol. Soc. Denmark*, **39**, 179-197.

McGregor, V.R. and Friend, C.R.L. (1992) *J. Geol.*, **100**, 207-219.

Mezger, K. (1990) Geochronology in granulites. in D.Vielzeuf and Ph. Vidal (eds), *Granulites and Crustal Evolution*, 451-470.

Mogk, D.W., Mueller, P.A., and Wooden, J.L. (1992) The nature of Archean terrane boundaries: an example from the northern Wyoming Province. *Precambrian Res.*, **55**, 155-168.

Moorbath, S., Welke, H., and Gale, N.H. (1969) The significance of lead isotope studies in ancient, high-grade metamorphic basement complexes, as exemplified by the Lewsian rocks of northwest Scotland. *Earth Planet. Sci. Lett.*, **6**, 245-256.

Moorbath, S., O'Nions, R.K., Pankhurst, R.J., Gale, N.H., and McGregor, V.R. (1972) Further rubidium-strontium age determinations on the very early Precambrian rocks of the Godthåb district, West Greenland. *Nature*, **240**, 78-82.

Moorbath, S., O'Nions, R.K., and Pankhurst, R.J. (1973) Early Archaean age for the Isua Iron Formation, West Greenland. *Nature*, **245**, 138-139.

Moorbath, S. and Pankhurst, R.J. (1976) Further Rb-Sr age and isotope evidence for the nature of the late Archaean plutonic event in West Greenland. *Nature*, **262**, 124-126.

Moorbath, S. (1977) Ages, isotopes and evolution of Precambrian continental crust. *Chem. Geol.*, **20**, 151-187.

Moorbath, S., Allaart, J.H., Bridgwater, D., and McGregor, V.R. (1977) Rb-Sr ages of early Archaean supracrustal rocks and Amîtsoq gneisses at Isua. *Nature*, **270**, 43-45.

Moorbath, S., Taylor, P.N., and Goodwin, R. (1981) Origin of granitic magma by crustal remobilisation: Rb-Sr and Pb-Pb geochronology and isotope geochemistry of the late Archaean Qorqut granite complex of southern West Greenland. *Geochim. et Cosmochim. Acta.*, **45**, 1051-1060.

Moorbath, S. (1984) Origin of granulites. *Nature*, **312**, 290.

Moorbath, S., Taylor, P.N., and Jones, N.W. (1986) Dating the oldest terrestrial rocks - fact and fiction. *Chem. Geol.*, **57**, 63-86.

Myers, J.S. (1978) Formation of banded gneisses by deformation of igneous rocks. *Precamb. Res.*, **6**, 43-64.

Myers, J.S. (1981) The Fiskenaesset anorthosite complex - a stratigraphic key to the tectonic evolution of the west Greenland complex 3000 - 2800 m.y. ago. *Spec. Pub. geol. Soc. Aust.*, **7**, 351-360.

Myers, J.S. (1985) Stratigraphy and structure of the Fiskenaesset Complex, southern West Greenland. *Bull. Grønlands geol. Unders.*, **150**, pp.72.

Nelson, B.K. and DePaolo D.J. (1985) Rapid production of continental crust 1.7 - 1.9 b.y. ago: Nd ans Sr isotopic evidence from the basement of the North American midcontinent. *Geol. Soc. Am. Bull.*, **96**, 746-754.

Nesbit, E.G. (1987) *The Young Earth - an introduction to Archaean geology.* Allen and Unwin, pp.402.

Newton, R.C., Smith, J.V., and Windley, B.F. (1980) Carbonic metamorphism, granulites and crustal growth. *Nature*, **288**, 45-50.

Newton, R.C. (1992) An overview of charnockite. *Precambrian Res.*, **55**, 399-405.

Nutman, A.P., Bridgwater, D., and Fryer, B.J. (1984a) The iron-rich suite from the Amîtsoq gneisses of southern West Greenland: early Archaean plutonic rocks of mixed crustal and mantle origin. *Contrib. Mineral. Petrol.*, **87**, 24-34.

Nutman, A.P., Allaart, J.H., Bridgwater, D., Dimroth, E., and Rosing, M. (1984b) Stratigraphic and geochemical evidence for the depositional environment of the early Archaean Isua supracrustal belt, West Greenland. *Precambrian Res.*, **25**, 365-396.

Nutman, A.P. and Bridgwater, D. (1986) Early Archaean Amîtsoq tonalites and granites of the Isukasia area, southern West Greenland: development of the oldest-known sial. *Contrib. Mineral. Petrol.*, **94**, 137-148.

Nutman, A.P., Friend, C.L., Baadsgaard, H., and McGregor, V.R. (1989) Evolution and assembly of Archaean gneiss terranes in the Godthåbsfjord region, southern West Greenland: structural, metamorphic and isotopic evidence. *Tectonics*, **8**, 573-589.

Nutman, A.P. (1990) New old rocks from Greenland. *7th Int. Conf. on Geochronology, Cosmochhronology and Isotope Geology*. Geol. Soc. of Australia, **27**, p.72.

Nutman, A.P., and Collerson K.D. (1991) Very early Archean crustal-accretion complexes preserved in the North Atlantic craton. *Geology*, **19**, 791-794.

O'Connor, J.T. (1965) A classification for quartz-rich igneous rocks based on feldspar ratios. *U.S. Geol. Surv. Prof. Paper.*, **525-B**, 79-84.

Olsen (1983) *In*: Atherton, M.P. and Gribble, C.D. (*Eds*) *Migmatites, Melting and Metamorphism*. Shiva Publications, Nantwich, Cheshire, U.K., 250-263.

O'Nions, R.K. and Pankhurst, R.J. (1978) Early Archaean rocks and geochemical evolution of the Earth's crust. *Earth Planet. Sci. Lett.*, **38**, 211-236.

O'Nions, R.K. and McKenzie D.P. (1988) Melting and continent generation. *Earth Planet. Sci. Lett.*, **90**, 449-456.

Pankhurst, R.J., Moorbath, S., and McGregor, V.R. (1973) Late event in the geological evolution of the Godthaab District, West Greenland. *Nat. Phy. Sci.,* **243**, 24-26.

Parrish, R.R., Roddick, J.C., Loveridge, W.D., and Sullivan, R.W. (1987) Uranium-lead analytical techniques at the geochronology laboratory, Geological Survey of Canada. in *Radiogenic Age and Isotopic Studies: Report 1, Geol. Surv. Can.*, Paper **87-2**, 3-7.

Parrish, R.R. and Krogh, T.E. (1987) Synthesis and purification of ^{205}Pb for U-Pb geochronology. *Chem. Geol. (Isotope Geosci. Sect.)*, **66**, 103-110.

Passchier, C.W., Myers, J.S. and Kroner, A. (1990) *Field geology of high-grade gneiss terrains*. Springer-Verlag, pp.150.

Paterson, L.A. (1985) Petrology of the Tsu Lake Gneiss in the Fort Smith area. Unpubl. M.Sc thesis. Univ. of Alberta. pp.308.

Peterman, Z.E. (1979) Strontium isotope geochemistry of late Archean to late Cretaceous tonalites and trondhjemites. in Trondhjemites, Dacites and Related Rocks. ed. Barker, F., 133-147. Elsevier, Amsterdam.

Petersen, T.S. (1977) FISK: a FORTRAN program to estimate the mode of (hornblende-) biotite gneisses and amphibolite from chemical analyses. *Computers and Geosciences*, **3**, 19-24.

Pride, C. and Muecke, G.K. (1980) Rare earth element geochemistry of the Scourian Complex N.W. Scotland - evidence for the granite-granulite link. *Contrib. Min. Petrol.*, **73**, 403-412.

Rameshwar Rao, D., Narayana, B.L., and Balaram, V. (1991) Nature and origin of lower crustal rocks of Dharmapuri area, Tamil Nadu, southern India -a geochemical approach. *Geochem. J.*, **25**, 57-74.

Rapp, R.P., Watson, E.B., and Miller, C.F. (1991) Partial melting of amphobolite/eclogite and the origin of Archean trondhjemites and tonalites. *Precamb. Res.*, **51**, 1-25.

Reed, S.J. (1980) The petrology of the high grade Archaean rocks from Nordlandet, southern West Greenland. Ph.D. thesis, University of Exeter, United Kingdom.

Riciputi, L., Valley, J. and McGregor, V.R. (1990) Conditions of Archean granulite metamorphism in the Godthåb - Fiskenaesset region, southern West Greenland. *J. Meta. Geol.*, **8**, 171-190.

Roddick, J.C., Loveridge, W.D., and Parrish, R.R. (1987) Precise U/Pb dating of zircon at the sub-nanogram Pb level. *Isotope Geosci.*, **66**, 111-121.

Rollinson, H.R. and Windley, B.F. (1980a) Selective elemental depletion during metamorphism of Archaean granulites, Scourie, NW Scotland. *Contrib. Mineral. Petrol.*, **72**, 257-263.

Rollinson, H.R. and Windley, B.F. (1980b) An Archaean granulite-grade tonalite-trondhjemite-granite suite from Scourie, NW Scotland: geochemistry and origin. *Contrib. Mineral. Petrol.*, **72**, 265-281.

Rudnick, R.L., McLennan, S.M., and Taylor, S.R. (1985) Large ion lithophile elements in rocks from high-pressure granulite facies terrains. *Geochim. et Cosmochim. Acta.*, **49**, 1645-1655.

Rudnick, R. and Taylor, S.R. (1986) Geochemical constraints on the origin of Archaean tonalitic-trondhjemitic rocks and implications for lower crustal composition. **in** Dawson, J.B., Carswell, D.A., Hall, J., and Wedepohl, K.H. (eds) *The Nature of the Lower Continental Crust*, Geol. Soc. Sp. Publ. **24**, 179-191.

Rudnick, R.L. and Presper, T. (1990) Geochemistry of intermediate- to high-pressure granulites. **in** D.Vielzeuf and Ph. Vidal (eds), *Granulites and Crustal Evolution*, 523-550.

Rudnick, R. (1990) Continental crust - Growing from below. *Nature*, **347**, 711-712.

Rudnick, R.L. (1992) Restites, Eu anomalies, and the lower continental crust. *Geochim. et Cosmochim. Acta.*, **56**, 963-970.

Rutter, M.J. and Wyllie, P.J. (1988) Melting of vapour-absent tonalite at 10 kbar to simulate dehydration-melting in the deep crust. *Nature*, **331**, 159-160.

Rushmer, T. (1991) Partial melting of two amphibolites: contrasting experimental results under fluid-absent conditions. *Contrib. Mineral. Petrol.*, **107**, 41-59.

Ryerson, F.J. and Watson, E.B. (1987) Rutile saturation in magmas: implications for Ti-Nb-Ta depletion in island-arc basalts. *Earth Planet. Sci. Lett.*, **86**, 225-239.

Schiøtte, L., Compston, W., and Bridgwater, D. (1988) Late Archaean ages for the deposition of clastic sediments belonging to the Malene supracrustals, southern west Greenland: evidence from an ion probe U-Pb zircon study. *Earth Planet. Sci. Lett.*, **87**, 45-58.

Schiøtte, L., Noble, S., and Bridgwater, D. (1990) U-Pb mineral ages from northern Labrador: Possible evidence for interlayering of early and middle Archean tectonic slices. *Geoscience Canada*, **17**, 227 - 231.

Schiøtte, L., and Compston, W. (1990) U-Pb age pattern for single zircons from the early Archaean Akilia association south of Ameralik fjord, southern West Greenland. *Chem. Geol. (Iso. Geosci. Sect.)*, **80**, 147-157.

Shaw, D.M. (1968) A review of K - Rb fractionation trends by covariance nanlysis. *Geochim. et Cosmochim. Acta.*, **32**, 573-601.

Shaw, D.M. (1972) The origin of the Apsley gneiss, Ontario. *Can. J. Earth Sci.*, **9**, 18-35.

Shaw, D.M., Cramer, J.J., Higgins, M.D., and Truscott, M.G. (1986) Composition of the Canadian Precambrian shield and the continental crust of the earth. **in** *The Nature of the Lower Continental Crust*. (ed) Dawson, J.B., Carswell, D.A., Hall, J., and Wedepohl, K.H. (eds) *Geol. Soc. Sp. Publ.* **24**, 275-282.

Sheraton, J.W., Skinner, A.C., and Tarney, J. (1973) The geochemistry of the Scourian gneisses of the Assynt district. **in** *The early Precambrian of Scotland and related rocks of Greenland*. (ed) Park, R.G. and Tarney, J., 30.

Skjerlie, K.P.. and A.D. Johnston (1992) Vapor-absent melting at 10 kbar of a biotite- and amphibole-bearing tonalitic gneiss: implications for the generation of A-type granites. *Geology*, **20**, 263-266.

Stacey, J.S. and Kramers, J.D. (1975) Approximation of terrestrial lead isotopic evolution by a two-stage model. *Earth Planet. Sci. Lett.*, **26**, 207-221.

Steger, H.F. (1983) Certified reference materials. CANMET Report **83-3E**, pp. 35, Energy, Mines and Resources, Canada.

Steiger, R.H. and Jager, E. (1977) Subcommission on geochronology: convention on the use of decay constants in geo- and cosmochronology. *Earth Planet. Sci. Lett.*, **36**, 359-362.

Streckeisen, A. (1973) Classification and nomenclature of plutonic rocks recommendations. *N. Jb. Miner. Mh.*, **4**, 149-164.

Strelow, F.W.E. (1960) Ion exchange selectivity scales for cations based on equilibrium distribution coefficients in hydrochloric acid. *Anal. Chem.*, **32**, 1185-1188.

Strelow, F.W.E., Rethemeyer, R., and Bothma, C.J.C. (1965) Ion exchange selectivity scales for cations in nitric acid and sulphuric acid media with a sulfonated polystyrene resin. *Anal. Chem.*, **37**, 106-111.

Strelow, F.W.E. (1978) Distribution coefficients and anion exchange behaviour of some elements in hydrobromic-nitric acid mixtures. *Anal. Chem.*, **50**, 1359-1361.

Tarney, J., Skinner, A.C., and Sheraton, J.W. (1972) A geochemical comparison of the major Archaean gneiss units from northwest Scotland and east Greenland. *24th Int. Geol. Cong.*, 162-174.

Tarney, J. (1976) Geochemistry of Archaean high-grade gneisses, with implications as to the origin and evolution of Precambrian Crust. **in** *The Early History of the Earth*. Ed. Windley, B.F., 405-417.

Tarney, J., Weaver, B., and Dury, S.A. (1979) Geochemistry of Archaean trondhjemitic and tonalitic gneisses from Scotland and east Greenland. **in** *Trondhjemites, Dacites and Related Rocks*. **ed.** Barker, F., 275-299. Elsevier, Amsterdam.

Tarney, J. and Weaver, B.L. (1987) Geochemistry of the Scourian complex: petrogenesis and tectonic models. in Park, R.G. and Tarney, J. (eds) *Evolution of the Lewsisian and Comparable Precambrian High Grade Terrains*, Geol. Soc. Sp. Publ. **27**, 45-56.

Tatsumi, Y., Hamilton, D.L., and Nesbitt, R.W. (1986) Chemical characteristics of fluid phase released from a subducted lithosphere and the origin of arc magmas: evidence from high-pressure experiments and natural rocks. *J. Volcanol. Geotherm. Res.*, **29**, 293-309.

Taylor, P.N., Moorbath, S., Goodwin, R., and Petrykowski, A.C. (1980) Crustal contamination as an indicator of the extent of early Archaean continental crust: Pb isotopic evidence from the late Archaean gneisses of West Greenland. *Geochim. et Cosmochim. Acta.*, **44**, 1437-1453.

Taylor, P.N., Jones, N.W., and Moorbath, S. (1984) Isotopic assessment of relative contributions from crust and mantle sources to the magma genesis of Precambrian granitoid rocks. *Phil. Trans. R. Soc., Lond., Ser. A.*, **310**, 605-625.

Taylor, S.R. and McLennan, S. (1985) The Continental Crust: its composition and evolution. Blackwell publishing. pp.312.

Taylor, S.R. (1990) Continental crust - Not mere scum of the Earth. *Nature*, **346**, 608-609.

Tilton, G.R. and Kwon, S.-T. (1990) Isotopic evidence for crust-mantle evolution with emphasis on the Canadian Shield. *Chem. Geol.*, **83**, 149-163.

Tuttle, O.F. and Bowen, N.L. (1958) Origin of granite in the light of experimental studies in the system $NaAlSi_3O_8$-$KAlSi_3O_8$-SiO_2-H_2O. *Geol. Soc. Amer. Mem.* **74**.

Valley, J.W. (1992) Granulite formation is driven by magmatic processes in the deep crust. *Earth-Sci. Rev.* **32**, 145-146.

van der Lann, S.R. and Wyllie, P.J. (1992) Constraints on Archean trondhjemite genesis from hydrous crystallization experiments on Nûk gneiss at 100 - 17 kbar. *J. Geol.*, **100**, 57-68.

Walker, R.L., Eby, R.E., Pritchard, C.A., and Carter, J.A. (1974) Simultaneous plutonium and uranium isotopic analysis from a single resin bead - a simplified chemical technique for assaying spent reactor fuels. *Anal. Lett.* **7**, 563-574.

Watson, E.B. and Capobianco, C.J. (1981) Phosphorus and the rare earth elements in felsic magmas: an assessment of the role of apatite. *Geochim. et Cosmochim. Acta.*, **45**, 2349-2358.

Watson, E.B. and Harrison, T.M. (1984) Accessory minerals and the geochemical evolution of crustal magmatic systems: a summary and prospectus of experimental approaches. *Physics of the Earth and Planetary Int.*, **35**, 19-30.

Weaver, B.L. and Tarney, J. (1980a) Rare earth geochemistry of Lewsisian granulite-facies gneisses, northwest Scotland: implications for the petrogenesis of the Archaean lower continental crust. *Earth Planet. Sci. Lett.*, **51**, 279-296.

Weaver, B.L. and Tarney, J. (1980b) Continental crust composition and nature of the lower crust: constraints from mantle Nd-Sr isotope correlation. *Nature*, **286**, 342-346.

Weaver, B.L. and Tarney, J. (1981) Lewsisian gneiss geochemistry and Archaean crustal development models. *Earth Planet. Sci. Lett.*, **55**, 171-180.

Weaver, B.L. and Tarney, J. (1983) Elemental depletion in Archaean granulite-facies rocks. *In*: Atherton, M.P. and Gribble, C.D. (*Eds*) *Migmatites, Melting and Metamorphism*. Shiva Publications, Nantwich, Cheshire, U.K., 250-263.

Weaver, B.L. and Tarney, J. (1984) Estimating the composition of the continental crust: an empirical approach. *Nature*, **310**, 575-577.

Weaver, B.L. (1991) The origin of ocean island basalt end-member compositions: trace element and isotopic constraints. *Earth Planet. Sci. Lett.*, **104**, 381-397.

Wells, P.R.A. (1980) Thermal models for the magmatic accretion and subsequent metamorphism of continental crust. *Earth Planet. Sci. Lett.*, **46**, 253-265.

Werner, C.D. (1987) Saxonian granulites - igneous or lithogenous. A contribution to the geochemical diagnosis of the original rocks in high-metamorphic complexes. in Gerstenberger, H. *ed*. Contributions to the geology of the Saxonian granulite massif (Sachsisches Granulitgebirge) Zfl-Mitteilungen Nr **133**, 221-250.

White and Chappell (1977) Ultrametamorphism and granitoid genesis. *Tectonophysics*, **43**, 7-22.

Whitehouse, M.J., and Moorbath, S. (1986) Pb-Pb systematics of Lewisian gneisses - implications for crustal differentiation. *Nature*, **319**, 488-489.

Whitehouse, M.J. (1988) Granulite facies Nd-isotopic homogenization in the Lewisian complex of northwest Scotland. *Nature*, **331**, 705-707.

Wilks, M.E. (1988) The Himalayas - a modern analogue for Archaean crustal evolution. *Earth Planet. Sci. Lett.*, **87**, 127-136.

Williams, I.S. and Claesson, S. (1987) Isotopic evidence for the Precambrian provenance and Caledonian metamorphism of high grade paragneisses from the Seve Nappes, Scandinavian Caledonides. *Contrib. Mineral. Petrol.*, **97**, 205-217.

Windley, B.F. (1984) The Evolving Continents. 2nd Ed., John Wiley and Sons. pp. 399.

Winther, K.T. and Newton, R.C. (1991) Experimental melting of hydrous low-K tholeiite: evidence on the origin of Archaean cratons. *Bull. geol. Soc. Denmark*, **39**, 213-228.

Wolf, M.B. and Wyllie, P.J. (1991) Dehydration-melting of solid amphibolite at 10 kbar: textural development, liquid inter-connectivity and applications to the segregation of magmas. *Min. and Petrol.*, **44**, 151-179.

Wyllie, P.J. (1984) Constraints imposed by experimental petrology on possible and impossible magma sources and products. *Phil. Trans. R. Soc., Lond., Ser. A.*, **310**, 439-456.

Wyllie, P.J. and Rutter, M.J. (1988) Melting sites at convergent plate boundaries with experimental data on vapor-absent tonalite gneiss. *Soc. Ital. di Min. e Petro.*, **43**, 1291-1306.

York, D. (1969) Least squares fitting of a straight line with correlated errors. *Earth Planet. Sci., Lett*, **5**, 320-324.

Yoshida, M., Santosh, M., and Shirahata, H. (1991) Geochemistry of gneiss-granulite transformation in the "Incipient Charnockite" zones of southern India. *Mineral. Petrol.* **45**, 69-83.

Zen, E-A. (1986) Aluminum enrichment in silicate melts by fractional crystallization: some mineralogic and petrographic constraints. *J. Petrol.* **27**, 1095 - 1117.

APPENDIX 1.

Sample Codes, Rock-types, Locations, and Grid References.

The identification code, rock-type, descriptive location, and grid reference of each sample analyzed in this study is listed below. Exceptions include the samples designated G86-9nn. These samples were kindly collected and supplied by V.R. McGregor for study. In lieu of grid reference co-ordinates for these samples a more detailed description of the sample location is given.

The rock-type deignation is based on a variety of criteria including:

a) O'Connor's (1965) granitoid classification scheme based on normative feldspar content (with modifications by Barker (1979).

b) major element chemistry (*e.g.*, trondhjemite definition, Barker (1979)).

c) quasi-modal QAP classification based on major element chemistry (Kalsbeek and Petersen, 1974; Streckeisen, 1973)

d) Dubon and Le Fort (1982) P-Q classification (which uses two parameters Q (Si/(3-(K + Na + 0.667Ca)) and P (K - (Na + Ca))) found in the PC-based programme NEWPET.

Sample Code	Rock-type	Location	Position	
			N	W
G87 - 1	granodioritic Nûk gneiss	By airport	64 11'16"	51 40'45"
G87 - 2	trondhjemitic Nûk gneiss	By airport	64 11'16"	51 40'45"
G87 - 3	trondhjemitic Nûk gneiss	By airport	64 11'16"	51 40'45"
G87 - 4	trondhjemitic Nûk gneiss	By airport	64 11'16"	51 40'45"
G87 - 5	granodioritic Nûk gneiss	By airport	64 11'16"	51 40'45"
G87 - 6	? amphibolite in gn	By airport	64 11'16"	51 40'45"
G87 - 10	? amph/gabbro gn	By runway	64 11'25"	51 40'45"
G87 - 12	trondhjemitic Nûk gneiss	N end of runway	64 11'53"	51 40'44"
G87 - 13	trondhjemitic Nûk gneiss	N end of runway	64 11'53"	51 40'44"
G87 - 14	trondhjemitic Nûk gneiss	By runway	64 11'24"	51 40'46"
G87 - 15	trond/granodioritic	Airport road	64 11'35"	51 41'23"
G87 - 16	qtz-dioritic Nûk gneiss	Airport road	64 11'27"	51 41'40"
G87 - 17	qtz-dioritic Nûk gneiss	Airport road	64 11'33"	51 41'49"
G87 - 18	qtz-dior/tonalitic Nûk gn	Airport road	64 11'33"	51 41'49"
G87 - 19	granitic gneiss	Airport road	64 11'33"	51 41'49"
G87 - 20	granodioritic Nûk gneiss	Airport road	64 11'33"	51 42'00"
G87 - 21	leucotonalitic Nûk gneiss	Airport road	64 11'28"	51 42'07"
G87 - 22	tonalitic Nûk gneiss	Airport road T	64 11'09"	51 42'37"
G87 - 24	tonalitic/trondj Nûk gn	Town road	64 11'11"	51 43'02"
G87 - 25	low Al trondh' Amîtsoq gn	Angissunguaq	64 04'26"	51 45'51"
G87 - 27	?trondh' gn in Amîtsoq gn	Angissunguaq	64 04'33"	51 46'35"
G87 - 34	tonalitic Nûk gneiss	Pularqavit	64 04'47"	51 47'49"
G87 - 35	trondhjemitic Nûk gneiss	Tartinguaq	64 07'10"	51 43'43"
G87 - 36	tonalitic Nûk gneiss	Tartinguaq	64 07'10"	51 43'43"
G87 - 39	dioritic Nûk gneiss	Tartinguaq	64 07'12"	51 45'13"
G87 - 40	dioritic/tonalitic Nûk gn	Tartinguaq	64 06'51"	51 46'54"
G87 - 42	tonalitic Nûk gneiss	Tartinguaq	64 06'51"	51 46'54"
G87 - 43	tonalitic Nûk gneiss	Tartinguaq	64 06'57"	51 46'36"
G87 - 44	trondhjemitic Nûk gneiss	Hundeo aw	64 07'39"	51 46'45"
G87 - 45	trondhjemitic Ikkatoq gn	NE-side Nuuk pen'	64 12'36"	51 29'49"
G87 - 46	trondhjemitic Ikkatoq gn	NE-side Nuuk pen'	64 12'42"	51 31'02"
G87 - 47	granodioritic Ikkatoq gn	NE-side Nuuk pen'	64 12'53"	51 31'30"
G87 - 57	granodioritic Nûk gneiss	Pipe-line traverse	64 12'21"	51 41'36"
G87 - 58	trondhjemitic Nûk gneiss	Pipe-line traverse	64 12'18"	51 41'34"
G87 - 59	?? tonalitic Nûk gneiss	Pipe-line traverse	64 11'13"	51 42'24"
G87 - 60	trondhjemitic Nûk gneiss	Pipe-line traverse	64 11'13"	51 42'24"
G87 - 61	granitic sheet	Pipe-line traverse	64 11'13"	51 42'24"
G87 - 64	trondhjemitic Amîtsoq gn	Rypeo	64 06'51"	51 42'38"
G87 - 67	dioritic gran (qtz norite)	Nordlandlet	64 11'46"	51 50'33"
G87 - 68	granitic sheet	Nordlandlet	64 11'46"	51 50'33"
G87 - 69	retro'dioritic(qtz norite)	Nordlandlet	64 11'46"	51 50'33"

Sample Code	Rock-type	Location	Position	
			N	W
G87 - 70	dioritic gran (qtz norite)	Nordlandlet	64 12’28"	51 50’56"
G87 - 72	tonalitic Amîtsoq gneiss	Ugujarssuit		
G87 - 78	trondhjemitic Amîtsoq gn	Qorqut		
G87 - 80	granodioritic Nûk gneiss	S’rn Store Malene	64 08’38"	51 41’05"
G87 - 85	qtz-dioritic Nûk gneiss	S’rn Store Malene	64 09’13"	51 41’45"
G87 - 86	tonalitic Nûk gneiss	S’rn Store Malene	64 09’36"	51 41’36"
G87 - 87	tonalitic Nûk gneiss	S’rn Store Malene	64 09’57"	51 41’12"
G87 - 88	trondhjemitic Nûk gneiss	S’rn Store Malene	64 10’06"	51 41’09"
G87 - 89a	trondhjemitic Nûk gneiss	S’rn Store Malene	64 10’19"	51 40’53"
G87 - 89b	qtz-dioritic Nûk gneiss	S’rn Store Malene	64 10’19"	51 40’53"
G87 - 90	tonalitic Nûk gneiss	A’port road quarry	64 11’35"	51 41’16"
G87 - 91	qtz-dioritic Nûk gneiss	A’port road quarry	64 11’35"	51 41’16"
G87 - 92	tonalitic Nûk gneiss	A’port road quarry	64 11’35"	51 41’16"
G87 - 93	grano/trondhj Nûk gneiss	A’port road quarry	64 11’35"	51 41’16"
G87 - 94	grano/trondhj Nûk gneiss	Building area road	64 11’25"	51 43’06"
G87 - 103	trondhjemitic Nûk gneiss	Marina	64 10’30"	51 43’00"
G87 - 111	trondhjemitic Nûk gneiss	Marina	64 10’30"	51 43’00"
G87 - 112	qtz-dioritic Nûk gneiss	Nuuk beach	64 10’00"	51 45’22"
G87 - 113	tonalitic Nûk gneiss	Nuuk beach	64 10’00"	51 45’22"
G87 - 114	trondhj/grano’ Nûk gneiss	Nuuk beach	64 10’00"	51 45’22"
G87 - 115	trondhj/grano’ Nûk gneiss	Nuuk beach	64 10’00"	51 45’22"
G87 - 116	trondhjemitic Nûk gneiss	S’rn Sadelo	64 15’42"	51 36’59"
G87 - 118	dioritic Nûk gneiss	S’rn Sadelo	64 14’34"	51 37’00"
G87 - 120	trondhjemitic Nûk gneiss	S’rn Sadelo	64 14’34"	51 37’00"
G87 - 121	trondhjemitic Nûk gneiss	S’rn Sadelo	64 14’33"	51 36’28"
G87 - 122	trondhjemitic Nûk gneiss	S’rn Sadelo	64 14’30"	51 36’08"
G87 - 123	tonalitic Nûk gneiss	S’rn Sadelo		
G87 - 124	tonalitic Nûk gneiss	S’rn Sadelo		
G87 - 127	granitic gneiss	N coast Nuuk pen’		
G87 - 128	dioritic granulite(norite)	Nordlandlet	64 11’51"	51 54’22"
G87 - 129	trondhj’ gran (enderbite)	Nordlandlet	64 11’51"	51 54’22"
G87 - 130	dioritic gran 2.5m(norite)	Nordlandlet	64 11’51"	51 54’22"
G87 - 131	dioritic gran 1 m (norite)	Nordlandlet	64 11’51"	51 54’22"
G87 - 133	retro’ granulite wt shear	Nordlandlet	64 11’51"	51 54’22"
G87 - 135	dioritic gran (qtz norite)	Nordlandlet	64 11’40"	51 56’09"
G87 - 136	tonalitic gran (enderbite)	Nordlandlet	64 11’40"	51 56’09"
G87 - 137	dioritic gran’ sl ret QN	Nordlandlet	64 11’40"	51 56’09"
G87 - 138	dioritic gran’ sl ret QN	Nordlandlet	64 11’40"	51 56’09"
G87 - 139	dioritic gran’ wt sm shear	Nordlandlet	64 11’40"	51 56’09"
G87 - 140	granodioritic Amîtsoq gn	Napassulik?		
G87 - 141	granitic sheet in G87-140	Napassulik?		

Sample Code	Rock-type	Location	Position	
			N	W
G87 - 142	trondhjemitic Nûk gneiss	Napassulik?		
G87 - 143	mylonitic shear zone	Napassulik?		
G87 - 144	trondhjemitic Nûk gneiss	SW. Bjørneøen	64 22’24"	51 23’38"
G87 - 145	granodioritic Nûk gneiss	SW. Bjørneøen	64 22’24"	51 23’38"
G87 - 146	trondhjemitic Nûk gneiss	SW. Bjørneøen	64 22’11"	51 23’50"
G87 - 147	trondhjemitic Nûk gneiss	SW. Bjørneøen	64 21’55"	51 21’55"
G87 - 148	qtz-dioritic Nûk gneiss	SW. Bjørneøen	64 21’55"	51 21’55"
G87 - 149	qtz-dioritic Nûk gneiss	SW. Bjørneøen	64 21’55"	51 21’55"
G87 - 150	tonalitic Nûk gneiss	N coast Sadelø	64 20’57"	51 25’54"
G87 - 151	tonalitic Nûk gneiss	N coast Sadelø	64 20’50"	51 26’18"
G87 - 152	qtz-dioritic Nûk gneiss	N coast Sadelø	64 20’46"	51 26’34"
G87 - 153	trondhj/grano’ Nûk gneiss	N coast Sadelø	64 20’46"	51 26’34"
G87 - 154	granodioritic Nûk gneiss	N coast Sadelø	64 20’41"	51 27’26"
G87 - 158	trondhjemitic Ikkatoq gn	Hjørataken		
G86 - 964	trondhjemitic Nûk gneiss			
G86 - 965	trondhjemitic Nûk gneiss			
G86 - 966	trondhjemitic Nûk gneiss			
G86 - 968	trondhjemitic Nûk gneiss			
G86 - 969	trondhjemitic Nûk gneiss			
G86 - 970	granodioritic Nûk gneiss			
G87 - 41	Nûk gneiss wt amphibolite	Tartinguaq	64 06’51"	51 46’54"
G87 - 54	metasedimentary(?) gneiss	NE-side Nuuk pen’	64 12’53"	51 31’54"
G87 - 66	metasedimentary(?) gneiss	Rypeø	64 06’36"	51 42’15"
G87 - 73	plag’ amphibolite dyke	Ugujarssuit		

APPENDIX 2.

ANALYTICAL METHODS

Sample Preparation

Rock samples collected in the field varied in size from 3 - 5 kg hand specimens for whole-rock isotopic and chemical analysis to *ca*. 20 kg for zircon and whole-rock analysis. A Cobra BBM 47L rock drill (Atlas Copco, Stockholm) with feather and wedges, was used to collect the large samples. Generally, when using the drill, two sets of holes were drilled. The first set was used to remove the weathered surface of the exposure, and the second set to release the sample. Other weathered surfaces were removed largely in the field, with additional, minor removal being performed in the rock crushing laboratory.

For thin-sections slabs were cut parallel and perpendicular to the gneissic fabric. The remaining material was broken into small fist-sized pieces weighing approximately 500 g which were passed through a coarse steel jaw-crusher and then through by a fine jaw-crusher to produce small rock chips 4 - 5 mm in size. For the large *c*. 20 kg samples a representative sample for geochemical analysis (weighing *ca*. 400 g) was taken from the initial coarse jaw crushed material by repeated quartering. This whole-rock sample was passed through the fine jaw-crusher following crushing of the larger subsample. The subsamples for zircon separation were ground using a Bico rotary mill with stainless steel plates. Great care was taken to prevent cross contamination of samples. The crushing and grinding equipment was rigorously cleaned and closely inspected between samples. When samples for zircon separation were being prepared, an attempt was made to process them in batches that were inferred from field evidence to be of similar age (*i.e.*, if at all possible probable Nûk gneisses were not milled following suspected Amîtsoq gneisses).

Similarly, the splits for whole-rock isotopic and geochemical analysis were ground to < 240 mesh using a motorized agate mortar and pestle which was scrupulously cleaned between samples, and 'contaminated' with an aliquot of the sample to be ground prior to final cleaning.

Tungsten-carbide grinding equipment was avoided because of the problem of tungsten contamination in neutron activation analysis. Although not determined in this study, tungsten activates readily under thermal neutron bombardment to produce the radioisotope ^{187}W (T½ = 23.8hrs). This radionuclide emits numerous gamma-rays, many of which cause spectral interferences with gamma-rays emitted by several other radioisotopes, particularly those used to characterize many of the REE.

X-Ray Fluorescence Analysis

All whole-rock samples in this study were analyzed, for the author, by X-ray fluorescence (XRF) using an automated Rigaku 3370 spectrometer at the Department of Geology, Washington State University, under Dr. Peter Hooper's supervision. Twenty-six major and trace elements were determined from a **single** fused bead.

Because of variations in loss on ignition (LOI), and the variable oxidation state of iron between unknowns and standards, the author was advised to report and use the major oxides "normalized to 100 % with Fe as FeO^* on a volatile-free basis" (P. Hooper, *pers comm*, 1989). However, a minor variation to this approach, using an average volatile content for normalization to 100 %, was taken. This is discussed more fully in the section on the accuracy of the XRF analyses.

Preparation of fused beads.

Representative aliquots of the agate-ground whole-rock powders weighing *ca*. 10 g were sent for analysis. For each sample 3.5 g of rock powder and 7.0 g of spectroscopically pure lithium tetraborate were combined in an automatic mixer for 10 minutes. The resulting mixture was transferred to a graphite crucible *ca*. 35 mm in diameter and fused (in batches of twenty-four) in a muffle furnace for five minutes at 1000°C. Following fusion, the graphite crucibles were removed from the furnace and left to cool. Each glass bead was ground in a Tema swing mill for about 30 seconds before the resulting glass powder was returned to its graphite crucible and fused a second time at 1000°C for five minutes.

Following the second fusion the cooled beads were labelled, and their lower flat surface ground, initially with a coarse (240) grit for about 10 seconds, and finally with a fine (600) grit for a further 10 seconds. The beads were then ultrasonically cleaned, and dried ready for analysis.

Analysis.

Elemental concentrations of the unknown samples were determined by comparing the characteristic X-ray intensity of each element with a calibration curve produced from the analysis of duplicate beads of eight USGS rock-standards of widely differing composition. The calibration standards included United States Geological Survey (USGS) reference materials PCC-1 (peridotite), BCR-1 and BIR-1 (basalts), W-2 and DNC-1 (diabases), AGV-1 (andesite), GSP-1 (granodiorite), and G-2 (granite). Where necessary, corrections were made for spectral interferences. During the analysis of unknowns internal standards were run every twenty-eight samples in order to assess instrument performance and to provide an estimate of reproducibility.

Samples were excited with primary rhodium X-rays produced by bombarding a Rh target with electrons accelerated through a potential difference of 50 kV and generated by a 50 mA current.

From the analysis of internal standards Hooper reports:

> "For the trace elements the precision for Ni, Cr, Sc, V, and Ba is significantly less than that obtained for Rb, Sr, Zr, Nb, Y, Ga, Cu, and Zn. This correlates with the much lower intensities for these first five elements (measured as cnts/sec/ppm) using the Rh tube. Some nickel in the Rh target exacerbates the Ni precision problem. Each of the elements Ni, Cr, Sc, V, and Ba can therefore be regarded only as semi-quantitative below the 30 ppm level. Rb, Sr, Zr, Nb, and Y have satisfactory precisions and accuracies down to one to three parts per million. Nb and Y could probably be measured to 0.1 parts per million."
>
> Hooper and Johnson, (1987).

To assess the accuracy and precision of the XRF analyses a number of coded replicates and standard reference materials were submitted with the two batches of samples analyzed. The standards included four aliquots of the GIT-IWG Ailsa Craig microgranite, AC-E (Govindaraju, 1987), and one aliquot of each of USGS W1 (diabase), SDC-1 (mica schist), SCo-1 (Cody shale), and CCRMP (Canadian Certified Reference Materials Project) SO-2 (soil).

Precision was assessed by analyzing seven aliquots of a typical thesis sample, G87-35. Three aliquots were analyzed in the first batch of samples, and four in the second batch, analyzed over a year later. The four aliquots of AC-E provide additional information on precision. The XRF results for the standards and replicate analyses of G87-35 are listed in Tables A2.1 to A2.7.

Precision

To estimate the precision of the XRF analyses it was considered important to use a representative thesis sample. The rationale being that a biased estimate of precision will generally result (particularly for trace elements) if the material used for estimating precision contains significantly higher concentrations of the elements of interest than those typically occurring in the 'unknown' samples. Variation in the results of the multiple XRF analyses of a sample (broadly referred to as precision, or reproducibility) has three main components: 1) variation in the stability and set-up of equipment, 2) counting statistics of X-ray generation and detection, and 3) sample inhomogeneity (because separate aliquots of a larger sample were analyzed in this case). The fine grain size (< 240 mesh) of the rock powder, coupled with the 3.5 g used for each analysis, should render the third factor insignificant. Thus it is apparent, all other factors remaining equal, that the greater the concentration of an element the better the counting statistics, and the less significant the second component will be to the overall precision of an analysis. Consequently, although four aliquots of the geostandard AC-E were included in the XRF analyses (largely to evaluate the accuracy of the method), it is considered that

Table A2.1 Results of multiple XRF analyses of G87-35.

Unnormalized results (weight %):

	(1)	(2)	(3)	(4)	(5)	(6)	(7)
SiO_2	74.04	73.95	73.82	71.97	72.05	72.80	72.61
Al_2O_3	16.24	16.29	16.17	15.73	15.82	15.84	16.12
TiO_2	0.187	0.185	0.186	0.194	0.189	0.183	0.190
FeO*	1.16	1.15	1.14	1.16	1.16	1.10	1.16
MnO	0.024	0.023	0.021	0.023	0.022	0.022	0.022
CaO	2.26	2.26	2.24	2.23	2.23	2.23	2.25
MgO	0.40	0.38	0.33	0.28	0.29	0.29	0.39
K_2O	1.97	1.97	1.97	1.95	1.96	1.93	1.97
Na_2O	5.72	5.72	5.72	5.59	5.58	5.61	5.49
P_2O_5	0.055	0.054	0.052	0.061	0.057	0.058	0.058
Total	102.06	101.98	101.65	99.19	99.36	100.06	100.26

Normalized oxides (weight %)

	(1)	(2)	(3)	(4)	(5)	(6)	(7)	Mean (n=7)	SD	CV (%)
SiO_2	72.16	72.13	72.23	72.17	72.13	72.37	72.03	72.17	.10	0.13
Al_2O_3	15.83	15.89	15.82	15.77	15.84	15.75	15.99	15.84	.07	0.47
TiO_2	0.182	0.180	0.182	0.195	0.189	0.182	0.188	0.19	.01	2.62
FeO*	1.13	1.12	1.12	1.16	1.16	1.09	1.15	1.13	.02	2.12
MnO	0.023	0.022	0.021	0.023	0.022	0.022	0.022	0.022	.001	3.90
CaO	2.20	2.20	2.19	2.24	2.23	2.22	2.23	2.22	.02	0.73
MgO	0.39	0.37	0.32	0.28	0.29	0.29	0.39	0.33	.05	13.54
K_2O	1.92	1.92	1.93	1.96	1.96	1.92	1.95	1.94	.02	0.92
Na_2O	5.57	5.58	5.60	5.61	5.59	5.58	5.45	5.57	.05	0.90
P_2O_5	0.054	0.053	0.051	0.061	0.057	0.058	0.058	0.058	.002	5.89

Normalized to 100 % assuming LOI of 0.534 %

Total Fe expressed as FeO*

	(1)	(2)	(3)	(4)	(5)	(6)	(7)	Mean (n=7)	SD	CV (%)
Ni	8	8	8	11	9	10	8	8.9	1.1	12.7
Cr	1	0	0	0	0	0	0	0.1	0.3	244.9
Sc	0	0	3	1	0	2	0	0.9	1.1	131.2
V	11	12	12	2	0	13	12	8.9	5.0	56.8
Ba	835	861	834	786	813	810	829	824	22.0	2.7
Rb	49	48	48	48	48	46	49	48	0.9	1.9
Sr	667	667	667	645	657	662	660	661	7.4	1.1
Zr	129	128	129	126	127	124	126	127	1.7	1.3
Y	3	3	3	2	4	4	4	3.3	0.7	21.3
Nb	0.6	0.8	0.0	4.7	3.9	2.3	3.3	2.2	1.7	75.3
Ga	--	--	--	16	19	19	19	18.3	1.3	7.1
Cu	3	4	6	7	4	5	4	4.7	1.3	27.1
Zn	41	41	42	38	42	42	42	41.1	1.4	3.3
Pb	23	20	21	20	19	21	18	20.3	1.5	7.3
La	7	12	13	15	34	25	7	16.1	9.2	57.0
Ce	47	45	43	35	36	30	33	38.4	6.0	15.7
Th	6	4	5	6	5	5	9	5.7	1.5	26.0

Trace element concentrations in parts per million (ppm) the seven aliquots of G87-35 give a better estimation of the precision of the XRF analyses, particularly for the trace elements measured.

Major and minor elements:

The excellent precision for the major element determinations, as indicated by the small coefficient of variations for the analyses of G87-35 (Table A2.1), is noteworthy. Except for MgO (which occurs at minor element levels in this sample) and FeO*, variations are significantly less than 1 percent for all the major elements. At 1.14 wt % the FeO* content of G87-35 is low and poor counting statistics are probably the cause of the greater variation displayed by the FeO* data. In a general sense this inference is supported by the much smaller variation in FeO* displayed by the quadruplicate analyses of AC-E (Table A2.2). This standard contains 2.25 wt % FeO* and the coefficient of variation is $<0.5\%$. The precision obtained from G87-35 for the minor oxides MnO and P_2O_5 is more than satisfactory for most applications. The analyses of AC-E give variations of < 1.3 % for all the oxides except MgO and P_2O_5. The poorer precision for the minor oxides is likely a consequence of poor counting statistics because of the soft nature of characteristic X-rays of Mg and P, coupled with their very low levels (MgO = 0.03 wt %, P_2O_5 = 0.014 wt %).

Although an analysis of variance was not performed on the means of the two batches of G87-35 data, a cursory examination of the oxide determinations shows no significant differences between the two groups.

Trace elements:

As noted earlier the precision for the transitional elements Ni, Cr, Sc, and V is poor at low concentrations. This observation of Hooper's is strongly supported by the G87-35 data (Table A2.1).

From the analyses of G87-35 the precision for the trace elements Rb, Ba, Sr, and Zr is in the 1 - 3 % range; for Pb, Zn, Ni, and Ce it is less than 16 %, and for Y, Cu, and Th less than 30 %. A notable irregularity is the imprecision displayed by Nb. Examination of the two batches of data show a significant difference in Nb concentrations and suggests that an important modification was made to the analysis procedure for Nb (possibly interference correction) at some time between the analysis of the two batches. The implications of this change are discussed in the following section on the accuracy of the XRF trace element analyses.

Accuracy

Major and minor elements:

Tables A2.2 to A2.7 list the measured and recommended elemental concentrations for the geostandards AC-E, W-1, SDC-1, SCo-1, and SO-2. In one column (B) the measured data are normalized to 100% on a volatile-free basis. In addition, using the recommended LOI for each standard (range: 0.31 % to 11.17 %, Govindaraju, 1989), the oxides have been recalculated to 100 % incorporating the LOI data (column C). As can be seen this results in a significant improvement in the agreement between the measured and recommended values, particularly for those samples which have a high loss on ignition (*e.g.*, SO-2 and SCo-1). The author did not determine the LOI for the one hundred and thirty samples analyzed in this study, however, because the LOI for felsic igneous rocks is commonly ≤ 1 % it is likely that this correction is an unnecessary refinement, which would have a visible effect only on the major oxides *e.g.*, silica and alumina. McGregor *et al.* (1986) reported whole-rock XRF analyses and LOI determinations, for eight representative type-Nûk gneisses. The silica content of these samples ranges from 51.65 to 71.76 wt. % (comparable to the range exhibited by the gneisses of this study) while, for the same set of samples, LOI varies between 0.49 and 0.61 wt. %, with a mean of 0.534 ± 0.049 (1σ). It should be noted that there is no correlation between silica content and LOI in these analyses. Consequently, this author felt justified in normalizing the measured major and minor oxides of this study to 100 % assuming a fixed LOI of 0.534 wt % throughout.

Table A2.2 X-ray fluorescence results for Ailsa Craig microgranite, AC-E.

	Aliquot (1)			Aliquot (2)			
	(A)	(B)	(C)	(A)	(B)	(C)	(D)
SiO_2	71.91	70.71	70.45	72.08	70.64	70.38	70.35
Al_2O_3	15.48	15.22	15.17	15.59	15.28	15.22	14.70
TiO_2	0.111	0.109	0.109	0.110	0.108	0.107	0.11
FeO*	2.30	2.26	2.25	2.28	2.23	2.23	2.28
MnO	0.061	0.060	0.060	0.062	0.061	0.061	0.058
CaO	0.38	0.37	0.37	0.38	0.37	0.37	0.34
MgO	0.02	0.02	0.02	0.05	0.05	0.05	0.03
K_2O	4.56	4.48	4.47	4.56	4.47	4.45	4.49
Na_2O	6.87	6.76	6.73	6.92	6.78	6.76	6.54
P_2O_5	0.007	0.007	0.007	0.009	0.009	0.009	0.014
LOI	---	---	0.37	---	---	0.37	0.37
Total	101.7	100.0	100.0	102.0	100.0	100.0	

	Aliquot (3)			Aliquot (4)			
	(A)	(B)	(C)	(A)	(B)	(C)	(D)
SiO_2	72.07	70.79	70.52	70.48	70.76	70.50	70.35
Al_2O_3	15.36	15.09	15.03	15.00	15.06	15.00	14.70
TiO_2	0.112	0.110	0.109	0.115	0.115	0.115	0.11
FeO*	2.29	2.25	2.24	2.26	2.27	2.26	2.28
MnO	0.060	0.059	0.059	0.060	0.060	0.060	0.058
CaO	0.38	0.37	0.37	0.36	0.36	0.36	0.34
MgO	0.00	0.00	0.00	0.00	0.00	0.00	0.03
K_2O	4.56	4.48	4.46	4.53	4.55	4.53	4.49
Na_2O	6.97	6.85	6.82	6.79	6.82	6.79	6.54
P_2O_5	0.011	0.011	0.011	0.013	0.013	0.013	0.014
LOI	---	---	0.37	---	---	0.37	0.37
Total	101.8	100.0	100.0	99.6	100.0	100.0	

(A) - measured values (weight %), unnormalizd
(B) - data normalized to 100 % on a volatile-free basis
(C) - data normalized to 100 % including literature LOI
(D) - recommended values (Govindaraju, 1987, 1989)

Table A2.3 X-ray fluorescence results for trace elements in AC-E.

					Mean		
Aliquot:	(1)	(2)	(3)	(4)	(n=3)	(n=4)	(Lit)
Ni	17	17	18	19	17	19	1.5
Cr	1	0	0	1	0.3	0.5	3.4
Sc	1	0	0	0	0.3	0.0	0.11
V	0	3	0	0	1.0	0.0	3
Ba	95	85	80	20	87	50	55
Rb	150	151	150	148	150	149	152
Sr	4	4	5	3	4	4	3
Zr	667	670	668	660	668	664	780
Y	185	185	184	187	185	186	184
Nb	135.6	137.2	135.0	128.7	136	132	110
Cu	6	6	9	5	7	7	4
Zn	207	207	208	204	207	206	224
Pb	39	38	41	31	39	36	39
La	52	70	62	65	61	64	59
Ce	171	188	188	185	182	187	154
Th	21	17	18	17	19	18	18.5
Ga	--	--	--	44	--	--	39

concentrations in parts per million (ppm)

(Lit) - recommended values (Govindaraju, 1987, 1989)

Table A2.4 X-ray fluorescence results for USGS W1.

	(A)	(B)	(C)	(D)
SiO_2	54.20	53.48	53.08	52.55 ± 0.30
Al_2O_3	15.34	15.14	15.02	14.99 ± 0.26
TiO_2	1.091	1.076	1.068	1.07 ± 0.06
FeO*	9.71	9.58	9.51	9.77 ± 0.34
MnO	0.175	0.173	0.171	0.168 ± 0.016
CaO	11.06	10.91	10.83	10.94 ± 0.17
MgO	6.74	6.65	6.60	6.62 ± 0.13
K_2O	0.65	0.64	0.637	0.639 ± 0.041
Na_2O	2.26	2.23	2.21	2.13 ± 0.11
P_2O_5	0.127	0.125	0.12	0.14 ± 0.01
LOI	---	---	0.74	0.74 ± 0.20
Total	101.35	100.0	100.0	
Ni	62			75 ± 9
Cr	116			120 ± 14
Sc	39			35 ± 2
V	261			260 ± 25
Ba	141			162 ± 5
Rb	21			21.4 ± 0.3
Sr	184			187 ± 7
Zr	94			100 ± 9
Y	23			26 ± 4
Nb	8.9			8 ± 2
Cu	107			114 ± 10
Zn	77			84 ± 6
Pb	10			7.5 ± 1.5
La	20			10.9 ± 1.3
Ce	14			23 ± 2
Th	2			2.4 ± 0.4

(oxides in weight %, trace element concentrations in ppm)

(A) - measured data (weight %), unnormalized

(B) - normalized to 100% on a volatile-free basis

(C) - normalized to 100% including literature LOI

(D) - Gladney _et al_., (1983)

Table A2.5 X-ray fluorescence results for USGS SDC-1.

	(A)	(B)	(C)	(D)
SiO_2	67.88	67.38	65.97	65.85 ± 0.43
Al_2O_3	16.37	16.25	15.91	15.75 ± 0.34
TiO_2	1.006	0.999	0.978	1.01 ± 0.04
FeO*	6.48	6.43	6.30	6.29 ± 0.28
MnO	0.118	0.117	0.115	0.114 ± 0.008
CaO	1.48	1.47	1.44	1.40 ± 0.07
MgO	1.74	1.73	1.69	1.69 ± 0.10
K_2O	3.34	3.32	3.25	3.28 ± 0.10
Na_2O	2.18	2.16	2.12	2.05 ± 0.09
P_2O_5	0.142	0.141	0.138	0.158 ± 0.025
LOI	---	---	2.1	2.1
Total	100.74	100.0	100.0	
Ni	35			38 ± 8
Cr	54			64 ± 7
Sc	14			17 ± 2
V	93			102 ± 12
Ba	653			630 ± 60
Rb	125			127 ± 7
Sr	181			183 ± 9
Zr	280			290 ± 30
Y	42			40 ± 6
Nb	20.6			18 ± 3
Cu	31			30 ± 3
Zn	95			103 ± 8
Pb	26			31 ± 3
La	35			42 ± 3
Ce	98			93 ± 7
Th	10			12.1 ± 0.9

(oxides in weight %, trace element concentrations in ppm)

(A) - measured data (weight %), unnormalized

(B) - normalized to 100% on a volatile-free basis

(C) - normalized to 100% including literature LOI

(D) - literature values (Gladney and Roelandts, 1988)

Table A2.6 X-ray fluorescence results for USGS SCo-1.

	(A)	(B)	(C)	(D)
SiO_2	66.51	68.97	62.83	62.78 ± 0.66
Al_2O_3	14.65	15.19	13.84	13.67 ± 0.21
TiO_2	0.623	0.646	0.59	0.628 ± 0.065
FeO*	4.98	5.16	4.70	4.67 ± 0.33
MnO	0.057	0.059	0.05	0.053 ± 0.004
CaO	2.78	2.88	2.63	2.62 ± 0.2
MgO	2.81	2.91	2.65	2.72 ± 0.18
K_2O	2.92	3.03	2.76	2.77 ± 0.08
Na_2O	0.90	0.93	0.85	0.899 ± 0.062
P_2O_5	0.210	0.218	0.20	0.206 ± 0.021
LOI	--	--	8.9	8.9
Total	96.44	100.0	100.0	
Ni	32			27 ± 4
Cr	67			68 ± 5
Sc	10			10.8 ± 1.1
V	138			131 ± 13
Ba	612			570 ± 30
Rb	121			112 ± 4
Sr	182			174 ± 16
Zr	167			160 ± 30
Y	27			26 ± 4
Nb	14.6			11 ± 3
Cu	34			28.7 ± 1.9
Zn	100			103 ± 8
Pb	36			25 ± 2
La	34			29.5 ± 1.1
Ce	49			62 ± 6
Th	9			9.7 ± 0.5

(oxides in weight %, trace element concentrations in ppm)

(A) - measured data (weight %), unnormalized

(B) - normalized to 100% on a volatile-free basis

(C) - normalized to 100% including literature LOI

(D) - literature values (Gladney and Roelandts, 1988)

Table A2.7 X-ray fluorescence results for CCRMP soil SO-2.

	(A)	(B)	(C)	(D)	(E)
SiO_2	57.46	61.20	54.04	53.42	53.46 ± 0.49
Al_2O_3	16.23	17.29	15.26	15.10	15.25 ± 0.34
TiO_2	1.516	1.615	1.43	1.43	1.43 ± 0.03
FeO*	7.99	8.51	7.51	7.10	7.15 ± 0.21
MnO	0.104	0.111	0.10	0.09	.093 ± .002
CaO	2.98	3.17	2.80	2.77	2.74 ± 0.14
MgO	0.91	0.97	0.86	0.89	0.89 ± 0.05
K_2O	3.18	3.39	2.99	2.94	2.95 ± 0.05
Na_2O	2.74	2.92	2.58	2.48	2.56 ± 0.07
P_2O_5	0.780	0.831	0.73	0.69	0.53 ± 0.04
LOI	---	---	11.7	11.7	
Total	93.89	100.0	100.0		
Ni	9			8	
Cr	8			12.3	
Sc	13			11.3	
V	65			57	
Ba	1093			1000	
Rb	79			77	
Sr	381			340	
Zr	753			760	
Y	47			40	
Nb	30.7			22	
Cu	4			8	
Zn	130			115	
Pb	23			20	
La	45			46.5	
Ce	138			112	
Th	7			3.8	

(oxides in weight %, trace element concentrations in ppm)

(A) - measured data (weight %), unnormalized
(B) - normalized to 100% on a volatile-free basis
(C) - normalized to 100% including literature LOI
(D) - literature values (Govindaraju, 1989)
(E) - Steger (1983); uncertainties at 95 % confidence level

In all cases the silica and alumina results are marginally higher than the recommended values for the standards. However, where uncertainties (1σ, unless otherwise stated) are reported for the standards they encompass the measured silica and alumina values in every case, except for W-1 which overlaps at the 2σ level. The largest discrepancies between recommended and the LOI-normalized oxide values occur for iron. This is largely a consequence of assuming the same ferrous:ferric ratio for samples as the 'average' of the set of eight calibration standards. For all the remaining major and minor elements the agreement between the LOI-corrected values and recommended values is excellent. A singular exception is the Na_2O determination of AC-E, the LOI-normalized values being *ca*. 0.3 wt % higher than the preferred Na_2O value (Govindaraju, 1989). However, detailed examination of the results of the interlaboratory study of this standard reveals that the standard deviation for the Na_2O analyses was 0.23 wt. % [n = 140] (Govindaraju, 1987), which almost overlaps the LOI-normalized Na_2O results at the 95% confidence level.

Trace elements:

The accuracy of the analyses of the standard materials display the salient features described by Hooper earlier. The agreement between the measured concentrations of Rb, Sr, Y, Zr, Nb, Cu, Zn, Pb, and even Th, and their recommended values is excellent. Further testament to this can be seen in Figure A1 where the Sr and Rb XRF concentrations of some sixty gneisses are plotted against the concentration determined by mass spectrometry isotope dilution (generally considered a definitive method of analysis for these elements). The agreement between the two methods of Rb analysis is exceptional. However, although not readily apparent from Figure A1, at levels < 10 ppm Rb (*i.e.*, typical of many granulites) the MSID results are considered to be superior to those of XRF. Only one Sr determination falls significantly off the Sr isocon.

At levels above 30 ppm the accuracy of Ni, Cr, Sc and V determinations

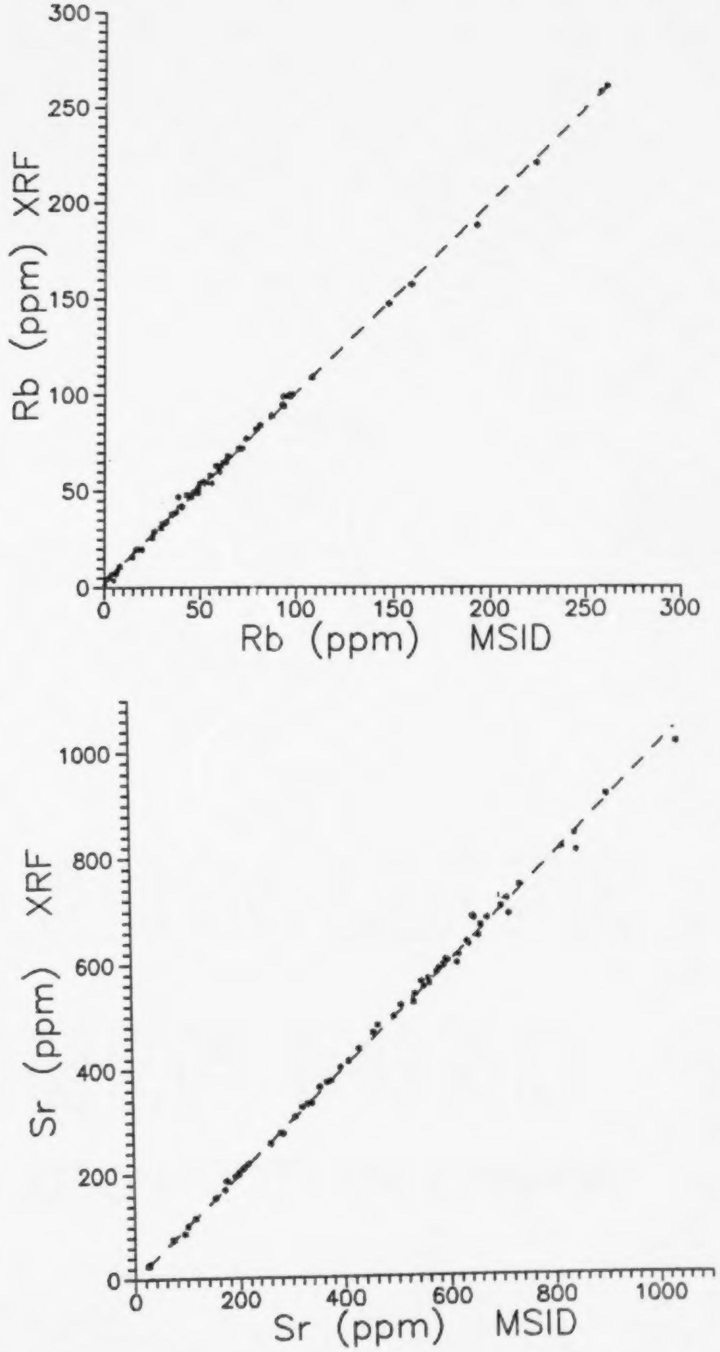

Figure A1. Comparison of the XRF and MSID determinations of Rb and Sr in thesis samples.

is generally very good. Accuracy for Ba, La and Ce is variable. The measured Ba values often agree with the reference concentrations at the 95% confidence level. A number of important points become apparent when one examines the trace element results for AC-E. Firstly, the Ni results are an order of magnitude greater than the recommended 1.5 ppm. The previously mentioned Ni impurities in the Rh X-ray tube explain this anomaly, and warn of the unreliability of Ni determinations at low concentrations. Again, as emphasised by Hooper, Cr, Sc, V, and Ba are to be considered only semi-quantitative at best when they are present at low levels. The data obtained for the standards suggests that the lower reliability limit for Cr, Sc, and V is about 10 ppm, and for Ba, 100-200 ppm.

When discussing the precision of the XRF analyses special note was made of the change in the Nb values for the two batches of G87-35 analyses, the second set of determinations being much higher than the first. Differences between the two batches of analyses are also displayed by the Nb determinations of AC-E (Table A2-3). However, unlike the analyses of G87-35, the Nb concentration of AC-E, determined in the second batch of samples, is **less than** that measured for the three aliquots of AC-E in the earlier batch. Even though there is reasonably good agreement between the Nb determinations and recommended values for all of the standards, the author feels that the Nb measurements are unreliable below *ca.* 3 - 4 ppm and that caution should be exercised when interpreting the Nb data for the gneisses analyzed in this study. This is particularly important when assessing negative Nb anomalies on 'spidergrams'.

Neutron Activation Analysis.

Neutron activation analysis (NAA) is recognized as a sensitive, generally matrix independent, multi-elemental technique for the analysis of a wide variety of materials. The principles of the method can be found in a number of texts, but the reader is referred to DeSoete *et al.*, (1972), and Erdtmann and Petri

(1986) for particularly thorough descriptions. In the context of using the Canadian SLOWPOKE II nuclear reactor for geochemical analyses see Duke (1983). Representative aliquots of whole-rock powders, weighing approximately 350 mg, were accurately weighed into nitric-acid washed polyethylene irradiation vials, capped, and hermetically sealed. Samples were irradiated for 2 hrs in batches of twelve at a nominal thermal neutron flux of 1 x 10^{12} n cm^{-2} s^{-1} at the SLOWPOKE II nuclear reactor of the University of Alberta. The controlling factor on sample throughput is generally not the irradiation of samples, but the counting of the induced radioactivity. The gamma-ray spectroscopy of the 12 samples irradiated each week (using a single spectroscopy system with an automatic sample changer) amounted to four-and-a-half days.

All irradiated samples were counted using an Ortec 86cm^3 active volume GEM vertical, coaxial hyperpure Ge detector, coupled to a Canberra Series 80 multichannel analyzer. The detector specifications include a relative efficiency of 21 %, and a measured FWHM of 2.1 keV and peak-to-Compton ratio of 60:1 measured from the 1332.5 keV photopeak of ^{60}Co. Signals were assigned to 4096 channels (0 - 1840 keV range) and the spectra accumulated were stored on floppy disc for off-line analysis. The detector was housed in a 10 cm Pb cave with graded shield. An automatic sample changer, built in-house, was utilized for the analyses.

The majority of samples were also counted using an Aptec low energy photon spectrometer (LEPS). Compared to large volume coaxial Ge detectors, LEPS detectors, because of their small size and thin Be window, have superior resolution and peak-to-background ratios at low photon energies (50 - 350 keV). This is particularly useful when determining of a number of the REE and other incompatible elements such as Hf, Ta, and Th. The LEPS was a hyperpure Ge detector, with an active area of 500 mm^2 and sensitive depth of 10 mm, had a measured resolution of 525 eV at 122 kev.

After a decay period of a six days the samples were individually counted for 30 minutes live-time at a sample-to-detector distance of 3 cm. Following a total decay period of *ca.* 21 days, each sample was recounted for 30,000 seconds live-time at a sample-to-detector distance of 1 cm. The additional decay time permits the decay of those medium-lived radioisotopes (*e.g.*, ^{24}Na) that activate readily and generate significant background. The higher background reduces signal-to-background ratios and thus increases detection limits for most elements. Samples were counted on the LEPS following the three week decay period for a minimum of 30000 seconds. From the combined analyses, and **depending upon the levels present**, the elements: La, Ce, Nd, Sm, Eu, Tb, Tm, Yb, Lu, Ta, Th, U, Ta, Hf, Ba, Rb, Cs, Sc, Co, Cr, Sb, Na and Fe were determined. Table 2.8 gives the relevant nuclear data for the elements determined by NAA.

Unfortunately, in many of the samples analyzed the levels of several elements were below the detection limit of the analysis scheme. This is, in part, a consequence of the high Na content of the majority of the samples studied, together with very low levels of some of the trace elements present (*e.g.*, Yb, Lu, Ta, U, Cs). To be statistically meaningful (*i.e*, 'detected') the integrated area of a photopeak must be $\geq 2.71 + (4.65 * \text{background})^{1/2}$ (where 'background' is the integrated region under the 'photopeak') (Currie, 1968). Given the background present at a particular energy, and the sensitivity for the element under consideration, it is possible to calculate an upper limit to the concentration of an element which is present below the detection limit. However, because background variation is sample specific no effort has been made to calculate these limits and 'ND' (not detected) is recorded in the results. A general indication of the detection limits for the elements determined by the various INAA schemes is given in Table A2.8. These detection limits were calculated from the various spectra obtained for samples G87-35 and G87-36. Again the reader is cautioned against assuming these values necessarily apply to all samples. The spectral background of each sample differs because of variable concentrations of Na, Sc, Fe, and Co (these elements contribute

Table A2.8 Nuclear data on elements determined by INAA.

Element	Radio-Isotope	T½	γ-ray (keV)	Detection Limit (ppm)*	Scheme
La	^{140}La	40.27 H	1596.2	1	A
			328.7	2	
			487.0	1	
Ce	^{141}Ce	32.38 D	145.0	0.4	B & C
Nd	^{147}Nd	10.98 D	91.1	1.2	B & C
Sm	^{153}Sm	1.948 D	103.2	0.5	A
			69.7		
Eu	^{152}Eu	12.7 Y	121.8	0.01	B & C
			1408.1	0.05	
Tb	^{160}Tb	72.1 D	86.8	0.15	B & C
			1178.*	0.04	
Tm	^{170}Tm	128.6 D	84.3	0.02	C
Yb	^{169}Yb	30.7 D	198.0	0.1	C
Yb	^{175}Yb	4.19 D	396.3	0.5	A
Lu	^{177}Lu	6.71 D	208.4	0.15	A
Hf	^{181}Hf	42.5 D	133.0	0.05	B & C
			482.2	0.02	
Ta	^{182}Ta	114.4 D	67.7	0.1	B & C
			152.4	0.04	
			1221.4	0.03	
Th	^{233}Pa	27.4 D	311.9	0.05	B & C
Rb	^{86}Rb	18.63 D	1076.6	2	B
Cs	^{134}Cs	2.062 Y	604.7	0.1	B
			795.8		
Ba	^{139}Ba	11.5 D	496.3	3	B
Na	^{24}Na	14.96 H	1368.6	65	A
			1732.2(DE)	630	
Sc	^{46}Sc	83.85 D	889.3	0.02	A & B
			1120.2	0.005	
Co	^{60}Co	5.272 Y	1173.2	0.06	A & B
			1332.5	0.12	
Fe	^{59}Fe	45.1 D	1099.2	50	A & B
			1291.6	35	
Cr	^{51}Cr	27.7 D	320.1	1	B & C
U	^{239}Np	2.355 D	277.6	1	A

* - based on 350 mg of G87-35 (Currie, 1968)
A - 1800 s count at 3 cm geometry (coaxial detector)
B - 30000 s count at 1 cm geometry (coaxial detector)
C - 30000 to 60000 s count (planar detector)

significantly to the background by Compton scattering) and hence will govern the detection limit for each element.

The spectra obtained were uploaded to the University of Alberta Amdahl mainframe computer and analyzed using Nuclear Data peak search routines. The resulting data were then downloaded to a PC and elemental concentrations determined using programmes written by the author. Analysis was performed via the semi-absolute method of neutron activation analysis (Bergerioux *et al.*, 1979). Accuracy of the procedure was checked by analyzing the USGS standards BCR-1, W-1, AGV-1, BHVO-1, SDC-1, and STM-1, the results indicate that the overall agreement between the recommended and measured values is very good.

Uranium Analysis by Delayed Neutron Counting.

The majority of whole-rock samples studied were analyzed by the author for their uranium content by the delayed neutron counting (DNC) method, at the University of Alberta SLOWPOKE II nuclear reactor. Representative ground samples, weighing between five and eight grammes, were packed in tared 7 mL polyethylene irradiation vials and weighed to the nearest milligram. The DNC array consisted of 6 BF_3 tubes (embedded in polyethylene) arranged coaxially about a sample pin-stop. Employing an irradiation-decay-count scheme of 20s - 10s - 20s, at a nominal thermal neutron flux of 1×10^{12} n. cm^{-2} s^{-1}, gave a sensitivity of 49.72 ± 0.61 (1σ) cts μg^{-1} natural uranium. Utilizing the described scheme the detection limit (Currie, 1968) for uranium in a 6 g sample is 56 ppb, and a concentration of 0.25 ppm U can be determined with a statistical uncertainty of $\leq$ 10 %.

The system was calibrated using multiple aliquots of the CANMET U standard DL-1a (U = 116 ± 3 ppm, 2σ) and accuracy checked by analyzing (in triplicate) the geostandards DL-1 (U = 41 ± 2 ppm) and BL-1 (U = 220 ± 10 ppm), and a single aliquot of USGS W1 (U = 0.57 ± 0.10 ppm). The results for these standards were in very good agreement with certified, or recommended, literature values.

The analysis of U by DNC suffers a systematic interference from the fast neutron induced fission of Th, the magnitude of which depends upon the sample Th/U ratio and the reactor thermal-to-fast neutron flux ratio. Analyses of a number of uranium-free Th standards under identical conditions to those employed for the uranium DNC determinations have shown that for the SLOWPOKE reactor the sensitivity for Th is 1.26 % ± 0.16 % (1σ) that of natural U (Duke, 1983). Given this datum, and the Th concentration of each sample (determined by INAA), the DNC U values were corrected for the Th interference with the incurred increase in uncertainty due to the propagation of errors. However, for the samples under study the increased uncertainty due to the Th correction was negligible. At the levels of uranium present in the rocks under study the uncertainty associated with the gross sample counts and stripping the counter background from the gross sample counts to obtain the net sample counts are the dominant sources of uncertainty. As a consequence of poorer counting statistics the largest uncertainty occurs for those samples with the lowest U concentrations (*e.g.*, the granulites from Nordlandet). The lowest U concentration determined (0.11 ppm for G87-130) has an uncertainty of ± 16.3 %, while at the 0.25 - 0.30 ppm U level the uncertainty is *c.* ± 10 %. The uncertainty decreased to ± 3.0 % at 3.28 ppm U (the highest U concentration in the samples analyzed).

Isotopic Analyses

The procedures utilized for the isotopic analysis of the samples studied here were modified as experience was gained. Changes were motivated by a desire for more rapid, simple, and reproducible manipulations, which invariably resulted in lower procedural blanks. Before any modifications were implemented for general use, however, aliquots of previously analyzed samples, and (or) standard reference materials, were analyzed using the new procedure, and procedural blanks run to assess the effects of the changes.

Reagents.

The mineral acids used in the whole-rock dissolution, and subsequent elemental purification steps, were produced by sub-boiling distillation in either Teflon® (Mattinson, 1972) or glass stills. Hydrofluoric acid and HBr were distilled once, while HCl and HNO_3 were doubly distilled. Ultrapure water was produced by a Millipore Corp. filtration system. Gold-label grade oxalic-acid (Aldrich Co.) was used without further purification once the reagent blank for Sm, Nd, Sr, and Pb had been determined and found to be negligible for the whole-rock analyses in question. Methyllactic acid (in solution) was purified by cation exchange chromatography. Cation exchange chromatography was also used to purify (remove Sr and to a lesser extent Pb) the $BaCl_2$ used in nitrate coprecipitation. For Pb analyses the $BaCl_2$ was further purified by double electrode stripping.

Sm-Nd, Rb-Sr, and Pb-Pb whole-rock isotopic analyses.

Aliquots of whole-rock powders, typically weighing 500 mg, were taken for unspiked analyses. Given the Nd, Sr, and Pb concentrations of the gneisses studied this generally resulted in a significant excess of the 0.2 ug Nd, *ca.* 0.5 ug Sr, and *ca.* 0.5 ug Pb required for mass spectrometric analysis. For isotope dilution, samples weighing *ca.* 200 mg were accurately weighed and spiked with a mixed ^{87}Rb-^{84}Sr and/or ^{149}Sm-^{145}Nd solution prior to decomposition. All samples were digested in screw topped Savillex® vessels using an 8:1 mixture of 25M HF:16M HNO_3. Decomposition was apparently complete after a few hours of heating, but samples were left a minimum of 12 hours to digest.

At the beginning of this study samples were processed in the manner described fully by Cavell (1985), and in a condensed, and more generally available form, in Baadsgaard *et al.* (1986). The essentials of the procedure are as follows: After decomposition, each sample was evaporated to dryness and the fluoride residue converted to nitrate by repeatedly treating the residue with 16N HNO_3, evaporating to dryness, and baking. The residue was then dissolved in 12 mL 7N HNO_3. This solution was evaporated to concentrated HNO_3, centrifuged, and the supernatant transferred to a silica tube. Lead and Sr were coprecipitated with $Ba(NO_3)_2$. The supernatant solution containing the REE and Rb was transferred to a 50 mL silica tube, diluted to 25 Ml and made ammoniacal to precipitate Fe, Al, and the REE. The Rb-enriched supernatant was transferred to another silica tube and Rb precipitated, with K, as a perchlorate by the addition of a few drops of perchloric acid. Aluminium was removed from the REE + Fe precipitate by adding one or two pellets of NaOH to dissolve the amphoteric Al-hydroxide. Following centrifuging the Al-rich supernatant was discarded. The REE and Fe were reprecipitated from a dilute HCl solution by adding NH_3 (to remove excess Na from the NaOH step). The REE-enriched precipitate was dissolved in a minimum of 2.3 N Hcl and the REE separated by cation exchange chromatography. Neodymium, and Sm, were separated from each other, and the remaining the rare earth elements, on a cation exchange column equilibrated with 0.2 M methyllatic acid (α-hydroxyisobutyric acid) ($pH = 4.43 \pm 0.01$; adjusted with NH_3) Eugster *et al.*, 1970. The Nd, and Sm, eluates were acidified to 0.1N HCl and the methyllactic acid and traces of ammonia removed by a third cation exchange column to give Nd or Sm ready for mass spectrometric analysis.

Lead (from the nitrate coprecipatation step) was purified from Ba and Sr using a column of DOWEX AG-X1 anion exchange resin (100-200 mesh) in chloride form, equilibrated with 1.5N HCl. Strontium, eluted from this anion exchange column, was purified by two passes through a DOWEX AG 50W-X8 cation exchange column, also in chloride form.

The blanks for the procedures as outlined were 0.3 ng Sm, 2.2 ng Nd, 1.5 ng Sr, 1.2 ng Pb, and 0.1 ng Rb.

Various aspects of these procedures were modified and, after the procedures had been tested, the majority of samples were treated as follows: Following decomposition samples were left to cool before being centrifuged to separate the Sr-, Pb-, and REE-bearing insoluble fluoride phase from the alkali-rich supernatant. In unspiked runs the supernatant was discarded, while for spiked runs it was saved for Rb purification.

The partitioning of Pb between the soluble and insoluble phases of a digested whole-rock sample (to which a known excess of Pb had been added) was determined by analyzing the Pb content of the two phases by atomic absorption spectrometry. Approximately 80% of the Pb was found to enter the insoluble phase while the remaining 20% remained in the supernatant solution. Given the relatively high Pb content of most of the samples in this study an 80% Pb yield at this step was judged acceptable and the simplicity of the separation far outweighed the effort required either to process a separate whole-rock aliquot for Pb, or to use a more involved chemical separation.

As before, the Pb-, REE-, and Sr-bearing fluoride residue was converted to more soluble nitrate salts by evaporating (and baking) the residue a number of times in with 16N HNO_3. The nitrate residue was then dissolved in 6N HCl and evaporated to dryness before being taken up in 1 mL 2.3N HCl ready for cation exchange chromatography. The solution was transferred to a 3 Ml silica glass test-tube and centrifuged. The supernatant was loaded on a 1 g DOWEX AG-50W X8 (100-200 mesh) cation exchange column equilibrated with a 0.1 M oxalic acid + 1.5N Hcl mixture. The column was calibrated for the REE, Sr and Pb (and at a later stage for Rb). Iron and Pb, together with any remaining alkalis were removed by washing the column with a total of 11 mL of the 0.1 M oxalic acid + 1.5N HCl mixture. This solution was retained for purification of Pb. The REE and alkaline earths form insoluble oxalate complexes, and are retained on the column. Cation exchange distribution coefficients (K_d's) for the REE and alkaline earths are quite similar in 2 to 6N HCl (Strelow, 1960; and Strelow *et al.*, 1965) and thus HCl solutions do not afford an effective means for the separation of these two groups. However, their K_d's in 2M HNO_3 are sufficiently different (Sr = 8.8, Ba = 13.0, REE range from 47.3(La) to 41.3(Yb)) to permit adequate separation. Consequently, Sr was removed from the column and collected using 2M HNO_3, and then, after further washing with

2M HNO_3 to remove most of the Ba, the REE were stripped and collected as a group in 6N HCl. After the HCl solution was evaporated to dryness, Nd (and Sm in spiked runs) was separated from the bulk of the other REE and purified, as described in detail earlier, using a cation exchange column equilibrated with 0.2 M methyllactic acid, followed by a final cation exchange column.

For the analysis of Rb the supernatant from the sample decomposition step was evaporated to dryness, and the conversion of the alkali fluoride salts to chlorides (via nitrates) achieved by twice evaporating the sample to dryness in the presence of 16N HNO_3, followed by evaporation from 6N HCl. The chloride residue was dissolved in 1.25 mL of 1.5 M HCl, transferred to a 3 mL Pyrex® tube, centrifuged, and the supernatant loaded on a 4 g DOWEX AG-50W X8 (100-200 mesh) cation exchange column equilibrated with 1.5N HCl. This column yielded purified Rb that never failed to give an excellent, stable, mass spectrometry run.

The Sr-bearing solution from the oxalic-acid columns was collected in 7 mL screw-top Savillex® beakers, and evaporated to dryness. The Sr-enriched residue was dissolved in 2 mL of 16N HNO_3 and Sr separated from Ca by coprecipitation with $Ba(NO_3)_2$. Precipitation was promoted by placing the capped Savillex vessels in an ultrasonic bath for about 20 minutes. The samples were then centrifuged, the supernatant discarded, and after drying on a hot plate (< 2 minutes) the precipitate was dissolved in a minimum of water (*c.* 20 uL) and the precipitation step repeated, as before, but from 1 mL of 16N HNO_3. Strontium was purified from Ba (and any residual Rb) by two passes through a 0.75 g DOWEX AG-50W X8 (100-200 mesh) cation exchange column equilibrated with 2.3N HCl.

The Pb- (and Fe-) containing solution, taken off the oxalic-acid column, was evaporated to dryness and the residue dissolved in 5 mL 0.7N HBr. The Pb was purified by a single pass through a DOWEX AG-X1 anion exchange resin (100-200 mesh) equilibrated with 0.7 HBr.

Procedural blanks for the modified procedures as outlined were 0.06 ng

Sm, 0.95 ng Nd, 0.3 ng Sr, 0.1 ng Pb, and 0.1 ng Rb.

Mass Spectrometric Analysis.

Lead was loaded as a chloride onto a single Re filament using the silica gel - phosphoric acid method (Cameron *et al.*, 1969). Neodymium, and Sm, were analyzed as metals following loading in 7N HNO_3 onto the side filament of a double Re filament assembly. Strontium and Rb were loaded as chlorides on the side filament of double Re assemblies and also run as metals.

Lead isotopic ratios were measured using a VG Micromass-30 single collector, solid-source mass spectrometer operating in semi-automatic mode. Multiple analyses of the NBS 981 common lead standard by the isotopic group of the Department of Physics, University of Alberta yielded mass fractionation correction factors of 1.2, 1.3, and 1.4 per mil/amu for $^{206}Pb/^{204}Pb$, $^{207}Pb/^{204}Pb$, and $^{208}Pb/^{204}Pb$, respectively. Replicate analyses of ten aliquots of NBS 981 (treated as 'unknowns') and corrected using the above mass fractionation factors gave:

$^{206}Pb/^{204}Pb = 16.934 \pm 0.009$ (n=10) [16.937 ± 0.011]
$^{207}Pb/^{204}Pb = 15.942 \pm 0.009$ (n=10) [15.491 ± 0.006]
$^{208}Pb/^{204}Pb = 36.720 \pm 0.038$ (n=10) [36.721 ± 0.027]

(all uncertainties at the 95% confidence level, values in square brackets were derived from the NBS 981 certificate). As can be seen the agreement between the arithmetic mean of the measured values and the certified values is excellent. Unspiked Nd (and the majority of unspiked Sr) isotopic measurements were performed using a five collector VG 354 solid-source mass spectrometer operating in peak switching mode. Reported $^{143}Nd/^{144}Nd$ isotopic ratios have been normalized to $^{146}Nd/^{144}Nd = 0.7219$, while $^{87}Sr/^{86}Sr$ ratios have been normalized to $^{86}Sr/^{88}Sr = 0.1194$.

Spiked Sm, Nd, Sr, and Rb analyses were performed on the MM-30 mass spectrometer. Initially, the Sm and Nd analyses were performed separately. The Nd concentration of a sample was determined from the measured $^{145}Nd/^{144}Nd$

spiked ratio. Mass fractionation was determined from the measured ^{146}Nd/^{144}Nd and ^{145}Nd/^{144}Nd ratios. The magnitude of the ^{144}Sm isobaric interference to ^{144}Nd was determined and corrected for, by monitoring the ^{147}Sm/^{144}(Nd + Sm) ratio. Similarly, the Sm concentration of each sample was determined from the measured ^{149}Sm/^{147}Sm spiked ratio, with mass fractionation being corrected for by measurement of the ^{148}Sm/^{147}Sm and ^{149}Sm/^{147}Sm ratios. Isobaric interference to ^{148}Sm by ^{148}Nd was monitored by measuring the ^{146}Nd/^{147}(Sm + Nd) ratio.

Because the methyllactic acid column separation gave high purity Nd and Sm fractions with very low levels of Ce and Gd, towards the end of this study the following modified analytical sequence was used in order to save analysis time. Samarium and Nd were consecutively eluted from the MLA columns into a single collection vessel and, following removal of the methyllactic acid (as described earlier), were loaded together on the same side filament for mass spectrometric analysis. For these analyses, the ^{145}Nd/^{146}Nd ratio was used to determine the Nd concentration with the mass fractionation correction being calculated from the measured ^{145}Nd/^{146}Nd and ^{142}Nd/^{146}Nd ratios. Any ^{142}Ce interference to ^{142}Nd was monitored by measuring the ratio of peaks at masses 140 and 142. As before, Sm was quantified using the measured ^{149}Sm/^{147}Sm spiked ratio. Mass fractionation was determined from the ^{149}Sm/^{147}Sm and ^{152}Sm/^{147}Sm ratios, and the possible ^{152}Gd isobaric interference to ^{152}Sm monitored by measuring the ratio ^{155}Gd/^{147}Sm. Programmes to correct for mass fractionation (assuming the linear law) and to perform the isotope dilution and ^{147}Sm/^{144}Nd calculations were written by the author.

Following individual Sm, and Nd runs, using the former combination of ratios, the remaining unloaded Sm and Nd aliquots were combined and analyzed using the second scheme. The differences in the ^{147}Sm/^{144}Nd ratios determined by the two procedures were statistically insignificant.

APPENDIX 3.

Single bead U-Pb Zircon Analyses.

Over the past twenty years major advances in the U-Pb dating of minerals, particularly zircon, have been made. Of special note in this field is the work of Krogh and various coworkers. Krogh (1973) presented the now well known and universally utilized hydrothermal procedure for the dissolution of zircons. Prior to this work dissolution was accomplished by the borax fusion technique which typically entailed a procedural Pb blank in the range 0.2 - 1.0 μg. The hydrothermal dissolution technique reduced this to 0.5 - 5.0 ng (Krogh, 1973) which meant that samples weighing 100-fold less than previous could be analyzed. Other advances, such as the development of multicollector thermal ionization mass spectrometers (with or without secondary electron multipliers), the synthesis and purification of ^{205}Pb for U-Pb dating (Krogh and Davis, (1975); Parrish and Krogh, (1987)), the abrasion technique to produce more concordant samples (Krogh (1982), the miniaturization of sample dissolution, and the production of ultra clean reagents and work environments, have all resulted in significant progress in the field of U-Pb analyses.

As a consequence precise U-Pb zircon analyses are now commonly performed on carefully prepared and selected samples typically weighing less than 100 μg (Krogh, 1973, 1982), and often weighing less than 20 μg (Parrish *et al.*, 1987). For the most precise analyses of these very small samples the procedural and loading blanks should be both as low, and reproducible, as possible. Following the procedures of Krogh (1973) a number of laboratories (*e.g.*, at the Royal Ontario Museum, and the geochronology laboratory of Geological Survey of Canada, Ottawa) that have been dedicated to the development and application of the method commonly report procedural blanks significantly less than 50 pg (*e.g.*, Roddick *et al.*, 1987). Assuming that no foreign particles contribute to the blank, the main components of a procedural blank will be: a) the reagent blank, b) container blank(s), and c) a processing or manipulation blank (*e.g.*, contribution from the chromatographic separation of Pb). Logically, other factors remaining equal, the fewer the number of manipulations in a procedure the lower procedural blank will be.

The author's initial attempts to separate and purify Pb from zircons using a modified column procedure of Krogh (1973) generally gave quite high and unsatisfactory Pb blanks. Consequently, the author decided to attempt a different approach for the separation of Pb. The method followed that of Manton (1988) who described the separation of Pb from young zircons using a single ion exchange bead. A dramatic reduction in the procedural blank resulted.

Theory of the single-bead technique.

Using Dowex 1-X8 (200 - 400 mesh) anion exchange resin Andersen and Knutsen (1962) showed that the distribution coefficient (K_d) for Pb(II) in HBr is greater, by over a factor of ten, than that for the same normality of HCl. Unfortunately, their results are only presented in a graphical manner, with the Pb(II) K_d reaching a maximum of *ca.* 800 at about 0.5N HBr. However, Strelow (1978), in a study to determine the distribution coefficients for 200 - 400 mesh anion exchange AG1-X8 resin for a number of elements in HBr-HNO_3 mixtures, lists the K_d for Pb(II) in 0.03N (14.4), 0.05N (52), 0.10N (242), 0.20N (635), 0.50N (821), and 1.0N (620) HBr (measured Pb(II) K_d-values in parentheses). A plot of the K_d-values against HBr normality is shown in Figure A3.1. As can be seen the K_d reaches a maximum slightly over 800, between 0.5 and 0.7N HBr.

Although various ions have been separated from complex mixtures by other workers using single ion exchange beads (particularly in the nuclear industry, *e.g.*, Walker *et al.*, 1974) Manton (1988) first applied the technique to the separation of Pb from young zircons.

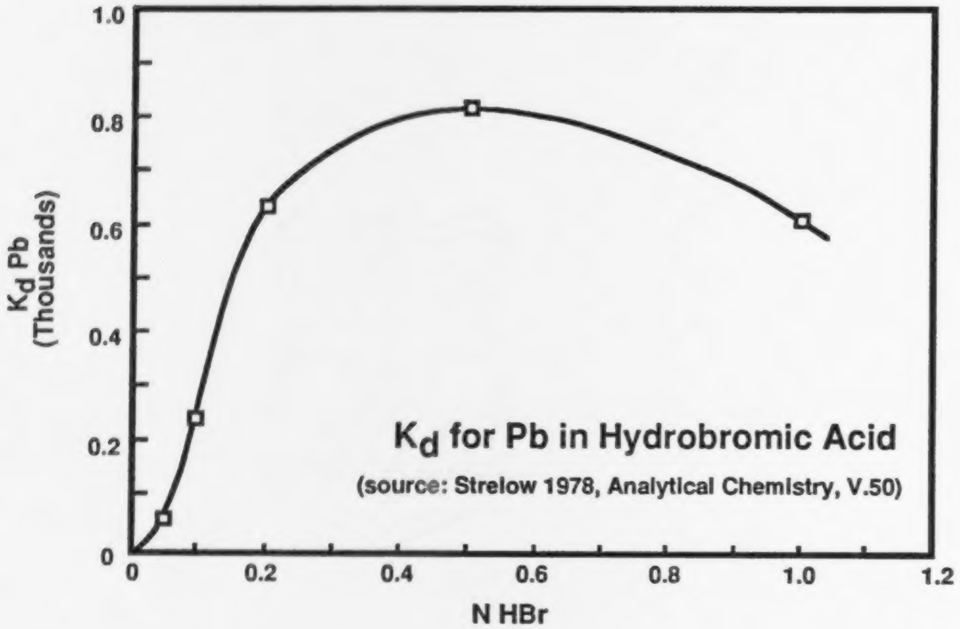

Figure A3.1 Variation of the distribution coefficient for Pb(II) with different HBr normalities (Dowex 1-X8 resin).

Using Pb as an example, the efficiency of separation (or yield) of ions from a liquid medium by ion exchange is given by:

$$\frac{I_B}{I} = \left(1 + \frac{M_L}{K_d.M_B}\right)^{-1} * 100\ \%$$

where:

I = Pb ions initially in solution

I_B = Pb ions bound to bead

M_L = mass of acid (g)

M_B = mass of bead(s) (g)

K_d = distribution coefficient of Pb for a particular acid normality

Given that a 20-mesh Dowex 1-X8 bead weighs *ca.* 375 μg, and assuming a K_d(Pb) of 700 for 0.7N HBr, and that 35 μL of 0.7N HBr is used, the efficiency of Pb extraction would in theory be *ca.* 88%. Use of two beads would increase this to *ca.* 94%, and with three beads to *ca.* 96%.

Methodology.

Following the picking, abrasion, weighing, and cleaning of zircons, samples weighing between 10 and 150 μg (as determined using a Cahn microbalance) were transferred to Teflon® mini-capsules (2 mL volume) in a clean air fumehood. A charge of 0.5 mL 25M HF and *ca.* 10 μL 7N HNO_3 was added to each sample (all acids were double/triple vapour distilled) and the microcapsules capped and batches of eight (including two blanks) were packed in a pressure bomb assembly. The assembly was placed in an oven at 190°-200°C and left for a minimum of 5 days to dissolve the zircons. Following cooling the microcapsules were opened in a clean air fumehood and examined for total dissolution of the zircons (the author had no samples that did not dissolve completely, however, sealing and further hydrothermal dissolution would have been employed if necessary). The clear sample solutions were spiked with a mixed ^{205}Pb - ^{235}U spike and the mixture evaporated to dryness (procedural blanks were not spiked at this point). Removal/conversion of the fluoride salts was promoted by twice adding *ca.* 10 μL 7N HNO_3 to the residue and evaporating to dryness. At this stage the nitrate residues were either dissolved in *ca.* 35 μL 0.7 M HBr or, in the early stages of the development of the method, first solubilized by adding 0.5 mL 7N HNO_3 to the dissolution bombs and heating overnight at 190° C before evaporating to dryness and dissolving the residue in *ca.* 35 μL 0.7 M HBr.

One to three rigorously cleaned 20 mesh, Dowex 1-X8 anion exchange beads (repeatedly washed and rinsed in double distilled 6N HCl and Millipore water, respectively) were added to each liquid sample (still in the dissolution bombs) using a Pt-Re wire with a loop *ca.* 1 mm in diameter at one end to select and hold the beads. The Pt-Re wire could be rigorously cleaned and never came into contact with the sample solution when adding the bead(s). Each bead was held firmly to the wire loop by surface tension but could be 'knocked off' into the sample solution with a drop of 0.7N HBr acid.

The kinetics of the extraction process for 20 mesh beads is slow in comparison to that for 100-200 or 200-400 mesh beads. To aid in equilibration the capped vessels containing the bead(s) and HBr were mechanically agitated to promote movement of the bead(s) in the acid. Following a minimum of an hour of agitation, samples were left at least 6 hours before the anion exchange bead(s) was/were removed from the HBr sample solution and transferred to a rigorously cleaned 3 mL Savillex® beaker. Again a Pt-Re wire was used and the individual beads transferred to the beaker by 'knocking' them off the wire with a falling drop of 6N HCl. The Pb bound to the beads was back extracted into *ca.* 50 μL 6N HCl. The capped Savillex® beakers containing the bead(s) and HCl were also shaken, approximately for one hour to maximize Pb extraction, prior to removing and discarding the anion exchange bead(s). At this stage approximately 6 μL of 1.75 N H_3PO_4 was added to the 6N HCl and the solution evaporated to a concentrated drop of phosphoric acid that contained the Pb ready for loading. All of the bead manipulations were performed in a clean air hood.

The 0.7N HBr sample solution, from which the Pb was extracted onto the 20 mesh anion exchange bead(s), was evaporated to dryness and taken up in 0.5 mL 7N HNO_3. Uranium was separated from this solution by standard anion exchange chromatography (100-200 mesh Dowex-1 X8, NO_3-form) on miniaturized columns. Following removal of Zr, Hf, REE, *etc.*, uranium was eluted, and collected in the microcapsule that had been used for the dissolution of the zircon(s) thus helping to minimize the U blank.

It would be possible to collect the Zr, Hf, REE, *etc*, (minus the U and Th) for isotopic (*e.g.*, Lu-Hf, Sm-Nd), or elemental analysis (Heaman *et al.*, 1990). If Hf could readily be separated from the Zr, and its isotopic composition determined by mass spectrometry, the combined U-Pb age data and Hf isotopic composition *determined on the same sample* would provide a very powerful geochemical tool.

U and Pb Mass Spectrometric Analyses.

The purified Pb samples (in concentrated phosphoric acid) were loaded on outgassed Re centre filaments using the silica-gel technique (Cameron, *et al.*, 1969). All U-Pb zircon analyses were performed using a VG 354 multicollector thermal ionization mass spectrometer. The majority of Pb samples were analyzed with the VG 354 operating in multi-collector mode (with Faraday cups as collectors), and the $^{206}Pb/^{204}Pb$ ratio generally checked or measured in single collector mode using a Daly amplifier. For very small samples all the Pb isotopic data were collected on the Daly multiplier in single collector mode. Common lead corrections were made using the model of Stacey and Kramers (1975). Uranium was loaded in HNO_3 on the side filament of an outgassed double Re assembly and analyzed as a metal. Again, depending upon the amount of uranium, analysis was carried out in either multi-collector or single collector using the Faraday or Daly collectors, respectively.

Summary.

The refined single-bead zircon technique gave procedural blanks of approximately 15 to 20 pg Pb, with a minimum of effort, that were quite reproducible. This was considered a great improvement on the conventional column separation which gave blanks of *ca.* 80 pg Pb. The Teflon® mini-capsules used for the dissolution of the zircon samples have a relatively large volume (2 mL) and hence surface area. Consequently, it is felt that the procedural blank could likely be lowered to the 5 pg level, or less, by employing 0.3 mL PTFE microcapsules for mineral dissolution and Pb extraction by the single bead method. Preliminary technique development using 0.3 mL PTFE vessels was very promising. The HBr acid used to dissolve the nitrate salts is strongly held in the vessel by surface tension permitting the microcapsule to be inverted and hence rotated. In this manner the anion exchange bead can roll around the solution maximizing Pb recovery. Unfortunately, time restraints did not permit the development of this variation of the technique.

APPENDIX 4.

Elemental and isotopic results.

Whole-rock elemental and isotopic results based on XRF, INAA, and MSID analyses.

	1	2	3	4	5	10	12
SiO2	72.97	71.14	71.92	71.47	72.87	50.71	69.39
Al2O3	15.36	16.63	16.09	16.49	15.87	19.41	17.31
TiO2	0.162	0.149	0.142	0.156	0.091	0.944	0.222
FeO*	0.98	1.21	1.08	1.05	0.56	8.42	1.36
MnO	0.020	0.030	0.025	0.022	0.015	0.129	0.021
CaO	1.76	2.73	2.46	3.01	1.93	8.75	3.08
MgO	0.28	0.30	0.26	0.31	0.10	5.05	0.56
K2O	2.92	1.59	1.84	1.21	2.35	1.47	1.31
Na2O	4.98	5.65	5.61	5.70	5.67	4.30	6.16
P2O5	0.041	0.053	0.034	0.041	0.018	0.286	0.058
Ni	8	10	7	7	9	68	11
Cr	1.78	2.75		2.08		19.5	9.00
Sc	1.45	1.79	1.61	1.73	1.22	19.8	1.70
Co	1.35	2.02	1.80	2.38	0.78	38.7	3.60
V	10	12	5	15	1	200	31
Rb	69.97	53	56	41	48.92	48.96	39.33
Sr	637.0	503	403	468	549.9	908.7	496.9
Nb	0.6	1.5	1.9	0.8	0.0	1.9	1.6
Cu	11	13	9	24	10	2	5
Zn	34	37	33	30	19	96	28
Pb	25	18	20	15	23	11	20
Th	6.60	0.93	0.20	1.38	1.29	0.87	1.85
Cs	0.82	1.58	0.76	0.84	0.50	1.06	0.78
Ba	1469	360	534	227	661	277	356
U	0.76	1.99	0.29	0.45	0.40	0.76	0.27
Ta	0.007	0.425	0.123	0.164	0.041	0.153	0.134
Hf	3.28	2.41	2.90	2.30	2.34	1.39	2.67
Zr	109	89	99	89	93	76	114
Y	3	4	3	1	3	14	2
La	19.8	6.72	5.39	10.9	7.95	20.3	13.4
Ce	32.0	12.4	8.92	17.8	12.3	46.3	21.6
Nd	9.040	4.770	2.910	5.250	3.070	22.00	8.447
Sm	1.233	0.988	0.515	0.820	0.429	5.343	1.012
Eu	0.441	0.457	0.415	0.369	0.432	1.712	0.491
Tb	0.110	0.160		0.105	0.035	0.560	0.125
Yb	0.287	0.360	0.260			0.880	0.385
Lu						0.114	

	13	14	15	16	17	18	20
SiO2	70.95	70.22	71.73	59.96	60.21	62.07	72.08
Al2O3	16.70	17.22	16.07	16.60	19.16	20.01	15.31
TiO2	0.172	0.125	0.169	0.801	0.877	0.401	0.267
FeO*	1.17	1.09	1.14	6.44	4.31	3.43	1.51
MnO	0.022	0.014	0.014	0.105	0.061	0.039	0.021
CaO	2.90	3.15	2.59	6.14	5.23	4.48	2.30
MgO	0.40	0.32	0.33	3.07	2.09	1.07	0.47
K2O	1.21	1.39	2.11	1.43	1.66	1.50	2.99
Na2O	5.90	5.90	5.27	4.63	5.59	6.23	4.45
P2O5	0.056	0.036	0.043	0.289	0.264	0.231	0.069
Ni	9	9	10	24	10	13	13
Cr	3.60	1.84	3.06	17.7	20.4	9.97	8.10
Sc	2.02	0.56	1.11	15.0	10.1	5.98	0.89
Co	2.42	2.42	2.30	23.2	19.0	9.13	4.01
V	18	20	0	135	112	67	25
Rb	35	30	45.05	40.36	55.28	52.24	73.73
Sr	473	750	596.9	564.9	554.7	583.9	322.6
Nb	2.0	0.0	0.0	7.9	6.4	3.7	1.7
Cu	6	22	5	50	441	52	6
Zn	38	18	28	85	63	52	32
Pb	15	16	16	14	13	17	20
Th	0.64	1.26	0.09	1.01	1.63	2.76	1.13
Cs	0.56	0.32	0.56	0.60	0.70	0.64	0.51
Ba	317	630	1251	446	477	426	1259
U	0.18	0.24	0.27	0.30	0.31	0.28	0.27
Ta	0.159	0.076	0.008	0.352	0.275	0.155	0.042
Hf	2.67	4.21	2.37	4.09	2.56	2.41	3.22
Zr	105	138	104	155	106	102	107
Y	2	1	1	19	12	8	3
La	9.09	9.49	7.44	31.4	30.5	26.5	13.7
Ce	15.5	13.8	11.2	65.6	66.3	50.6	23.3
Nd	5.542	3.870	3.660	27.70	30.03	21.87	7.920
Sm	0.905	0.516	0.489	6.040	4.748	3.399	1.003
Eu	0.832	0.640	0.489	1.336	0.930	0.881	0.740
Tb	0.094	0.068	0.048	0.606	0.637	0.371	0.107
Yb	0.247	0.127		1.640	1.100	0.450	0.172
Lu				0.230			

	21	22	24	34	35	36	39
SiO2	68.26	64.02	68.25	66.48	72.16	63.49	51.81
Al2O3	16.18	16.95	16.93	16.16	15.83	17.77	18.94
TiO2	0.387	0.618	0.349	0.456	0.182	0.725	0.787
FeO*	3.32	4.43	2.30	3.96	1.13	4.57	8.59
MnO	0.042	0.067	0.025	0.070	0.023	0.067	0.115
CaO	3.37	5.06	3.36	4.38	2.20	4.04	8.50
MgO	1.27	2.06	1.11	1.78	0.39	1.73	4.97
K2O	1.61	1.07	1.89	1.81	1.92	1.88	1.12
Na2O	4.88	4.92	5.13	4.21	5.57	4.97	4.33
P2O5	0.147	0.274	0.140	0.156	0.054	0.227	0.296
Ni	14	22	19	21	8	9	36
Cr	14.5	29.2	15.8	45.5	1.55	3.50	35.2
Sc	5.38	7.46	2.58	8.40	1.79	12.2	24.0
Co	9.31	14.4	8.20	12.3	1.78	12.6	32.5
V	49	86	39	64	11	85	190
Rb	71.48	26.10	50.00	63.03	46.36	78.94	32.51
Sr	395.6	718.7	621.0	369.7	664.0	592.5	820.8
Nb	6.3	0.0	2.9	7.6	0.6	4.1	2.1
Cu	26	43	19	6	3	48	0
Zn	69	75	45	61	41	80	91
Pb	13	9	13	13	23	14	17
Th	4.05	1.01	0.66	5.24	5.33	5.25	1.44
Cs	0.67	0.33	0.65	2.77	1.04	1.93	2.10
Ba	380	595	1375	451	835	795	344
U	0.60	0.36	0.40	0.72	0.75	0.70	0.88
Ta	0.597	0.101	0.087	0.549	0.190	0.229	0.411
Hf	3.83	4.34	3.75	4.15	3.44	4.36	1.09
Zr	150	184	156	153	129	188	67
Y	6	10	3	11	3	10	14
La	39.7	31.7	16.6	26.6	24.2	28.8	17.0
Ce	71.0	69.3	29.4	48.7	40.8	57.4	37.9
Nd	23.26	28.24	10.30	18.43	12.22	20.88	20.71
Sm	3.278	4.291	1.491	3.068	1.654	3.526	4.190
Eu	0.759	1.270	0.758	0.990	0.552	1.050	1.380
Tb	0.348	0.330	0.123	0.471	0.135	0.517	0.536
Yb	0.640	0.790	0.270	1.260	0.175	0.850	0.949
Lu				0.180		0.104	0.118

	40	42	43	44	57	58	60
SiO2	59.80	64.87	64.43	71.70	70.68	68.07	69.26
Al2O3	17.02	16.88	16.03	16.17	16.56	17.81	16.88
TiO2	0.635	0.490	0.537	0.132	0.160	0.281	0.258
FeO*	6.35	4.45	5.51	0.95	1.15	1.78	1.69
MnO	0.120	0.070	0.121	0.022	0.025	0.022	0.022
CaO	7.51	5.28	4.71	1.77	2.66	3.53	3.24
MgO	2.86	1.90	2.02	0.71	0.49	0.64	0.66
K2O	0.82	1.37	1.46	1.27	2.36	1.28	1.59
Na2O	4.19	4.07	4.42	6.70	5.34	5.94	5.79
P2O5	0.152	0.094	0.221	0.032	0.046	0.106	0.086
Ni	38	27	25	8	11	8	12
Cr	36.8	21.8	39.0		2.07	4.67	8.20
Sc	15.7	10.8	12.6	1.73	1.61	0.88	1.04
Co	22.6	13.2	15.7	1.57	2.98	4.03	4.96
V	122	80	62	10	26	31	30
Rb	11	82	61	42	67	43	45.47
Sr	214	244	177	411	504	749	596.5
Nb	4.6	7.2	11.1	0.0	2.3	0.0	0.0
Cu	26	8	5	8	18	11	27
Zn	53	53	79	26	30	35	37
Pb	11	16	18	11	16	15	17
Th	2.47	4.91	1.68	0.38	0.17	0.29	0.70
Cs		2.37	1.40	0.40	1.14	0.93	0.42
Ba	75	239	175	224	536	565	723
U	0.76	0.84	0.95	0.42	0.22	0.29	0.20
Ta	0.411	0.569	0.898	0.121	0.062	0.084	
Hf	5.10	3.87	3.85	2.09	2.27	3.25	2.72
Zr	175	153	141	85	93	155	119
Y	23	21	24	4	2	1	2
La	17.2	18.3	13.0	4.12	5.50	8.40	17.3
Ce	35.8	34.9	29.4	8.90	9.79	15.10	27.9
Nd	16.50	15.90	15.46	3.400	3.333	5.590	8.080
Sm	3.720	3.090	3.612	0.636	0.620	0.784	0.978
Eu	0.896	0.676	0.976	0.320	0.420	0.670	0.642
Tb	0.623	0.542	0.612	0.096	0.067	0.049	0.074
Yb	1.700	1.270	2.090	0.306	0.213		0.112
Lu	0.252	0.180	0.231				

	80	85	86	87	88	89A	89B
SiO_2	71.80	61.18	69.78	67.84	71.33	70.71	60.46
Al_2O_3	16.08	17.65	15.77	16.72	16.31	16.52	16.07
TiO_2	0.161	0.760	0.334	0.497	0.152	0.201	0.750
FeO*	1.05	5.30	2.91	2.97	1.22	1.30	7.29
MnO	0.021	0.070	0.048	0.055	0.024	0.026	0.130
CaO	2.35	5.63	3.56	3.20	2.83	3.06	6.30
MgO	0.21	2.56	0.95	1.06	0.43	0.41	2.93
K_2O	2.43	1.09	1.17	1.53	1.29	1.81	1.22
Na_2O	5.31	4.95	4.84	5.43	5.83	5.35	4.18
P_2O_5	0.039	0.280	0.112	0.177	0.041	0.074	0.138
Ni	8	26	15	10	13	8	25
Cr		39.1	16.0	16.2	4.83		45.7
Sc	1.53	12.5	5.70	4.55	2.66	2.13	20.5
Co	1.61	17.0	10.0	7.21	2.62	2.42	23.3
V	17	100	36	43	25	19	154
Rb	64.07	30.44	49.89	92.64	51.56	64	43.00
Sr	580.0	648.6	333.1	411.0	466.4	537	280.5
Nb	0.0	3.5	6.2	6.6	2.0	1.1	6.3
Cu	5	63	25	32	10	3	22
Zn	41	62	45	65	30	32	77
Pb	21	12	15	17	17	17	15
Th	2.43	4.72	2.74	4.44	3.01	4.55	4.42
Cs	0.96	1.32	1.07	1.36	1.41	1.71	1.65
Ba	1005	815	333	273	226	413	267
U	0.52	0.35	0.92	0.56	0.84	0.60	1.87
Ta	0.131		0.459	0.490	0.651	0.180	0.853
Hf	2.82	5.72	4.23	4.75	2.07	3.12	3.64
Zr	103	250	165	196	89	135	137
Y	4	13	10	8	6	6	26
La	9.77	73.3	7.50	24.2	10.6	17.9	22.6
Ce	18.0	133	23.4	47.9	20.1	31.7	45.0
Nd	6.291	48.30	7.293	20.25	8.013	10.09	19.99
Sm	1.120	8.454	1.633	3.168	1.439	1.557	4.080
Eu	0.413	1.940	0.509	0.591	0.404	0.440	1.070
Tb	0.120	0.594	0.315	0.329	0.195	0.168	0.621
Yb		1.040	0.813	0.501	0.430		2.170
Lu			0.114				

	90	91	92	93	94	103	111
SiO2	64.00	60.91	64.57	71.52	70.31	69.59	69.73
Al2O3	16.65	16.83	17.10	15.84	17.00	17.01	17.03
TiO2	0.494	0.586	0.701	0.210	0.149	0.214	0.226
FeO*	4.59	5.71	4.41	1.32	0.91	1.33	1.35
MnO	0.098	0.110	0.047	0.022	0.014	0.020	0.018
CaO	4.88	5.57	4.53	2.43	2.68	3.49	3.56
MgO	2.17	3.26	1.34	0.49	0.53	0.65	0.61
K2O	1.42	1.63	1.42	2.44	2.56	1.36	1.24
Na2O	4.98	4.66	5.11	5.12	5.26	5.70	5.60
P2O5	0.175	0.217	0.244	0.071	0.063	0.108	0.097
Ni	26	37	6	9	12	18	10
Cr	26.1	92.0	3.40	4.90	7.08	6.49	12.0
Sc	20.8	13.6	7.76	0.79	1.12	1.27	1.35
Co	15.6	20.0	10.6	2.56	3.22	5.42	4.84
V	86	104	86	19	15	19	29
Rb	47.92	59.43	55.02	58.20	48.84	47.00	40.59
Sr	534.3	536.6	659.4	617.6	620.6	676.5	651.0
Nb	7.1	4.6	4.3	0.0	1.3	0.8	0.5
Cu	27	0	31	7	12	19	12
Zn	80	98	58	34	24	33	34
Pb	16	14	15	20	20	16	15
Th	2.60	2.54	8.93	0.49	1.21	0.77	0.89
Cs	0.65	1.03	0.62	0.51	0.52	1.29	0.73
Ba	463	505	724	1269	1962	533	539
U	0.70	0.77	0.46	0.24	0.23	0.37	0.49
Ta	0.350	0.474	0.266		0.056	0.126	0.040
Hf	2.28	2.46	5.06	2.57	2.62	2.29	5.46
Zr	101	110	225	105	118	98	251
Y	23	15	8	2	1	2	2
La	24.3	26.5	59.8	9.51	18.5	8.71	12.1
Ce	60.2	50.1	105	15.6	26.8	16.2	21.4
Nd	35.39	23.62	32.54	4.910	7.820	6.330	6.690
Sm	8.055	4.192	4.162	0.670	0.922	1.068	0.964
Eu	1.220	0.755	1.125	0.332	0.611	0.539	0.430
Tb	1.070	0.427	0.490		0.089	0.121	0.057
Yb	1.740	0.863	0.511				0.172
Lu		0.137					

	112	113	116	118	120	121	122
SiO2	53.20	67.28	72.08	53.87	72.75	72.33	74.74
Al2O3	18.56	16.86	16.07	19.18	15.47	15.84	14.78
TiO2	1.080	0.412	0.198	1.038	0.206	0.164	0.128
FeO*	7.73	3.08	1.33	7.65	1.15	1.14	0.68
MnO	0.112	0.037	0.016	0.103	0.020	0.020	0.012
CaO	7.95	4.27	3.31	7.26	2.09	2.65	1.68
MgO	4.04	1.20	0.46	3.55	0.33	0.34	0.30
K2O	1.24	1.13	0.89	0.93	1.95	1.31	1.44
Na2O	5.01	5.04	5.11	5.48	5.44	5.62	5.68
P2O5	0.550	0.150	0.007	0.406	0.059	0.049	0.022
Ni	41	13	10	24	9	13	8
Cr	63.0	12.2	3.10	33.9	4.83	6.34	
Sc	19.7	4.24	1.01	21.9	1.66	2.10	1.30
Co	29.2	10.7	3.25	26.2	2.62	2.81	1.05
V	152	58	21	136	23	24	10
Rb	24.99	32.22	17.79	19.65	35.15	39.31	28
Sr	1046	846.8	715.4	849.5	563.4	430.8	377
Nb	3.2	1.2	0.0	5.0	1.4	1.7	1.1
Cu	57	20	27	43	13	6	13
Zn	109	53	21	98	35	29	17
Pb	17	16	16	12	15	24	16
Th	0.62	3.21	7.63	1.35	0.51	2.56	4.73
Cs	0.47	0.55		0.51	0.41	0.58	0.41
Ba	428	630	703	620	1107	366	463
U	0.32	0.28	0.26	0.59	0.13	0.52	0.38
Ta	0.353	0.079		0.276	0.025	0.187	0.024
Hf	3.15	3.25	3.89	6.15	3.24	2.78	2.45
Zr	147	145	169	226	130	100	83
Y	18	5	1	20	1	3	0
La	40.4	39.4	57.8	31.9	10.4	10.5	17.8
Ce	93.0	70.6	87.4	73.9	19.3	19.2	30.5
Nd	45.00	23.18	21.61	40.83	8.230	7.622	9.800
Sm	8.820	2.759	1.798	7.431	1.155	1.269	1.465
Eu	2.350	1.260	0.732	2.770	0.551	0.396	0.392
Tb	1.120	0.205	0.162	0.680	0.074	0.148	0.174
Yb	1.590			1.240	0.138	0.216	
Lu	0.201			0.132			

	123	124	127	142	144	145	146
SiO2	62.85	67.40	72.13	72.28	70.39	72.23	71.59
Al2O3	16.16	16.74	15.84	15.27	17.08	15.96	16.23
TiO2	0.591	0.558	0.140	0.184	0.167	0.111	0.137
FeO*	6.03	3.56	0.73	1.80	0.99	0.77	1.07
MnO	0.119	0.050	0.013	0.032	0.022	0.019	0.032
CaO	5.93	3.13	1.78	2.59	2.60	2.03	2.50
MgO	2.16	1.11	0.17	0.64	0.27	0.17	0.31
K2O	1.07	1.70	3.57	2.08	2.09	2.66	1.81
Na2O	4.40	5.05	5.06	4.54	5.82	5.49	5.73
P2O5	0.161	0.159	0.034	0.045	0.041	0.026	0.049
Ni	24	6	10	14	9	7	10
Cr	23.8			4.86	1.40	1.10	2.14
Sc	15.1	6.89	1.30	3.22	1.80	1.46	1.96
Co	17.2	8.90	1.16	4.22	2.26	1.16	1.87
V	100	63	7	18	24	11	5
Rb	38.52	120.48	62	112	56	61.76	60.35
Sr	171.7	445.1	599	134	701	457.4	364.0
Nb	9.6	7.2	0.0	7.5	1.1	0.5	3.2
Cu	9	7	11	7	5	8	7
Zn	64	79	21	43	35	25	35
Pb	14	18	26	32	17	18	17
Th	2.78	7.29	8.17	7.57	0.74	1.00	2.33
Cs	1.29	4.39	0.49	3.34	0.90	0.98	1.36
Ba	217	387	1530	343	516	666	380
U	0.96	1.17	0.28	3.28	0.40	0.45	0.42
Ta	0.667	0.790		0.386	0.165	0.054	0.220
Hf	4.44	3.87	2.43	3.82	1.90	1.91	2.73
Zr	175	147	95	104	88	77	94
Y	30	14	2	9	4	4	4
La	17.0	33.7	30.5	22.2	13.3	4.42	9.44
Ce	35.1	63.9	45.4	42.5	19.1	11.7	17.2
Nd	18.58	22.73	12.53	13.37	10.14	4.350	6.060
Sm	4.151	3.720	1.560	2.951	1.792	0.850	1.107
Eu	1.014	0.673	0.602	0.587	0.370	0.343	0.265
Tb	0.663	0.434	0.132	0.345	0.186	0.101	0.132
Yb	1.870	0.964					
Lu	0.346	0.126					

	147	148	149	150	151	152	153
SiO2	69.34	60.88	61.68	68.51	63.57	54.98	71.15
Al2O3	16.39	16.44	16.32	17.08	16.88	17.47	16.61
TiO2	0.358	0.589	0.661	0.367	0.575	0.767	0.151
FeO*	2.53	5.75	5.87	2.29	4.97	7.73	1.04
MnO	0.039	0.100	0.101	0.035	0.093	0.119	0.018
CaO	3.29	6.17	5.76	4.15	5.73	8.52	2.58
MgO	0.69	3.75	3.22	0.70	1.74	4.81	0.36
K2O	2.01	1.58	1.64	1.16	0.91	0.54	2.06
Na2O	4.74	4.04	4.00	5.08	4.87	4.38	5.43
P2O5	0.086	0.170	0.198	0.083	0.127	0.155	0.073
Ni	9	51	40	7	25	89	9
Cr	2.70	128	104		19.6	114	3.00
Sc	3.80	13.9	14.4	4.92	12.1	21.1	1.63
Co	5.85	23.0	21.9	6.54	14.1	30.8	2.52
V	31	95	86	43	91	155	12
Rb	66	54	56	66	37.32	4	56
Sr	317	356	335	527	153.8	266	534
Nb	4.1	6.9	7.7	1.5	7.7	2.5	1.7
Cu	4	65	10	7	4	12	39
Zn	29	70	73	39	55	88	30
Pb	13	14	13	15	17	10	21
Th	6.09	4.21	4.62	0.64	2.81	0.31	1.50
Cs	0.95	1.19	1.22	3.69	1.77		1.15
Ba	629	323	339	260	113	134	622
U	0.74	0.73	0.66	0.37	1.57	0.29	0.98
Ta	0.272	0.381	0.610	0.261	0.614	0.242	0.138
Hf	3.55	2.89	3.97	1.40	3.75	0.98	2.93
Zr	127	136	146	93	140	65	118
Y	8	15	15	4	29	10	6
La	16.6	20.9	15.1	2.73	15.4	12.3	11.4
Ce	34.6	41.9	47.0	6.56	41.4	24.8	22.0
Nd	12.60	17.95	18.21	2.700	17.46	9.860	7.950
Sm	2.230	3.379	3.680	0.820	4.172	2.194	
Eu	0.751	1.089	1.120	0.490	1.090	0.987	0.497
Tb	0.211	0.453	0.472	0.156	0.749	0.357	0.172
Yb	0.658	1.050	1.020		2.450	0.917	
Lu		0.111	0.130		0.335	0.130	

	154	964	965	966	968	969	970
SiO2	70.55	69.84	68.02	67.41	69.79	69.13	71.40
Al2O3	16.81	16.96	17.38	17.96	16.71	17.32	16.34
TiO2	0.150	0.204	0.380	0.301	0.235	0.199	0.175
FeO*	0.83	1.47	2.15	1.98	1.61	1.60	1.09
MnO	0.019	0.023	0.021	0.026	0.021	0.020	0.022
CaO	2.31	3.08	4.45	3.85	2.90	3.03	2.73
MgO	0.29	0.52	0.82	0.83	0.63	0.54	0.34
K2O	3.43	1.85	0.93	1.55	1.98	1.64	2.38
Na2O	5.04	5.46	5.26	5.47	5.54	5.94	4.94
P2O5	0.037	0.067	0.054	0.089	0.064	0.054	0.047
Ni	10	11	11	11	11	12	10
Cr	3.63	0.50	3.90	4.30	6.76	7.10	3.50
Sc	1.48	2.03	3.36	3.93	2.04	1.91	1.85
Co	2.08	3.73	5.87	5.79	3.85	3.66	2.26
V	22	20	34	29	26	26	17
Rb	97.68	47	29.57	51	49	43	59
Sr	600.1	669	739.7	576	381	421	396
Nb	0.9	0.0	0.0	0.8	0.0	0.0	0.0
Cu	20	11	13	5	2	7	10
Zn	26	54	37	53	29	36	34
Pb	24	15	16	16	13	15	18
Th	2.52	1.80	0.75	2.76	1.65	1.51	2.47
Cs	1.53	4.29	1.65	1.03		1.03	1.34
Ba	918	1040	299	500	390	362	559
U	0.68	0.32	0.32	0.35	0.40	0.21	0.23
Ta	0.060	0.130	0.114	0.207	0.024	0.037	0.191
Hf	1.17	2.45	2.74	2.26	2.50	2.44	2.10
Zr	59	106	129	112	97	92	88
Y	3	1	3	3	1	2	5
La	10.2	12.8	3.80	8.80	5.80	6.20	11.4
Ce	20.9	23.5	7.80	18.8	12.2	13.3	21.0
Nd	9.240	9.320	4.540	8.250	5.100	4.040	10.06
Sm	1.731	1.553	1.158	1.350	0.813	0.661	1.848
Eu	0.492	0.440	0.599	0.436	0.397	0.315	0.452
Tb	0.167	0.115	0.127	0.162			0.200
Yb							0.326
Lu							

	19	27	61	68	114	115	141
SiO2	73.46	71.42	74.95	74.20	74.85	76.70	70.76
Al2O3	14.64	16.45	14.13	14.35	14.75	14.10	15.84
TiO2	0.166	0.143	0.054	0.085	0.154	0.053	0.099
FeO*	1.09	1.09	0.34	0.69	0.86	0.33	0.88
MnO	0.019	0.020	0.007	0.009	0.013	0.007	0.013
CaO	1.58	2.30	1.17	1.13	3.22	2.86	1.10
MgO	0.25	0.42	0.01	0.06	0.29	0.08	0.21
K2O	4.22	1.86	5.31	5.44	0.69	0.55	7.36
Na2O	4.01	5.71	3.49	3.48	4.62	4.78	3.18
P2O5	0.038	0.042	0.004	0.022	0.010	0.003	0.024
Ni	10	11	8	8	7	8	8
Cr	2.60	1.19		1.90	3.60		
Sc	2.65	1.59	0.51	0.74	1.28	0.52	1.05
Co	1.92	1.75	0.35	1.62	2.28	0.93	1.10
V	15	2	4	10	13	23	14
Rb	96.25	59.72	96.41	106	16.81	8.21	173
Sr	204.0	421.4	217.6	322	640.6	510.7	248
Nb	4.4	3.2	0.0	0.0	0.0	0.0	2.4
Cu	6	9	9	39	18	16	8
Zn	21	31	10	13	20	11	20
Pb	22	38	30	26	16	15	44
Th	7.48	3.93	4.48	22.2	2.48	6.05	1.70
Cs	0.48	0.98	0.29	0.16	0.47	0.17	1.99
Ba	900	223	673	2024	286	219	2132
U	0.56	0.48	0.51	1.20	0.38	0.67	0.48
Ta	0.243	0.235	0.020			0.020	0.304
Hf	2.93	2.60	1.98	3.11	3.09	5.42	0.85
Zr	101	100	49	98	113	161	43
Y	6	5	2	4	1	1	4
La	20.6	14.2	5.27	35.4	5.99	13.6	3.69
Ce	34.1	27.3	9.06	61.2	10.6	26.5	6.47
Nd	12.18	9.490	3.250	19.72	4.430	10.61	2.630
Sm	2.137	1.596	0.517	2.640	0.611	1.481	0.493
Eu	0.550	0.454	0.396	0.480	0.573	0.614	0.769
Tb	0.240	0.149		0.163		0.103	0.101
Yb		0.178		0.157			
Lu				0.018			

	25	64	72	78	140
SiO2	75.74	70.71	68.50	71.55	73.20
Al2O3	13.73	16.46	16.34	15.99	13.77
TiO2	0.168	0.211	0.423	0.170	0.255
FeO*	0.91	1.30	2.86	1.27	2.68
MnO	0.018	0.018	0.035	0.018	0.089
CaO	2.58	2.19	3.39	2.88	1.97
MgO	0.75	0.74	1.21	0.53	0.23
K2O	0.96	1.81	1.56	1.70	3.77
Na2O	4.58	5.98	5.05	5.29	3.45
P2O5	0.032	0.050	0.111	0.068	0.052
Ni	14	9	24	17	12
Cr	13.8	1.87	16.7	18.6	6.29
Sc	2.40	1.34	6.18	1.50	3.61
Co	7.87	2.49	9.23	3.40	2.87
V	18	22	43	21	2
Rb	42	51	94.09	56.52	93.37
Sr	412	515	365.1	379.3	199.4
Nb	0.0	0.0	2.7	0.0	4.8
Cu	10	10	14	15	38
Zn	18	25	43	26	36
Pb	24	21	19	25	23
Th	0.60	3.86	8.22	5.17	9.34
Cs	0.61	0.76	3.34	1.22	1.35
Ba	209	304	530	361	764
U	0.79	0.53	1.02	0.53	0.49
Ta		0.005	0.250		0.189
Hf	3.33	3.34	4.49	3.02	12.40
Zr	135	125	166	106	402
Y	4	4	5	3	53
La	15.5	23.1	13.0	22.9	67.5
Ce	27.4	32.5	23.2	43.3	140
Nd	11.85	7.530	7.951	14.88	53.99
Sm	1.729	1.066	1.412	2.326	9.690
Eu	0.761	0.708	0.570	0.554	1.914
Tb		0.169	0.136	0.178	1.370
Yb		0.241			5.480
Lu					0.636

	67	69	70	128	129	130	131
SiO2	61.09	62.82	60.94	55.63	73.44	54.85	53.70
Al2O3	16.27	16.25	17.60	17.53	15.98	17.75	17.48
TiO2	0.647	0.602	0.603	0.774	0.060	0.776	0.870
FeO*	6.58	5.93	5.79	7.85	0.54	8.04	8.11
MnO	0.112	0.107	0.104	0.113	0.016	0.133	0.129
CaO	6.70	5.74	6.25	8.20	3.41	8.18	8.91
MgO	2.85	2.74	2.49	4.13	0.16	4.48	5.12
K2O	0.72	1.01	0.80	0.69	0.89	0.59	0.68
Na2O	4.36	4.18	4.75	4.34	4.99	4.50	4.29
P2O5	0.133	0.089	0.125	0.198	0.004	0.162	0.180
Ni	36	40	32	61	9	91	104
Cr	31.5	26.2	45.0	156	1.02	169	190
Sc	18.5	16.5	15.4	19.8	0.81	22.2	22.8
Co	23.0	22.3	20.3	30.2	1.50	30.9	33.9
V	130	114	101	164	16	159	193
Rb	3.84	26.32	6.05	5.26	9	4.84	2.17
Sr	196.6	208.3	377.5	312.1	691	285.0	308.2
Nb	6.1	4.3	3.0	2.9	0.0	3.1	1.7
Cu	5	69	13	0	11	9	5
Zn	73	77	68	95	11	91	96
Pb	10	11	10	9	15	8	9
Th	0.22	0.74			1.22	0.17	0.28
Cs		1.18	0.39	0.80	0.054		
Ba	246	276	287	165	658	175	136
U	0.16	0.23	0.28	0.56	0.29	0.11	0.15
Ta	0.453	0.366	0.291	0.230	0.014	0.197	0.254
Hf	2.53	3.17	2.91	0.66	2.64	0.98	1.41
Zr	117	157	116	49	115	54	76
Y	16	I4	8	11	0	12	11
La	12.5	11.8	9.80	9.52	14.2	9.85	9.90
Ce	24.9	20.6	20.9	19.7	22.5	21.2	22.2
Nd	10.79	9.930	9.430	9.241	4.703	11.16	11.16
Sm	2.473	2.251	2.040	2.086	0.452	2.700	2.517
Eu	1.010	0.746	0.839	1.030	0.662	0.947	1.150
Tb	0.467	0.408	0.304	0.279	0.075	0.399	0.410
Yb	1.510	1.300	1.000	0.951	0.280	1.030	1.090
Lu	0.208	0.173	0.151	0.112	0.040	0.137	0.154

	133	135	136	137	138	139
SiO2	59.92	57.01	66.01	56.84	57.55	56.74
Al2O3	17.56	17.00	16.88	17.00	16.27	16.86
TiO2	0.710	0.774	0.683	0.767	0.750	0.750
FeO*	6.48	7.85	3.79	7.86	7.83	8.01
MnO	0.104	0.134	0.063	0.123	0.136	0.136
CaO	4.90	7.64	4.68	7.54	7.96	7.90
MgO	3.42	4.07	1.79	4.08	3.99	4.15
K2O	2.08	0.59	0.47	0.68	0.33	0.64
Na2O	4.16	4.27	5.01	4.45	4.49	4.15
P2O5	0.128	0.137	0.088	0.126	0.157	0.126
Ni	67	70	29	74	61	77
Cr	127	127	9.20	138	119	140
Sc	15.5	22.7	7.61	20.6	25.1	21.8
Co	23.4	27.1	12.3	28.2	29.4	30.6
V	112	158	68	131	145	155
Rb	93.26	3.60	0.76	6.95	0.248	11.02
Sr	283.7	333.0	703.8	340.6	261.5	309.0
Nb	7.8	3.9	0.5	4.4	3.0	3.9
Cu	11	12	23	10	5	22
Zn	104	92	49	86	82	89
Pb	14	8	10	10	7	10
Th	1.77	0.19		0.31		0.28
Cs	2.81					
Ba	417	235	358	423	127	295
U	0.54	0.13	0.21	0.19	0.15	0.20
Ta	0.750	0.184	0.216		0.184	0.172
Hf	2.60	2.55	5.84	2.00	1.50	2.25
Zr	103	116	284	107	75	106
Y	8	17	3	12	14	13
La	14.0	9.68	7.08	13.0	7.30	10.2
Ce	24.5	23.5	11.6	22.4	16.5	21.6
Nd	10.65	14.15	5.050	11.62	8.820	11.41
Sm	1.933	3.285	0.976	2.308	2.238	2.497
Eu	0.720	1.130	0.511	0.879	0.909	1.040
Tb	0.284	0.550	0.103	0.377	0.383	0.425
Yb	0.626	1.520	0.310	1.009	1.264	0.919
Lu		0.199	0.041	0.138	0.198	0.114

	6	45	46	47	158
SiO2	51.05	70.26	70.89	74.30	70.47
Al2O3	13.50	16.37	15.93	14.53	15.94
TiO2	1.217	0.211	0.243	0.110	0.255
FeO*	13.07	2.01	2.25	1.34	2.43
MnO	0.219	0.033	0.039	0.024	0.034
CaO	10.10	3.36	3.11	2.31	3.28
MgO	6.41	0.59	0.77	0.22	0.76
K2O	1.08	1.88	1.53	2.35	1.28
Na2O	2.71	4.70	4.64	4.27	4.96
P2O5	0.107	0.062	0.065	0.020	0.063
Ni	78	11	19	7	16
Cr	189	2.39	9.60	1.50	7.97
Sc	41.8	1.85	2.24	1.55	3.06
Co	48.0	4.25	6.16	1.51	6.39
V	354	20	16	5	29
Rb	6.37	80.96	108.10	60.87	87.0
Sr	94.8	209.9	199.1	173.1	191.9
Nb	4.7	6.7	5.9	9.1	5.9
Cu	79	5	5	8	7
Zn	90	44	47	32	50
Pb	10	13	15	15	18
Th	0.76	4.35	6.26	9.12	4.21
Cs		3.33	5.98	1.30	0.91
Ba	69	564	543	750	268
U	0.72	0.79	2.73	0.76	0.61
Ta		0.708	0.676	0.369	0.480
Hf	2.43	3.45	3.10	2.72	3.57
Zr	86	122	130	74	118
Y	29	9	7	5	9
La	6.35	22.3	26.4	28.7	12.1
Ce	14.9	39.6	49.3	57.4	24.0
Nd	12.54	13.09	16.15	17.41	9.120
Sm	3.924	2.074	2.474	3.069	1.961
Eu	1.030	0.779	0.683	0.955	0.608
Tb	0.850	0.306	0.346	0.265	0.331
Yb	2.655	0.870	0.644	0.335	0.612
Lu	0.360	0.117			

	59	143	54	66	155	156	73
SiO2	61.81	70.54	76.57	81.63	60.61	61.36	49.90
Al2O3	11.12	14.17	11.79	9.97	16.42	17.89	15.45
TiO2	0.378	0.546	0.377	0.210	0.378	0.709	0.720
FeO*	4.92	4.02	3.50	1.23	5.61	4.91	10.38
MnO	0.132	0.166	0.069	0.019	0.051	0.045	0.188
CaO	7.17	2.85	0.83	1.72	1.40	3.53	11.25
MgO	8.20	1.41	2.12	0.56	8.59	3.93	7.75
K2O	3.36	1.58	3.10	1.61	2.36	0.98	0.88
Na2O	2.23	4.06	1.05	2.49	3.98	5.87	2.91
P2O5	0.148	0.126	0.056	0.026	0.062	0.239	0.048
Ni	233	25	15	25	18	27	87
Cr	398	15.5	6.20	43.6	8.70	33.0	249
Sc	22.3	12.3	5.78	4.10	2.22	12.2	40.4
Co	33.3	11.8	3.56	6.63	13.5	16.2	46.9
V	99	46	18	37	63	100	238
Rb	115	133	80	60	69	26	10
Sr	317	109	31	353	211	476	79.0
Nb	4.4	15.1	47.9	2.9	0.8	2.7	0.7
Cu	0	185	5	15	1	63	58
Zn	76	85	224	37	98	47	73
Pb	13	30	20	18	8	12	18
Th	7.32	7.28	11.4	3.36	1.50	1.46	0.48
Cs	1.26	6.40	6.60	1.92	2.46	0.80	
Ba	748	168	498	653	408	290	32
U	0.66	3.02	3.14	0.97	0.36	0.43	0.68
Ta	0.520	1.230	0.218	0.260	0.084	0.099	
Hf	1.91	9.13	13.83	2.23	3.16	4.24	1.31
Zr	77	296	397	88	117	165	51
Y	10	61	129	5	5	10	20
La	24.8	37.0	63.5	14.5	16.4	28.0	2.87
Ce	52.1	80.7	139	28.5	30.8	57.4	7.71
Nd	24.85	38.86	65.00	13.51		25.20	
Sm	4.058	8.190	17.50	2.230	1.500	4.430	1.870
Eu	0.901	1.260	2.810	0.587	0.444	1.110	0.630
Tb	0.473	1.470	3.450	0.256	0.166	0.399	0.454
Yb	0.577	6.320	8.390	0.473			1.600
Lu		0.742	1.547	0.058		0.107	0.219

G87	206Pb 204Pb	207Pb 204Pb	208Pb 204Pb	87Sr/ /86Sr	87Rb/86Sr (meas)	87Rb/86Sr (calc)	143Nd 144Nd	147Sm 144Nd
1	13.643	14.342	35.590	0.715414	0.3180	0.3280	0.510371	0.0824
2	19.492	15.707	33.673	0.714865	nd	0.3052	0.511315	0.1253
3	13.241	14.308	32.859	0.718687	nd	0.4027	0.510910	0.1072
4	14.764	14.587	34.587	0.713401	nd	0.2537	0.510571	0.0944
5	13.257	14.328	33.465	0.714262	0.2576	0.2633	0.510399	0.0844
10	14.948	14.615	33.275	0.707212	0.1559	0.1559	0.510870	0.1043
12	13.262	14.291	34.227	0.713061	0.2291	0.2458	0.510281	0.0724
13	12.990	14.245	33.305	0.711047	nd	0.2143	0.510693	0.0987
14	13.107	14.250	33.500	0.707224	nd	0.1158	nd	nd
15	12.900	14.170	32.554	0.711258	0.2185	0.2272	0.510352	0.0780
16	13.406	14.278	34.319	0.710707	0.2068	0.2183	0.510751	0.0997
17	13.151	14.249	33.809	0.714239	0.2885	0.2834	0.510685	0.0856
18	13.091	14.207	34.026	0.713994	0.2590	0.2674	0.510658	0.0939
20	12.910	14.128	33.022	0.729503	0.6573	0.6873	0.510273	0.0765
21	13.631	14.244	35.252	0.723586	0.5196	0.5219	0.510523	0.0855
22	13.828	14.390	33.581	0.706609	0.1043	0.1220	0.510600	0.0918
24	13.584	14.307	33.077	0.712089	nd	0.2332	0.510502	0.0875
34	15.604	14.907	36.309	0.723601	0.4940	0.5066	0.510728	0.1005
35	13.853	14.432	35.198	0.710238	0.2021	0.2127	0.510467	0.0818
36	14.778	14.595	38.150	0.718381	0.3859	0.4014	0.510747	0.1020
39	16.800	14.947	33.836	0.707544	0.1146	0.1212	0.511162	0.1223
40	15.971	14.909	36.667	0.709372	nd	0.1488	nd	nd
42	16.183	14.892	38.441	0.742874	nd	0.9762	nd	nd
43	15.226	14.658	33.529	0.749514	nd	1.0017	0.511476	0.1412
44	18.727	15.169	36.763	nd	nd		nd	nd
57	13.284	14.318	33.017	0.717445	nd	0.3852	0.510985	0.1124
58	13.092	14.231	33.118	0.708999	nd	0.1662	0.510451	0.0847
59	14.671	14.522	34.634	0.744332	nd	1.0539	0.510742	0.0987
60	13.203	14.289	33.203	0.711614	0.2207	0.2261	0.510071	0.0731
80	13.523	14.330	33.137	0.716357	0.3199	0.3403	0.510847	0.1076
85	13.806	14.380	36.812	0.707731	0.1358	0.1399	0.510368	0.0768
86	15.708	14.872	35.984	0.723057	0.4340	0.4716	0.511198	0.1352
87	14.030	14.472	34.327	0.729272	0.6535	0.6689	0.510530	0.0945
88	14.237	14.565	34.147	0.716618	0.3202	0.3327	0.510886	0.1085
89A	14.630	14.665	34.540	0.716232	nd	0.3453	0.510592	0.0932
89B	19.084	15.577	36.748	0.723863	0.4443	0.5024	0.511213	0.1233
90	14.271	14.459	35.993	0.713576	0.2596	0.2719	0.511296	0.1376
91	14.319	14.487	34.375	0.716393	0.3207	0.3237	0.510822	0.1072
92	13.654	14.358	39.929	0.713803	0.2416	0.2597	0.510295	0.0761
93	13.129	14.263	32.853	0.714145	0.2728	0.3062	0.510325	0.0825
94	12.906	14.191	33.094	0.711928	0.2278	0.2465	0.510262	0.0712
103	13.255	14.227	32.876	0.710497	0.2011	0.2129	0.510777	0.1020
111	13.257	14.228	32.927	0.709220	0.1804	0.1788	0.510521	0.0871
112	12.980	14.094	33.088	0.705042	0.0685	0.0746	0.510562	0.0962
113	13.342	14.229	35.195	0.706806	0.1093	0.1176	0.510232	0.0720
116	13.629	14.324	38.463	0.705432	0.0719	0.0807	0.509771	0.0503
118	14.597	14.562	34.293	0.704901	0.0669	0.0718	0.510853	0.1100
120	12.810	14.222	33.182	0.709982	0.1815	0.1944	0.510432	0.0848
121	13.533	14.348	33.821	0.714804	0.2642	0.2797	0.510767	0.1006
122	13.853	14.443	35.329	0.713134	nd	0.2151	0.510598	0.0904
123	16.630	15.097	35.584	0.738755	0.7643	0.8075	0.511392	0.1350

G87	206Pb 204Pb	207Pb 204Pb	208Pb 204Pb	87Sr/ /86Sr	87Rb/86Sr (meas)	87Rb/86Sr (calc)	143Nd 144Nd	147Sm 144Nd
124	nd	nd	nd	nd	nd	nd	0.510703	0.0992
127	16.125	14.878	34.272	nd	nd	nd	0.510308	0.0763
142	14.488	14.190	35.040	0.808070	nd	2.4433	0.511012	0.1088
144	13.328	14.560	33.126	0.712156	0.2265	0.2314	0.511060	0.0559
145	13.71	14.52	33.41	0.719153	0.3911	0.4051	0.511000	0.1182
146	14.606	14.579	34.081	0.723607	0.4909	0.5018	0.510942	0.1104
147	nd	nd	nd	nd	nd	nd	nd	nd
148	17.330	15.229	37.829	0.720074	nd	0.4396	0.510959	0.1138
149	17.160	15.207	37.846	0.721812	nd	0.4846	0.511008	0.1221
150	13.422	14.300	33.109	0.718165	0.3442	0.3629	nd	0.4498
151	17.687	15.288	34.585	0.735000	0.7040	0.7352	0.511466	0.1444
152	13.806	14.456	33.226	0.702369	0.0340	0.0435	0.511375	0.1345
153	13.444	14.320	33.142	0.715802	nd	0.3038	nd	nd
154	13.626	14.343	33.424	0.722084	0.4716	0.4823	0.510906	0.1132
964	13.152	14.114	33.525	0.709842	nd	0.2034	0.510824	0.1007
965	13.425	14.163	33.004	0.707159	0.1156	0.1209	0.511750	0.1542
966	14.707	14.437	33.655	0.712436	nd	0.2564	0.510698	0.0989
968	13.617	14.202	33.615	0.716840	nd	0.3726	0.510549	0.0964
969	13.505	14.168	33.312	0.714623	nd	0.2959	0.510550	0.0989
970	14.738	14.441	33.441	0.719369	nd	0.4318	0.510922	0.1110
45	nd	nd	nd	nd	1.1203	1.1570	0.510825	0.0958
46	17.364	14.815	34.186	0.763801	1.5795	1.5863	0.510765	0.0926
47	14.795	14.387	37.282	0.734938	nd	1.0449	0.510988	0.1065
158	13.681	14.039	33.368	0.757554	1.3180	1.3277	0.511361	0.1300
19	13.566	14.301	34.374	0.761647	1.3727	1.4127	0.510833	0.1061
27	12.476	13.673	33.324	0.725118	nd	0.4356	0.510322	0.1017
61	13.297	14.207	33.298	0.760241	1.2882	1.3214	0.510658	0.0963
68	14.254	14.583	44.764	0.741687	nd	0.9561	0.510282	0.0809
114	13.279	14.188	33.739	0.707477	0.0759	0.0918	0.510561	0.0833
115	13.857	14.307	34.606	0.705527	0.0465	0.0617	0.510433	0.0843
141	12.313	13.448	32.643	0.794307	nd	2.0365	0.510853	0.1135
6	17.491	15.265	35.940	0.711647	0.1947	0.2694	0.512520	0.1896
41	15.884	14.803	33.639	0.721982	0.2226	0.4417	0.512066	0.1686
54	17.414	14.901	37.875	nd	nd	nd	0.511613	0.1455
66	14.114	14.353	33.919	nd	nd	nd	0.510920	0.0998
143	17.134	15.000	34.686	0.710297	nd	3.5331	0.511531	0.1332
25	13.481	13.961	34.948	0.723747	nd	0.2956	0.510112	0.0882
64	13.004	13.951	33.391	nd	nd	nd	0.509904	0.0855
78	12.641	13.784	33.829	0.725008	nd	0.4461	0.510219	0.0944
140	12.159	13.544	34.981	0.780725	1.3643	1.3567	0.510643	0.1085

G87	206Pb 204Pb	207Pb 204Pb	208Pb 204Pb	87Sr/ /86Sr	87Rb/86Sr (meas)	87Rb/86Sr (calc)	143Nd 144Nd	147Sm 144Nd
67	13.263	14.302	32.843	0.703691	0.0564	0.1028	0.511443	0.1384
69	13.916	14.447	33.976	0.716750	nd	0.3938	0.511532	0.1472
70	13.529	14.410	33.103	0.703541	0.0464	0.0540	0.511394	0.1308
128	14.390	14.614	33.272	0.704144	0.0487	nd	0.511452	0.1368
129	13.167	14.306	33.244	0.703251	nd	0.0377	0.509903	0.0581
130	12.951	14.247	32.926	0.702235	0.0491	0.0419	0.511390	0.1462
131	13.120	14.290	32.848	0.702398	0.0204	0.0471	0.511390	0.1362
133	14.054	14.388	33.841	0.743716	0.9546	1.0458	0.510992	0.1097
135	12.876	14.173	33.559	0.703883	nd	0.0695	0.511487	0.1402
136	13.005	14.257	32.972	0.701918	0.0031	0.0165	0.511050	0.1166
137	13.067	14.268	33.388	0.704123	0.0590	0.0782	0.510955	0.1200
138	12.690	14.175	32.586	0.701482	0.0034	0.0113	0.511734	0.1531
139	13.277	14.268	33.640	0.704153	nd	0.0656	0.511358	0.1323
266926	13.591	14.361	33.171	nd	nd	nd	0.511536	0.1450
341901	13.534	14.421	32.930	nd	nd	nd	0.510911	0.1136
341911	14.628	14.781	42.248	nd	nd	nd	0.510720	0.0999
341918	13.390	14.400	33.346	nd	nd	nd	0.511225	0.1236
341919	13.341	14.390	32.891	nd	nd	nd	0.510479	0.0885
341938	27.002	17.432	40.499	nd	nd	nd	nd	nd
341939	13.970	14.503	33.777	nd	nd	nd	0.511547	0.1422
341971	24.744	16.839	36.323	nd	nd	nd	0.513881	nd
341976	13.034	14.328	34.566	nd	nd	nd	0.510218	0.0749

APPENDIX 5.

CIPW Norms

C.I.P.W. norms were calculated using the programme 'NEWPET' written by D. Clarke. The major element data differ slightly from those reported in Appendix 4 because i) iron has been divided into ferrous and ferric ($Fe_2O_3 = 0.25 * FeO$, except for samples analyzed by A. Stelmach) in the manner described in Chapter 3 under 'Classification' and ii) the data have been recalculated on an anhydrous basis.

The following key has been used:

Symbol	**Mineral**
Q	Quartz
C	Corundum
Z	Zircon
Or	Orthoclase
Ab	Albite
An	Anorthite
Di	Diopside
Hy	Hypersthene
Ol	Olivine
Mt	Magnetite
Il	Ilmenite
Ap	Apatite

Normative minerals are in weight percent, An (%) and Ab-Or-An data calculated from molecular %

G87-	1	2	3	4	5	10	12	13	14	15
SiO_2	73.34	71.49	72.28	71.83	73.24	50.86	69.73	71.30	70.58	72.09
TiO_2	0.16	0.15	0.14	0.16	0.09	0.95	0.22	0.17	0.13	0.17
Al_2O_3	15.43	16.71	16.17	16.58	15.96	19.47	17.40	16.78	17.31	16.16
Fe_2O_3	0.27	0.47	0.30	0.29	0.16	2.35	0.38	0.33	0.30	0.32
FeO	0.74	0.78	0.82	0.80	0.42	6.33	1.03	0.88	0.82	0.86
MnO	0.02	0.03	0.03	0.02	0.02	0.13	0.02	0.02	0.01	0.01
MgO	0.28	0.30	0.27	0.31	0.10	5.07	0.56	0.40	0.32	0.33
CaO	1.77	2.74	2.47	3.02	1.94	8.78	3.10	2.91	3.16	2.60
Na_2O	5.01	5.67	5.64	5.73	5.70	4.31	6.19	5.93	5.93	5.29
K_2O	2.94	1.59	1.84	1.22	2.36	1.48	1.32	1.22	1.40	2.12
P_2O_5	0.04	0.05	0.03	0.04	0.02	0.29	0.06	0.06	0.04	0.04
Q	28.5	25.8	26.3	26.5	26.6	0.0	20.8	25.0	23.1	26.8
C	0.90	0.80	0.48	0.43	0.55	0.00	0.30	0.55	0.39	0.53
Z	0.02	0.02	0.02	0.02	0.02	0.02	0.02	0.02	0.03	0.02
Or	17.4	9.4	10.9	7.2	14.0	8.7	7.8	7.2	8.3	12.5
Ab	42.4	48.0	47.7	48.5	48.3	31.6	52.3	50.2	50.2	44.8
An	8.5	13.2	12.1	14.7	9.5	29.4	15.0	14.1	15.5	12.6
Di	0.0	0.0	0.0	0.0	0.0	10.0	0.0	0.0	0.0	0.0
Hy	1.6	1.6	1.7	1.8	0.8	0.0	2.6	2.1	1.9	1.9
Ol	0.0	0.0	0.0	0.0	0.0	11.7	0.0	0.0	0.0	0.0
Mt	0.4	0.7	0.4	0.4	0.2	3.4	0.6	0.5	0.4	0.5
Il	0.31	0.28	0.27	0.30	0.17	1.80	0.42	0.33	0.24	0.32
Ap	0.10	0.13	0.08	0.10	0.04	0.68	0.14	0.13	0.09	0.10
An (%)	15.9	20.6	19.2	22.3	15.6	46.7	21.3	20.9	22.5	21.0
Or	24.5	12.8	14.8	9.8	18.7	12.2	9.9	9.6	10.7	17.2
Ab	63.5	69.2	68.8	70.1	68.6	46.8	70.9	71.5	69.2	65.4
An	12.0	18.0	16.4	20.1	12.7	41.1	19.1	18.9	20.1	17.4

G87-	16	17	18	19	20	21	22	24	34	35
SiO_2	60.17	60.45	62.35	73.83	72.43	68.57	64.28	68.57	66.77	72.53
TiO_2	0.80	0.88	0.40	0.17	0.27	0.39	0.62	0.35	0.46	0.18
Al_2O_3	16.66	19.24	20.10	14.71	15.39	16.25	17.02	17.01	16.23	15.91
Fe_2O_3	1.80	1.30	0.96	0.43	0.42	0.93	1.24	0.64	1.11	0.32
FeO	4.85	3.17	2.58	0.70	1.14	2.50	3.33	1.73	2.98	0.85
MnO	0.11	0.06	0.04	0.02	0.02	0.04	0.07	0.03	0.07	0.02
MgO	3.08	2.10	1.07	0.25	0.47	1.28	2.07	1.11	1.79	0.39
CaO	6.16	5.26	4.50	1.59	2.32	3.38	5.08	3.37	4.40	2.21
Na_2O	4.65	5.62	6.26	4.03	4.47	4.90	4.94	5.15	4.22	5.60
K_2O	1.43	1.67	1.51	4.24	3.01	1.62	1.07	1.90	1.82	1.93
P_2O_5	0.29	0.27	0.23	0.04	0.07	0.15	0.27	0.14	0.16	0.05
Q	9.6	6.6	8.0	30.2	28.8	23.6	16.8	21.9	22.0	26.9
C	0.00	0.00	0.55	0.70	0.73	0.63	0.00	0.69	0.00	0.71
Z	0.03	0.02	0.02	0.02	0.02	0.03	0.04	0.03	0.03	0.03
Or	8.5	9.9	8.9	25.0	17.8	9.6	6.3	11.2	10.7	11.4
Ab	39.3	47.5	53.0	34.1	37.8	41.5	41.8	43.6	35.7	47.4
An	20.4	22.4	20.8	7.6	11.0	15.8	21.1	15.8	20.0	10.6
Di	6.8	1.6	0.0	0.0	0.0	0.0	1.9	0.0	0.7	0.0
Hy	10.6	7.8	6.0	1.3	2.5	6.4	8.4	4.9	8.0	2.0
Ol	0.0	0.0	0.0	0.0	0.0	0.0	0.0	0.0	0.0	0.0
Mt	2.6	1.9	1.4	0.6	0.6	1.3	1.8	0.9	1.6	0.5
Il	1.53	1.67	0.76	0.32	0.51	0.74	1.18	0.67	0.87	0.35
Ap	0.69	0.63	0.55	0.09	0.16	0.35	0.65	0.33	0.37	0.13
An %	32.8	30.7	27.0	17.4	21.5	26.4	32.3	25.5	34.5	17.5
Or	12.0	11.9	10.4	36.4	25.8	13.8	8.8	15.3	15.6	15.8
Ab	59.1	61.0	65.4	52.6	58.2	63.4	61.8	63.1	55.3	69.5
An	28.9	27.1	24.2	11.1	16.0	22.8	29.4	21.6	29.1	14.7

G87-	36	39	40	41	42	43	44	45	46	47
SiO_2	63.73	51.96	60.02	52.15	65.13	64.68	72.07	70.60	71.23	74.67
TiO_2	0.73	0.79	0.64	0.58	0.49	0.54	0.13	0.21	0.24	0.11
Al_2O_3	17.83	19.00	17.08	14.04	16.94	16.10	16.25	16.45	16.00	14.60
Fe_2O_3	1.53	2.39	1.77	2.94	1.24	1.54	0.21	0.56	0.63	0.37
FeO	3.23	6.46	4.78	7.94	3.35	4.15	0.77	1.51	1.69	1.01
MnO	0.07	0.12	0.12	0.21	0.07	0.12	0.02	0.03	0.04	0.02
MgO	1.74	4.98	2.87	8.07	1.91	2.03	0.71	0.59	0.78	0.22
CaO	4.05	8.53	7.53	10.14	5.30	4.73	1.78	3.37	3.12	2.32
Na_2O	4.99	4.34	4.21	2.94	4.08	4.43	6.74	4.72	4.66	4.29
K_2O	1.88	1.13	0.82	0.94	1.38	1.46	1.27	1.89	1.54	2.36
P_2O_5	0.23	0.30	0.15	0.06	0.09	0.22	0.03	0.06	0.07	0.02
Q	15.2	0.0	11.8	0.0	20.5	18.7	22.7	27.1	29.5	34.8
C	0.76	0.00	0.00	0.00	0.00	0.00	0.62	0.66	1.14	0.83
Z	0.04	0.01	0.04	0.01	0.03	0.03	0.02	0.02	0.03	0.01
Or	11.1	6.7	4.9	5.5	8.1	8.7	7.5	11.2	9.1	14.0
Ab	42.2	36.7	35.6	24.9	34.6	37.5	57.0	39.9	39.5	36.3
An	18.6	29.0	25.3	22.4	23.8	19.7	8.6	16.3	15.1	11.4
Di	0.0	9.3	9.2	22.4	1.5	1.9	0.0	0.0	0.0	0.0
Hy	7.9	1.7	9.1	15.6	8.4	9.8	2.9	3.5	4.2	2.0
Ol	0.0	10.9	0.0	3.8	0.0	0.0	0.0	0.0	0.0	0.0
Mt	2.2	3.5	2.6	4.3	1.8	2.2	0.3	0.8	0.9	0.5
Il	1.38	1.50	1.21	1.10	0.93	1.02	0.25	0.40	0.46	0.21
Ap	0.54	0.70	0.36	0.13	0.22	0.53	0.08	0.15	0.15	0.05
An %	29.4	42.7	40.1	45.9	39.4	33.1	12.5	27.8	26.4	22.8
Or	14.9	8.9	7.2	10.2	11.9	12.7	9.8	16.0	13.8	21.9
Ab	60.1	52.2	55.6	48.6	53.4	58.4	78.9	60.6	63.4	60.3
An	25.0	38.9	37.2	41.2	34.7	28.9	11.3	23.4	22.8	17.8

G87-	57	58	59	60	80	85	86	87	88	89A
SiO_2	71.04	68.40	62.06	69.60	72.17	61.41	70.10	68.15	71.69	71.07
TiO_2	0.16	0.28	0.38	0.26	0.16	0.76	0.34	0.50	0.15	0.20
Al_2O_3	16.64	17.90	11.16	16.96	16.16	17.72	15.84	16.79	16.39	16.60
Fe_2O_3	0.32	0.50	1.37	0.47	0.29	1.48	0.81	0.83	0.34	0.36
FeO	0.86	1.34	3.71	1.27	0.79	3.99	2.19	2.24	0.92	0.98
MnO	0.03	0.02	0.13	0.02	0.02	0.07	0.05	0.06	0.02	0.03
MgO	0.49	0.65	8.23	0.66	0.22	2.57	0.95	1.06	0.43	0.41
CaO	2.68	3.55	7.19	3.25	2.37	5.65	3.57	3.22	2.84	3.07
Na_2O	5.36	5.97	2.24	5.82	5.34	4.97	4.86	5.45	5.86	5.38
K_2O	2.37	1.28	3.38	1.60	2.45	1.09	1.17	1.54	1.30	1.82
P_2O_5	0.05	0.11	0.15	0.09	0.04	0.28	0.11	0.18	0.04	0.07
Q	23.9	19.8	11.7	21.2	26.0	11.6	27.3	21.4	25.4	25.3
C	0.50	0.50	0.00	0.00	0.52	0.00	0.36	0.75	0.27	0.38
Z	0.02	0.03	0.02	0.02	0.02	0.05	0.03	0.04	0.02	0.03
Or	14.0	7.6	20.0	9.4	14.5	6.5	6.9	9.1	7.7	10.8
Ab	45.4	50.5	19.0	49.3	45.2	42.1	41.1	46.1	49.6	45.5
An	13.0	16.9	10.4	15.5	11.5	22.8	17.0	14.8	13.8	14.8
Di	0.0	0.0	19.4	0.1	0.0	2.8	0.0	0.0	0.0	0.0
Hy	2.3	3.2	16.5	3.2	1.5	10.0	5.3	5.3	2.3	2.3
Ol	0.0	0.0	0.0	0.0	0.0	0.0	0.0	0.0	0.0	0.0
Mt	0.5	0.7	2.0	0.7	0.4	2.1	1.2	1.2	0.5	0.5
Il	0.31	0.54	0.72	0.49	0.31	1.45	0.64	0.95	0.29	0.38
Ap	0.11	0.25	0.35	0.20	0.09	0.67	0.27	0.42	0.10	0.18
An %	21.2	24.0	34.2	22.8	19.3	33.8	28.0	23.2	20.8	23.4
Or	18.7	9.7	39.5	12.2	19.5	8.7	10.2	12.5	10.3	14.6
Ab	64.1	68.6	39.8	67.8	64.9	60.4	64.6	67.2	71.0	65.4
An	17.3	21.7	20.7	20.0	15.5	30.9	25.1	20.3	18.7	20.0

G87-	89B	90	91	92	93	94	103	111	112	113
SiO_2	60.66	64.26	61.14	64.83	71.88	70.67	69.93	70.08	53.30	67.59
TiO_2	0.75	0.50	0.59	0.70	0.21	0.15	0.22	0.23	1.08	0.41
Al_2O_3	16.13	16.72	16.89	17.17	15.92	17.09	17.10	17.12	18.59	16.94
Fe_2O_3	2.03	1.28	1.59	1.23	0.37	0.25	0.37	0.38	3.39	0.86
FeO	5.48	3.46	4.30	3.32	0.99	0.68	1.00	1.02	4.71	2.32
MnO	0.13	0.10	0.11	0.05	0.02	0.01	0.02	0.02	0.11	0.04
MgO	2.94	2.18	3.27	1.35	0.49	0.53	0.65	0.62	4.05	1.20
CaO	6.32	4.90	5.59	4.55	2.44	2.70	3.50	3.58	7.96	4.29
Na_2O	4.19	5.00	4.68	5.13	5.15	5.28	5.73	5.63	5.02	5.06
K_2O	1.22	1.43	1.63	1.42	2.46	2.57	1.37	1.25	1.24	1.13
P_2O_5	0.14	0.18	0.22	0.24	0.07	0.06	0.11	0.10	0.55	0.15
Q	12.6	15.2	10.1	16.9	26.2	23.4	22.6	23.7	0.0	21.9
C	0.00	0.00	0.00	0.00	0.53	0.87	0.08	0.23	0.00	0.00
Z	0.03	0.02	0.02	0.05	0.02	0.02	0.02	0.05	0.03	0.03
Or	7.2	8.5	9.7	8.4	14.5	15.2	8.1	7.4	7.3	6.7
Ab	35.5	42.3	39.6	43.4	43.6	44.7	48.5	47.6	42.5	42.8
An	21.6	19.0	20.3	19.6	11.6	13.0	16.7	17.1	24.5	20.2
Di	7.3	3.5	4.9	1.1	0.0	0.0	0.0	0.0	9.2	0.1
Hy	11.1	8.4	11.5	6.8	2.4	2.1	2.8	2.8	3.9	5.9
Ol	0.0	0.0	0.0	0.0	0.0	0.0	0.0	0.0	4.4	0.0
Mt	2.9	1.9	2.3	1.8	0.5	0.4	0.5	0.6	4.9	1.3
Il	1.43	0.94	1.12	1.34	0.40	0.28	0.41	0.43	2.05	0.79
Ap	0.33	0.42	0.51	0.58	0.17	0.15	0.26	0.23	1.31	0.36
An %	36.5	29.7	32.6	29.9	20.1	21.5	24.5	25.3	35.3	30.7
Or	10.8	11.7	13.4	11.4	20.1	20.1	10.6	9.8	9.5	9.3
Ab	56.6	62.1	58.4	62.1	63.9	62.8	67.5	67.4	58.6	62.9
An	32.5	26.2	28.2	26.5	16.1	17.2	21.9	22.8	31.9	27.9

G87-	116	118	120	121	122	123	124	127	142	144
SiO_2	72.44	53.99	73.11	72.70	75.13	63.08	67.70	72.50	72.63	70.75
TiO_2	0.20	1.04	0.21	0.16	0.13	0.59	0.56	0.14	0.18	0.17
Al_2O_3	16.15	19.23	15.55	15.92	14.85	16.21	16.81	15.92	15.34	17.16
Fe_2O_3	0.37	2.78	0.32	0.32	0.19	1.68	0.99	0.21	0.50	0.28
FeO	1.00	5.18	0.87	0.86	0.51	4.54	2.68	0.55	1.36	0.75
MnO	0.02	0.10	0.02	0.02	0.01	0.12	0.05	0.01	0.03	0.02
MgO	0.46	3.56	0.33	0.34	0.30	2.17	1.11	0.17	0.64	0.27
CaO	3.32	7.28	2.10	2.66	1.68	5.95	3.15	1.79	2.60	2.61
Na_2O	5.13	5.49	5.47	5.65	5.71	4.41	5.08	5.09	4.57	5.85
K_2O	0.89	0.93	1.96	1.32	1.45	1.07	1.71	3.59	2.09	2.10
P_2O_5	0.01	0.41	0.06	0.05	0.02	0.16	0.16	0.03	0.05	0.04
Q	30.8	0.0	28.5	28.2	32.1	16.5	22.2	24.9	30.8	22.4
C	0.72	0.00	0.76	0.48	0.88	0.00	1.27	0.49	0.95	0.62
Z	0.03	0.05	0.03	0.02	0.02	0.04	0.03	0.02	0.02	0.02
Or	5.3	5.5	11.6	7.8	8.6	6.3	10.1	21.2	12.4	12.4
Ab	43.4	46.5	46.3	47.8	48.3	37.3	43.0	43.1	38.6	49.5
An	16.4	25.1	10.0	12.9	8.2	21.3	14.6	8.7	12.6	12.7
Di	0.0	6.9	0.0	0.0	0.0	6.0	0.0	0.0	0.0	0.0
Hy	2.4	3.6	1.9	1.9	1.4	8.6	6.0	1.1	3.4	1.6
Ol	0.0	5.6	0.0	0.0	0.0	0.0	0.0	0.0	0.0	0.0
Mt	0.5	4.0	0.5	0.5	0.3	2.4	1.4	0.3	0.7	0.4
Il	0.38	1.98	0.39	0.31	0.24	1.13	1.07	0.27	0.35	0.32
Ap	0.02	0.96	0.14	0.12	0.05	0.38	0.38	0.08	0.11	0.10
An %	26.3	33.7	16.9	20.2	13.8	34.9	24.2	15.9	23.5	19.5
Or	7.8	6.9	16.4	10.9	12.6	9.4	14.4	28.0	18.8	16.0
Ab	67.9	61.7	69.4	71.1	75.3	58.9	64.9	60.5	62.1	67.6
An	24.3	31.4	14.2	18.0	12.1	31.7	20.7	11.4	19.1	16.4

G87-	145	146	147	148	149	150	151	152	153	154
SiO_2	72.60	71.95	69.66	61.11	61.91	68.83	63.83	55.15	71.51	70.91
TiO_2	0.11	0.14	0.36	0.59	0.66	0.37	0.58	0.77	0.15	0.15
Al_2O_3	16.04	16.32	16.46	16.50	16.38	17.16	16.94	17.53	16.70	16.90
Fe_2O_3	0.22	0.30	0.71	1.60	1.64	0.64	1.39	2.15	0.29	0.23
FeO	0.58	0.81	1.91	4.33	4.42	1.72	3.74	5.81	0.78	0.62
MnO	0.02	0.03	0.04	0.10	0.10	0.04	0.09	0.12	0.02	0.02
MgO	0.17	0.31	0.69	3.76	3.24	0.71	1.74	4.82	0.36	0.29
CaO	2.04	2.51	3.31	6.19	5.78	4.17	5.75	8.55	2.59	2.32
Na_2O	5.51	5.76	4.76	4.06	4.02	5.11	4.89	4.39	5.46	5.07
K_2O	2.67	1.82	2.02	1.58	1.65	1.17	0.92	0.54	2.07	3.45
P_2O_5	0.03	0.05	0.09	0.17	0.20	0.08	0.13	0.15	0.07	0.04
Q	25.4	25.3	25.3	12.0	14.1	23.9	16.4	2.1	25.5	22.6
C	0.42	0.42	0.64	0.00	0.00	0.10	0.00	0.00	0.95	0.70
Z	0.02	0.02	0.03	0.03	0.03	0.02	0.03	0.01	0.02	0.01
Or	15.8	10.8	11.9	9.4	9.7	6.9	5.4	3.2	12.2	20.4
Ab	46.7	48.7	40.3	34.3	34.0	43.2	41.4	37.2	46.2	42.9
An	10.0	12.2	15.9	22.2	21.8	20.2	21.6	26.5	12.4	11.3
Di	0.0	0.0	0.0	6.1	4.6	0.0	5.1	12.1	0.0	0.0
Hy	1.2	1.9	4.1	12.2	11.7	3.9	6.8	13.9	1.9	1.5
Ol	0.0	0.0	0.0	0.0	0.0	0.0	0.0	0.0	0.0	0.0
Mt	0.3	0.4	1.0	2.3	2.4	0.9	2.0	3.1	0.4	0.3
Il	0.21	0.26	0.68	1.12	1.26	0.70	1.10	1.46	0.29	0.29
Ap	0.06	0.12	0.20	0.40	0.47	0.20	0.30	0.37	0.17	0.09
An %	16.8	19.0	27.1	37.8	37.7	30.6	32.9	40.2	20.2	19.9
Or	21.0	14.4	16.9	13.8	14.4	9.5	7.6	4.6	16.6	26.4
Ab	65.8	69.3	60.6	53.6	53.4	62.9	61.9	57.0	66.6	59.0
An	13.2	16.3	22.5	32.6	32.2	27.7	30.4	38.4	16.8	14.6

G87-	158	964	965	966	968	969	970
SiO_2	70.80	70.19	68.35	67.74	70.13	69.47	71.76
TiO_2	0.26	0.21	0.38	0.30	0.24	0.20	0.17
Al_2O_3	16.01	17.04	17.46	18.05	16.79	17.41	16.42
Fe_2O_3	0.68	0.41	0.60	0.55	0.45	0.45	0.30
FeO	1.83	1.10	1.62	1.49	1.21	1.20	0.82
MnO	0.03	0.02	0.02	0.03	0.02	0.02	0.02
MgO	0.77	0.52	0.82	0.84	0.63	0.54	0.34
CaO	3.29	3.09	4.47	3.87	2.91	3.04	2.74
Na_2O	4.98	5.49	5.29	5.50	5.57	5.96	4.97
K_2O	1.29	1.86	0.93	1.55	1.99	1.65	2.39
P_2O_5	0.06	0.07	0.05	0.09	0.06	0.05	0.05
Q	27.8	23.3	22.6	19.7	22.5	20.6	27.0
C	0.60	0.54	0.00	0.51	0.35	0.41	0.79
Z	0.02	0.02	0.03	0.02	0.02	0.02	0.02
Or	7.6	11.0	5.5	9.2	11.7	9.8	14.1
Ab	42.1	46.5	44.7	46.5	47.1	50.5	42.0
An	15.9	14.9	21.2	18.6	14.0	14.7	13.3
Di	0.0	0.0	0.6	0.0	0.0	0.0	0.0
Hy	4.4	2.7	3.7	3.9	3.1	2.9	1.9
Ol	0.0	0.0	0.0	0.0	0.0	0.0	0.0
Mt	1.0	0.6	0.9	0.8	0.7	0.7	0.4
Il	0.49	0.39	0.73	0.57	0.45	0.38	0.33
Ap	0.15	0.16	0.13	0.21	0.15	0.13	0.11
An %	26.3	23.2	30.8	27.4	21.9	21.6	23.0
Or	11.1	14.6	7.4	11.9	15.5	12.5	19.6
Ab	65.5	65.6	64.0	64.0	66.0	68.6	61.9
An	23.3	19.8	28.5	24.1	18.5	18.9	18.5

G87-	27	61	68	114	115	141	6	25	54	64
SiO_2	71.78	75.34	74.58	75.23	77.10	71.12	51.14	76.13	76.91	71.06
TiO_2	0.14	0.05	0.09	0.15	0.05	0.10	1.22	0.17	0.38	0.21
Al_2O_3	16.53	14.20	14.42	14.83	14.18	15.92	13.53	13.80	11.84	16.54
Fe_2O_3	0.27	0.10	0.19	0.24	0.09	0.25	3.64	0.25	0.98	0.36
FeO	0.85	0.26	0.52	0.65	0.25	0.66	9.82	0.68	2.63	0.98
MnO	0.02	0.01	0.01	0.01	0.01	0.01	0.22	0.02	0.07	0.02
MgO	0.42	0.01	0.06	0.29	0.08	0.21	6.42	0.76	2.13	0.74
CaO	2.31	1.18	1.14	3.24	2.88	1.10	10.11	2.59	0.83	2.20
Na_2O	5.74	3.51	3.50	4.64	4.81	3.20	2.72	4.60	1.06	6.01
K_2O	1.87	5.34	5.47	0.70	0.55	7.40	1.08	0.96	3.12	1.82
P_2O_5	0.04	0.00	0.02	0.01	0.00	0.02	0.11	0.03	0.06	0.05
Q	25.2	31.8	30.5	37.8	40.6	21.2	0.2	38.7	52.4	22.9
C	0.96	0.52	0.74	0.57	0.46	0.71	0.00	0.55	5.35	0.80
Z	0.02	0.01	0.02	0.02	0.03	0.01	0.02	0.03	0.08	0.03
Or	11.1	31.6	32.3	4.1	3.3	43.8	6.4	5.7	18.4	10.8
Ab	48.6	29.7	29.6	39.3	40.7	27.1	23.0	39.0	9.0	50.9
An	11.2	5.8	5.5	16.0	14.3	5.3	21.5	12.6	3.8	10.6
Di	0.0	0.0	0.0	0.0	0.0	0.0	23.0	0.0	0.0	0.0
Hy	2.2	0.3	0.8	1.5	0.5	1.4	18.1	2.7	8.8	3.0
Ol	0.0	0.0	0.0	0.0	0.0	0.0	0.0	0.0	0.0	0.0
Mt	0.4	0.1	0.3	0.4	0.1	0.4	5.3	0.4	1.4	0.5
Il	0.27	0.10	0.16	0.29	0.10	0.19	2.32	0.32	0.72	0.40
Ap	0.10	0.01	0.05	0.02	0.01	0.06	0.25	0.08	0.13	0.12
An %	17.9	15.6	14.9	27.7	24.8	15.6	46.9	23.4	28.4	16.4
Or	15.0	45.8	46.7	6.7	5.3	56.2	12.2	9.5	58.1	14.3
Ab	69.8	45.7	45.3	67.4	71.2	36.9	46.6	69.3	30.0	71.7
An	15.2	8.4	8.0	25.9	23.5	6.8	41.1	21.2	11.9	14.1

G87-	66	72	73	78	140	143	155	156
SiO_2	82.04	68.81	50.02	71.90	73.54	70.83	60.85	61.61
TiO_2	0.21	0.43	0.72	0.17	0.26	0.55	0.38	0.71
Al_2O_3	10.02	16.41	15.49	16.07	13.84	14.23	16.49	17.96
Fe_2O_3	0.34	0.80	2.89	0.35	0.75	1.12	1.57	1.37
FeO	0.92	2.15	7.80	0.96	2.02	3.03	4.23	3.70
MnO	0.02	0.04	0.19	0.02	0.09	0.17	0.05	0.05
MgO	0.56	1.21	7.77	0.53	0.23	1.41	8.62	3.95
CaO	1.73	3.40	11.28	2.90	1.98	2.86	1.40	3.54
Na_2O	2.51	5.07	2.91	5.32	3.46	4.08	3.99	5.89
K_2O	1.62	1.57	0.88	1.71	3.79	1.59	2.37	0.99
P_2O_5	0.03	0.11	0.05	0.07	0.05	0.13	0.06	0.24
Q	56.3	23.3	0.0	27.1	33.2	31.3	10.2	8.7
C	1.07	0.46	0.00	0.37	0.56	0.91	4.95	1.32
Z	0.02	0.03	0.01	0.02	0.08	0.06	0.02	0.03
Or	9.6	9.3	5.2	10.1	22.4	9.4	14.0	5.8
Ab	21.2	42.9	24.7	45.0	29.3	34.5	33.8	49.9
An	8.4	16.2	26.6	13.9	9.5	13.4	6.6	16.0
Di	0.0	0.0	23.6	0.0	0.0	0.0	0.0	0.0
Hy	2.5	5.7	1.8	2.5	3.4	7.6	27.4	14.4
Ol	0.0	0.0	12.4	0.0	0.0	0.0	0.0	0.0
Mt	0.5	1.2	4.2	0.5	1.1	1.6	2.3	2.0
Il	0.40	0.81	1.37	0.32	0.49	1.04	0.72	1.35
Ap	0.06	0.26	0.11	0.16	0.12	0.30	0.15	0.57
An %	27.2	26.2	50.4	22.6	23.4	26.8	15.5	23.3
Or	23.6	13.1	9.0	14.0	35.5	15.8	24.8	7.8
Ab	55.6	64.2	45.1	66.5	49.4	61.6	63.6	70.7
An	20.7	22.8	45.9	19.4	15.1	22.5	11.6	21.4

G87-	67	69	70	128	129	130	131	133	135	136
SiO_2	61.30	63.06	61.17	55.78	73.82	55.04	53.87	60.10	57.19	66.30
TiO_2	0.65	0.60	0.61	0.78	0.06	0.78	0.87	0.71	0.78	0.69
Al_2O_3	16.32	16.31	17.67	17.58	16.06	17.81	17.53	17.61	17.05	16.95
Fe_2O_3	1.94	1.65	1.61	2.39	0.15	1.64	2.26	2.24	2.19	1.06
FeO	4.87	4.46	4.36	5.74	0.40	6.61	6.10	4.50	5.91	2.86
MnO	0.11	0.11	0.10	0.11	0.02	0.13	0.13	0.10	0.13	0.06
MgO	2.86	2.75	2.50	4.14	0.16	4.50	5.14	3.43	4.08	1.80
CaO	6.72	5.76	6.27	8.22	3.43	8.21	8.94	4.91	7.66	4.70
Na_2O	4.37	4.20	4.77	4.36	5.01	4.52	4.30	4.17	4.28	5.03
K_2O	0.73	1.01	0.81	0.70	0.89	0.60	0.68	2.09	0.59	0.47
P_2O_5	0.13	0.09	0.13	0.20	0.00	0.16	0.18	0.13	0.14	0.09
Q	13.9	17.0	12.1	4.0	33.4	1.0	0.0	10.2	6.8	21.3
C	0.00	0.00	0.00	0.00	0.63	0.00	0.00	0.00	0.00	0.00
Z	0.02	0.03	0.02	0.01	0.02	0.01	0.02	0.02	0.02	0.06
Or	4.3	6.0	4.8	4.1	5.3	3.5	4.0	12.4	3.5	2.8
Ab	37.0	35.5	40.4	36.9	42.4	38.2	36.4	35.3	36.2	42.5
An	22.8	22.7	24.4	26.4	17.0	26.6	26.5	23.2	25.6	22.3
Di	8.0	4.4	4.9	10.8	0.0	10.8	13.6	0.3	9.5	0.4
Hy	9.7	10.7	9.7	12.5	0.9	15.6	13.7	13.8	13.5	7.7
Ol	0.0	0.0	0.0	0.0	0.0	0.0	0.4	0.0	0.0	0.0
Mt	2.8	2.4	2.3	3.5	0.2	2.4	3.3	3.3	3.2	1.5
Il	1.23	1.15	1.15	1.47	0.11	1.48	1.66	1.35	1.47	1.30
Ap	0.32	0.21	0.30	0.47	0.01	0.38	0.43	0.30	0.32	0.21
An %	36.7	37.5	36.3	40.3	28.6	39.6	40.7	38.3	40.0	33.1
Or	6.5	9.0	6.6	5.9	8.1	5.0	5.8	16.9	5.2	4.0
Ab	59.2	56.8	59.5	56.2	65.6	57.4	55.8	51.3	56.9	64.3
An	34.3	34.2	33.9	37.9	26.3	37.6	38.4	31.8	37.9	31.8

G87-	137	138	139
SiO_2	57.02	57.73	56.91
TiO_2	0.77	0.75	0.75
Al_2O_3	17.05	16.32	16.91
Fe_2O_3	2.19	2.18	2.23
FeO	5.91	5.89	6.03
MnO	0.12	0.14	0.14
MgO	4.09	4.01	4.17
CaO	7.98	7.56	7.92
Na_2O	4.47	4.51	4.17
K_2O	0.68	0.33	0.64
P_2O_5	0.13	0.16	0.13
Q	5.5	7.3	6.4
C	0.00	0.00	0.00
Z	0.02	0.02	0.02
Or	4.0	2.0	3.8
Ab	37.8	38.1	35.3
An	24.5	23.3	25.6
Di	10.0	12.5	10.6
Hy	13.3	11.8	13.4
Ol	0.0	0.0	0.0
Mt	3.2	3.2	3.2
Il	1.46	1.43	1.43
Ap	0.30	0.37	0.30
An %	39.3	36.6	40.6
Or	6.1	3.0	5.7
Ab	57.0	61.5	56.0
An	63.9	35.5	38.3

APPENDIX 6.

Whole-rock normalized plots

This appendix includes chondrite-normalized REE patterns and spidergrams of selected samples.

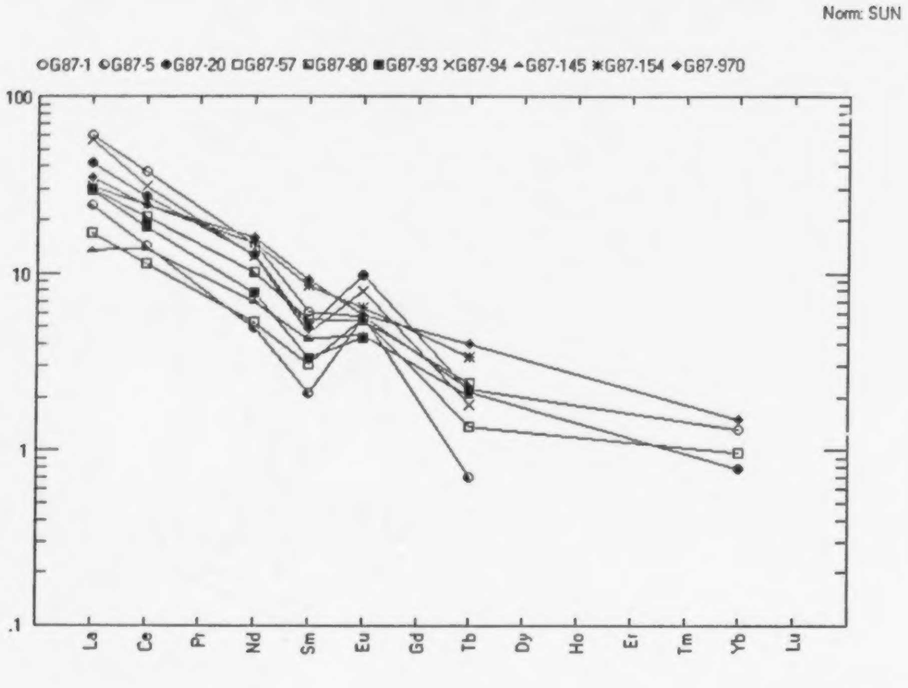
Norm: SUN
○G87-1 ◎G87-5 ●G87-20 □G87-57 ▣G87-80 ■G87-93 ×G87-94 ▲G87-145 ✱G87-154 ◆G87-970
100
10
1
.1
La
Ce
Pr
Nd
Sm
Eu
Gd
Tb
Dy
Ho
Er
Tm
Yb
Lu

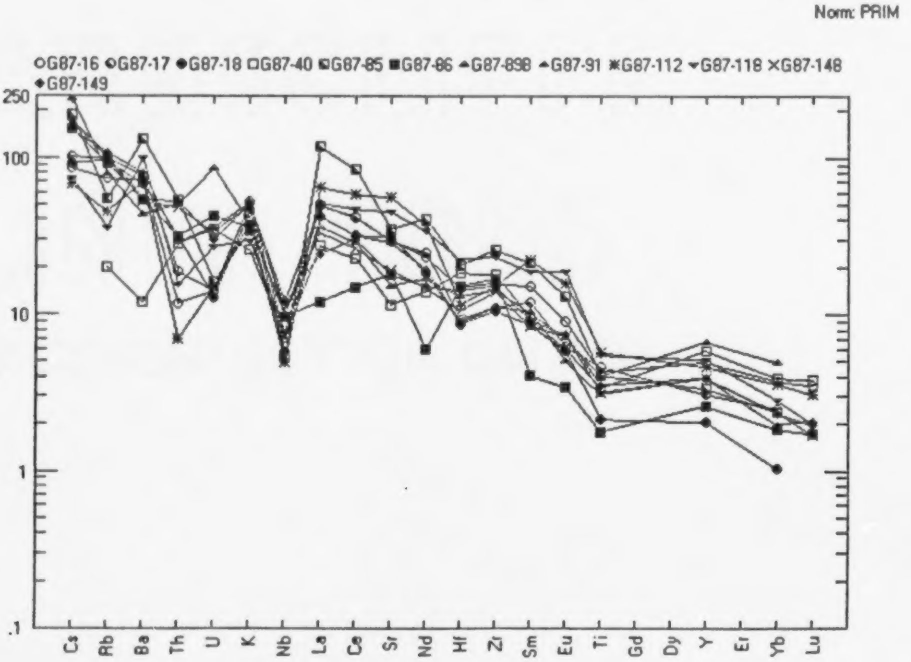
Norm: PRIM
○G87-16 ◎G87-17 ●G87-18 □G87-40 ▣G87-85 ■G87-86 ▲G87-89B ▲G87-91 ✱G87-112 ▼G87-118 ×G87-148
◆G87-149
250
100
10
1
.1
Cs
Rb
Ba
Th
U
K
Nb
La
Ce
Sr
Nd
Hf
Zr
Sm
Eu
Ti
Gd
Dy
Y
Er
Yb
Lu

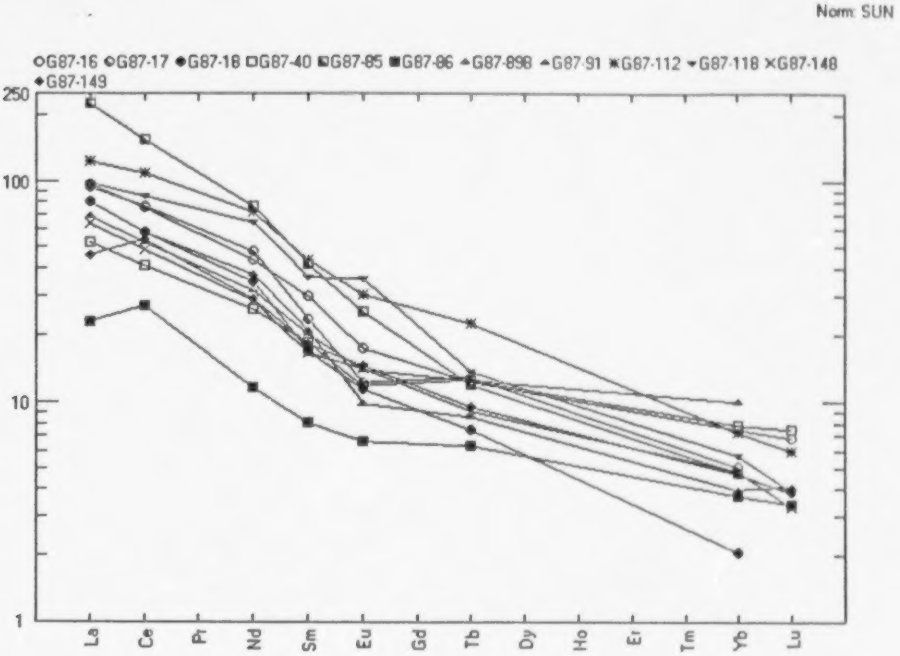
Norm: SUN
○G87-16 ◇G87-17 ●G87-18 □G87-40 ◘G87-85 ■G87-86 ▲G87-89B ▲G87-91 ✱G87-112 ▼G87-118 ×G87-148
◆G87-149
250
100
10
1
La
Ce
Pr
Nd
Sm
Eu
Gd
Tb
Dy
Ho
Er
Tm
Yb
Lu

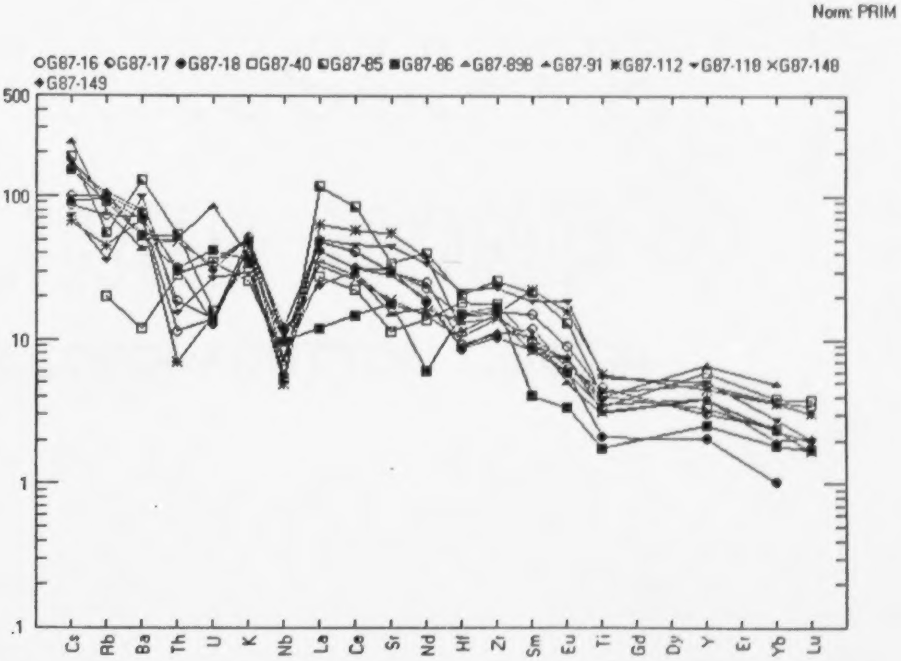
Norm: PRIM
○G87-16 ◇G87-17 ●G87-18 □G87-40 ◘G87-85 ■G87-86 ▲G87-89B ▲G87-91 ✱G87-112 ▼G87-118 ×G87-148
◆G87-149
500
100
10
1
.1
Cs
Rb
Ba
Th
U
K
Nb
La
Ce
Sr
Nd
Hf
Zr
Sm
Eu
Ti
Gd
Dy
Y
Er
Yb
Lu

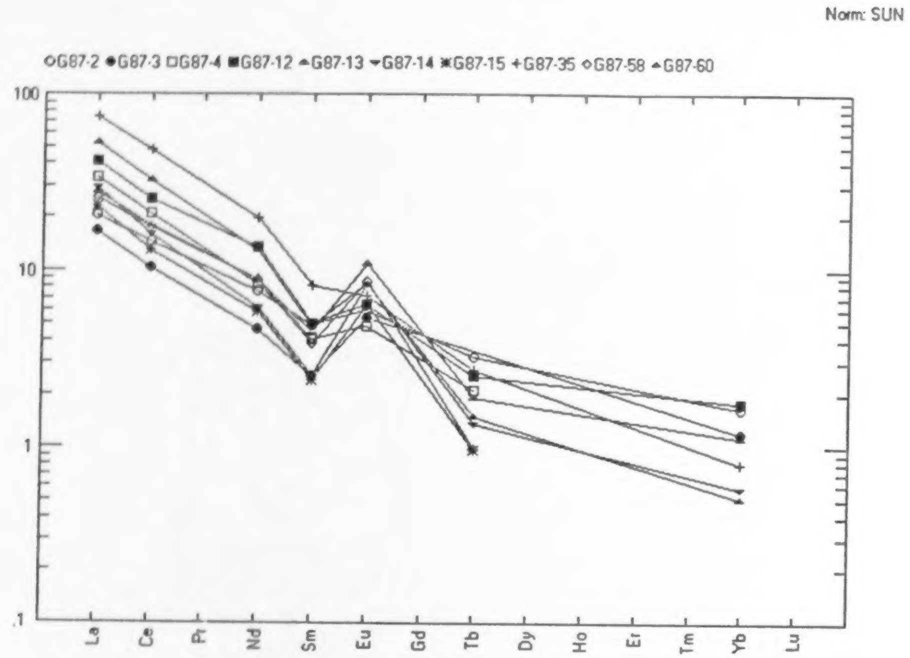
Norm: SUN
○G87-2 ●G87-3 □G87-4 ■G87-12 ▲G87-13 ▼G87-14 ✱G87-15 +G87-35 ◇G87-58 ▲G87-60
100
10
1
.1
La
Ce
Pr
Nd
Sm
Eu
Gd
Tb
Dy
Ho
Er
Tm
Yb
Lu

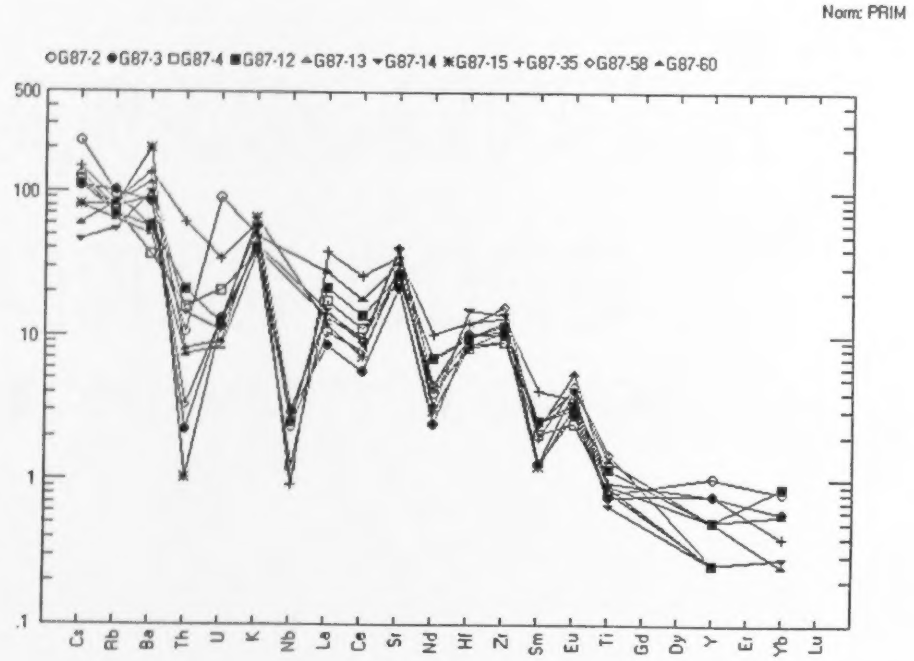
Norm: PRIM
○G87-2 ●G87-3 □G87-4 ■G87-12 ▲G87-13 ▼G87-14 ✱G87-15 +G87-35 ◇G87-58 ▲G87-60
500
100
10
1
.1
Cs
Rb
Ba
Th
U
K
Nb
La
Ce
Sr
Nd
Hf
Zr
Sm
Eu
Ti
Gd
Dy
Y
Er
Yb
Lu

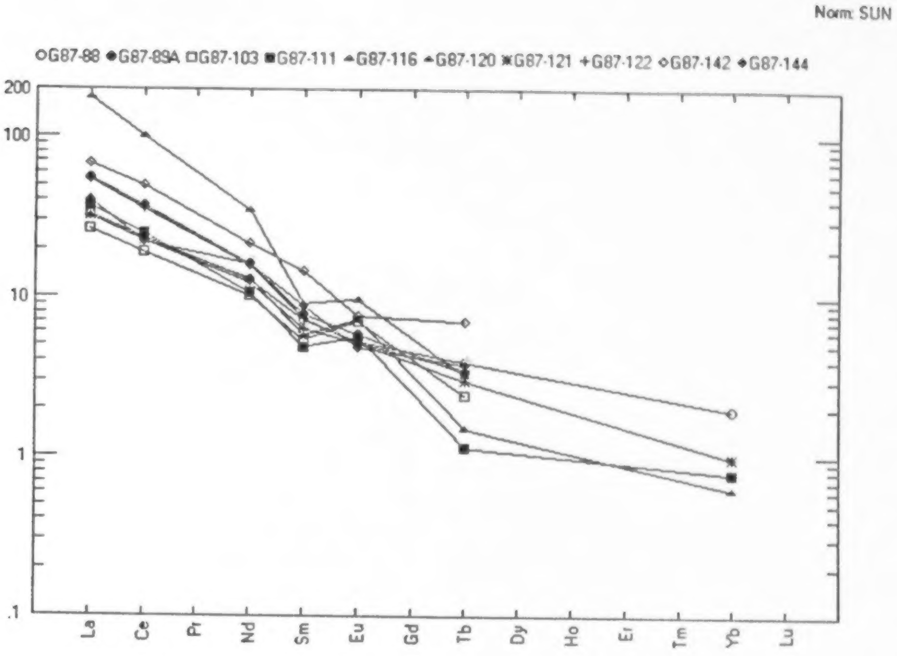
Norm: SUN
○G87-88 ●G87-89A □G87-103 ■G87-111 ▲G87-116 ▲G87-120 ✱G87-121 +G87-122 ◇G87-142 ◆G87-144
200
100
10
1
.1
La
Ce
Pr
Nd
Sm
Eu
Gd
Tb
Dy
Ho
Er
Tm
Yb
Lu

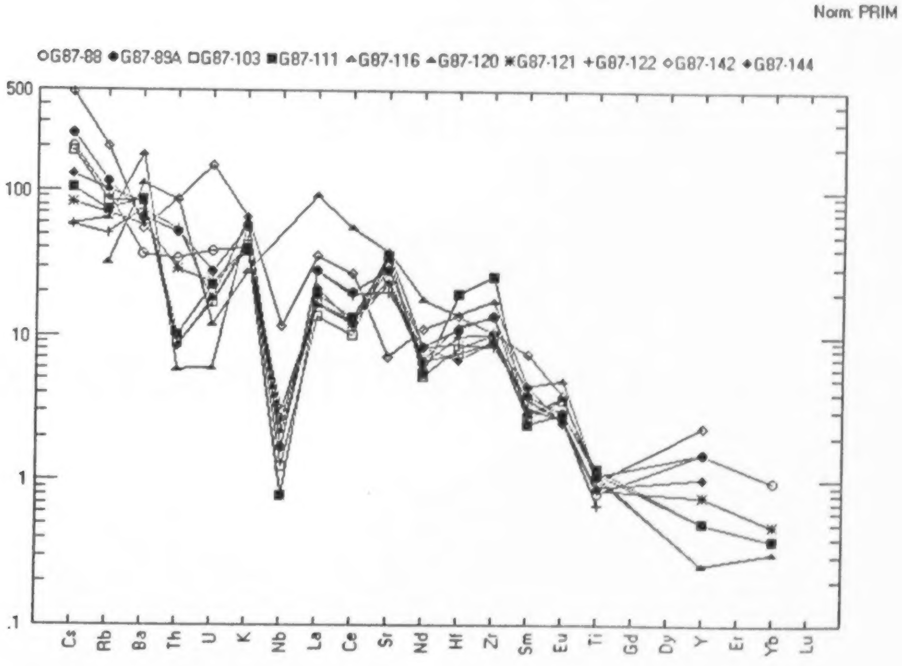
Norm: PRIM
○G87-88 ●G87-89A □G87-103 ■G87-111 ▲G87-116 ▲G87-120 ✱G87-121 +G87-122 ◇G87-142 ◆G87-144
500
100
10
1
.1
Cs
Rb
Ba
Th
U
K
Nb
La
Ce
Sr
Nd
Hf
Zr
Sm
Eu
Ti
Gd
Dy
Y
Er
Yb
Lu

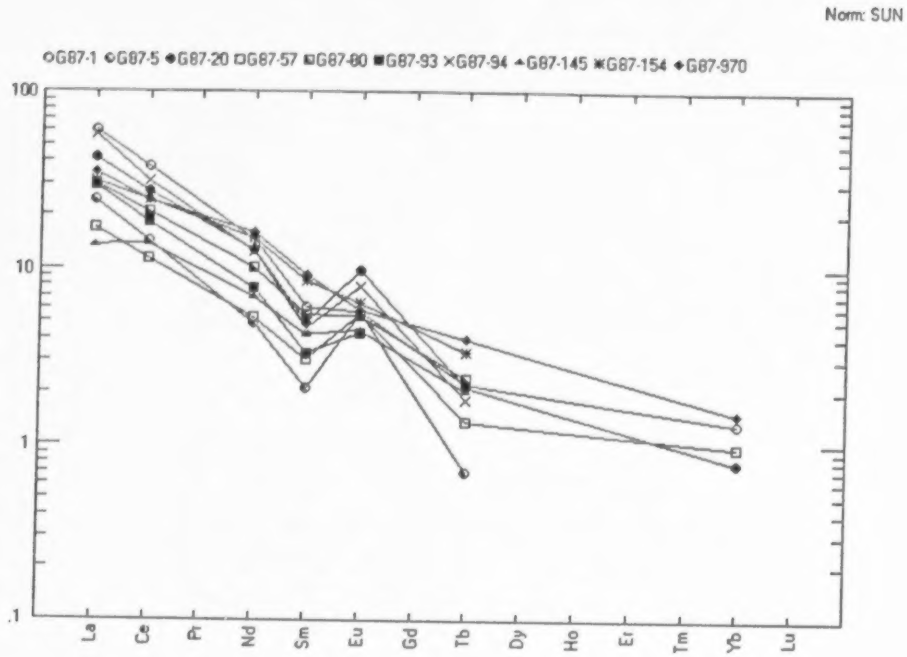
Norm: SUN
○G87-1 ◎G87-5 ●G87-20 □G87-57 ▣G87-80 ■G87-93 ×G87-94 ▲G87-145 ✱G87-154 ◆G87-970
100
10
1
.1
La
Ce
Pr
Nd
Sm
Eu
Gd
Tb
Dy
Ho
Er
Tm
Yb
Lu

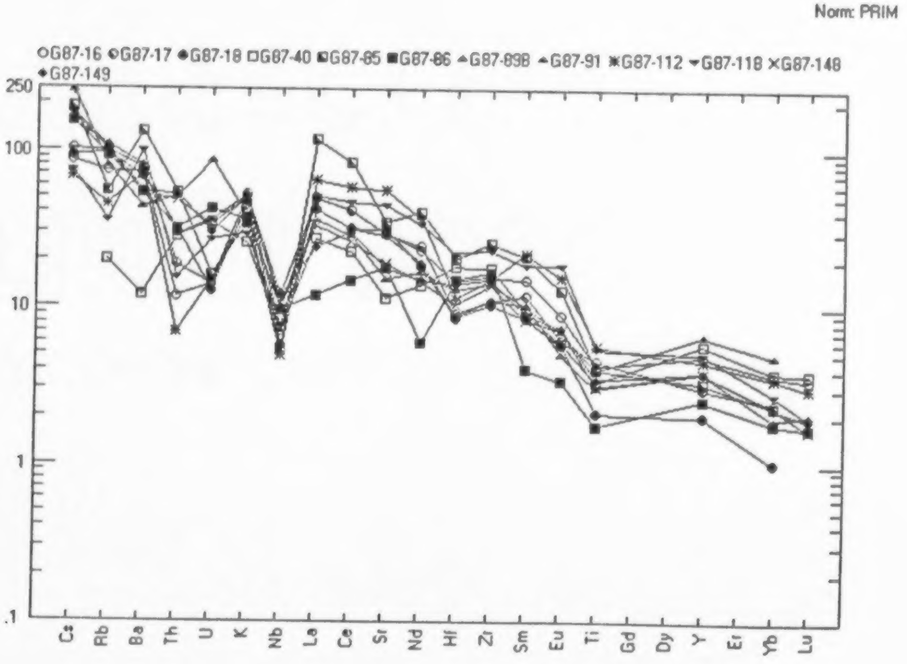
Norm: PRIM
○G87-16 ◎G87-17 ●G87-18 □G87-40 ▣G87-85 ■G87-86 ▲G87-89B ▲G87-91 ✱G87-112 ▼G87-118 ×G87-148
◆G87-149
250
100
10
1
.1
Cs
Rb
Ba
Th
U
K
Nb
La
Ce
Sr
Nd
Hf
Zr
Sm
Eu
Ti
Gd
Dy
Y
Er
Yb
Lu

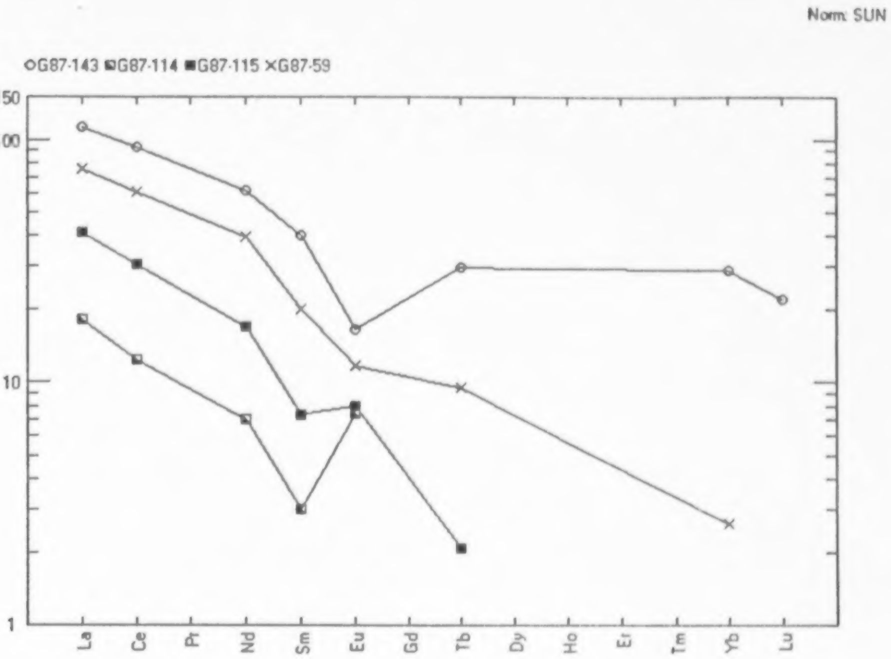
Norm: SUN
○G87-143 ▨G87-114 ■G87-115 ×G87-59
150
100
10
1
La
Ce
Pr
Nd
Sm
Eu
Gd
Tb
Dy
Ho
Er
Tm
Yb
Lu

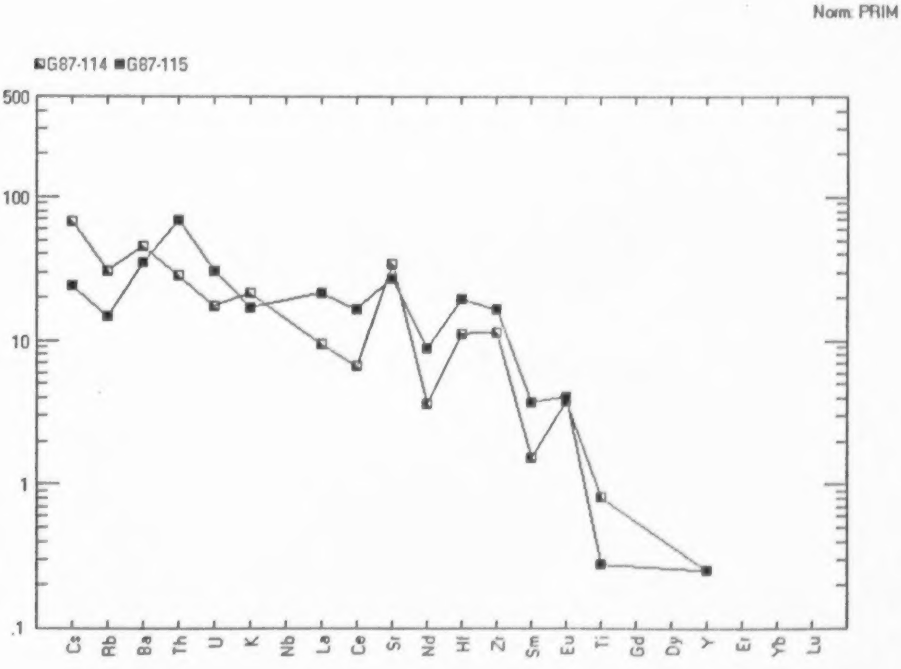
Norm: PRIM
▨G87-114 ■G87-115
500
100
10
1
.1
Cs
Rb
Ba
Th
U
K
Nb
La
Ce
Sr
Nd
Hf
Zr
Sm
Eu
Ti
Gd
Dy
Y
Er
Yb
Lu

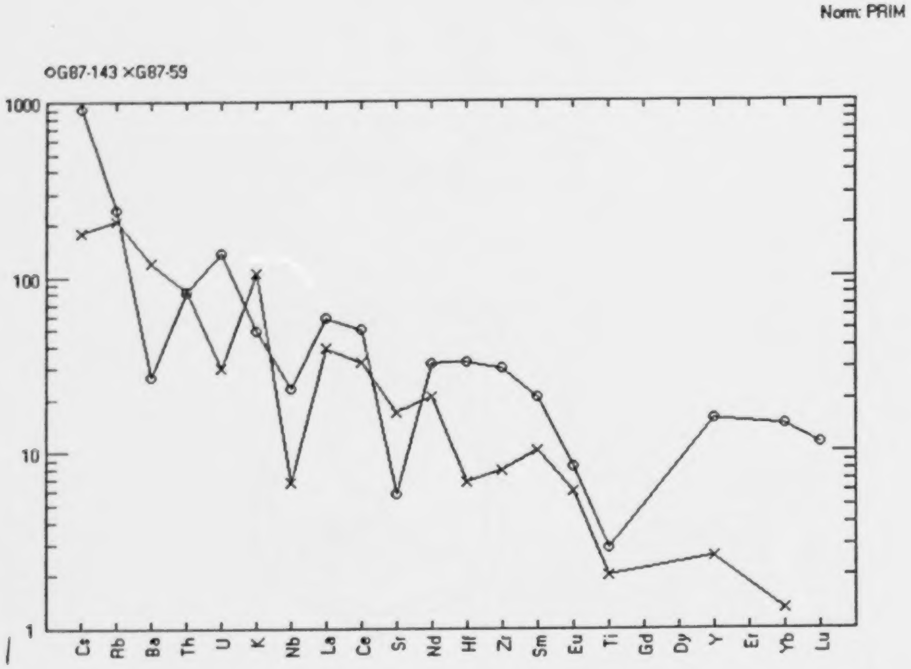
Norm: PRIM
○G87-143 ×G87-59
1000
100
10
1
Cs
Rb
Ba
Th
U
K
Nb
La
Ce
Sr
Nd
Hf
Zr
Sm
Eu
Ti
Gd
Dy
Y
Er
Yb
Lu

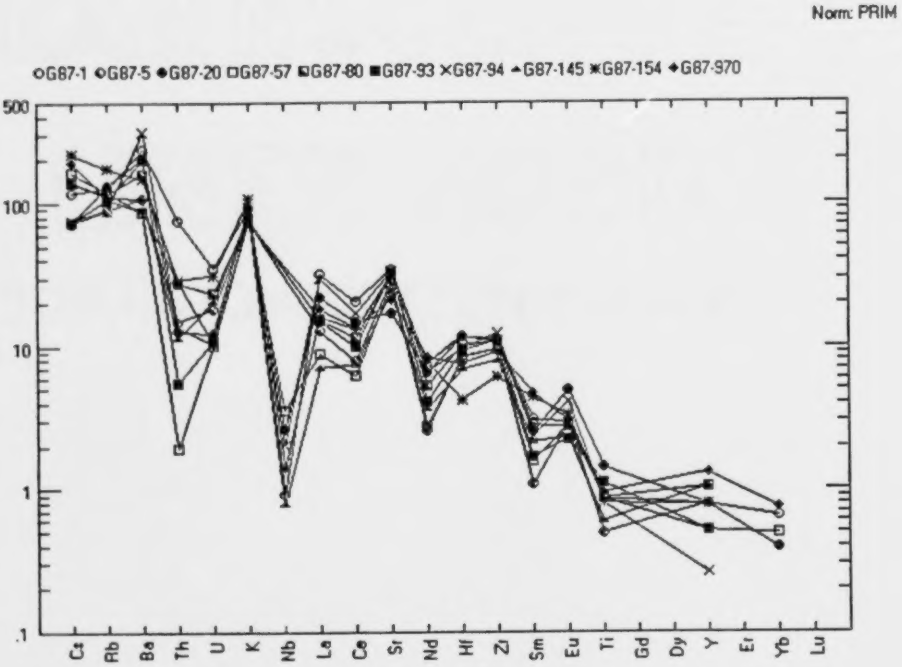
Norm: PRIM
○G87-1 ◇G87-5 ●G87-20 □G87-57 ▣G87-80 ■G87-93 ×G87-94 ▲G87-145 ✱G87-154 ◆G87-970
500
100
10
1
.1
Cs
Rb
Ba
Th
U
K
Nb
La
Ce
Sr
Nd
Hf
Zr
Sm
Eu
Ti
Gd
Dy
Y
Er
Yb
Lu